TECHNISCHE UNIVERSITÄT MÜNCHEN
Lehrstuhl für Informationstechnische Regelung

Distributed Algorithm Analysis and Topology Design in Coevolutionary Networks

Dong Xue

Vollständiger Abdruck der von der Fakultät für Elektrotechnik und Informationstechnik der Technischen Universität München zur Erlangung des akademischen Grades eines

Doktor-Ingenieurs (Dr.-Ing.)

genehmigten Dissertation.

Vorsitzender: Prof. Dr.-Ing. Wolfgang Kellerer

Prüfer der Dissertation:

1. Prof. Dr.-Ing. Sandra Hirche
2. Prof. dr. ir. Ming Cao
   University of Groningen, the Netherlands

Die Dissertation wurde am 21.06.2018 bei der Technischen Universität München eingereicht und durch die Fakultät für Elektrotechnik und Informationstechnik am 19.09.2018 angenommen.

To my parents and myself ...

Munich, June 2018
Dong (Tony) XUE

Abstract

The term "distributed" appears as a thematic element in the problems of system analysis, control synthesis, and algorithm design of network systems consisting of numerous possibly heterogeneous subsystems that are typically distributed spatially over a large area. Research in the field of social network analysis has flourished in recent years, resulting in many important concepts about modern network science. Early work in network science considered individual entities to interact cooperatively. However, most real-world networks display various contrasting relationships (such as friendly/hostile, like/dislike, trust/distrust, and cooperation/competition) between social entities. Such antagonistic interactions in the graphic representation of networks are represented by edges with negative weights, spurring the study of dynamical processes over a signed graph. In contrast to the consensus on cooperative networks, opinion formations in signed graphs may result in other complex outcomes, including neutrality, polarization, and separation. Furthermore, conventional research on network systems usually assumes that the topology of the interaction network remains unchanged during the evolving dynamical processes. Many social observations show evidence of a feedback loop between the dynamics of the network and individuals' states. Networks with this coevolving property are called coevolutionary or adaptive networks. These kinds of social networks require the development of novel mathematical models and distributed algorithms to respond efficiently to emerging challenges.

The present thesis addresses the study of opinion dynamics evolving on coopetitive (cooperative-competitive) networks and topology-design problems for network systems from a coevolutionary point of view. The antecedent of protocol design for opinion dynamics is to examine the accessibility problem: whether there are admissible control laws to polarize, reconcile, or neutralize individuals' opinions in a social group. The next investigation is how opinion-forming processes evolve over social networks with antagonistic interactions and exogenous influences. Furthermore, the shift from single-issue opinion-forming to opinion evolution over a sequence of issues sparks us to evaluate individuals' social influence on the outcomes of group discussions. From a practically applicable perspective, the hope is that the topology-manipulation mechanism can itself perform in a distributed manner without complete information of network topology and a central decision-maker.

The main contributions of this thesis are as follows. First, sufficient and necessary conditions for those accessibility problems are provided, with particular emphasis on the joint impact of the dynamical properties of subsystems and their interaction structure. A mathematical model based on a port-Hamiltonian representation of opinion dynamics is proposed to capture the information-diffusion process and to predict how public opinions evolve through social entities in the long run. For opinion formation along a sequence of issues, a mathematical formulation is introduced to characterize the coevolution of opinion dynamics and the influence of networks. Finally, we review the topology-design problem in the spirit of coevolution networks and develop some distributed strategies to implement topology operations in an iterative fashion. The developed strategies can be performed using only local knowledge of network topology and in the absence of a central coordinator for decision-making. All of the obtained results are elucidated and validated via numerical demonstrations and tests.

Zusammenfassung

Der Begriff der Verteiltheit taucht als thematisches Element in Problemstellungen der Analyse, Steuerung und Regelung von Systemen auf, sowie im Entwurf von Algorithmen in Netzwerksystemen, die aus zahlreichen und möglicherweise heterogenen Subsystemen bestehen und in der Regel räumlich über große Gebiete verteilt sind. Forschung im Bereich der Analyse von sozialen Netzwerken ist in vergangenen Jahren aufgeblüht, mit dem Ergebnis vielfältiger neuer Konzepte in der modernen Wissenschaft von Netzwerken. Frühe Arbeiten der Netzwerkwissenschaften handelten von einzelnen Entitäten, die kooperativ interagieren. Die meisten realen Netzwerke weisen jedoch vielfältige gegensätzliche Beziehungen zwischen sozialen Entitäten auf (zB freundschaftlich/befeindet, mögen/nicht mögen, Vertrauen/Misstrauen, kooperativ/im Wettbewerb stehend). Solch gegensätzliche Interaktionen werden in Netzwerken als Kanten mit negativer Gewichtung repräsentiert, was Studien von dynamischen Prozessen auf vorzeichenbehafteten Graphen hervorruft. Im Gegensatz zu Konsensus in kooperativen Netzwerken können Meinungsverteilungen in vorzeichenbehafteten Netzwerken komplexe Zustände einnehmen, unter anderem Neutralität, Polarisation und Separation. Darüberhinaus, is es in Arbeiten zu Netzwerksystemen gebräuchlich, die Topologie des Interaktionsnetzwerkes während des darauf evolvierenden dynamischen Prozesses als unverändert anzunehmen. Viele soziale Beobachtungen weisen auf Rückkoppelungsschleifen zwischen der Dynamik des Netzwerkes und einzelner Zustände hin. Netzwerke mit solch einer koevolvierenden Eigenschaft werden als koevolutionäre oder adaptive Netzwerke bezeichnet. Diese Art von sozialen Netzwerken bedürfen der Erarbeitung neuer mathematischer Modelle und verteilter Algorithmen, um effektiv auf aufkommende Herausforderungen reagieren zu können.

Die vorliegende Arbeit handelt von Meinungsdynamiken, die auf kooperativ und wettbewerblichen Netzwerken evolvieren, sowie von Problemen des Topologieentwurfs für Netzwerksysteme aus einer koevolutionären Perspektive. Im Protokollentwurf für Meinungsdynamiken beschäftigen wir uns mit dem Zugangsproblem: Gibt es zulässliche Regelgesetze die individuelle Meinungen in einer sozialen Gruppe polarisieren, neutralisieren oder wieder zusammenführen. Danach behandeln wir die Fragestellung wie meinungsformende Prozesse in sozialen Netzwerken mit antagonistischen Interaktionen und unter exogenen Einflüssen evolvieren. Ferner führt uns der Unterschied zwischen Meinungsbildung zu Einzelthemen und der Meinungsbildung über eine Sequenz von Themen hin zur Untersuchung des sozialen Einflusses von Individuen auf die Endergebnisse in Gruppendiskussionen. Aus einem praktischen Standpunkt heraus untersuchen wir Mechanismen zur Manipulation von Topologien ohne vollständige Information von Netzwerktopologien und ohne zentralen Entscheidungsträger.

Die wesentlichen Beiträge dieser Arbeit sind wie folgt. Zunächst werden hinreichende und notwendige Bedingungen für eine Klasse an Zugangsproblemen präsentiert, mit besonderem Fokus auf den gemeinsamen Einfluss der dynamischen Eigenschaften der Subsysteme und ihrer Interaktionsstruktur. Ein mathematisches Modell basierend auf einer Port-Hamilton'schen Repräsentation von Meinungsdynamiken wird eingeführt, die den Informationsdiffusionsprozess abbilden, sowie Aussagen über die Langzeitevolution von öffentlichen Meinungen durch soziale Entitäten erlauben. Zum Problem der Meinungsbildung über eine Sequenz von Themen wird eine mathematische Formulierung vorgestellt, die es erlaubt die Koevolution von Meinungsdynamiken und den Einfluss des Netzwerkes zu charakterisieren. Letztlich geben wir einen Überblick zum Problem des Topologieentwurfs unter der Perspektive koevolutionärer Netzwerke und entwickeln verteilte Strategien, um Topologiemanipulationen interaktiver Art vorzunehmen. Die entwickelten Strategien können unter lediglich lokalem Wissen der Netzwerktopologie ausgeführt werden, sowie unter Abwesenheit eines zentrale Koordinators für die Entscheidungsfindung. Die vorgestellten Ergebnisse werden mittels numerischer Simulation demonstriert, getestet und validiert.

Contents

Notations

Abbreviations

LTI	linear time-invariant
LMI	linear matrix inequality
SC	strongly connected
QSC	quasi-strongly connected
SB	structurally balanced
ISB	in-isolated structurally balanced
PH	port-Hamiltonian
PCH	port-controlled Hamiltonian
PI	power iteration
SIS	susceptible-infected-susceptible
SIR	susceptible-infected-removed
SIRS	susceptible-infected-recovered-susceptible
SEIR	susceptible-exposed-infected-recovered

Conventions

Scalars, vectors and matrices

Scalars and *scalar functions* are denoted by lower and upper case letters in italic type, respectively. *Vectors* are denoted by lower case letters in bold type, as the vector $\boldsymbol{x}$ is composed of elements x_i. *Matrices* are denoted by upper case letters in bold type, as the matrix $\boldsymbol{X}$ is composed of elements $[\boldsymbol{X}]_{ij}$ (i-th row, j-th row). In order to avoid excessive notational clutter when dealing with vectors and matrixes, dimensions are only rarely mentioned explicitly.

x	scalar
$\boldsymbol{x}$	vector

$\boldsymbol{f}(\cdot)$	vector-valued function or vector field
$\boldsymbol{X}$	matrix
$\mathbf{1}$	column vector of all ones with appropriate dimensions
$\mathbf{0}$	column vector of all zeros with appropriate dimensions
$\boldsymbol{e}_i$	i-th canonical basis of Euclidean space
$\boldsymbol{I}$	identity matrix with appropriate dimensions
$(\cdot)^\mathsf{T}$	transpose of vectors or matrices
$\boldsymbol{M}^{-1}$	inverse of square matrix $\boldsymbol{M}$
$\lvert x \rvert$	absolute value of scalar x
$\lvert \boldsymbol{x} \rvert$	entry-wise absolute value of vector $\boldsymbol{x}$, i.e., $\lvert \boldsymbol{x} \rvert = [\lvert x_1 \rvert, \ldots, \lvert x_n \rvert]^\mathsf{T}$
$\lvert \boldsymbol{X} \rvert$	entry-wise absolute value of matrix $\boldsymbol{X}$, i.e., $[\lvert \boldsymbol{X} \rvert]_{ij} = \lvert [\boldsymbol{X}]_{ij} \rvert$
$\lVert \boldsymbol{x} \rVert_l$	$l = 1, 2, \infty$ vector norm of $\boldsymbol{x}$
$\lVert \boldsymbol{X} \rVert_l$	$l = 1, 2, \infty$ matrix norm of $\boldsymbol{X}$ induced by l vector norm
$\boldsymbol{X} > 0$	matrix with positive entries
$\boldsymbol{X} \geq 0$	matrix with non-negative entries
$\boldsymbol{X} \succ 0$	symmetric, positive definite matrix
$\boldsymbol{X} \succeq 0$	symmetric, non-negative definite matrix
$\boldsymbol{X} \prec 0$	symmetric, negative definite matrix
$\boldsymbol{X} \preceq 0$	symmetric, non-positive definite matrix

Spaces and sets

Spaces and sets are denoted by upper case letters in blackboard bold type.

$\mathbb{R}$	set of real numbers
$\mathbb{R}_{>0}$	set of positive real numbers
$\mathbb{R}_{\geq 0}$	set of non-negative real numbers
$\mathbb{R}^n$	n-dimensional Euclidean space
$\mathbb{R}^{n \times m}$	space of $n \times m$-dimensional matrices
$\mathbb{Z}$	set of integers
$\mathbb{Z}_{>0}$	set of positive integers
$\mathbb{Z}_{\geq 0}$	set of non-negative integers
$\mathbb{C}$	set of complex numbers
$\mathbb{C}_{>0}$	set of complex numbers with positive real parts

$\mathbb{C}_{<0}$	set of complex numbers with negative real parts
$\mathbb{C}_{\geq 0}$	set of complex numbers with non-negative real parts
$\mathbb{C}_{\leq 0}$	set of complex numbers with non-positive real parts
$\lvert\mathbb{X}\rvert$	cardinality of set $\mathbb{X}$
$\mathbb{X}^n$	n-dimensional manifold
$T_{\boldsymbol{x}}\mathbb{X}^n$	tangent space of $\mathbb{X}^n$ on $\boldsymbol{x} \in \mathbb{X}^n$
$\mathbb{S}^n$	n-dimensional simplex
$\mathbb{D}^n$	n-dimensional orthoplex

Symbols

Operator

$\otimes$	Kronecker product
$\circ$	Hadamard product
$\lambda_i(\boldsymbol{X})$	i-th smallest eigenvalue of matrix $\boldsymbol{X}$
$\mathsf{sr}(\boldsymbol{X})$	spectral radius of matrix $\boldsymbol{X}$
$\mathsf{sp}(\boldsymbol{X})$	set of eigenvalue of square matrix $\boldsymbol{X}$
$\ker \boldsymbol{X}$	kernel of matrix $\boldsymbol{X}$
$\mathrm{tr}(\boldsymbol{X})$	trace of matrix $\boldsymbol{X}$
$\max$	maximum function
$\min$	minimum function
$\arg\max$	arguments of the maximum
$\arg\min$	arguments of the minimum
$\mathrm{diag}(x_1, x_2)$	diagonal matrix with scalars x_1, x_2 on diagonal
$\mathrm{diag}(\boldsymbol{X}_1, \boldsymbol{X}_2)$	(block)-diagonal matrix with matrices $\boldsymbol{X}_1, \boldsymbol{X}_2$ on diagonal
$\mathrm{d}_{\mathbb{X}}$	metric on $\mathbb{X}^n$
$\mathrm{int}(\mathbb{X}^n)$	interior of $\mathbb{X}^n$

Graph theory

$\mathcal{G}$	graph

$\mathbb{V}$	set of nodes
$\mathbb{E}$	set of edges
$\boldsymbol{A}$	adjacency matrix
$\boldsymbol{L}$	Laplacian matrix
$\mathbb{N}^i$	neighborhood set of node $i \in \mathbb{V}$
$\deg_i$	degree of node $i \in \mathbb{V}$

List of Figures

List of Tables

We cannot understand the implications of network system mechanisms without attending to the network structure in which the mechanisms are unfolding, and we cannot understand the implications of a network structure without attending to the mechanisms that are unfolding on it.

Noah E. Friedkin

Chapter 1

Introduction

This chapter introduces some background information on network systems and distributed control. First, a short historical review of complex networks and an introduction of the current status of research are provided. Then, we address the major challenges and open questions that arise from the urgent need for the advancement of mathematical modelings and algorithm designs to meet the distributed requirement, as well as from the advent of the rapid development of social networks. Finally, an outline of this thesis and its main contributions are provided.

1.1 Historical Context

Complex networks represent a class of systems in which nodes represent the constituent entities, and links model their interaction. Examples of such systems range from biological networks, such as genetic pathways, anatomical metabolic networks, and ecological systems, to society and civil engineering, such as the internet, smart power grids, supply chains, water-distribution and transportation systems, and the world trade web, among others.

The investigation of complex networks dates back to the late 1940s and early 1950s and has become a significant multidisciplinary field of research with contributions from mathematics, informatics, physics, and computer science, as well as social science, biology, and other theoretical and applied sciences (see [Bar16] for the historical review). Studies in network science have mainly concentrated on modeling, evaluating, and decomposing network representations of natural phenomena to provide a deeper understanding of the underlying systems [WS98; BA99; New00]. However, there have been few investigations of the various types of dynamical processes evolving on the networks.

The 20th century witnessed a fundamental tendency toward filling the gap between complex network analysis and system and control theory. To a certain degree, this is a consequence of the advancement in sensing and communication technology, the progress in distributed theory in system analysis, control synthesis and algorithm design, and the strong imbalance between limited computational and communication resources and a massive increase in the volume of information. This requires the development of mathematical dynamic models and systematic analysis techniques that transcend the conventional theory applied to complex networks. This trend also gave birth to the network system analysis, an emerging interdisciplinary branch of network science.

Network (or networked) systems represent a class of dynamical systems whose dynamics evolve on a set of nodes in a network and where the interplay between the dynamics occurs at the network's edges [PG16]. So, what is the exact relationship between network systems and complex networks? Unfortunately, no precise definition exists, although scientists from diverse backgrounds have been trying to explain this. All the same, network system research differs, to a certain extent, from most literature found on complex networks. For instance, the traditional robustness studies in complex networks concern the ability of the network to maintain its original structure and the connectedness of the underpinning graph under node/edge failures. The robustness of network systems measures how well a dynamical system embedded in a network behaves in the presence of internal model uncertainty and external random disturbance. For some "simple" dynamical processes [YSL15; YSL16], those two concepts of robustness coincide and can be assessed through a unified measure, the *Kirchhoff index* [ESM+11]. However, the existence of a unique metric simultaneously reflecting both functional and structural robustness is not available for the generic case. Moreover, work in complex networks has paid considerably less attention to the problem of network controllability, which examines under what conditions the dynamics of network systems can be steered from arbitrary states to any desired state within a finite amount of time [LSB11]. Consequently, much follow-up literature has renewed classical control theory content in the context of complex networks, including edge controllability [NV12], network observability [LSB13], and network reachability [LSB13]. An intense scientific debate about this distinction is occurring in the realm of social network analysis [PT17; PT18]. Traditional studies of social networks focus mainly on topological properties to denote a structure, constituted by social actors (individuals or organizations) and their social ties, while the application of control theory to social networks concerns the development of dynamical models to describe social processes over networks and mathematical armamentaria for theoretical analysis. In other words, scientists from the systems and control community consider dynamical processes (namely, opinion dynamics) over a social network rather than the network itself.

Without providing a definite resolution of this argument, we emphasize that this thesis is written by researchers from the systems and control community. Hence, following the mainstream philosophy of most control theorists, the research of complex networks focuses on their topological dynamics, where prominent examples include the formation of small-world [WS98] and scale-free networks [BA99], while the research of network systems concerns the dynamics of networks, whose related problems involve opinion formation [PT17], synchronization of phase oscillators [DB14], and epidemic spreading [NPP16]. Despite their strong interrelation and potential cross-fertilization, most research achievements from two fields are derived almost independently in network science.

1.2 Distributed Control on Coevolutionary Networks

The number of constituent subsystems of a network system varies from hundreds of entities of smart-sensor networks to millions of individuals in social networks and billions of neurons in the human brain. These subsystems are typically spread over a broad

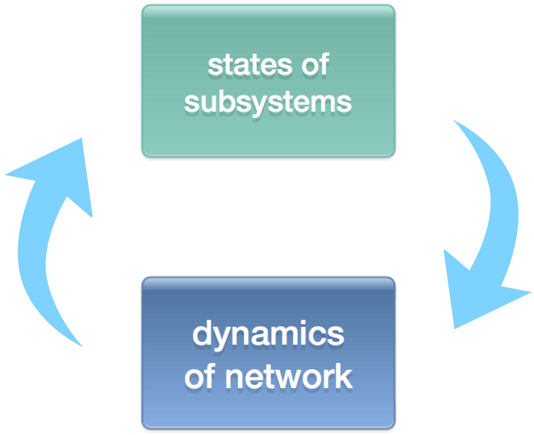

Figure 1.1: A schematic representation of a coevolutionary network which has a feedback loop between the dynamics of the interaction network and the states of the dynamical subsystems.

area, making collective decision-making challenging without a centralized controller to access all the network information. Numerous research efforts have been devoted to developing distributed methods for system analysis [RC11], control synthesis[RB08], and optimization problems [Ned15]. The underlying principle of the distributed fashion is the nearest-neighbor rule. For instance, in distributed system analysis [JLM03; OSM04], individual entities interact with nearby agents that are physically accessible or communicative. Methods to design distributed control laws use local model information shared among neighbors [DMUH15]. To optimize a system of multiple agents embedded in a communication network, distributed algorithms aim to make each agent aware of (and communicate with) its local neighbors only [Ned15].

Most existing results for distributed applications consider that the interaction structure of network systems remains unchanged over time, or that the temporal aspect of networks can be neglected for practical purposes. Unfortunately, the dynamics describing the interaction topology are often time-varying or state-dependent. There has been much interest in the systems and control community in the study of the dynamics of networks from several directions [Mes05; KM06; BHT09; MT14; DLR15; HO16]. However, little progress has been made to theoretically explore the relationship between network evolution and states of dynamical processes over it.

Recent developments in social networks point to a coevolving phenomenon between the topology of interactions and the dynamics of node performance [Laz01; MCP+13]. On the one hand, individuals' opinions are shaped by the interactions of neighbors under social pressure [MB16]. On the other hand, social entities prefer to modify their interconnection relationships based on phenotypic cues [RCW16]; namely, the tendency to form new social ties with others of similar groups (homophily) or diverse types (heterophily). As shown in Figure 1.1, this finding establishes a feedback loop between the dynamics of system networks and the states of constituent subsystems. Networks that possess such a feedback loop are called coevolutionary or adaptive networks [GB08].

The study of coevolutionary networks has been a work in progress that lacks an established structure. This thesis is a step toward the application of distributed control design and system analysis to coevolutionary networks, which is on the frontier, with limited results. Considering opinion-formation problems in social networks, we commit to provide mathematical models to characterize coevolving properties and algorithmic tools for quantitative and qualitative analysis. In a parallel line of research, the concept of coevolutionary networks stimulates us to reexamine distributed topology design problems, providing a deep understanding of the relationship between distributed computation and topology variation.

1.3 State of the Art

This section introduces research achievements related to the topics of interest in this thesis. They are not presented chronologically but instead divided into three parts by theme.

1.3.1 Opinion Dynamics in Social Networks

Recent years have witnessed a growing interest in the studies of social networks across a broad range of disciplines including sociology, psychology, mathematics, economics, and political sciences [MSLC01; FIA11; Fri15; VPS+16; LMSM17]. Facilitated by recent advancement in analyzing multi-agent systems [ME10] and constructing distributed algorithms [Ned15], social network analysis has attracted considerable attention within the systems and control community in the past decade as well; see [PT17; PT18; PRD18] for an excellent tutorial. Opinion dynamics have always been the prominent focus subject for the multidisciplinary study of dynamical phenomena in social networks [DeG74; FIRT15; RFTI15; VBZ+16]. Social entities share and aggregate thoughts, ideas, feelings, experiences, and observations over social networks, and generate new concepts, trends, and reflections at the same time. Such social activities among humans can also find their similar counterparts in engineered systems, e.g., robot and sensor networks [RC11], and natural communities, e.g., bacteria, neurons, and fireflies [MGTH09]. One central line of research in the modeling of opinion pooling can be traced back to the early influential works of French [Fre56], Harary [Har59], Abelson [Abe64], and DeGroot [DeG74], nowadays known as the French-DeGroot (or DeGroot-type) model for discrete-time systems and Abelson-type model for continuous-time systems. The basis for these models is an empirical observation that individuals update their opinions as a convex combination of their own and neighbors' beliefs; this observation is widely taken as a historical milestone of "cognitive and behavioral algebra" in experimental social psychology [All85]. All afore-cited works are derived by assuming explicitly or implicitly that individuals cooperatively interaction with each other. By using graphs to represent the interaction patterns, such pairwise interactions can be represented by edges of non-negative weights in the graph of the corresponding social network. However, this assumption is not always appropriate since there exist various competition, rebellion, and betrayal in many real-life networks such as Epinions, Slashdot, and WikiElections [FIA11]. Other sources of negative ties include the boomerang effect [AG14] or the individuals' reactance [DS05]. In the graph representation, those antagonistic interrelations appear in the form of negatively weighted edges in the so-called signed graphs [Zas82]. In the past few years, elaboration on investigating opinion forming on signed networks has emerged [Alt12; Alt13]. The settled opinions of individuals on a single issue over coopetitive (cooperative-competitive) networks, may exhibit not only opinion consent, but also other complex outcomes including neutrality, polarization, and separation. *Similar to the classic controllability problem in control theory, we investigate* *polarizability, consensusability, and neutralizability of opinion dynamics on signed graphs in Section 3.1.*

Furthermore, the aforecited literature primarily focuses on understanding the connection between the opinion evolution and the interactions via communication networks. However, the psychological fact shows that social entities, primarily humans, are not absolutely rational and even ordinarily intentional [Tot13]. Moreover, individual diversity has a significant impact on the opinion formulation of social entities. Individuals, who live in the same community, may still have different educational experience, dissenting political views, and contrasting aesthetic standards, substantially affecting their decision making. The existing methods including the gauge transformation [Alt13] and lifting approach [XCJ16] employ the discrete-time DeGroot-type model [DeG74] or the continuous-time Abelson-type model [Abe64], and thus are only valid in the absence of self-dynamics. So there is a great need for constructing an appropriate methodology to study the opinion-forming problem of heterogeneous agents with self-cognition. *In this thesis, a novel mathematical model of opinion dynamics is presented in Chapter 3 that emphasizes the fundamental importance of individuals' dynamical properties on opinion formation.*

The conventional modeling methods of social networks often postulate that a social actor communicates directly with other connected peers. In practice, however, interaction in the form of communication or observation between social actors occurs not directly but rather through some intermediates or a shared environment. An analogy can be found in biological systems [CB06; DMPTH10], where bacteria produce, release, and measure signaling molecules (known as autoinducers) which disseminate in the environment, influencing population coordination and bacterial infection processes. This mechanism, termed *quorum-sensing* transitions [RS10], appears to be "déjà vu" in social science. In reality, aside from actor-to-actor communication, the messages delivered either through the traditional media, e.g., TV, radio, and newspaper, or trendy socio-technical platforms, e.g., blogs, Facebook, and Twitter are also important sources of formulating and changing people's attitudes towards relevant topics. For instance, according to a study of the impact of media bias on US voting [DK07], Fox News, a cable and satellite TV news channel, helps Republicans gain an estimated 3 to 8 percent of additional votes between 1996 and 2000. Meanwhile, media are affected, to different extents, by their audiences and other presses. Nowadays, viewers no longer passively receive messages but may behave proactively. Another significant class of social networks where quorum sensing can take place is the system of governance in which a small deliberative group assembles in a large organization. Those elected or appointed members coming from different interest communities are authorized to deal with issues in particular domains. Real-life examples include committees in universities or enterprises, School Boards in public school districts, Boards of Directors in the organizations, and elected officials and standing policy bodies in the Congress [FJB16]. *Based on the new proposed mathematical model of opinion dynamics, we further examine how media influence shapes public opinions in a quorum-sensing environment as presented in Section 3.2.*

1.3.2 Evolution of Social Influence and Power

In the study of opinion dynamics, it is of particular interest to evaluate *social influence* or *power* of individuals in a collective debate on a given issue. The seminal work of French in the 1950s [Fre56] initiated the investigation of the total (direct and indirect) influence of the individual's initial idea on the final collective opinion outcome. Recently, the focus has been shifted from single-issue opinion forming to opinion evolution over sequences of issues, and in the latter individuals can modify their relative influence structures in response to their evaluations of social power [JMFB15; FJB16]. Such self-modification of the influence network across an issue sequence is rooted in the theory of reflected appraisal [Fri11]. Indeed, the appraisal phenomenon is natural human behavior and is omnipresent in social contexts. The modeling of the coevolution of opinion dynamics and an accompanying self-appraisal mechanism, now known as the DeGroot-Friedkin model [JMFB15], essentially captures the psychological behavior: the status of individuals (assertive advocacy vs. silence, confidence vs. uncertainty, intransigence vs. accommodation) in group discussions is likely to alter adaptively in correspondence to their previously appraised power and influence. Empirical validation of the DeGroot-Friedkin model can then be found in [FJB16]. Furthermore, other research efforts on developing the DeGroot-Friedkin model include relaxation to reducible influence networks [JFB17], extensions to dynamic interaction topology [YLA+18], and distributed modeling in both continuous time [CLB+17] and discrete time [XLJB16]. Aside from the self-esteem mechanism, interpersonal assessment for individuals to cognitively evaluate (positively or negatively) peers in social activities, is another driving force recognized in social psychology [Hei58], as Gecas and Schwalbe have noted [GS83], "... that our self-concepts are formed as reflections of the responses and evaluations of others in our environment." Such interpersonal appraisal mechanism specifies the qualitative and quantitative degrees of the interactive relationships between agents.

In contrast to previous achievements, one of the objectives of this thesis is to address the qualitative and quantitative analysis of social power and self-appraisal mechanism in the presence of interpersonal positive or negative evaluations.

1.3.3 Distributed Topology Design Problems

As the network topology captures salient features of the interaction relationships between subsystems/entities in a network, extensive literature [CP11; XGH14; FLJ14; SSLD15; Lun15] appearing in the last few years is concerned with topology manipulation to enhance network performances including connectivity, robustness, resilience, coherence, controllability, and observability. The works on topology operations including addition/deletion/reallocation split into two lines of research according to the elementary components of networks, i.e., nodes and links. Take controlling topology to mitigate epidemic spreading over networks, as an example. The first line of research specializes in either inoculating [PZE+14] or quarantining [MSMH14] particular individual nodes, making them immunized against the disease and more importantly unable to propagate it. An intimately related problem to nodal operations is the optimal protection resource allocation [XHC+17]. In realistic scenarios, for instance, individuals possessing more resources can afford more doctors or accept better medical treatments. Another research direction concerns link removal [BS11; MSK+11; TPER12; SAPV15] and link relocation [TK12; DYL+15; CA16; BKCM17] to slow virus dissemination.

In general, the node and link operation problems mentioned can be formulated as an optimization problem which is NP-complete and NP-hard [NPP16]. About the computational complexity of problems in systems and control, please refer to the tutorial introduction [BT00]. Although this class of optimization problems is more likely to be solved by brute-force searching all possibility and selecting the best solutions, the computation complexity increases rapidly as the size of networks grows and quickly becomes unfeasible even for some moderate networks. As a result, extensive papers instead look for convex relaxation and heuristic algorithms to approximate the optimal solution. For example, a relaxation method based on semi-definite programming (SDP) [BS11] or its generalization, mixed-integer quadratic constraint programming [DM11], can be applied to tackle this problem, whereas this method does not scale to massive networks. Alternatively, various heuristics based on different network metrics are proposed in literature [HK02; MH07; MSK+11; SMHH11; TPER12]. In addition, a growing body of researchers tends to employ a solution framework based on supermodular/submodular optimization and greed algorithm to pursue a suboptimal or near-optimal solution in polynomial time [CBP14; SS15; SCL16; BM16]. All methods proposed above highly depend on the knowledge of the complete network structure. Unfortunately, the global information of network topology is difficult to access in a large-scale real-world network due to geographical constraints or privacy concerns. As such, distributed methods appear in the recent literature [TK12; XGH14; MK14; GQH18]. Despite using only local topology information, these distributed approaches still fall in the centralized design framework because they need a central entity to make a decision on topology operations.

In this thesis, we are interested in developing distributed algorithms for topology design problems and primarily aim to provide topology manipulation strategies that are itself performed in a fully distributed way in the absence of a central coordinator collecting network information and making decisions.

1.4 Outline and Contributions

The three focal points of this thesis are: (1) distributed opinion dynamics analysis on signed graphs; (2) distributed evaluation of interpersonal social influence along issue sequences; and (3) distributed algorithm design for topology manipulation. At first glance, these three topics could be regarded, to a great extent, as being independent of one another. Nevertheless, we will see in the sequel to this thesis that they are closely related. The second part can be treated, in some sense, as a generic instance of the first because of the paradigm shift from simultaneous opinion-pooling on topics to successive opinion-formation on issues. Furthermore, inspired by the exploration of coevolution between dynamical processes and network topology, an iterative strategy for topological operations is developed in the third part, which fundamentally improves the quality of service in distributed algorithm design.

In the remainder of this section, the major contributions of each chapter are outlined in more detail.

Chapter 2: Background and Related Work

This chapter consists of necessary background information and preliminary knowledge. We present an intuitive example to give a flavor of the two thematic elements of this thesis: signed graphs and coevolution between the dynamics of networks and the states of constituent subsystems. Moreover, we introduce some powerful tools employed in this thesis for modeling and analysis, and we also provide formal definitions and discussions related to the prominent network metrics. Partial discussion in this section is based on [MXH18].

Chapter 3: Opinion Dynamics on Coopetitive Social Networks

In this chapter, we address the problem of opinion dynamics on social networks with cooperative and competitive interactions. Particular emphasis is placed on the joint impact of the dynamical properties of individuals and the interaction topology among them. First, we address the existence problem: whether there exist admissible control rules to form a consensus, polarization, or neutralization of opinions of homogeneous individuals in a large population. Sufficient and/or necessary conditions on polarizability, consensusability, and neutralizability are provided. With consideration of heterogeneity of individuals, we then investigate how the opinion-forming process evolves over social networks under media influence. In this endeavor, a mathematical model of opinion dynamics is introduced, which captures the information-diffusion process under consideration: it uses the community-based network structure and accounts for personalized biases among individuals in social networks. By employing the port-Hamiltonian system theory to analyze the modeled opinion dynamics, we predict how public opinions evolve over time for social entities and find applications in political strategy science. A key technical observation is that as a result of the port-Hamiltonian formulation, the mathematical passivity property of individuals' self-dynamics facilitates the convergence analysis of opinion evolution. We show that public opinions become polarized or neutralized, and investigate how an autocratic media coalition might emerge that ignores public opinions. We also assess the role of interpersonal communication and media exposure, which themselves constitute an important topic in mathematical sociology. The contributions presented in this chapter are based on [ZX16; LXHB18; XHC18a].

Chapter 4: Opinion Dynamics and Self-Appraisal of Social Power on Signed Networks

In this chapter, we investigate opinion-formation problems along with a sequence of issues entangled with the evolution of individuals' social influence. Most related existing work assumes explicitly or implicitly that the interpersonal influence weights are always non-negative; by contrast, we argue that such interpersonal influences can be both positive and negative, especially when subjective self-esteem evolves over time. This more general view is also motivated by the social phenomenon of the coexistence of various contrasting relationships (e.g., friendly/hostile, like/dislike, trust/distrust.) between social entities in real-world social networks. Hence, we propose a mathematical formulation of social power and the evolution of self-appraisal in signed social networks. We focus in particular on identifying the effect of social power on shaping public opinions. By applying classical Lyapunov theory to the tangent bundle, we show the global exponential convergence of the proposed self-appraisal model for almost all appraisal networks. Furthermore, a graph-theoretic interpretation of individuals' influence is provided to expose topologically how individuals allocate their relative importance to others through interaction networks. This interpretation facilitates the extension of obtained results to networks with weaker topological constraints. Finally, we prove the complete dependence of eventual self-appraisal of individuals' social power on the interpersonal appraisal profile. The results in this chapter are based on [LXHB18; XHC18b].

Chapter5: Distributed Topology Operations for Enhancing Network Performance

In this section, we study the topology-design problem in network systems and focus on developing the optimal strategy for link operations concerning specific network measures. First, a distributed-control design method is presented to guarantee robustness of interconnected systems under topological uncertainty. Based on this result, the optimal communication topology is derived from the minimization problem of the $\mathcal{H}_2$ norm. However, this distributed-control design approach depends on the complete information of network topology, hence we develop a distributed topology design method to enhance the connectivity of complex networks in the absence of global details of network topology. Even though the proposed method merely relies on local topology information, the requirement that there exists a central entity for decision-making is a significant obstruction. In response to this problem, a new distributed strategy for link operation is provided, which does not require full knowledge of network topology and a central decision-maker. Apart from its low computational complexity and communication frequency, such a distributed algorithm provides a suboptimal solution which is very close to the real global optimum. The analysis of optimality is discussed from both algebraic and topological perspectives. The results in this chapter are mainly based on the author's own works in [XH13; XGH13; XGH14; XH18a; XH18b].

Chapter6: Conclusions and Outlook

This chapter concludes with a discussion of the results developed in this thesis and an outlook on open problems.

The good thing about science is that it's true whether or not you believe in it.

Neil deGrasse Tyson

Chapter 2

Background and Related Work

The purpose of this chapter is twofold. We first aim at providing the necessary background information and preliminary knowledge for a better understanding of this thesis. The second goal is to get down to the bedrock of this thesis and the precise motivation behind each chapter.

2.1 Consensus Theory

In recent year it has been seen that the so-called linear consensus algorithm is at the heart of many network systems problems. Applications range from biological network analysis such as bird flocking, fish swarming, and firefly synchronization, to social and artificial engineering such as unmanned aerial vehicle formation, truck platooning, and heliostat alignment. In fact, consensus problems have a long history in computer science and are of central importance in the field of distributed computation. The pioneering works studying the distributed computation in systems and control field can be traced back to 80s [BV82; TBA86; BT89]. From the 2000s onwards, the development and advancement in multi-agent systems and social networks have sparked a considerable renewed interest in distributed computation across a broad range of disciplines. Nowadays, the terminology consensus is not only a simple algorithm as it is born but also grows into a systematic theory, playing a key role in the studies of network systems.

A discrete-time linear consensus algorithm is an averaging procedure among n states, which has the representation

$$\boldsymbol{x}(t+1) = \boldsymbol{P}(x)(t) \qquad \Leftrightarrow \qquad x_i(t+1) = \sum_{j=1}^{n} p_{ij} x_j(t), \tag{2.1}$$

where $\boldsymbol{x} = [x_1, \ldots, x_n]^\mathsf{T}$ is a vector of states x_i of nodes and the transition matrix $\boldsymbol{P} = [p_{ij}] \in \mathbb{R}_{\geq 0}^{n\times n}$ is right stochastic, i.e., $\sum_{j=1}^{n} p_{ij} = 1$, for all $i = 1, \ldots, n$. An important feature of this updated law is the fact that each local state evolves iteratively to the relative interior of the convex hull spanned by its past state and the incoming states. This mathematical formulation also appears in opinion dynamics and is referred to as the French–DeGroot model [Fre56; DeG74]. The averaging principle exposes that each individual updates its opinion to a convex combination of its neighbors' and its won at each time step. Due to this convex combination mechanism, a consensus state, where $x_1 = \ldots, = x_n$, is reached asymptotically, and the consensus set is uniformly exponential stable. A continuous counterpart of the consensus model (2.1), is referred to as Abelson's model in social networks [Abe64], is introduced by

$$\dot{\boldsymbol{x}}(t) = -\boldsymbol{L}(x)(t) \qquad \Leftrightarrow \qquad \dot{x}_i(t) = \sum_{j=1, j\neq i}^{n} l_{ij}(x_i(t) - x_j(t)), \tag{2.2}$$

where the semi-positive definite matrix $\boldsymbol{L} \succeq 0$ is a weighted Laplacian, i.e., $l_{ii} = -\sum_{j=1}^{n} l_{ij}$ and has the same sparsity structure as $\boldsymbol{P}$. The differential updated law (2.2) generates $\boldsymbol{P}$ in an infinitesimal manner, i.e., $\mathrm{e}^{-\boldsymbol{L}(t-t_0)}\boldsymbol{x}(t_0) = \boldsymbol{P}^{t-t_0}$ for any $0 \leq t_0 < t$.

The linear consensus algorithm (2.1) admits the useful interpretation of n agents embedded into a weighted directed (communication network) graph[1] $\mathcal{G} = (\mathbb{V}, \mathbb{E}, w(\mathbb{E}))$. Within this graph embedding, each node (or vertex) in $\mathbb{V} = \{1, \ldots, n\}$ indexes one agent, and directed edges $(j, i) \in \mathbb{E} \subseteq \mathbb{V} \times \mathbb{V}$ indicate whether there is a communication link from agent j to agent i. The weighting function $w : \mathbb{E} \to \mathbb{R}_{\leq 0}$ assigns to each communication link a positive value $w((j, i)) = p_{ij} \geq \bar{p} > 0$ if $(j, i) \in \mathbb{E}$, where $\bar{p}$ denotes a constant threshold value. Similarly, the graph for the continuous-time version (2.2) has weights $w((j, i)) = -l_{ij}$ and by that, the components $-l_{ij}$ are intensities expressing the constant rate at which state information is transmitted from agent j to i. With the help of algebraic graph theory, the interpretation as averaging procedure among dynamical agents that interact over a network with structure given by $\mathbb{E}$ yields a wide range of applications. For example, in multi-agent systems [RB08; RC11], to name a few, consensus algorithm has been seen as the pillar of coordination and formation control. In distributed computation and decision making [Ned15], and distributed filtering [MB10], the consensus algorithm is used as network protocols to achieve information diffusion among interacting systems. With development of research in multi-agent systems and wireless communication technology, many new contents, second-order model [RA05], heterogeneous interaction topology [XH13], finite-time convergence [Xia10], switched topologies [XW06], time-delay [OSM04], packet-loss [ZT10], event-triggered control [SDJ13] and nonlinear protocols [HH08], have emerged. Furthermore, while the linear consensus algorithm is usually defined on Euclidean space, important generalizations to a consensus on nonlinear space have been made, see for instance [Sep11] for an overview. Applications have been seen in many scientific disciplines such as in physical chemistry or biology (see for instance [SRJ16]), in neuroscience (see for example [BHD10]), and in electric power systems (see [DB14] and reference therein), etc.

Among others, consensus on general functions [Cor08] is of great interest to illustrate how the dynamics of nodes influence the interconnection structure of a network. Consider a consensus protocol

$$\dot{x}_i(t) = \sum_{j=1, j\neq i}^{n} l_{ij}(h(x_i) - h(x_j)), \tag{2.3}$$

[1] For a short introduction to the relevant notations and concepts of graph theory for this thesis, please see Section A.1.

where h is an increasing function e.g., $\ln(x)$, e^x, x^q with $q>0$, on the different domain of definition [MXH18]. The consensus algorithm (2.3) in stack vector form can be given by

$$\dot{\boldsymbol{x}}(t) = -\boldsymbol{K}(\boldsymbol{x})\boldsymbol{x}(t), \qquad [\boldsymbol{K}]_{ij} := \begin{cases} l_{ij}\frac{h(x_j)-h(x_i)}{x_j-x_i}, & \text{if } \ j \neq i, \\ \sum_{k\neq i}[\boldsymbol{K}]_{ik}, & \text{if } \ j = i, i \in \mathbb{V}, \end{cases} \tag{2.4}$$

where $\boldsymbol{K}$ is a weighted Laplacian of a "virtual" graph with non-negative finite entries and non-trivial branch. More importantly, the transformation from a non-linear time-variant network protocol to a linear time-varying consensus form give an insight into the coupling relation between the dynamics of nodes and networks. On the one hand, the adjacent interconnections in the network influence the states of nodes and, on the other hand, they continuously change their interaction along the time scale. The feedback loop between the topology of interactions and the states of the nodes provides an intuitive instance of the concept of coevolutionary network. This coevolving phenomenon motivates us to review the studies of opinion dynamics in social networks and topology design problems in complex networks.

Apart from interdependence relation of the dynamics of the network and individuals' states, consensus algorithms on signed graphs[2] also spark extensive interest researchers in the field of social networks [Alt13], multi-agent systems [YCFC18] and power grids [CWL+16]. On a signed graph, the weights of edges are allowed to be negative, and thereby the coexistence of positively and negatively weighted links is typical, e.g., the friend/foe, dislike/like and trust/distrust relationship between individuals in social networks, and the attractive and repulsive force interactions in physical systems.

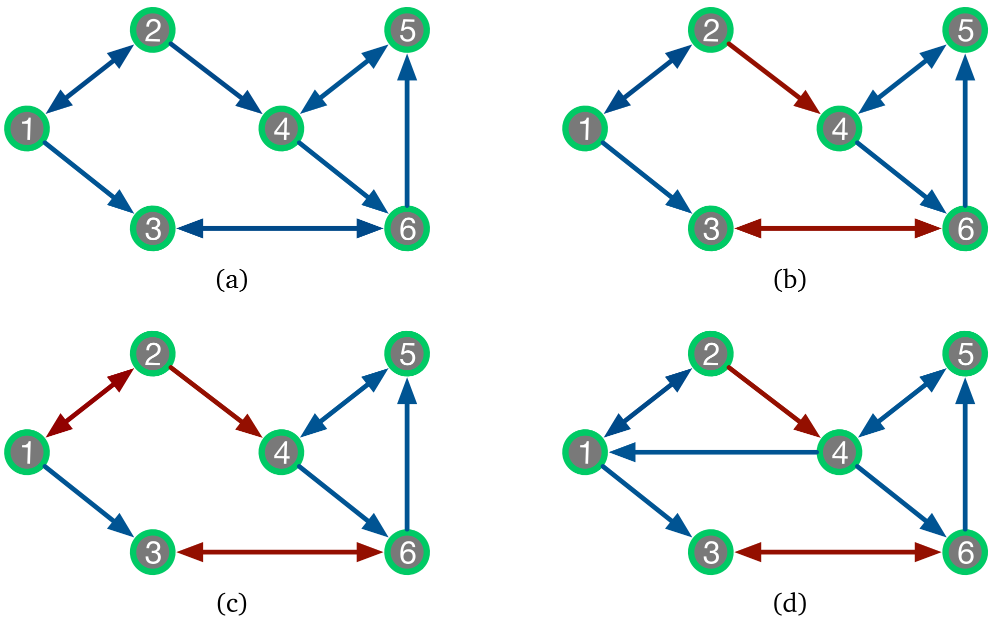

Figure 2.1: Directed signed graphs: weights associated to arrowed lines (positive couplings in blue and negative in red).

We present here some illustrative examples to give a flavor of the consensus problems on signed graphs. Consider the linear consensus protocol (2.2) evolving on the directed

[2] For more details on the signed graph, please refer to Section A.1.3

signed graphs shown in Figure 3.3 where each graph may or may not contain edges with negatively signed weighted and all graphs are strongly connected. It is well-known that consensus can be achieved asymptotically on an unsigned network if the underlying graph is strongly connected, as shown in Figure 2.2a. By observing Figure 2.2b and Figure 2.2c, consensus dynamics over signed graphs, rarely exhibit unanimous behavior, specifically conformity, due to the coexistence of positive and negative weights on edges. Even though the states of nodes in Figures 2.2d converge eventually to a common value, it is a trivial case, regardless of initial conditions. Those new state separation has motivated us to study the dynamical processes when the network contains links with negative weights, serving as a starting point for Chapter 3 and Chapter 4

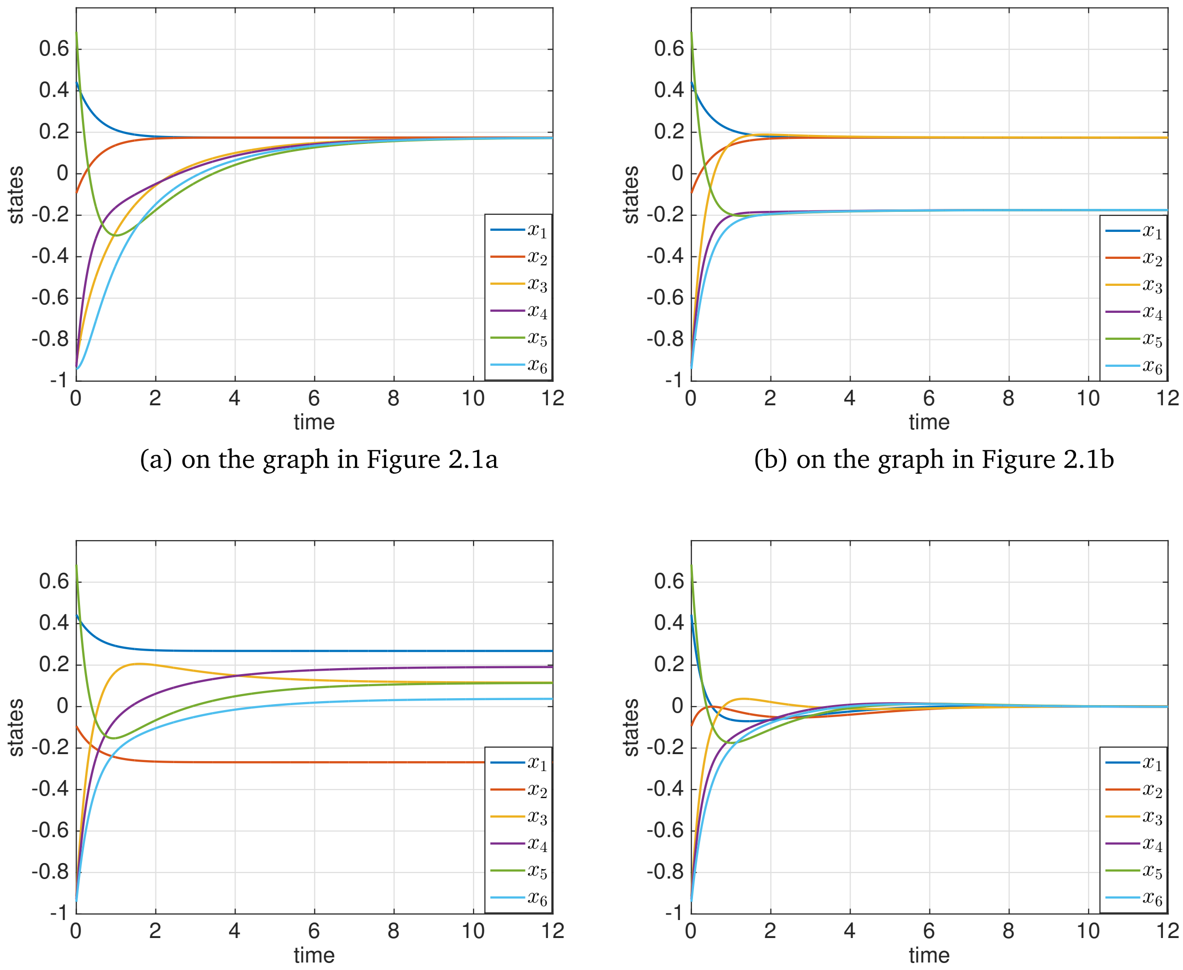

(a) on the graph in Figure 2.1a

(b) on the graph in Figure 2.1b

(c) on the graph in Figure 2.1c

(d) on the graph in Figure 2.1d

Figure 2.2: Evolution of inidivudals' states on signed graphs.

2.2 Preliminaries on Modeling and Analysis Approaches for Network Systems

In this section, we present a sketch of differential Lyapunov theory and port-Hamiltonian approach, both playing an important role in modeling and analysis of network systems in this thesis.

2.2.1 Incremental Stability Analysis and Contraction Theory

Lyapunov's second method or the method of Lyapunov functions, though developed in the late 19th century, serves as one of the most fundamental tools in the study of deterministic differential equations. The technique facilitates to examine the stability of a dynamical system independent of a detailed ODE representation. Same as other stability criteria, the Lyapunov theory of nonlinear systems is conventionally regarded relative to some nominal reference or equilibrium point. It is well known that a nonlinear system may have multiple equilibrium points and hence investing the stability of such a system can only be addressed concerning a certain equilibrium point. Only when the equilibrium point is unique, the global stability may take in consideration, which is a significant difference between linear and nonlinear dynamics regarding stability. However, there are many engineering problems of interest such as so-called "tracking" and "regulation" problems, for which not all equilibrium points or reference trajectories are easy to find. Frequently, one may be interested not in the stability of trajectories concerning a particular attractor, but rather the stability of trajectories in reference to one another, which is another aspect to distinguish linear and nonlinear systems in the analysis of stability. For linear systems, these two concepts coincide with each other, but the latter is indeed much stronger in the nonlinear case.

Works along the study of "relative stability" of trajectories split commonly into two lines: differential and integral framework [SPB14]. The former often termed *contraction theory* [LS98] rooting in continuum mechanics and differential geometry focuses on analyzing the dynamical behavior of a "virtual displacement" between two infinitesimally separated trajectories. Intuitively, a system is stable in some region if initial conditions or temporary disturbances are "forgotten" in some sense, namely if the ultimate behavior of the system is irrelevant to the initial conditions. In the context of the integral approach to the relative stability of trajectories, incremental stability relies on seeking an appropriate incremental Lyapunov function [Ang02]. Rather than with a single fixed trajectory, the word incremental implies the fact that solutions of dynamical systems are compared with one another.

Contraction theory and incremental stability have fueled the research activities in the field of power systems [SS07], robot control [CS09], and social networks [YLA+18]. Nevertheless, very little progress has been made on connecting contraction analysis to Lyapunov theory. Only very recently in the context of Finsler geometry, the authors of [FS14] make a step toward filling this gap. For more details on contraction theory, incremental stability, and other relevant notions, we refer the interested readers to the afore-cited literature and reference therein. In what follows, we introduce a discrete-time counterpart of the differential Lyapunov theory, which enables us to conduct convergence and stability analysis in Chapter 4.

Consider a manifold $\mathbb{X}^n$ and a deterministic discrete-time nonlinear system described by the difference equation

$$\boldsymbol{x}(t+1)=\boldsymbol{f}(\boldsymbol{x},t), \quad \text{and } \boldsymbol{x}(0):=\boldsymbol{x}_0\in\mathbb{X}^n \tag{2.5}$$

where $\boldsymbol{f}:\mathbb{X}^n\times\mathbb{R}\to\mathbb{X}^n$ is continuously differentiable. Let $\boldsymbol{\phi}(\cdot;t_0,\boldsymbol{x}_0)$ be the semi-flow of the system (2.5) starting from the initial condition $\boldsymbol{x}_0\in\mathbb{X}^n$ at time t_0, i.e., $\boldsymbol{\phi}(t_0;t_0,\boldsymbol{x}_0)=\boldsymbol{x}_0$. Following [FS14], we consider *forward invariant* and *connected* subset $\mathbb{M}^n\subset\mathbb{X}^n$ for (2.5), on which $\boldsymbol{\phi}(t;t_0,\boldsymbol{x}_0)$ is *forward complete* for every $\boldsymbol{x}_0\in\mathbb{M}^n$.

To make this chapter self-contained, we recall the definition of incremental stability.

Definition 2.1. Consider the nonlinear system (2.5) on a given manifold $\mathbb{X}^n$. Let $\mathbb{M}^n\subset\mathbb{X}^n$ be a connected and forward invariant set and $\mathrm{d}_{\mathbb{X}}:\mathbb{X}^n\times\mathbb{X}^n\to\mathbb{R}$ be a continuous distance metric[3] on $\mathbb{X}^n$. The system (2.5) is

(i) *incrementally stable* (IS) on $\mathbb{M}^n$ with respect to $\mathrm{d}_{\mathbb{X}}$ if there exists a function α of $\mathcal{K}$ class[4] such that for all $\boldsymbol{x}_1,\boldsymbol{x}_2\in\mathbb{M}^n$ and $t\geq t_0\in\mathbb{R}$, there is

$$\mathrm{d}_{\mathbb{X}}(\boldsymbol{\phi}(t;t_0,\boldsymbol{x}_1),\boldsymbol{\phi}(t;t_0,\boldsymbol{x}_2))\leq\alpha\big(\mathrm{d}_{\mathbb{X}}(\boldsymbol{x}_1,\boldsymbol{x}_2)\big);$$

(ii) *incrementally asymptotically stable* (IAS) on $\mathbb{M}^n$ if it is incrementally stable and for all $\boldsymbol{x}_1,\boldsymbol{x}_2\in\mathbb{M}^n$ and $t_0\in\mathbb{R}$, there is

$$\lim_{t\to\infty}\mathrm{d}_{\mathbb{X}}(\boldsymbol{\phi}(t;t_0,\boldsymbol{x}_1),\boldsymbol{\phi}(t;t_0,\boldsymbol{x}_2))=0;$$

(iii) *incrementally exponentially stable* (IES) on $\mathbb{M}^n$ if there exist scalars $c_1\geq 1$, and $1>c_2>0$ such that for all $\boldsymbol{x}_1,\boldsymbol{x}_2\in\mathbb{M}^n$ and $t\geq t_0\in\mathbb{R}$, one has

$$\mathrm{d}_{\mathbb{X}}\big(\boldsymbol{\phi}(t;t_0,\boldsymbol{x}_1),\boldsymbol{\phi}(t;t_0,\boldsymbol{x}_2)\big)\leq c_1c_2^{t-t_0}\mathrm{d}_{\mathbb{X}}(\boldsymbol{x}_1,\boldsymbol{x}_2).$$

In general, one can associate a *variational system* to the system of form (2.5) by

$$\delta\boldsymbol{x}(t+1)=\frac{\partial\boldsymbol{f}(\boldsymbol{x},t)}{\partial\boldsymbol{x}}\delta\boldsymbol{x}(t), \tag{2.6}$$

where $\delta\boldsymbol{x}(t):\mathbb{R}\to T_{\boldsymbol{x}}\mathbb{X}^n$ represents a *virtual displacement*. The combination of (2.5) and (2.6) is referred to as the *prolonged system* [FSS13].

Before embarking on the main results, the following Finsler geometry is important in the deduction of the discrete-time differential Lyapunov theorem for contraction analysis.

Definition 2.2. A *Finsler* structure $F(\boldsymbol{x},\delta\boldsymbol{x})\in T\mathbb{X}^n\to\mathbb{R}_{\geq0}$ on manifold $\mathbb{X}^n$ satisfies the following conditions:

(i) F is a smooth function on $T\mathbb{X}^n\backslash\{\mathbf{0}\}$;

(ii) $F(\boldsymbol{x},\delta\boldsymbol{x})\geq0$ where the equality holds iff $\delta\boldsymbol{x}=\mathbf{0}$;

---

[3] Given a manifold $\mathbb{X}^n$, a function $\mathrm{d}:\mathbb{X}^n\times\mathbb{X}^n\to\mathbb{R}$ is said to be a *metric* or *distance* function on $\mathbb{X}^n$ if it satisfies $\mathrm{d}(\boldsymbol{x}_1,\boldsymbol{x}_2)=\mathrm{d}(\boldsymbol{x}_2,\boldsymbol{x}_1)$ (symmetry), $\mathrm{d}(\boldsymbol{x}_1,\boldsymbol{x}_2)>0$ when $\boldsymbol{x}_1\neq\boldsymbol{x}_2$ (positivity), $\mathrm{d}(\boldsymbol{x}_1,\boldsymbol{x}_2)=0$ when $\boldsymbol{x}_1=\boldsymbol{x}_2$ (non-degeneracy), and $\mathrm{d}(\boldsymbol{x}_1,\boldsymbol{x}_2)+\mathrm{d}(\boldsymbol{x}_2,\boldsymbol{x}_3)\geq\mathrm{d}(\boldsymbol{x}_1,\boldsymbol{x}_3)$ (triangle-inequality), for all $\boldsymbol{x}_1,\boldsymbol{x}_2,\boldsymbol{x}_3$

[4] The a function $\alpha:\mathbb{R}_{\geq0}\to\mathbb{R}_{\geq0}$ belong to $\mathcal{K}$ class means it is continuous, strictly increasing, and has $\alpha(0)=0$.

(iii) $F(\boldsymbol{x}, c\,\boldsymbol{\delta x}) = c\,F(\boldsymbol{x}, \boldsymbol{\delta x})$ on $T\mathbb{X}^n$ for $c \geq 0$;

(iv) $F(\boldsymbol{x}, \boldsymbol{\delta x}_1 + \boldsymbol{\delta x}_2) < F(\boldsymbol{x}, \boldsymbol{\delta x}_1) + F(\boldsymbol{x}, \boldsymbol{\delta x}_2)$ for $\boldsymbol{\delta x}_1 \neq \boldsymbol{\delta x}_2$.

The development of the Finsler structure in the tangent bundle enables us to induce a well-defined distance on $\mathbb{X}^n$

$$\mathrm{d}_{\mathbb{X}}(\boldsymbol{x}_1, \boldsymbol{x}_2) := \inf_{\Gamma(\boldsymbol{x}_1, \boldsymbol{x}_2)} \int_0^1 F(\gamma(s), \dot{\gamma}(s))ds, \tag{2.7}$$

where $\gamma : [0,1] \to \mathbb{X}^n$ is a curve on $\mathbb{X}^n$ satisfying $\gamma(0) = \boldsymbol{x}_1$, $\gamma(1) = \boldsymbol{x}_2$, and $\Gamma(\boldsymbol{x}_1, \boldsymbol{x}_2)$ is the collection of those piecewise continuous curves.

Theorem 2.1: Discrete-time Differential Lyapunov theorem for Contraction Analysis

Consider the system (2.5) on a smooth manifold $\mathbb{X}^n$ with a continuously differentiable vector-valued function $\boldsymbol{f}$ in a connected and positively invariant set $\mathbb{M} \subset \mathbb{X}^n$. If there exist a Finsler structure $F(\boldsymbol{x}, \boldsymbol{\delta x}) \in T\mathbb{X}^n \to \mathbb{R}_{\geq 0}$, a function $\alpha : \mathbb{R}_{\geq 0} \to \mathbb{R}_{\geq 0}$, scalars $c_1, c_2 \in \mathbb{R}_{\geq 0}$, $l \in \mathbb{R}_{\geq 1}$ and a candidate Lipschitz continuous Lyapunov function $V(\boldsymbol{x}, \boldsymbol{\delta x}) \in T\mathbb{X}^n \to \mathbb{R}_{\geq 0}$, such that, in coordinates,

$$\begin{aligned} &c_1 F\big(\boldsymbol{x}(t), \boldsymbol{\delta x}(t)\big)^l \leq V\big(\boldsymbol{x}(t), \boldsymbol{\delta x}(t)\big) \leq c_2 F\big(\boldsymbol{x}(t), \boldsymbol{\delta x}(t)\big)^l \\ &V\big(\boldsymbol{x}(t+1), \boldsymbol{\delta x}(t+1)\big) - V\big(\boldsymbol{x}(t), \boldsymbol{\delta x}(t)\big) \leq -\alpha\Big(V\big(\boldsymbol{x}(t), \boldsymbol{\delta x}(t)\big)\Big) \end{aligned} \tag{2.8}$$

for $t \in \mathbb{R}_{\geq 0}$, $\boldsymbol{x} \in \mathbb{M}^n \subset \mathbb{X}^n$, and $\boldsymbol{\delta x} \in T_{\boldsymbol{x}}\mathbb{X}^n$, then system (2.5) is

(i) IS on $\mathbb{M}^n$ if $\alpha(V) = 0$ for each $V \in \mathbb{R}_{\geq 0}$;

(ii) IAS on $\mathbb{M}^n$ if α is a function of $\mathcal{K}$ class;

(iii) IES on $\mathbb{M}^n$ if $\alpha(V) = c_3 V > 0$ for $c_3 \in \mathbb{R}_{>0}$ and each $V \in \mathbb{R}_{\geq 0}$.

Moreover, if condition (2.8) is satisfied for some function α of class $\mathcal{K}$, then we say that the function V is the contraction measure and is contracted by the system (2.5) on the contraction $\mathbb{M}$.

Proof. Bearing the way of extending contraction analysis to a discrete-time setting in mind, see, e.g., [TRK16], this proof follows along the same step as in the proof of Theorem 1 in [FS14] and thus, the details are omitted. □

2.2.2 Port-Hamiltonian Representation of Network Systems

The port-Hamiltonian approach has been recognized as one of the most fundamental network-systematic tools in modeling, regulation, and optimization; see [vdS14] for a nice literature review. A prominent merit of the port-Hamiltonian formalism is that it underscores the physics of the systems by exposing the relationship between the energy (information) storage, dissipation, and interconnection structure. Furthermore, port-Hamiltonian systems are modular, which means that a power-preserving interconnection between port-Hamiltonian subsystems leads to another port-Hamiltonian system with composite energy (information) storage, dissipation, and interconnection structure.

Consider an input-output dynamical system

$$\dot{\boldsymbol{x}}(t) = \boldsymbol{f}(\boldsymbol{x}) + \boldsymbol{g}(\boldsymbol{x})\boldsymbol{u}(t), \quad \boldsymbol{y} = \boldsymbol{h}(\boldsymbol{x}) \tag{2.9}$$

where $\boldsymbol{x} \in \mathbb{R}^{n_x}$, $\boldsymbol{u} \in \mathbb{R}^{n_u}$ and $\boldsymbol{y} \in \mathbb{R}^{n_y}$ are the state, control input and output, respectively. Let $\boldsymbol{f}, \boldsymbol{g}$ be locally Lipschitz and $\boldsymbol{h}$ be continuous, satisfying $\boldsymbol{f}(0) = 0$, $\boldsymbol{g}(0) = 0$ and $\boldsymbol{h}(0) = 0$. Consequently, the solution to the system (2.9) is unique for any locally bounded input u and the initial condition $\boldsymbol{x}(0) \in \mathbb{R}^{n_x}$.

We say the system (2.9) admits a port-Hamiltonian representation (in a generalized sense) if there exist $n_x \times n_x$ matrices $\boldsymbol{J}(\boldsymbol{x})$, $\boldsymbol{R}(\boldsymbol{x})$ satisfying $\boldsymbol{J}(\boldsymbol{x}) = -\boldsymbol{J}^\top(\boldsymbol{x})$ and $\boldsymbol{R}(\boldsymbol{x}) = \boldsymbol{R}^\top(\boldsymbol{x}) \succeq 0$, and a smooth function $S(\boldsymbol{x})$, called Hamiltonian, such that (2.9) can be rewritten in the form

$$\dot{\boldsymbol{x}}(t) = (\boldsymbol{J}(\boldsymbol{x}) - \boldsymbol{R}(\boldsymbol{x}))\frac{\partial S}{\partial \boldsymbol{x}}(\boldsymbol{x}) + \boldsymbol{g}(\boldsymbol{x})\boldsymbol{u}, \quad \boldsymbol{y} = \boldsymbol{g}^\top(\boldsymbol{x})\frac{\partial S}{\partial \boldsymbol{x}}(\boldsymbol{x}). \tag{2.10}$$

An appealing feature of the port-Hamiltonian system is the passivity property when $S \geq 0$, namely

$$\dot{S}(\boldsymbol{x}) = -\frac{\partial S^\top}{\partial \boldsymbol{x}}\boldsymbol{R}(\boldsymbol{x})\frac{\partial S^\top}{\partial \boldsymbol{x}} + \frac{\partial S^\top}{\partial \boldsymbol{x}}\boldsymbol{g}(\boldsymbol{x})\boldsymbol{u} \leq \boldsymbol{y}^\top \boldsymbol{u}.$$

We call system (2.9) with the passivity property a port-controlled Hamiltonian (PCH) system, denoted by $(\boldsymbol{J}, \boldsymbol{R}, S)$.

Application areas of port-Hamiltonian approach to modeling and analysis have increased sharply as the emerging topics have proliferated, and now include power grids [FOSS13], chemical reaction networks [SSS14], consensus and coordination controls [SM13], physically network systems [vdS17], optimal and stochastic control theory [DS14], etc. As one will see in Chapter 3, the intrinsic passivity property facilitates the convergence analysis of opinion dynamics admitting port-Hamiltonian representation. More importantly, the port-Hamiltonian system theory might provide a key basis for getting an insight into how agents behave confronting a massive body of external influences.

2.3 An Introductory Overview of Network Metrics

Complex networks or networks in a general context, capture the topology structure for a wide range of chemical, mechanical and civil engineering, biological or social systems. Over the last 80 years, a steady stream of research efforts has been devoted to investigating the performance of complex networks in the field of network science, resulting in various follow-up indices evaluating the network quality.

Among other performances, the network connectivity is of paramount interest, which measures how well a network is connected. A plenty measures arisen from different contexts have been introduced to examine qualitatively and quantitatively the connectivity of networks including the vertices (edge) connectivity which amounts to the minimum number of vertices (edges) whose removal makes network disconnected. Another remarkable metric to quantify the connectivity of a network is the second smallest (the first nonzero) eigenvalue of the Laplacian matrix, also well known as the algebraic connectivity which was introduced by Fiedler in his seminal paper [Fie73]. In addition to unfolding the variation of network connectivity sensitively in contrast to vertex- and edge-connectivity, algebraic connectivity is closely related to the convergence speed of distributed computation algorithm and information diffusion processes over networks. It is, however, of no help in a disconnected graph, thus necessitating the appearance of the so-called natural connectivity [JBYJZ10] which is given by the logarithm of the average Estrada index of the network [EH08]. The natural connectivity indeed mirrors strong discrimination in measuring the connectivity of complex networks, even for disconnected graphs. A general notion of natural connectivity taking its origin in statistical physics, as known as communicability [EHB12], quantifies how "easy" to deliver a message from one node to one another. Thanks to its clear physical meaning, communicability has been widely used to measure the robustness or resilience networks against the loss of links and nodes. Another popular notion closely related to communicability is the so-called centrality which focuses on identifying the most "important" nodes in a network. There is a massive body of centrality metrics with different definitions for recognizing important nodes in a network, such as degree- [AJB10], betweenness- [Bar04], closeness- [KK10] and motif-centrality [WLY14]. Due to the application in Google's PageRank algorithm [BP98] and community detection [For10], eigenvector centrality using the dominant eigenvector of graph adjacency matrix attracts widespread attention and serves as a prime measure that identifies the critical nodes in a network [CL12]. Commonly, nodal criticality is analogous to node centrality, a concomitant of which is the edge centrality measuring the most important edges in a graph. Other notions of network performance include vulnerability [RMD15], lethality [JMBO01], and structural robustness [Bar16], etc. These network performances and their associated metrics usually overlap, more or less, with one another.

Nowadays, fundamental questions about network performance are mainly concerned with the following aspects.

- From an algebraic point of view, the problem to identify these measures of networks performance is generally NP-hard [MSK+11] or NP-complete [KKM97]. Moreover, since many real-life networks consist of millions or even billions of edges/nodes, they commonly do not possess a center for gathering the complete network information. This urges the need for the development of novel distributed algorithms that go beyond the existing algorithms designed in a centralized manner [GVJ12; LQ13; BM13; LB14; Ned15]. Additionally, various malicious attacks and natural disasters make networks in practice liable to be disconnected, thus necessitating the development of new performance indices that apply to this scenario, such as subgraph centrality [ERV05] and local natural connectivity [Sha11].

- The past decade has witnessed a burgeoning interest in reconsidering the traditional measure and spawning new network metrics from a control-theoretical perspective. Many control theorists commit themselves to this recent branch of research and bring about miscellaneous network metrics including the extensions of traditional concepts in control theory to network science, such as controllability [LSB11] with a vast applications to multi-agent systems [NWX13; LFJ14], observability [LSB13], reachability [ZC16] and functional robustness [YSC+13], and the emergence of new metrics in order to meet the distributed requirement, such as information centrality [PYSL16] and coherence [SSLD15].

- With the advent of wire or wireless communication, the sharp separation between complex network and communication technology has been questioned, and a growing number of the dedicated literature focus on filling this gap. Despite its evident benefits arising in many network applications, the introduction of communication technology for transmitting information between spatially distributed entities in networks, spurs the scientists to consider the emerging contents network such as security [CDH+16] and privacy-preservation [ZGP13], beyond the traditional network performance.

Towards this end, Chapter 5 address the endeavor for enhancing network performance by conducting network topology manipulation in a distributed fashion.

Since universal ultimate agreement is an ubiquitous outcome of a very broad class of mathematical models, we are naturally led to inquire what on earth one must assume in order to generate the bimodal outcomes of community cleavage studies.

Robert P. Abelson

Chapter 3

Opinion Dynamics on Coopetitive Social Networks

This chapter studies the opinion formation problems on social networks with coopetitive (cooperative-competitive) interrelationships of a group of individuals. Distinct from many other processes on cooperative networks, opinion dynamics rarely exhibit unanimous behavior, specifically consensus, due to the possible existence of antagonistic interactions among the group members. Consequently, collective behaviors of opinion discussion in coopetitive networks may result in clustering wherein polarity that the opinions oppositely separate is of significant interests in social activities. Meanwhile, the neutrality that people turn to keep neutral also stands for a substantial instance case in political and commercial negotiations, urging the need for scrupulous studies. Until now, the existing mathematical models describing opinion dynamics primarily characterize what network structure leads to different dynamical behaviors of opinion formation. In this section, we introduce a new opinion-forming model specifying the thematic diversification of individuals' self-dynamics and the interaction structures among them in the process of opinion discussion.

Our first concern addresses the fundamental question: Under what conditions, there exists certain kind of distributed protocols such that the opinion dynamics over networks are consensus, polarized, and neutralized, respectively. Therefore, sufficient and/or necessary conditions on consensusability, polarizability, and neutralizability are provided.

Then we elaborate on how opinions evolve under the exogenous influence. Its importance lies in the fact that individuals can access, more or less, to pervasive mass and electronic media in their surrounding social context. Motivated by the market segmentation and business concentration in media industries, we analyze the evolutionary properties of the developed model for opinion dynamics at the level of community architectures. By employing the port-Hamiltonian (PH) formulation to represent the opinion dynamics, we can gain insight into how agents behave confronting a massive body of external information sources. In connection with the concept "*internalization*" in psychological and sociological studies [You16], the port-Hamiltonian formulation explains how the inward information or messages flow through social entities without relying on detailed descriptions of social psychology. Moreover, the convergence analysis follows naturally from the PH representation, underlining the joint impact of local dynamic natures and topological properties on shaping public opinion. Besides, the sociological postulate "iron law of oligarchy" [Mic15] motivates our further investigation on how media control the opinion-pooling process in an autocratic context. From a control-theoretic perspective, we explore the intrinsic mechanisms and ruling strategies of dominant groups manipulating outcomes of social systems. Thus, our developments may open up avenues for policy intervention or prevention.

This chapter is organized as follows. The accessibility problems of opinion dynamics are first investigated in Section 3.1. Section 3.2 examines the formation of heterogeneous individuals' opinions in the presence of interpersonal communication and media exposure. A short overview of relevant literature and the conclusion of this chapter are given in Section 3.3 and Section 3.4, respectively.

3.1 Modulus Consensusabililty of Opinion Dynamics on Signed Networks

Before embarking on designing a consensus/polarization/neturalization opinion protocol, it is essential to address the existence question: whether or not there exists the possibility to make the opinion dynamics consensusalized/polarized/neutralized.

3.1.1 Problem Formulation

Consider a network of $n \geq 2$ individuals described by a signed graph $\mathcal{G} = (\mathbb{V}, \mathbb{E}, \boldsymbol{A})$ associated with a signed Laplacian $\boldsymbol{L} \in \mathbb{R}^{n\times n}$. Each individual i is associated with a vector $\boldsymbol{x}_i \in \mathbb{R}^{n_x}$ that represents its opinions on n_x different subjects. In the chapter, we focus on continuous-value opinions like the degree of preference to issues or the tendency to change thoughts: sign qualifies the current belief tendency -positive for support, negative for protest and zero for neutrality-, and modulus quantifies the magnitude. The time-evolution of the opinion vector $\boldsymbol{x}_i$ obeys the linear time-invariant (LTI) dynamics

$$\dot{\boldsymbol{x}}_i(t) = \boldsymbol{F}\boldsymbol{x}_i(t) + \boldsymbol{G}\boldsymbol{u}_i(t), \quad i \in \mathbb{V}, \tag{3.1}$$

where $\boldsymbol{u}_i \in \mathbb{R}^{n_u}$ is the control input of individual i. The state matrix $\boldsymbol{F} \in \mathbb{R}^{n_x \times n_x}$ characterizes the level of "anchorage" on their topic-specific opinions, which has been formed by some exogenous conditions, e.g., the past social experience, or endogenous factors, e.g., personal intelligence and character. The input matrix $\boldsymbol{G} \in \mathbb{R}^{n_x \times n_u}$ stands for the susceptibility of agents to the interpersonal influence. We consider a distributed feedback control involving coopetitive interaction as follows,

$$\boldsymbol{u}_i(t) = -\boldsymbol{K} \sum_{(j,i)\in\mathbb{E}} |a_{ij}|(\boldsymbol{x}_i(t) - \operatorname{sgn}(a_{ij})\boldsymbol{x}_j(t)), \quad i \in \mathbb{V}, \tag{3.2}$$

where $\boldsymbol{K} \in \mathbb{R}^{n_u \times n_x}$ is the feedback gain matrix. In the recent literature of opinion evolution on signed graphs [Alt13; PMC16], the control protocol (3.2) can often be found.

After denoting $\boldsymbol{u}(t) := [\boldsymbol{u}_1^\top(t), \ldots, \boldsymbol{u}_n^\top(t)]^\top$, we consider the following admissible set,

$$\begin{aligned} \mathbb{U} = \{\boldsymbol{u}(t) \in \mathbb{R}^{nn_u} | \boldsymbol{u}_i(t) = -\boldsymbol{K} \sum_{j=1}^{n} |a_{ij}|(\boldsymbol{x}_i(t) - \operatorname{sgn}(a_{ij})\boldsymbol{x}_j(t)),& \\ \forall t > 0,\ \boldsymbol{K} \in \mathbb{R}^{n_u \times n_x},\ i = 1, \ldots, n\}.& \end{aligned} \tag{3.3}$$

The admissible control set (3.3) covers a relatively large number of distributed protocols with antagonistic interactions. The premise of the stage of protocol design is to determine under what conditions, the opinion dynamics of interest is polarizable, consensusable, and neutralizable w.r.t. such an admissible control set $\mathbb{U}$. To investigate such question, we first provide the formal definitions of the polarizability, consensusability, and neutralizability in the context of the so-called modulus consensusability of an opinion system w.r.t. $\mathbb{U}$.

Definition 3.1: Stationary Modulus Consensusability

The system (3.1) is stationary *modulus consensusable* w.r.t. $\mathbb{U}$, if one can find a controller $\boldsymbol{u} \in \mathbb{U}$ and scalars $\pi_i, \pi_j \in \{\pm 1\}$, $\forall i, j \in \mathbb{V}$ such that for any initial value $\boldsymbol{x}_i(0)$, the solution of (3.1) on a graph $\mathcal{G} = (\mathbb{V}, \mathbb{E}, \boldsymbol{A})$ satisfies

$$\lim_{t\to\infty} \pi_i \boldsymbol{x}_i(t) = \boldsymbol{v}, \quad \text{and } \lim_{t\to\infty} \|\boldsymbol{x}_i(t)\| < \infty, \quad \forall i, j \in \mathbb{V}, \tag{3.4}$$

where $\boldsymbol{v} \in \mathbb{R}^{n_x}$ is a constant vector. Specifically, stationary modulus consensusability can be classified into the following cases:

a). if $\boldsymbol{v} = \boldsymbol{0}$, we say the system (3.1) is *neutralizable* w.r.t. $\mathbb{U}$;

b). if $\boldsymbol{v} \neq \boldsymbol{0}$, we say the system (3.1) is stationary *bipartite consensusable* w.r.t. $\mathbb{U}$. In addition, if $\pi_i = \pi_j$ holds for all $i, j \in \mathbb{V}$, we say the system (3.1) is stationary *consensusable* w.r.t. $\mathbb{U}$; otherwise, we say the system (3.1) is stationary *polarizable* w.r.t. $\mathbb{U}$.

Remark 3.1. *To avoid being too conceptual, we use the terminology "neutralization" to characterize the phenomenon where social actors increasingly become getting used to indifference no matter what their initial intentions were. It is a more descriptive term in social science than the technical term of stabilization used in Altafinis' work [Alt13].*

A diagrammatic illumination is presented in Figure 3.1 to illustrate the relations of the concepts proposed in Definition 3.1. Apart from neutrality in the modulus consensus, the nontrivial case that the opinions reach consensus or oppositely separate, is named as bipartite consensus. Polarizability (resp. consensusability) concerns the phenomenon of polarity (resp. consensus) [Alt13; PMC16], but the detailed content here is slightly different. As the opinion variable is a vector rather than a scalar, the case when some (not all) of the entries of the opinion vector are 0 is also allowed for bipartite consensusability. We also point out that the opinion states should be bounded no matter how extreme they could be since infinite values of opinions make no sense from the perspective of sociology and psychology.

At the end of this subsection, we fix some notations and terminologies. In the remainder of this section, symbols $\pi_i \in \{\pm 1\}$ characterizes the signatures of individual opinions at steady-state, while the structural balance[1] of a graph, if it has, is specified by $\beta_i \in \{\pm 1\}$. As we shall see, there is no explicit dependence between the two sequences of scalars, with few exceptions.

[1] As defined in Section A.1.3, a signed digraph $\mathcal{G}$ is structurally balanced if the node set can be split into two disjoint subsets (i.e., $\mathbb{V}^+ \cup \mathbb{V}^- = \mathbb{V}$, $\mathbb{V}^+ \cap \mathbb{V}^- = \emptyset$) such that the weights of $(j, i) \in \mathbb{E}$ are positive for all $i \in \mathbb{V}^+, j \in \mathbb{V}^+$ and $i \in \mathbb{V}^-, j \in \mathbb{V}^-$, and negative for all $i \in \mathbb{V}^+, j \in \mathbb{V}^-$ and $\forall j \in \mathbb{V}^+, i \in \mathbb{V}^-$. Especially, a structurally balanced graph allows one to associate each node $i = \{1, \ldots, N\}$ with a scalar $\beta_i \in \{\pm 1\}$ such that $\beta_i = 1$ if $i \in \mathbb{V}^+$ and $\beta_i = -1$ if $i \in \mathbb{V}^-$.

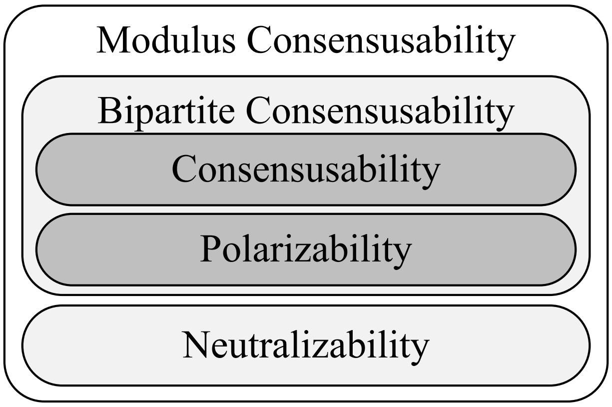

Figure 3.1: A schematic illustation of the relations between the concepts in Definition 3.1.

3.1.2 Bipartition Consensusability of Opinion Dynamics

In comparison to the trivial case in modulus consensus, the bipartite consensus is of great interest to sociological studies. Such bipartition of opinions is known to have a tight connection to the structural balance of the underlying interaction topology. Following this line of thought, we first provide sufficient conditions for stationary bipartite consensusability of opinion dynamics (3.1).

Theorem 3.1: Sufficient Conditions for Stationary Bipartite Consensusability

Given a graph $\mathcal{G} = (\mathbb{V}, \mathbb{E}, \boldsymbol{A})$ and arbitrary initial condition $\boldsymbol{x}(0) \in \mathbb{R}^{nn_x} \setminus \boldsymbol{0}$, the system (3.1) is stationary bipartite consensusable w.r.t. $\mathbb{U}$, if the following conditions are satisfied:

i). $\mathcal{G}$ is structurally balanced and quasi-strongly connected;

ii). $(\boldsymbol{F}, \boldsymbol{G})$ is stabilizable;

iii). $\boldsymbol{F}$ has semi-simple[a] zero eigenvalues and all its other eigenvalues have negative real parts.

Moreover, the system (3.1) is stationary consensusable if $\mathcal{G}$ is an unsigned graph, otherwise stationary polarizable if $\mathcal{G}$ is a signed graph.

[a] A semi-simple eigenvalue possesses equal algebraic and geometric multiplicities

Proof. The structurally balanced property of $\mathcal{G}$ means that there exist n scalars $\beta_i \in \{\pm 1\}$ such that $\beta_i \beta_j a_{ij} = \hat{a}_{ij} \geq 0$. By denoting $\hat{\boldsymbol{x}}_i(t) := \beta_i \boldsymbol{x}_i(t)$, one can obtain its time-derivative from (3.1) as follows

$$\dot{\hat{\boldsymbol{x}}}_i(t) = \boldsymbol{F}\hat{\boldsymbol{x}}_i(t) - \boldsymbol{G}\boldsymbol{K}\sum_{j=1}^{n} \hat{a}_{ij}(\hat{\boldsymbol{x}}_i(t) - \hat{\boldsymbol{x}}_j(t)), \qquad i \in \mathbb{V}. \tag{3.5}$$

With the adoption of the Kronecker product, the system (3.5) can be rewritten in a compact form as below.

$$\dot{\hat{\boldsymbol{x}}}(t) = \left(\boldsymbol{I}_n \otimes \boldsymbol{F} - \hat{\boldsymbol{L}} \otimes \boldsymbol{G}\boldsymbol{K}\right)\hat{\boldsymbol{x}}(t), \tag{3.6}$$

where $\hat{\boldsymbol{x}}(t) = [\hat{\boldsymbol{x}}_1^{\mathsf{T}}(t), \ldots, \hat{\boldsymbol{x}}_n^{\mathsf{T}}(t)]$ and $\hat{\boldsymbol{L}}$ is the Laplacian matrix associated to the unsigned graph $(\mathbb{V}, \mathbb{E}, \hat{\boldsymbol{A}})$ where $[\hat{\boldsymbol{A}}]_{ij} = \hat{a}_{ij}$ for $i \neq j$ and $[\hat{\boldsymbol{A}}]_{ij} = 0$ for $i = j$.

The stationary bipartite consensusability of (3.1) is closely related to the stationary consensusability of (3.6). According to [MZ10, Theorem 2], there exists a controller $\boldsymbol{u} \in \mathbb{U}$ for unsigned graphs such that the solutions to the system (3.5) converge asymptotically to a common trajectory for any nonzero initial value $\hat{\boldsymbol{x}}_i(0)$, if the unsigned graph $(\mathbb{V}, \mathbb{E}, |\boldsymbol{A}|)$ associated to $\mathcal{G}$ is quasi-strongly connected and $(\boldsymbol{F}, \boldsymbol{G})$ is stabilizable. The nonzero initialization $\boldsymbol{x}(0) \in \mathbb{R}^{nn_x} \setminus \boldsymbol{0}$ and the constraint iii) further imply that $\hat{\boldsymbol{x}}(t)$ does not converge to a nonzero and bounded vector-valued equilibrium as $t \to \infty$ for all $i \in \mathbb{V}$. By setting $\pi_i = \beta_i$ for all $i \in \mathbb{V}$, the system (3.6) achieving stationary consensus, i.e., $\lim_{t\to\infty} \hat{\boldsymbol{x}}(t) = \boldsymbol{v}$, implies the establishment of stationary bipartite consensus for the opinion dynamics (3.1), i.e., $\lim_{t\to\infty} \pi_i \boldsymbol{x}_i(t) = \boldsymbol{v}$. In summary, the original system (3.1) is stationary bipartite consensusable if condition i), ii) and iii) occur.

Moreover, a signed graph $\mathcal{G}$ associated with at least one negative weighted edge results in opinion polarization otherwise opinion consensus. $\square$

Remark 3.2. *The conditions in Theorem 3.1 involve two aspects, i.e., the requirements for the network topology and the subsystem dynamics. In condition i), quasi-strongly connectivity ensures that there exists at least one agent who can deliver directly or indirectly his/her willing to the remaining members. Moreover, the structural balance of graphs paves the way for the bipartite consensus of opinions. Condition ii) and iii) emphasize the importance of the dynamical properties of individuals. Specifically, to exclude the situation of neutralization and the meaningless case in which opinions are unbounded, the specification of the spectrum of system matrix $\boldsymbol{F}$ is of significance. Besides, the stabilizability of $(\boldsymbol{F}, \boldsymbol{G})$ implies that the individual is open to interpersonal influence.*

In Theorem 3.1, we only focus on the sufficient conditions for stationary bipartite consensusability, wherein graphs being structurally balanced are indispensable in the sufficient criterion. Through the next analysis, however, we will address that this graph property is not necessary for an opinion dynamics to achieve stationary bipartite consensus.

Theorem 3.2: Necessary Conditions for Stationary Bipartite Consensusability

Given a graph $\mathcal{G} = (\mathbb{V}, \mathbb{E}, \boldsymbol{A})$, the system (3.1) is stationary bipartite consensusable w.r.t. $\mathbb{U}$, only if the following conditions hold:

i). $\mathcal{G}$ is quasi-strongly connected and there exists a non-negative scalar $\alpha \geq 0$ satisfying the following relation

$$\alpha_i \equiv \alpha, \quad \forall i \in \mathbb{V} \tag{3.7}$$

where $\alpha_i := \sum_{j=1}^{n} (|\tilde{a}_{ij}| - \tilde{a}_{ij})$ and $\tilde{a}_{ij} := \pi_i \pi_j a_{ij}$;

ii). $(\boldsymbol{F}, \boldsymbol{G})$ is stabilizable;

iii). $\boldsymbol{F} - \alpha \boldsymbol{G} \boldsymbol{K}$ has semi-simple zero eigenvalues and all other eigenvalues have negative real parts.

Proof. We first prove $\mathcal{G}$ is quasi-strongly connected by contradiction. If $\mathcal{G}$ is not quasi-strongly connected, then it has either at least two nodes without inward edges or two separate subgraphs [RB05]. The first situation means that there exist at least two "isolated" actors (say agent i and agent j) whose opinions remain independent of the others' thoughts. Accordingly, the dynamics of these two agents reduce to $\dot{\boldsymbol{x}}_k = \boldsymbol{F} x_k$ with $k = i, j$. It is evident that such subsystems cannot reach bipartite consensus for arbitrary initial states. For the second case, even if the stationary bipartite consensus is achieved in each subgraph, it is unlikely to established across the entire graph $\mathcal{G}$ for all initial configurations. As a result, the contradictions arising in both two cases allow us to state that the quasi-strongly connected property of a graph is necessary for the stationary bipartite consensusability.

Next, we begin to demonstrate the relation (3.7). According to Definition 3.1, the system (3.1) being stationary bipartite consensusable means there exists a sequence of scalars $\pi_i, \pi_j \in \{\pm 1\}$ and a constant vector $\boldsymbol{v} \in \mathbb{R}^{n_x} \setminus \{\mathbf{0}\}$ such that $\lim_{t\to\infty} \pi_i \boldsymbol{x}_i(t) = \boldsymbol{v}$ is valid for all $i \in \mathbb{V}$. After denoting $\tilde{\boldsymbol{x}}_i := \pi_i \boldsymbol{x}_i$ for $i \in \mathbb{V}$, in analogy with the system dynamics (3.5), one can obtain

$$\dot{\tilde{\boldsymbol{x}}}_i(t) = \boldsymbol{F}\tilde{\boldsymbol{x}}_i(t) - \boldsymbol{G}\boldsymbol{K}\sum_{j=1}^{n}(|\tilde{a}_{ij}|\tilde{\boldsymbol{x}}_i(t) - \tilde{a}_{ij}\tilde{\boldsymbol{x}}_j(t)), \quad i \in \mathbb{V}, \tag{3.8}$$

where $\tilde{a}_{ij} := \pi_i \pi_j a_{ij}$. With the notation $\tilde{\boldsymbol{x}} = [\tilde{\boldsymbol{x}}_1^{\mathsf{T}}, \ldots, \tilde{\boldsymbol{x}}_n]^{\mathsf{T}}$, the compact form of (3.8) is given by

$$\dot{\tilde{\boldsymbol{x}}}(t) = (\boldsymbol{I}_n \otimes \boldsymbol{F} - \widetilde{\boldsymbol{L}} \otimes \boldsymbol{G}\boldsymbol{K})\tilde{\boldsymbol{x}}(t), \tag{3.9}$$

where

$$\widetilde{\boldsymbol{L}} := \mathsf{diag}(\boldsymbol{\pi})\boldsymbol{L}\,\mathsf{diag}(\boldsymbol{\pi}) = \begin{bmatrix} \sum_{j=1}^{n}|\tilde{a}_{1j}| & \widetilde{\boldsymbol{L}}_{12} \\ \widetilde{\boldsymbol{L}}_{21} & \widetilde{\boldsymbol{L}}_{22} \end{bmatrix}, \quad \text{and} \quad \boldsymbol{\pi} = [\pi_1, \cdots, \pi_n]^{\mathsf{T}}. \tag{3.10}$$

Arisen from the fact that the system (3.1) is stationary bipartite consensusable, the stationary consensusability of the dynamics (3.8) is unambiguous.

To promote the analysis, we introduce an auxiliary variable $\boldsymbol{\xi}_i = \tilde{\boldsymbol{x}}_1 - \tilde{\boldsymbol{x}}_i$ $(i = 2, 3, \ldots, n)$ which obeys the following time evolution rule

$$\begin{aligned}\dot{\xi}_i(t) = \boldsymbol{F}\xi_i(t) - \boldsymbol{G}\boldsymbol{K}\sum_{j=1}^{n}\Big[(\tilde{a}_{1j} - \tilde{a}_{ij})\xi_j(t) + |\tilde{a}_{ij}|\xi_i(t)\Big] \\ - \boldsymbol{G}\boldsymbol{K}\tilde{\boldsymbol{x}}_1(t)\sum_{j=1}^{n}\Big[(|\tilde{a}_{1j}| - \tilde{a}_{1j}) - (|\tilde{a}_{ij}| - \tilde{a}_{ij})\Big].\end{aligned} \tag{3.11}$$

We can immediately infer that the auxiliary system (3.11) is asymptotically stable, i.e., $\lim_{t\to\infty} \xi_i(t) = \mathbf{0}$ as the system (3.8) is stationary consensusable. Consequently, the third item in the right-hand side of (3.11) needs to approach to $\mathbf{0}$ as $t \to \infty$ for all $i = 2, \ldots, n$. That is to say, the conditions

$$\sum_{j=1}^{n}\Big[(|\tilde{a}_{1j}| - \tilde{a}_{1j}) - (|\tilde{a}_{ij}| - \tilde{a}_{ij})\Big] = 0, \text{ for } i = 2, \ldots, n. \tag{3.12}$$

and/or $\lim_{t\to\infty} \boldsymbol{G}\boldsymbol{K}\tilde{\boldsymbol{x}}_1(t) = \mathbf{0}$ succeed.

In order to rule out the second situation, bearing the relation $\lim_{t\to\infty} \tilde{\boldsymbol{x}}_i(t) = \boldsymbol{v}$ in mind, we first postulate, without loss of generality, that $\lim_{t\to\infty} \boldsymbol{G}\boldsymbol{K}\tilde{\boldsymbol{x}}_i(t) = \boldsymbol{G}\boldsymbol{K}\boldsymbol{v} = \mathbf{0}$ holds for all

$i \in \mathbb{V}$, meaning $\boldsymbol{v} \in \ker \boldsymbol{G}\boldsymbol{K}$. The limiting behavior of the dynamics (3.8) and its stationary consensusability manifest that $\boldsymbol{F}\boldsymbol{v} = \mathbf{0}$, i.e., $\boldsymbol{v} \in \ker \boldsymbol{F}$. Meanwhile, let $\boldsymbol{e}(t) := \tilde{\boldsymbol{x}}(t) - \mathbf{1}_n \otimes \boldsymbol{v}$ be an error vector. Thanks to the fact that

$$(\boldsymbol{I}_n \otimes \boldsymbol{F} - \widetilde{\boldsymbol{L}} \otimes \boldsymbol{G}\boldsymbol{K})(\mathbf{1}_n \otimes \boldsymbol{v}) = \mathbf{1}_n \otimes (\boldsymbol{F}\boldsymbol{v}) - (\widetilde{\boldsymbol{L}}\mathbf{1}_n) \otimes (\boldsymbol{G}\boldsymbol{K}\boldsymbol{v}) = \mathbf{0}_{nn_x},$$

it follows that

$$\dot{\boldsymbol{e}}(t) = (\boldsymbol{I}_n \otimes \boldsymbol{F} - \widetilde{\boldsymbol{L}} \otimes \boldsymbol{G}\boldsymbol{K})\boldsymbol{e}(t). \tag{3.13}$$

By noticing that $\lim_{t\to\infty} \boldsymbol{e}(t) = \mathbf{0}$, one can infer $\mathrm{sp}\{\boldsymbol{I}_n \otimes \boldsymbol{F} - \widetilde{\boldsymbol{L}} \otimes \boldsymbol{G}\boldsymbol{K}\} \subseteq \mathbb{C}_{<0}$. Therefore, the system (3.9) is asymptotically stable, i.e., $\lim_{t\to\infty} \tilde{\boldsymbol{x}}(t) = \mathbf{0}$, which is contradictory to the definition of the stationary bipartite consensus. To this end, we can conclude that the equality (3.12) is necessary for bipartite consensusability of the opinion system (3.1), which can be cast equivalently into the condition

$$\sum_{j=1}^{n} (|\tilde{a}_{ij}| - \tilde{a}_{ij}) = \alpha, \quad \forall i \in \mathbb{V}, \tag{3.14}$$

where $\alpha \geq 0$ is a non-negative scalar. As a result, the dynamics (3.11) can be compactly written as

$$\dot{\xi}(t) = (\boldsymbol{I}_{n-1} \otimes \boldsymbol{F} - \widetilde{\mathscr{L}} \otimes \boldsymbol{G}\boldsymbol{K})\xi(t), \tag{3.15}$$

where $\xi(t) = [\xi_2^{\mathsf{T}}(t), \ldots, \xi_n^{\mathsf{T}}(t)]^{\mathsf{T}}$ and $\widetilde{\mathscr{L}} = \widetilde{\boldsymbol{L}}_{22} - \mathbf{1}_{n-1}\widetilde{\boldsymbol{L}}_{12}$.

Next, we illustrate the stabilizability of $(\boldsymbol{F}, \boldsymbol{G})$ in condition ii). The equality (3.14) can be rephrased to $\widetilde{\boldsymbol{L}}\mathbf{1} = \alpha\mathbf{1}$, thus facilitating the matrix decomposition as follows

$$\begin{bmatrix} 1 & 0 \\ \mathbf{1}_{n-1} & \boldsymbol{I}_{n-1} \end{bmatrix}^{-1} \widetilde{\boldsymbol{L}} \begin{bmatrix} 1 & 0 \\ \mathbf{1}_{n-1} & \boldsymbol{I}_{n-1} \end{bmatrix} = \begin{bmatrix} \alpha & \widetilde{\boldsymbol{L}}_{12} \\ \mathbf{0} & \widetilde{\mathscr{L}} \end{bmatrix}. \tag{3.16}$$

Then, the fact that the matrix transformation from $\boldsymbol{L}$ to $\mathrm{diag}(\pi)\boldsymbol{L}\,\mathrm{diag}(\pi)$ is a similar transformation leads to $\mathrm{sp}\{\boldsymbol{L}\} = \mathrm{sp}\{\widetilde{\boldsymbol{L}}\}$, which immediately implies $\mathrm{sp}\{\boldsymbol{L}\} = \mathrm{sp}\{\widetilde{\mathscr{L}}\} \cup \{\alpha\}$. Therefore, one can compute

$$\mathrm{sp}\{\boldsymbol{I}_{n-1} \otimes \boldsymbol{F} - \widetilde{\mathscr{L}} \otimes \boldsymbol{G}\boldsymbol{K}\} = \bigcup_{\lambda \in \mathrm{sp}\{\boldsymbol{L}\} \setminus \{\alpha\}} \mathrm{sp}\{\boldsymbol{F} - \lambda \boldsymbol{G}\boldsymbol{K}\}. \tag{3.17}$$

Thereby, the asymptotic stability of the auxiliary system (3.15) accords to

$$\mathrm{sp}\{\boldsymbol{F} - \lambda \boldsymbol{G}\boldsymbol{K}\} \subseteq \mathbb{C}_{<0}, \quad \forall \lambda \in \mathrm{sp}\{\widetilde{\mathscr{L}}\}. \tag{3.18}$$

As reported in [MZ10], $(\boldsymbol{F}, \boldsymbol{G})$ is stabilizable if formula (3.18) is available. In conclusion, the stabilizability of $(\boldsymbol{F}, \boldsymbol{G})$ is necessary for stationary bipartite consensusability of the opinion dynamics (3.1).

The system matrix in (3.8), in spirit similar to (3.17), has the spectrum

$$\mathrm{sp}\{\boldsymbol{I}_n \otimes \boldsymbol{F} - \widetilde{\boldsymbol{L}} \otimes \boldsymbol{G}\boldsymbol{K}\} = \bigcup_{\lambda \in \mathrm{sp}\{\widetilde{\mathscr{L}}\} \cup \{\alpha\}} \mathrm{sp}\{\boldsymbol{F} - \lambda \boldsymbol{G}\boldsymbol{K}\}. \tag{3.19}$$

Based upon the fact that $\mathrm{sp}\{\boldsymbol{F} - \lambda \boldsymbol{G}\boldsymbol{K}\} \subseteq \mathbb{C}_{<0}$ for all $\lambda \in \mathrm{sp}\{\widetilde{\mathscr{L}}\}$, the spectral property of the matrix $\boldsymbol{F} - \alpha \boldsymbol{G}\boldsymbol{K}$ primarily characterizes the dynamical behavior of the system (3.9). Then, the statement that $\tilde{\boldsymbol{x}}$ converges to a bounded constant non-zero vector $\mathbf{1} \otimes \boldsymbol{v}$ for almost initial conditions, indicates condition iii) holds. Therefore, we complete the proof. $\square$

Remark 3.3. *The most noticeable point of Theorem 3.2 is no explicit requirement of structurally balanced graphs for the stationary bipartite consensus dynamics. Nevertheless, one still can extract the structurally balanced condition from the equality relation* (3.7) *but far more than that. Structural balance theory [Hei46] states that for an unweighted graph being not exactly structurally balanced, the least number of edges that must be changed in sign can be used to compute a distance to structural balance (i.e., a metric measuring the amount of structural unbalance in the network.). This statement has an immediate extension in weighted graphs [EK10]. In specific, we can argue that the quantity* $\sum_i \alpha_i = \sum_{i,j}(|\tilde{a}_{ij}| - \tilde{a}_{ij})$ *can be treated as an unbalance metric which measures the distance to a desired structurally balanced structure specified by* $\boldsymbol{\pi} = [\pi_1, \ldots, \pi_n]^\mathsf{T}$*. Since such a metric captures the collective effect of unbalance, the index* α_i *distinguishes the individual contribution of node* i *to disrupt the global structural balance w.r.t.* $\boldsymbol{\pi}$*. Hence, the relation* (3.7) *reads that all agents contribute an equal impact on network unbalance. In the special case of* $\alpha_i = 0$ *for all* $i \in \mathbb{V}$*, all nodes exhibit a local structural balance, and the network entails a global structurally balanced structure: the community splits into two hostile camps, individuals with the same sign of* π_i *come from the same camp, the social ties inside each fraction are cooperative, and the interrelations cross fractions are competitive. Hence, Theorem 3.2 reveals an appealing and previously unexplored, relationship between structurally balanced bipartition of topology and state clustering of opinion dynamics. In particular, the scenario* $\alpha > 0$ *meaning the mismatch of the bipartition pattern between opinion organization and network structure, mirrors real-world phenomena, especially, in political and commercial voting. The U.S. House Vote [XHC18b] in the two-party congress serves as a typical example. Although the underlying interconnection topology of Republicans and Democrats exhibits a naturally structural balance, representatives from the same party would not always vote for the same (pros or cons, usually) and the vote result is of high dependence on the specific content of topics.*

Until now, the discussion is carried out in terms of sufficient and necessary conditions, respectively. In the following theorem, we make a further step towards filling this gap.

Theorem 3.3: Sufficient and Necessary Conditions for Stationary Bipartition Consensusability

Let the system (3.1) be of a non-Hurwitz matrix $\boldsymbol{F}$ and satisfy

$$\pi_i \pi_j = \beta_i \beta_j, \quad \forall i, j \in \mathbb{V}. \tag{3.20}$$

The opinion dynamics (3.1) evolving over a structurally balanced graph $\mathcal{G}$ is stationary bipartite consensusable w.r.t. $\mathbb{U}$ for any nonzero initial conditions, if and only if the following statements hold:

i) $\mathcal{G}$ is quasi-strongly connected;

ii). $(\boldsymbol{F}, \boldsymbol{G})$ is stabilizable;

iii). $\boldsymbol{F}$ has semi-simple zero eigenvalues and all other eigenvalues have negative real parts.

Proof. Sufficiency is an immediate result of Theorem 3.1. Here we only need to prove the necessity.

The assembly line of Theorem 3.2 exposes that a quasi-strongly connected graph is necessary. The relation (3.20) results in $\alpha_i = \sum_{j=1}^{n}(|\tilde{a}_{ij}| - \tilde{a}_{ij}) = 0$ for $i \in \mathbb{V}$, implying $\alpha = 0$. Meanwhile, the dynamics (3.8) becomes

$$\dot{\tilde{\boldsymbol{x}}}_i(t) = \boldsymbol{F}\tilde{\boldsymbol{x}}_i(t) - \boldsymbol{G}\boldsymbol{K}\sum_{j=1}^{n}(|\hat{a}_{ij}|\tilde{\boldsymbol{x}}_i(t) - \hat{a}_{ij}\tilde{\boldsymbol{x}}_j(t)), \tag{3.21}$$

where $\hat{a}_{ij} = \beta_i\beta_j a_{ij} \geq 0$ due to the structural balance of the graph. Consequently, the auxiliary system (3.11) here reduces to

$$\dot{\xi}_i(t) = \boldsymbol{F}\xi_i(t) - \boldsymbol{G}\boldsymbol{K}\sum_{j=1}^{n}\left[(\hat{a}_{1j} - \hat{a}_{ij})\xi_j(t) + \hat{a}_{ij}\xi_i(t)\right], \tag{3.22}$$

where $\xi_i = \tilde{\boldsymbol{x}}_1 - \tilde{\boldsymbol{x}}_i$ and $i = 2, \ldots, n$. The compact form of (3.22) can be given by

$$\dot{\xi}(t) = (\boldsymbol{I}_{n-1} \otimes \boldsymbol{F} - \hat{\mathscr{L}} \otimes \boldsymbol{G}\boldsymbol{K})\xi(t), \tag{3.23}$$

where $\hat{\mathscr{L}} := \hat{\boldsymbol{L}}_{22} - \boldsymbol{1}_{n-1}\hat{\boldsymbol{L}}_{12}$ upon the matrix partition

$$\hat{\boldsymbol{L}} = \mathrm{diag}(\boldsymbol{\beta})\boldsymbol{L}\,\mathrm{diag}(\boldsymbol{\beta}) = \begin{bmatrix} \sum_{j=1}^{n}\hat{a}_{1j} & \hat{\boldsymbol{L}}_{12} \\ \hat{\boldsymbol{L}}_{21} & \hat{\boldsymbol{L}}_{22} \end{bmatrix}, \quad \text{and} \quad \boldsymbol{\beta} = [\beta_1, \cdots, \beta_n]^{\mathsf{T}}. \tag{3.24}$$

The remainder of the proof mimics the procedure of Theorem 3.2 which entails condition ii) and iii). Remarkably, by revisiting the similarity transformation (3.16) with Laplacian matrix $\hat{\boldsymbol{L}}$ associated to the unsigned graph $(\mathbb{V}, \mathbb{E}, \hat{\boldsymbol{A}})$ which is quasi-strongly connected, $\hat{\mathscr{L}}$ inherits all nonzero eigenvalues of $\hat{\boldsymbol{L}}$. □

3.1.3 Neutralizability of Opinion Dynamics

Bipartite consensus describes that the outcome of opinion-forming processes performs either unanimous or opposite behaviors in a group of social entities. For several reasons, such as for political or economic concerns, social members occasionally tend to remain neutral in social activities, thus motivating us to discuss the neutralizability of opinion dynamics.

The answer to neutralizability of systems (3.1) with a Hurwitz matrix $\boldsymbol{F}$ is affirmative. In this scenario, an intuitive choice for the state-feedback matrix $\boldsymbol{K}$ is the zero matrix and individuals, who are immune to the social influence, persist in neutral attitudes for all topics. Thus, we restrict ourselves to the case of the non-Hurwitz $\boldsymbol{F}$ while dealing with neutralizability.

Theorem 3.4: Sufficient and Necessary Conditions for Neutralizability of Opinion Dynamics

Given a graph $\mathcal{G} = (\mathbb{V}, \mathbb{E}, \boldsymbol{A})$ and arbitrary nonzero initial conditions, the system (3.1) with a non-*Hurwitz*[a] matrix $\boldsymbol{F}$ is neutralizable w.r.t. to $\mathbb{U}$, if and only if the following conditions are satisfied,

i) $(\boldsymbol{F}, \boldsymbol{G})$ is stabilizable.

ii) $\mathcal{G}$ is neither structurally balanced nor contains in-isolated structurally balanced subgraphs.

[a] A square matrix is called Hurwitz matrix (or sometimes stable matrix) if all its eigenvalues have strictly negative real parts.

Proof. The compact form of the system (3.1) can be written by

$$\dot{\boldsymbol{x}}(t) = (\boldsymbol{I}_n \otimes \boldsymbol{F} - \boldsymbol{L} \otimes \boldsymbol{G}\boldsymbol{K})\boldsymbol{x}(t), \tag{3.25}$$

from which, one can easily obtain

$$\mathsf{sp}\{\boldsymbol{I}_n \otimes \boldsymbol{F} - \boldsymbol{L} \otimes \boldsymbol{G}\boldsymbol{K}\} = \bigcup_{\lambda \in \mathsf{sp}\{\boldsymbol{L}\}} \mathsf{sp}\{\boldsymbol{F} - \lambda \boldsymbol{G}\boldsymbol{K}\}.$$

Therefore, the neutralizability problem can be transformed to show $\mathsf{sp}\{\boldsymbol{F} - \lambda\boldsymbol{G}\boldsymbol{K}\} \subseteq \mathbb{C}_{<0}$ for all $\lambda \in \mathsf{sp}\{\boldsymbol{L}\}$.

Sufficiency: Since $\mathcal{G}$ is not structurally balanced and contains no isolated structurally balanced subgraphs, it is already known that $0 \notin \mathsf{sp}\{\boldsymbol{L}\}$ [PMC16]. In addition, the stabilizability of $(\boldsymbol{F}, \boldsymbol{G})$ always allows one to find a matrix $\boldsymbol{K}$ such that the matrix $\boldsymbol{F} - \lambda\boldsymbol{G}\boldsymbol{K}$ is stable for all $\lambda \in \mathsf{sp}\{\boldsymbol{L}\}$, thereby evidencing the neutralizability of the compact system (3.25) w.r.t. $\mathbb{U}$.

Necessity: The background that the system (3.25) is neutralizable w.r.t. $\mathbb{U}$ amounts to $\mathsf{sp}\{\boldsymbol{F} - \lambda\boldsymbol{G}\boldsymbol{K}\} \subseteq \mathbb{C}_{<0}$ for all $\lambda \in \mathsf{sp}\{\boldsymbol{L}\}$. We posit that graph $\mathcal{G}$ is structurally balanced or contains at least one in-isolated structurally balanced subgraph, which leads to $0 \in \mathsf{sp}\{\boldsymbol{L}\}$. The condition $\mathsf{sp}\{\boldsymbol{F} - \lambda\boldsymbol{G}\boldsymbol{K}\} \subseteq \mathbb{C}_{<0}$ with $\lambda = 0$ means $\boldsymbol{F}$ is a stable matrix which is contradictory to the fact that $\boldsymbol{F}$ is not Hurwitz. Therefore, we derive the necessity of condition ii). In reference to condition i), we can adopt the same method presented in [MZ10] to display that stabilizability of $(\boldsymbol{F}, \boldsymbol{G})$ is necessary. Thus, the proof is completely finished. □

3.2 Opinion Dynamics on Coopetitive Social Networks with Media Influence

So far, a mathematical model that reflects the influence of self-dynamics and interpersonal interactions is introduced in the previous section. In this section, we study the opinion formation problems in a generic setting concerning the individual's heterogeneity and media influence. Throughout this section, we shall use the terminology "agents" for all social entities living on a network and model them by nodes in a graph. Among others, we shall refer to "media" or "leaders" as the social entities who have predominance in social activities, which correspond to the dominant nodes in the graph. We shall adopt "actors" to describe the entities that amount to the other standard nodes in the graph.

3.2.1 Problem Formulation and Elementary Results

Consider a network of $n \geq 2$ actors described by a signed graph $\mathcal{G}^a = (\mathbb{V}^a, \mathbb{E}^a, \boldsymbol{A}^a)$ associated with a signed Laplacian $\boldsymbol{L}^a \in \mathbb{R}^{n\times n}$. In contrast to the state-feedback homogeneous model (3.1), we deal with opinion dynamics of the following fashion

$$\dot{\boldsymbol{x}}_i(t) = \boldsymbol{F}_i x_i(t) + \boldsymbol{G}_i \boldsymbol{u}_i(t), \quad \boldsymbol{y}_i(t) = \boldsymbol{H}_i \boldsymbol{x}_i(t) \tag{3.26a}$$

$$\boldsymbol{u}_i(t) = \sum_{j=1}^{n} |a_{ij}| \Big(\boldsymbol{y}_j(t) \operatorname{sgn} a_{ij} - \boldsymbol{y}_i(t) \Big), \tag{3.26b}$$

where $\boldsymbol{x}_i \in \mathbb{R}^{n_x}$, $\boldsymbol{u}_i, \boldsymbol{y}_i \in \mathbb{R}^{n_y}$ stand for the actor states, control inputs and outputs, respectively. The matrices $\boldsymbol{F}_i$, $\boldsymbol{G}_i$, and $\boldsymbol{H}_i$ with appropriate dimensions denote the open loop system matrix, the control input to the state map, and the state to output map, respectively. As discussed in the previous section, the interconnection network can accommodate antagonistic interactions with negative weights $a_{ij} < 0$. In comparison to the dynamics (3.1), it is worthy to note that each individual entails heterogeneous dynamics. In the real world, individuals even living in the same house may be tremendously distinct in educational background, life history, personal preference, etc., and all these discrepancies, in turn, influence the decision-making of each actor.

In order to conduct the system analysis, we first provide the formal definition of modulus synchronization.

Definition 3.2: Output Modulus Synchronization

An opinion dynamic is said to establish *output modulus synchronization* under a prescribed control protocol, if for any initial states, the following statement

$$\lim_{t\to\infty} |\boldsymbol{y}_i(t)| - |\boldsymbol{y}_j(t)| = \boldsymbol{0}, \quad \lim_{t\to\infty} \|\boldsymbol{y}_i(t)\| < \infty, \tag{3.27}$$

holds for all $i, j \in \mathbb{V}^a$. With additional conditions, the output modulus synchronization can be further categorized:

1). if $\lim_{t\to\infty} \boldsymbol{y}_i(t) = \boldsymbol{0}$ for all $i \in \mathbb{V}^a$, then we say the protocol establishes *output neutralization*;

2). if $\lim_{t\to\infty} \boldsymbol{y}_i(t) - \boldsymbol{y}_j(t) = \boldsymbol{0}$ for all $i, j \in \mathbb{V}^a$, then we say the protocol establishes *output conformity*;

3). if there exists at least one pair of nodes $i, j \in \mathbb{V}^a$ satisfying $\lim_{t\to\infty} \boldsymbol{y}_i(t) + \boldsymbol{y}_j(t) = \boldsymbol{0}$, then we say the protocol establishes *output polarization*.

The integration of situation 2) and 3) is referred to the case where the protocol establishes *output bipartite synchronization*.

We highlight, to avoid any confusion, that the definition above slightly differs from Definition 3.1, as well as the usual *modulus consensus* definition in [Alt13; PMC16], where the outputs or rather states of all social actors are required to converge in modulus to a constant. Definition 3.2 only concerns whether or not the deviations between modular outputs vanish, while the outputs themselves may or may not converge to a static equilibrium vector. In comparison to the modulus consensus in Definition 3.1, the concept of modulus synchronization encompasses a wider range of opinion formation in modulus.

Moreover, the adoption of conformity instead of consensus is to avoid confusion with the static equilibrium case.

Throughout this section, we are mainly interested in the opinion dynamics which consist of individual subsystems admitting a port-Hamiltonian (PH) representation. A short sketch of the port-Hamiltonian approach to network system modeling and analysis is presented in Section 2.2.2. See [vdS14] and the references therein, for more details and a literature review.

Assumption 3.1. Actors with dynamics (3.26) admit PH representations in the form of PCH systems $(\boldsymbol{J}_i^a, \boldsymbol{R}_i^a, S_i^a)$:

$$\dot{\boldsymbol{x}}_i(t) = (\boldsymbol{J}_i^a - \boldsymbol{R}_i^a)\frac{\partial S_i^a}{\partial \boldsymbol{x}_i}(\boldsymbol{x}_i) + \boldsymbol{G}_i \boldsymbol{u}_i(t), \quad \boldsymbol{y}_i(t) = \boldsymbol{G}_i^\top \frac{\partial S_i^a}{\partial \boldsymbol{x}_i}(\boldsymbol{x}_i). \tag{3.28}$$

with $\boldsymbol{J}_i^a = -(\boldsymbol{J}_i^a)^\top$, $\boldsymbol{R}_i^a = (\boldsymbol{R}_i^a)^\top \succeq 0$, and the Hamiltonian function $S_i^a \geq 0$.

More details on the interpretation of the above model and its sociological implications will be provided later.

For cooperative networks, it is widely known [HCFS15] that the output synchronization of passive agents can be achieved if the interaction graph is strongly connected and balanced. Therefore, we start off by providing some sufficient conditions for output modulus synchronization of opinion systems (3.26a) with the control law (3.26b).

Proposition 3.1: Sufficient Conditions for Output Modulus Synchronization without Media

Consider an opinion forming process with evolutionary dynamics (3.26) satisfying Assumption 3.1 additionally with radially unbounded Hamiltonian functions S_i^a for all $i \in \mathbb{V}^a$. If the signed graph $\mathcal{G}^a$ is quasi-strongly connected and balanced, then the protocol (3.26b) establishes output modulus synchronization.

Proof. Due to the PH representation of actors, the Hamiltonian of the entire network is given by the summation of the individual Hamiltonian $S^a = \sum_i^n S_i^a$ whose time-derivative along the trajectories of the system dynamics (3.26) satisfies

$$\dot{S}^a(\boldsymbol{x}) = \frac{d}{dt}\sum_i^n S_i^a(\boldsymbol{x}_i) \leq \sum_i^n \boldsymbol{y}_i^\top(t)\boldsymbol{u}_i(t) = \sum_{i,j}^n a_{ij}\boldsymbol{y}_i^\top(t)\boldsymbol{y}_j(t) - |a_{ij}|\boldsymbol{y}_i^\top(t)\boldsymbol{y}_i(t), \tag{3.29}$$

in which $\boldsymbol{x} = [\boldsymbol{x}_1^\top, \ldots, \boldsymbol{x}_n^\top]^\top \in \mathbb{R}^{nn_x}$. As the digraph is balanced, i.e., $\sum_j^n |a_{ij}| = \sum_j^n |a_{ji}|$, the additive power is further equal to

$$\begin{aligned}\sum_i^n \boldsymbol{y}_i^\top(t)\boldsymbol{u}_i(t) &= \sum_{i,j}^n \Big(a_{ij}\boldsymbol{y}_i^\top(t)\boldsymbol{y}_j(t) - \frac{1}{2}|a_{ij}|\big(\boldsymbol{y}_i^\top(t)\boldsymbol{y}_i(t) + \boldsymbol{y}_j^\top(t)\boldsymbol{y}_j(t)\big)\Big) \\ &= -\frac{1}{2}\sum_{i,j}^n |a_{ij}| \big\|\boldsymbol{y}_j(t)\operatorname{sgn} a_{ij} - \boldsymbol{y}_i(t)\big\|_2^2 \leq 0\end{aligned} \tag{3.30}$$

Since S^a is proper (due to the local positive definiteness and the radial unboundedness), the inequality (3.30) along with (3.29) implies that the solution $\boldsymbol{x}(t)$ to the interconnected systems (3.26) is bounded and stays in a compact set. Due to the fact that $\boldsymbol{H}_i$ is a real matrix, it is obvious that $\boldsymbol{y}(t)$ is also bounded, i.e., $\lim_{t\to\infty}\boldsymbol{y}(t) < \infty$. By the application of

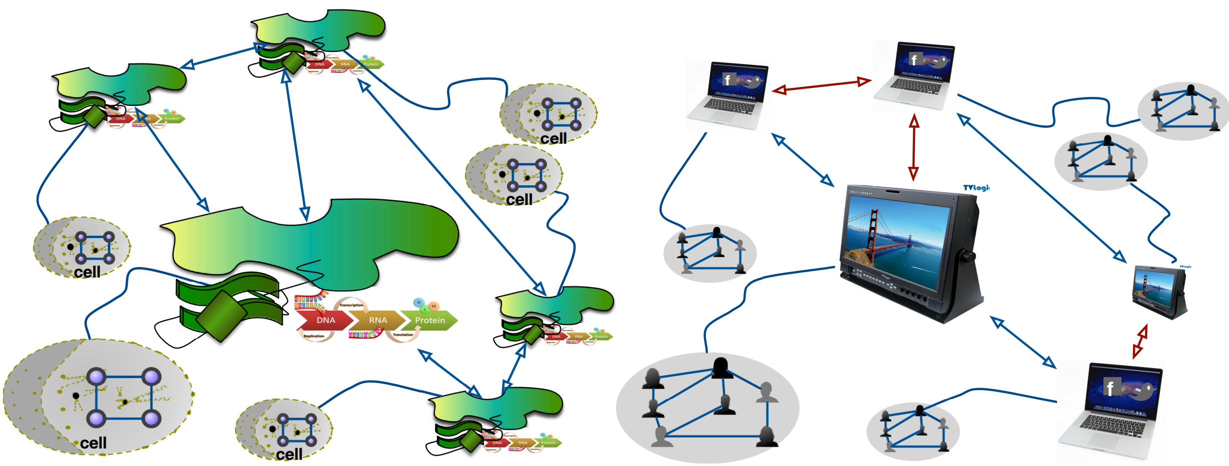

(a) a bacterial quorum-sensing network

(b) a social network with cooperative (in red) and competitve (in blue) interactions

Figure 3.2: A schematic representation of interconnection networks under consideration.

LaSalle invariant principle [Kha02] and the property $\operatorname{sgn} a_{ij} = \{\pm 1\}$, $\boldsymbol{x}(t)$ converges to a ω-limit set[2] in which $|\boldsymbol{y}_i(t)| = |\boldsymbol{y}_j(t)|$ for all $i, j \in \mathbb{V}^a$. It is known that a balanced graph is quasi-strongly connected if and only if it is strongly connected. Following Theorem 8.5 of [HCFS15], the system (3.29) reaches output modulus synchronization

$$\lim_{t\to\infty} |\boldsymbol{y}_i(t)| - |\boldsymbol{y}_j(t)| = \boldsymbol{0}, \qquad \forall\, i, j \in \mathbb{V}^a, \quad \forall \boldsymbol{x}(0) \in \mathbb{R}^{nn_x}. \tag{3.31}$$

Thus, the proof is complete. □

In reality, however, people are more or less exposed to pervasive mass and electronic media in their surrounding social context. Hence, a natural question is how the opinions of actors evolve under the influence of social media. To this end, we first modify the model of opinion dynamics (3.26) in the following way. Consider the existence of $p \geq 1$ media in a social network. Let $\mathcal{G}^m = (\mathbb{V}^m, \mathbb{E}^m)$ be the graph describing the underlying interconnection structure among media. To capture market segmentation in media industries, the appearance of p media gives rise to an p-subgraph decomposition[3] in the actor-to-actor communication network $\mathcal{G}^a$: Let $\mathcal{G}_k^a = (\mathbb{V}_k^a, \mathbb{E}_k^a)$ be the subgraph characterizing the interconnection relation among actors confronting medium $k \in \mathbb{V}^m$, where $|\mathbb{V}_k^a| = n_k$ and $(i, j) \in \mathbb{E}_k^a$ for $i, j \in \mathbb{V}_k^a$ means $(i, j) \in \mathbb{E}^a$. As shown in Figure 3.2, an analogous network architecture can also be found in biological systems because of the so-called quorum-sensing phenomenon [RS10]. The quorum-sensing mechanism exposes that bacteria produce, release, and measure signaling molecules (known as autoinducers) that disseminate in the environment, influencing population coordination and bacterial infection processes.

[2] An ω-limit set is the state of a dynamical system reaches after an infinite amount of time when time goes forward [GH83].

[3] For convenience, we label the first n_1 nodes of the graph as the actors exposed to media 1 and so on. Therefore, one can have $n_1 + \cdots + n_p = n$, $\mathbb{V}_1^a \cup \cdots \cup \mathbb{V}_p^a = \mathbb{V}_a$, and $\mathbb{E}_1^a \cup \cdots \cup \mathbb{E}_p^a = \mathbb{E}^a$.

As such, the media exposure and the community-based architecture render the actors the following opinion update rule

$$\dot{\boldsymbol{x}}_i(t) = \boldsymbol{F}_{\gamma(i)}\boldsymbol{x}_i(t) + \boldsymbol{G}_{\gamma(i)}\boldsymbol{u}_i(t), \quad \boldsymbol{y}_i(t) = \boldsymbol{H}_{\gamma(i)}\boldsymbol{x}_i(t), \tag{3.32a}$$

$$\boldsymbol{u}_i(t) = \sum_{j\in\mathbb{V}^a_{\gamma(i)}} a_{ij}\big(\boldsymbol{y}_j(t) - \boldsymbol{y}_i(t)\big) + b_{i\gamma(i)}\big(\boldsymbol{\eta}_{\gamma(i)}(t) - \boldsymbol{y}_i(t)\big), \tag{3.32b}$$

where $a_{ij} \in \mathbb{R}_{\geq 0}$ and $b_{ik} \in \mathbb{R}_{\geq 0}$ stand for the degree of confidence or susceptibility to interactions. $\gamma : \mathbb{V}^a \to \mathbb{V}^m$ is a surjective function defined between two sets of indices (not necessarily injective). Two actors $i, j \in \mathbb{V}^a$ are said to be in the same group if and only if $\gamma(i) = \gamma(j)$. In the control law (3.32b), $\boldsymbol{\eta}_{\gamma(i)}$ is the output of medium $\gamma(i) \in \mathbb{V}^m$ which is guided by the update rule

$$\dot{\boldsymbol{\chi}}_k(t) = \boldsymbol{\Psi}_k\boldsymbol{\chi}_k(t) + \boldsymbol{\Theta}_k\boldsymbol{\nu}_k(t), \qquad \boldsymbol{\eta}_k(t) = \boldsymbol{\Xi}_k\boldsymbol{\chi}_k(t), \tag{3.33a}$$

$$\boldsymbol{\nu}_k(t) = \sum_{l\in\mathbb{V}^m} |c_{kl}|\big(\boldsymbol{\eta}_l(t)\operatorname{sgn} c_{kl} - \boldsymbol{\eta}_k(t)\big) + \sum_{j\in\mathbb{V}^a_k} d_{kj}\big(\boldsymbol{y}_j(t) - \boldsymbol{\eta}_k(t)\big), \tag{3.33b}$$

where $\boldsymbol{\chi}_k \in \mathbb{R}^{n_x}$ and $\boldsymbol{\nu}_k, \boldsymbol{\eta}_k \in \mathbb{R}^{n_y}$ respectively are state, input, and output of medium k. In reference to (3.33b), $c_{kl} \in \mathbb{R}$ and $d_{kj} \in \mathbb{R}_{\geq 0}$ are coupling strength of the interrelation with media and individuals, respectively. Note that different from the opinion dynamics (3.26) over actor-to-actor networks, we assume no antagonism in the communication links among actors to avoid unnecessary complexity, i.e., $a_{ij} \geq 0$ for all $i, j \in \mathbb{V}^a$. Moreover, the competition relationships among media, if exists, lead to negative coefficients c_{kl}. Qualitatively, the development in this section can be adapted to the negative ties among individuals as well. Thus, the signed Laplacian matrix $\boldsymbol{L}^m \in \mathbb{R}^{p\times p}$ associated to the graph $\mathcal{G}^m$ is given by

$$[\boldsymbol{L}^m]_{kl} := \begin{cases} -c_{kl} & \text{if } k \neq l \\ \sum_{l=1}^{p} |c_{kl}| & \text{if } k = l \end{cases}. \tag{3.34}$$

Apart from the cell-based architecture in biological systems [GN02](as shown in Figure 3.2), the proposed compartmental model (3.32), (3.33) is indeed ultimately related to the emergence and prevalence of clustering phenomena in human society [HCS+17]. For example, homophily [RCW16] (medium is "heard" only by persons with views being not too far away) provides the sociological explanation for the appearance of social agglomerations. This modeling framework of social networks is reminiscent of many real-world scenarios (microbial world, human society, etc.; see Table 3.1), but we will not expand further.

Remark 3.4. *It is necessary to point out that the results developed in the following analysis are independent of the specific community-detection algorithm, especially of topological operations such as zoom in or out of compartments, which do not change the collective opinion evolution in social spaces. In fact, the topological architecture in which each group $\mathcal{G}^a_k$ connects to one medium k does not represent a restriction and applies to a more general setup wherein the opinions of media available for an actor group are in the same phase. Throughout this section, we only focus on the model* (3.32) *for simplicity of analysis and clarity of presentation.*

In what follows, we study in depth the asymptotic dynamical behavior of individual opinions under the joint influence of continuous communication with neighboring peers and the assimilation of information advocated on media.

Table 3.1: Glossary of Terms

social network	social entity	social actor	social medium	social community
graph theory	node	standard node	dominant node	subgroup
biology	organism	species	intermediate	cell
governance	people	civilian	legislator	factor
election	citizen	constituent	elected official	political party
activity	participator	member	radical leader	clique
factory	staff	worker	managers	office
company	staff	clerk	administrator	department
news	gossiper	audience	press	clustered viewer
marketing	user	customer	advertiser	user group

3.2.2 Convergence Behavior Analysis

In this subsection, we first introduce some notational conventions and topological properties of the underpinning interaction network before jumping into the quest of the convergence analysis.

Let $\boldsymbol{L}_k^a \in \mathbb{R}_{\geq 0}^{n_k \times n_k}$ be the Laplacian matrix of the subgraph $\mathcal{G}_k^a$ where $k \in \{1, \dots, p\}$, so that $\boldsymbol{L}^a = \mathrm{diag}(\boldsymbol{L}_1^a, \dots, \boldsymbol{L}_p^a)$. Thus, we can formalize the interaction structure encoded in control protocol (3.32b) and (3.33b) by an $(n+p)\times(n+p)$ Laplacian matrix $\boldsymbol{\mathcal{L}} \triangleq \begin{bmatrix} \boldsymbol{L}^a + \boldsymbol{B} & -\boldsymbol{\mathcal{B}} \\ -\boldsymbol{\mathcal{D}} & \boldsymbol{L}^m + \boldsymbol{D} \end{bmatrix}$ where

$$
\begin{aligned}
&\boldsymbol{\mathcal{B}} \in \mathbb{R}_{\geq 0}^{n \times p} = \mathrm{diag}(\boldsymbol{b}_1, \dots, \boldsymbol{b}_p), \quad \text{with } \boldsymbol{b}_k = \left[b_{(\sum_{l=1}^{k-1} n_l + 1)k}, \dots, b_{(\sum_{l=1}^{k} n_l)k} \right]^{\mathsf{T}} \\
&\boldsymbol{B} \in \mathbb{R}_{\geq 0}^{n \times n} = \mathrm{diag}(\boldsymbol{B}_1, \dots, \boldsymbol{B}_p), \quad \text{with } \boldsymbol{B}_k = \mathrm{diag}\left(b_{(\sum_{l=1}^{k-1} n_l + 1)k}, \dots, b_{(\sum_{l=1}^{k} n_l)k} \right), \\
&\boldsymbol{\mathcal{D}} \in \mathbb{R}_{\geq 0}^{p \times n} = \mathrm{diag}(\boldsymbol{d}_1, \dots, \boldsymbol{d}_p), \quad \text{with } \boldsymbol{d}_k = \left[d_{k(\sum_{l=1}^{k-1} n_l + 1)}, \dots, d_{k(\sum_{l=1}^{k} n_l)} \right] \\
&\boldsymbol{D} \in \mathbb{R}_{\geq 0}^{p \times p} = \mathrm{diag}\left(\sum_{j \in \mathbb{V}_1^a} d_{1j}, \dots, \sum_{j \in \mathbb{V}_p^a} d_{pj} \right).
\end{aligned}
\tag{3.35}
$$

In the following, we use the graph $\mathcal{G}(\boldsymbol{\mathcal{L}}) = (\mathbb{V}, \mathbb{E}, \boldsymbol{W})$ to represent the underpinning interconnected structure of the entire social network consisting of actors and media, wherein $\mathbb{V} = \{1, \dots, n, n+1, \dots, n+p\}$ is a vertex set[4] and the edge set $\mathbb{E} \subseteq \mathbb{V} \times \mathbb{V}$ has elements $(j, i) \in \mathbb{E}$ if $[\boldsymbol{W}]_{ij} \neq 0$ and $j \neq i$. Moreover, $\boldsymbol{W}$ is the designated adjacency matrix of graph $\mathcal{G}(\boldsymbol{\mathcal{L}})$ whose elements are defined by $[\boldsymbol{W}]_{ij} := w_{ij} = -[\boldsymbol{\mathcal{L}}]_{ij}$ and $[\boldsymbol{W}]_{ii} := w_{ii} = 0$ where $i, j \in \mathbb{V}$.

Similar to the treatment of actor systems, we restrict ourselves to the passive media dynamics satisfying the following assumptions.

4 The media are labeled by $\{n+1, \dots, n+p\}$ in the graph $\mathcal{G}$.

Assumption 3.2. Media (3.33) identify the PH representation (2.10) with $\boldsymbol{J}_k^m = -(\boldsymbol{J}_k^m)^\top$, $\boldsymbol{R}_k^m = (\boldsymbol{R}_k^m)^\top \succeq 0$, and a Hamiltonian $S_k^m \geq 0$ for all $k \in \mathbb{V}^m$.

Assumption 3.3. In each actor subgroup, at least one actor is listening to the medium, i.e., $\sum_{i \in \mathbb{V}_k^a} b_{ik} > 0$ for all $k \in \mathbb{V}^m$ and the actor-medium interaction is equivalently reciprocal, i.e., $b_{ik} = d_{ki}$ for all $i \in \mathbb{V}^a$ and $k \in \mathbb{V}^m$.

Note that Assumption 3.3 is necessary to derive the primary results in this section. The following lemma provides some topological properties of the entire social network under consideration.

Lemma 3.1: Network Topological Properties

For a social network with n actors and p media,

1). the graph $\mathcal{G}(\boldsymbol{\mathcal{L}})$ is structurally balanced if and only if the media graph $\mathcal{G}^m$ is structurally balanced.

Furthermore, when Assumption 3.3 holds

2). if media graph $\mathcal{G}^m$ and all actor subgraphs $\mathcal{G}_k^a$ $(k \in \mathbb{V}^m)$ are respectively balanced, then the graph $\mathcal{G}(\boldsymbol{\mathcal{L}})$ is balanced;

3). if the media graph $\mathcal{G}^m$ is quasi-strongly connected and all subgraphs $\mathcal{G}_k^a$ $(k = 1, \ldots, p)$ are strongly connected, then

3.1). the graph $\mathcal{G}(\boldsymbol{\mathcal{L}})$ is quasi-strongly connected;

3.2). there is at least one dominant node (medium) being a root of graph $\mathcal{G}(\boldsymbol{\mathcal{L}})$;

3.3). there is at least one standard node (actor) being a root of graph $\mathcal{G}(\boldsymbol{\mathcal{L}})$.

Proof. On the one hand, by noticing that the edges with negative weight only appear in the interaction among media, a structurally balanced $\mathcal{G}(\boldsymbol{\mathcal{L}})$ immediately leads to the structural balance of the media graph $\mathcal{G}^m$. On the other hand, since each group of actors only listens to one specific medium, when $\mathcal{G}^m$ is structurally balanced, $\mathbb{V}^m$ is split into two hostile camps and nodes in $\mathbb{V}^a$ are allowed to connect to any one of them, leading to the structural balance of the graph $\mathcal{G}(\boldsymbol{\mathcal{L}})$. Therefore, the claim 1). is true.

Without loss of generality, supposed $1 \in \mathbb{V}^m$ (equivalently, node $n+1 \in \mathbb{V}$ in the graph $\mathcal{G}(\boldsymbol{\mathcal{L}})$) be the root of the quasi-strongly connected graph $\mathcal{G}^m$. Thus, the medium 1 has at least one path to connect to any other media. On basis of Assumption 3.3, the strong connectedness of each actor subgraph $\mathcal{G}_k^a$ implies each medium k in $\mathbb{V}^m$ has a path to communicate with nodes in V_k^a. Consequently, one always can find a path connecting from media 1 to all actors and thus statements 3.1) and 3.2) hold.

Moreover, there exists at least one actor in $\mathbb{V}_1^a$, supposed the node with label $1 \in \mathbb{V}^a$ (equivalently, node $1 \in \mathbb{V}$ in graph $\mathcal{G}(\boldsymbol{\mathcal{L}})$), satisfying $d_{(n+1)1} = b_{1(n+1)} > 0$ according to Assumption 3.3. That is to say, both actor 1 and media $n+1$ on graph $\mathcal{G}(\boldsymbol{\mathcal{L}})$ have a link connecting to another. Following the fact that the media node $1 \in \mathbb{V}^m$ is a root of graph $\mathcal{G}(\boldsymbol{\mathcal{L}})$, the actor $1 \in \mathbb{V}^a$ has a path on graph $\mathcal{G}(\boldsymbol{\mathcal{L}})$ to reach other nodes in $\mathbb{V}$ in terms of the transition though medium $n+1 \in \mathbb{V}$. Therefore, actor 1 is also a root of graph $\mathcal{G}(\boldsymbol{\mathcal{L}})$ and the proof is finished. □

In analogy with Proposition 3.1 derived from actor-to-actor networks, we can provide a criterion for output modulus synchronization of the network $\mathcal{G}(\boldsymbol{\mathcal{L}})$.

Theorem 3.5: Sufficient Conditions for Output Modulus Synchronization with Media

Consider a social network of n actors with opinion dynamics (3.32) satisfying Assumption 3.1 and of p media (3.33) satisfying Assumption 3.2. If the following topological conditions hold:

1). Assumption 3.3 holds;

2). subgraphs $\mathcal{G}_k^a$ are strongly connected and balanced for all $k \in \mathbb{V}^m$;

3). media graph $\mathcal{G}^m$ is quasi-strongly connected, balanced;

then the actors (3.32) reach output modulus synchronization.

Proof. Straightforwardly, the graph $\mathcal{G}(\boldsymbol{\mathcal{L}})$ is quasi-strongly connected and balanced according to Lemma 3.1.

Let the Hamiltonian of the entire social network be

$$S(\boldsymbol{x}, \boldsymbol{\chi}) = \sum_i^n S_i^a(\boldsymbol{x}) + \sum_k^p S_k^m(\boldsymbol{\chi}), \tag{3.36}$$

where $\boldsymbol{x} = [\boldsymbol{x}_1^\top, \ldots, \boldsymbol{x}_n^\top]^\top$ and $\boldsymbol{\chi} = [\boldsymbol{\chi}_1^\top, \ldots, \boldsymbol{\chi}_p^\top]^\top$ are the stacked state vectors of actors and media, respectively. By treating media as members of the actor-network, Proposition 3.1 with the Hamiltonian function (3.36) implies that the protocol (3.32b) synchronizes the outputs of systems (3.32a) in modulus, i.e.,

$$\lim_{t\to\infty} |\boldsymbol{y}_i(t)| - |\boldsymbol{y}_j(t)| = \boldsymbol{0}, \tag{3.37}$$

for all initial conditions $\boldsymbol{x}(0) \in \mathbb{R}^{nn_x}$, $\boldsymbol{\chi}(0) \in \mathbb{R}^{pn_x}$. Thus, the proof is complete. □

Although not explicit in Theorem 3.5, the media (3.33a) also establishes output modulus synchronization under the control rule (3.33b), i.e., $\lim_{t\to\infty} |\boldsymbol{\eta}_k(t)| - |\boldsymbol{\eta}_l(t)| = \boldsymbol{0}$, for all $k, l \in \mathbb{V}^m$. More significantly, one can also check that $\lim_{t\to\infty} |\boldsymbol{y}_i(t)| - |\boldsymbol{\eta}_k(t)| = \boldsymbol{0}$ for all $i \in \mathbb{V}^a$ and $k \in \mathbb{V}^m$.

In cooperative networks [HCFS15], no precise extraction of the trivial case that the synchronous trajectories asymptotically vanish independent of initial states is made on the notion of synchronization. However, it is important to highlight such distinction of synchronous behavior in opinion dynamics, since the "degenerate" case implies all of the opinions become neutralized in the end and is of essential interest in its own right.

To promote the further analysis, we define an equivalence relation $\simeq_e$ on system matrices $\boldsymbol{F}_i$ and $\boldsymbol{F}_j$ by $\boldsymbol{F}_i \simeq_e \boldsymbol{F}_j$ if they satisfy the properties[5]

1). $\mathsf{sp}(\boldsymbol{F}_k) \cap \imath\mathbb{R} \neq \emptyset$ $(k = i, j)$ and are semi-simple;

2). $\mathsf{sp}(\boldsymbol{F}_i) \cap \imath\mathbb{R} = \mathsf{sp}(\boldsymbol{F}_j) \cap \imath\mathbb{R}$;

[5] Here, $\imath$ is the imaginary unit, i.e., $\imath^2 = -1$ and $\imath\mathbb{R}$ represents the imaginary axis containing the number zero.

3). the eigen-spaces corresponding respectively to $\mathrm{sp}(\boldsymbol{F}_i)\cap \imath\mathbb{R}$ and $\mathrm{sp}(\boldsymbol{F}_j)\cap \imath\mathbb{R}$ are the same.

Note that the definition of this equivalence relation implies the matrix $\boldsymbol{F}_k$ $(k=i,j)$ has at least one eigenvalue 0 or a pair of purely imaginary eigenvalues and their geometric multiplicity is equal to their algebraic multiplicity. In particular, those eigenvalues on the imaginary axis and the associated eigenspace are the same for all elements in the equivalence class $[\boldsymbol{F}_i]_{\simeq_e}$.

Towards this end, the following theorem serves as the investigation of the non-trivial case where output modulus synchronization implies output conformity or output polarization.

Theorem 3.6: Sufficient Conditions for Output Bipartite Synchronization with Media

Let the assumptions and conditions of Theorem 3.5 hold. If the following conditions are satisfied:

1). the media graph $\mathcal{G}^m$ is structurally balanced;

2). $\boldsymbol{F}_i \simeq_e \boldsymbol{F}_j \simeq_e \boldsymbol{\Psi}_k$ for all $i,j\in\mathbb{V}^a$ and $k\in\mathbb{V}^m$;

3). for all $i\in\mathbb{V}^a$, one has $\boldsymbol{H}_i^\top \boldsymbol{H}_i \succ 0$;

then the actor-network (3.32) reaches output bipartite synchronization: if $c_{kl}\geq 0$ for all $k,l\in\mathbb{V}^m$, then the conformity of output opinion is reached; otherwise, output opinions polarize.

Proof. As graph $\mathcal{G}(\boldsymbol{\mathcal{L}})=(\mathbb{V},\mathbb{E})$ is structurally balanced thanks to the first statement of Lemma 3.1, we can denote $\mathbb{V}^-$ and $\mathbb{V}^+$ as two “antagonistic camps” such that $\mathbb{V}^-\cap\mathbb{V}^+=\emptyset$ and $\mathbb{V}^-\cup\mathbb{V}^+=\mathbb{V}$. Without loss of generality, let $\beta_i=1$ if $i\in\mathbb{V}^+$ and $\beta_i=-1$ if $i\in\mathbb{V}^-$. By denoting the augmented variable

$$\boldsymbol{z}:=[\boldsymbol{z}_1^\top,\ldots,\boldsymbol{z}_{n+p}^\top]^\top=[\boldsymbol{y}^\top,\boldsymbol{\eta}^\top]^\top,$$

the time-derivative of the Hamiltonian (3.36) S becomes

$$\dot{S}(\boldsymbol{x},\boldsymbol{\chi})\leq\sum_{i,j}^{n+p}\Big(w_{ij}\boldsymbol{z}_i^\top(t)\boldsymbol{z}_j(t)-\frac{1}{2}|w_{ij}|\big(\boldsymbol{z}_i^\top(t)\boldsymbol{z}_i(t)+\boldsymbol{z}_j^\top(t)\boldsymbol{z}_j(t)\big)\Big) \tag{3.38}$$

$$=-\frac{1}{2}\sum_{i,j}^{n+p}|w_{ij}|\big\|\boldsymbol{z}_j(t)\,\mathrm{sgn}\,w_{ij}-\boldsymbol{z}_i(t)\big\|_2^2 \tag{3.39}$$

$$=-\frac{1}{2}\sum_{i,j}^{n+p}|w_{ij}|\big\|\beta_j\boldsymbol{z}_j(t)-\beta_i\boldsymbol{z}_i(t)\big\|_2^2, \tag{3.40}$$

where the inequality (3.38) is similar in the spirit to (3.29), and the last equation (3.40) comes from the fact $\mathrm{sgn}\,w_{ij}=\beta_i\beta_j$ for $(j,i)\in\mathbb{E}$ as the graph $\mathcal{G}(\boldsymbol{\mathcal{L}})$ is structurally balanced.

According to LaSalle invariance principle, $[\boldsymbol{x}^\top,\boldsymbol{\chi}^\top]^\top$ thus converges to the ω-limit set $\Omega(\boldsymbol{x}(0),\boldsymbol{\chi}(0))$ in which one has $\beta_j\boldsymbol{z}_j=\beta_i\boldsymbol{z}_i$ for all $i,j\in\mathbb{V}$. On this controlled invariant subspace $\Omega(\boldsymbol{x}(0),\boldsymbol{\chi}(0))$, the dynamic of actors (3.32a) reduces to an unforced system $\dot{\boldsymbol{x}}_i(t)=\boldsymbol{F}_{\gamma(i)}\boldsymbol{x}_i(t)$. Moreover, the zero vector is not an asymptotic equilibrium of this autonomous system since $\mathsf{sp}(\boldsymbol{F}_{\gamma(i)})$ contains at least one marginally stable eigenvalue according to condition 2). The equivalence relation among all matrices $\mathsf{sp}(\boldsymbol{F}_i)$ $(i \in \mathbb{V}^a)$ guarantees that the unforced systems perform the same long-term dynamical behavior. Thus, any actor $i \in \mathbb{V}^a$ must obey $\lim_{t\to\infty} |\boldsymbol{y}_i(t)| \neq \boldsymbol{0}$ due to $\boldsymbol{H}_i \boldsymbol{x}_i \neq 0$ for all $\boldsymbol{x}_i \in \mathbb{R}^{n_x}/\{\boldsymbol{0}\}$. Combining with Theorem 3.5, one can conclude that the actor-network reaches the polarization of output opinions if there exists at least one negatively weighted edge in graph $\mathcal{G}^m$; otherwise, output conformity is achieved. The proof is complete. □

Remark 3.5. *It is worthy to note that when the system matrices $\boldsymbol{F}_i$ for all $i \in \mathbb{V}^a$ have no purely imaginary eigenvalue except one or multiple semi-simple zero eigenvalues satisfying condition 2) of Theorem 3.6, the opinion evolving process collapses to the stationary equilibrium setting, similar to the study in [Alt13; PMC16]. That is, the asymptotic states of the opinion dynamics are the same constant vector for all actors. Otherwise, each component of the opinion trajectories steered by dynamics* (3.32a) *exhibits a simple harmonic oscillation as time progresses.*

According to Theorem 3.6, the output bipartite synchronization of opinion evolution is determined by two factors. One is the communication topological structure among participating entities. That is, the graph-theoretic conditions,(quasi-)strongly connectedness and balancedness for asymptotic synchronization of passive multi-agent systems [HCFS15], are customized distributively to subgraphs of social networks. More notably, the structurally balanced condition is a significant source of the opinion cleavage in society. The network of media with different memes might split into two disjoint camps such that media in the same club mimic the memes with each other while media coming from distinct groups confront each other for some reasons, e.g., grabbing higher audience ratings.

Moreover, the dynamical properties of agents are in close relation with the (nontrivial) synchronous behaviors of opinions in a large population. Non-identical self-dynamics are introduced to characterize the diversity of individuals in e.g., human thoughts and faiths. The inherent requirement on their dynamic intersection is a prerequisite to realizing conformity among cooperative entities or polarization on cooperative networks. This finding is reminiscent of the real-life fact that individuals who may be unmatched in many aspects, e.g., age, height, color, etc., should have some commonalities such as the moral compass of society, in the hope of participating collective group behaviors.

Obviously, it is not challenging to produce a counterpart of Theorem 3.6 in the purely actor-to-actor interaction networks $\mathcal{G}^a = (\mathbb{V}^a, \mathbb{E}^a, \boldsymbol{A})$.

Corollary 3.1: Sufficient Conditions for Output Bipartite Synchronization without Media

Consider a network of actors with dynamics (3.26) satisfying Assumption 3.1 additionally with the radially unbounded Hamiltonian functions S_i^a for all $i \in \mathbb{V}^a$. Assume the signed graph $\mathcal{G}^a$ is quasi-strongly connected and balanced. If the following conditions are satisfied:

1). the node graph $\mathcal{G}^a$ is structurally balanced;

2). $\boldsymbol{F}_i \simeq_e \boldsymbol{F}_j$ for $i, j \in \mathbb{V}^a$;

3). for all $i \in \mathbb{V}^a$, one has $\boldsymbol{H}_i^\top \boldsymbol{H}_i \succ 0$;

then actor systems (3.26) achieve output bipartite synchronization: if $a_{ij} \geq 0$ for all $i, j \in \mathbb{V}^a$, then output opinions become conformity; otherwise, opinions polarize.

Since the structural balance and imbalance of the graphs are two mutually exclusive properties, a criterion concluding output neutralization in a coopetitive organization can be deduced from Theorem 3.5 and Theorem 3.6.

Theorem 3.7: Sufficient Conditions for Output Neutralization under Media Influence

Let the assumptions of Theorem 3.5 hold. If the media graph is strongly connected and structurally unbalanced, then the actors (3.32a) reach output neutralization under protocol (3.32b) for all initial condition. In addition, if the system is zero-state detectable, then the actor-network $\mathcal{G}^a$ entails state neutralization for all initial condition.

Proof. According to the proof of Theorem 3.6, the inequality (3.39) can further lead to

$$\dot{S}(\boldsymbol{x},\boldsymbol{\chi}) \leq -\boldsymbol{z}^\top(t)\boldsymbol{\mathcal{L}}\boldsymbol{z}(t) \leq -\varepsilon\sum_{i=1}^{n+p}\|\boldsymbol{z}_i(t)\|_2^2, \quad \exists\,\varepsilon>0, \tag{3.41}$$

where the balanced condition of graph $\mathcal{G}(\boldsymbol{\mathcal{L}})$ is used due to Lemma 3.1, i.e., $\sum_j^{n+p}|w_{ij}| = \sum_j^{n+p}|w_{ji}|$ for all $i\in\mathbb{V}$. Moreover, inequality (3.41) also follows from Corollary 3 of [Alt13] that if the strongly connected signed graph $\mathcal{G}(\boldsymbol{\mathcal{L}})$ is structural unbalance, then the smallest eigenvalue of $\boldsymbol{\mathcal{L}}$ is a positive real number and the other eigenvalues have positive real parts.

The application of LaSalle invariance principle to the inequality (3.41) shows that $[\boldsymbol{x}^\top,\boldsymbol{\chi}^\top]^\top$ converges to the ω-limit set $\Omega(\boldsymbol{x}(0),\boldsymbol{\chi}(0))$ on which one can obtain $\lim_{t\to\infty}\boldsymbol{z}_i(t) = \boldsymbol{0}$. Namely, the social network is asymptotically neutral for arbitrary initial conditions $[\boldsymbol{x}^\top(0),\boldsymbol{\chi}^\top]^\top(0)$. Straightforwardly, one can derive $\lim_{t\to\infty}\boldsymbol{y}_i(t) = \boldsymbol{0}$ whatever the initial conditions are.

Furthermore, the zero-state detectability of systems leads to the reasoning that if $\boldsymbol{u}_i \equiv 0$ and $\boldsymbol{y}_i = 0$ in the ω-limit set $\Omega(\boldsymbol{x}(0),\boldsymbol{\chi}(0))$, one may induce $\boldsymbol{x}_i(t)\to\boldsymbol{0}$ as $t\to\infty$ for all $i\in\mathbb{V}^a$. Namely, the actor-network $\mathcal{G}^a$ establishes state neutralization for arbitrary initial conditions. □

Remark 3.6. *In general, the quest for a global criterion to identify bipartite synchronization from modulus context is an open problem for more general nonlinear systems. Although the nonlinear case is beyond the scope of the chapter, it is worth mentioning that by linearization of the nonlinear dynamics in the vicinity of the original and by using Theorem* (3.6) *rooted in the linear case, one may explore some local criteria as a stepping stone.*

Before ending this subsection, we provide some necessary remarks on the proposed modeling methodology. The adoption of the port-Hamiltonian representation to identify a prominent class of opinion dynamics provides substantial benefits in the mathematical analysis due to the natural passivity. In particular, the developed methodology allows for the interpretation of *internalization*, a concept studied in social psychology and sociology [You16], from system and control theory. The first message is that the PH picture captures how the message- or information-flow derived from external communication with other peers and exposure to media gets through each social actor. The passivity inequality $\dot{S}_i^a(\boldsymbol{x}_i) \leq \boldsymbol{y}_i^\top(t)\boldsymbol{u}_i(t)$ implies that the internalizing rate of in-coming knowledge or ideas never excesses information potential available for actors. In addition, the PH modeling of actors illustrates that the vector field that generates an opinion flow inside actors can decompose into a conservative and a dissipative component. Among them, the dissipative system concerning a non-negative definite matrix $\boldsymbol{R}_i^a$ governs the convergence performance of opinion dynamics, since the opinion Hamiltonian (Lyapunov-like function) decreases (gradient-descent) along the dissipative vector field. Therefore, the symmetric matrix $\boldsymbol{R}_i^a$ serves, in some sense, as a measure assessing the capability of actors to internalize information, ideas, knowledge from the external environment. In this regard, actors whose symmetric dynamic is of predominance often behave more active in social activities and impose significant influence on the collective decision-making processes. In other words, actors who are relatively conservative performs back and forth or in a quandary. Intuitively, the skew-symmetric matrix $\boldsymbol{J}_i^a$ appeared in the PH representation reflects how conservative social entities are.

3.2.3 Autocratic Media Controlling Social Opinion Formation

In the system of governance, one pitfall of the representative democracy mechanism is that elected officials are in no need to fulfill promises made before being elected, and even promote their self-interests once elected. Besides, information broadcasters like, e.g., television, newspapers, celebrity blogs, are supposed to propagate informative messages to their audiences, while they may mislead the public attitudes towards political or social events by using deliberate manipulations or even lies [LBB+18].

Those undesirable instances suggest the appearance of autocratic media in social networks. More formally, they fall into a broad topic, what the sociologists call “corruption” meaning the misuse of authorized power (by heritage, education, marriage, election, appointment or whatever else) to acquire private benefits or reach ulterior purposes, e.g., in politics, economics, and culture [JS17]. If corruption happens in the minority, its damages include the loss of democracy, deprivation of liberty, demagoguery of public opinions, etc., necessitating the rigorous examination of the interaction organization and intrinsic mechanism in those scenarios.

First, we endow a mathematical narrative to the corruption in social networks, i.e., $\sum_{i=1}^{n}\sum_{k=1}^{p} d_{ik} = 0$ which means no medium is affected by actors in a society with autocratic leaders. To this end, we consider the input signals for actors and media in the following pattern

$$\boldsymbol{u}_i(t) = \sum_{j\in\mathbb{V}^a_{\gamma(i)}} a_{ij}(\boldsymbol{y}_j(t)-\boldsymbol{y}_i(t)) + b_{i\gamma(i)}\big(\boldsymbol{H}_{\gamma(i)}\boldsymbol{\Pi}_{\gamma(i)}\boldsymbol{\chi}_{\gamma(i)}(t)-\boldsymbol{y}_i(t)\big) + \boldsymbol{\Gamma}_{\gamma(i)}\boldsymbol{\chi}_{\gamma(i)}(t), \tag{3.42}$$

$$\boldsymbol{\nu}_k(t) = \sum_{l=1}^{p} |c_{kl}|(\boldsymbol{\eta}_l(t)\operatorname{sgn} c_{kl} - \boldsymbol{\eta}_k(t)) \tag{3.43}$$

where matrices $\boldsymbol{\Pi}_{\gamma(i)}$ and $\boldsymbol{\Gamma}_{\gamma(i)}$ are solutions to the equations

$$\boldsymbol{F}_{\gamma(i)}\boldsymbol{\Pi}_{\gamma(i)} + \boldsymbol{G}_{\gamma(i)}\boldsymbol{\Gamma}_{\gamma(i)} = \boldsymbol{\Pi}_{\gamma(i)}\boldsymbol{\Psi}_{\gamma(i)}, \tag{3.44}$$

$$\boldsymbol{H}_{\gamma(i)}\boldsymbol{\Pi}_{\gamma(i)} = \boldsymbol{\Xi}_{\gamma(i)}, \tag{3.45}$$

for $i = 1,\ldots,n$. Now, we begin to examine the convergence behavior of opinion formation in a corrupted social context.

Theorem 3.8: Convergence Behavior of Opinion Formation in a Corrupted Social Context

Consider the entire social network $\mathcal{G}(\boldsymbol{\mathcal{L}})$ satisfying $\sum_{i=1}^{n}\sum_{k=1}^{p} d_{ki} = 0$. If the following conditions hold,

1). the media graph $\mathcal{G}^m$ is quasi-strongly connected, balanced and structurally balanced;

2). the media-to-actor couplings are lower bounded away from zero, i.e., $b_{i\gamma(i)} \geq \epsilon > 0$, for all $i \in \mathbb{V}^a$ and a positive constant ϵ;

3). $\boldsymbol{\Psi}_k \simeq_e \boldsymbol{\Psi}_l$ for all $k, l \in \mathbb{V}^m$;

4). for all $k \in \mathbb{V}^m$, $\boldsymbol{\Xi}_k^{\top}\boldsymbol{\Xi}_k \succ 0$;

then the control laws (3.42)-(3.45) solve the output bipartite synchronization problem for the passive actor systems (3.32a) with detectable $(\boldsymbol{H}_i, \boldsymbol{F}_i)$ for all $i \in \mathbb{V}^a$. More importantly, the stably synchronized output trajectory of actors completely relies on the output of media.

Proof. After denoting an error variable $\boldsymbol{\zeta}_i = \boldsymbol{x}_i - \boldsymbol{\Pi}_{\gamma(i)}\boldsymbol{\chi}_{\gamma(i)}$ for $i \in \mathbb{V}^a$, we compute its time-derivative from (3.32a) by

$$\dot{\boldsymbol{\zeta}}_i(t) = (\boldsymbol{F}_{\gamma(i)} - b_{i\gamma(i)}\boldsymbol{G}_{\gamma(i)}\boldsymbol{H}_{\gamma(i)})\boldsymbol{\zeta}_i(t) - \boldsymbol{\Pi}_{\gamma(i)}\boldsymbol{\Theta}_{\gamma(i)}\boldsymbol{\nu}_{\gamma(i)}(t), \tag{3.46}$$

where (3.42)-(3.45) are employed. In equation (3.46), the first term $\boldsymbol{F}_{\gamma(i)} - b_{i\gamma(i)}\boldsymbol{G}_{\gamma(i)}\boldsymbol{H}_{\gamma(i)}$ on the right-hand side is Hurwitz as a consequence of the passivity assumption and detectability of $(\boldsymbol{H}_i, \boldsymbol{F}_i)$. By adopting Corollary 3.1 to the media-network, the media state $\boldsymbol{\chi}_{\gamma(i)}(t)$ with $\gamma(i) \in \mathbb{V}^m$ asymptotically reaches the output bipartite synchronization, as well as $\boldsymbol{\nu}_{\gamma(i)}(t) \to 0$ when time goes to infinity $t \to \infty$. Then, the error variable $\boldsymbol{\zeta}_i$ obeying time evolution rule (3.46) converges to an asymptotically stable equilibrium state, i.e., $\lim_{t\to\infty}\boldsymbol{\zeta}_i(t) = \boldsymbol{0}$ for all $i = 1, \ldots, N$. Combining with condition (3.45), one can immediately deduce $\boldsymbol{y}_i \to \boldsymbol{\eta}_{\gamma(i)}$ as $t \to \infty$.

Note that media asymptotically achieve the output bipartite synchronize at their own risk without the involvement of actors. In a more abstract setting, the outputs of media play a virtual role of external references for the dynamical system (3.32a), which are tracked by actors under the control law (3.42). Therefore, one can conclude that actors asymptotically follow a non-zero synchronization trajectory which does not depend on dynamical properties of actors. □

Remark 3.7. *In control theory, equations* (3.44) *and* (3.45) *resemble* Francis *equations in the output regulation problem. For this reason, the solvability conditions suggested by [TSH01] are available to examine the existence of matrices* $\boldsymbol{\Pi}_{\gamma(i)}$ *and* $\boldsymbol{\Gamma}_{\gamma(i)}$ *such that equations* (3.44) *and* (3.45) *hold. Theorem 3.8 claims that members of media-networks ignore the ideas of actors while forming opinions. In fact, the medium, which produces the reference-synchronization signal, plays the role of an exosystem for actors. Thus, one can apply the internal model principle to media systems by following the classical namesake in the control field [FW76]. By exploring an internal model in media dynamics, we can explicitly derive the analytic expression of equilibrium opinion trajectories of agents. See [WSA11; PJ14] for the internal-model-based synchronization problem on cooperative networks and the references therein for more details.*

We now provide some important remarks on the proposed theory. The overarching point is that the influence of information exchange among actors vanishes in this case. That is, the diffusion-like term $\sum_{j\in\mathbb{V}^a_{\gamma(i)}} a_{ij}(\boldsymbol{y}_j-\boldsymbol{y}_i)$ in (3.42) degenerates implicitly to zero since the outputs of actors belonging to the same subgroup become identical with each other, owing to (3.45). Notably, an additional term $\boldsymbol{\Gamma}_{\gamma(i)}\boldsymbol{\chi}_{\gamma(i)}$ appears in the opinion protocol (3.42) in comparison to the democratic controller (3.32b).

On the network interconnection structure, condition 2) given in Theorem 3.8 guarantees that every medium has a direct influence on its own viewers. The topological constraints including connectivity and (structural) balance, are imposed only on the media-graph and the explicit knowledge of the interaction among actors is not required. That is to say, the results are valid for any interconnection configuration of actor subgraphs $\mathcal{G}^a_{\gamma(i)}$. We even allow the extreme case in which actors do not communicate with one another and only believe information spread through public media, i.e., $\sum_{i,j=1}^{n} a_{ij}=0$.

3.2.4 Numerical Evaluations

In this subsection, we provide some numerical tests to qualitatively and quantitatively demonstrate the developed results.

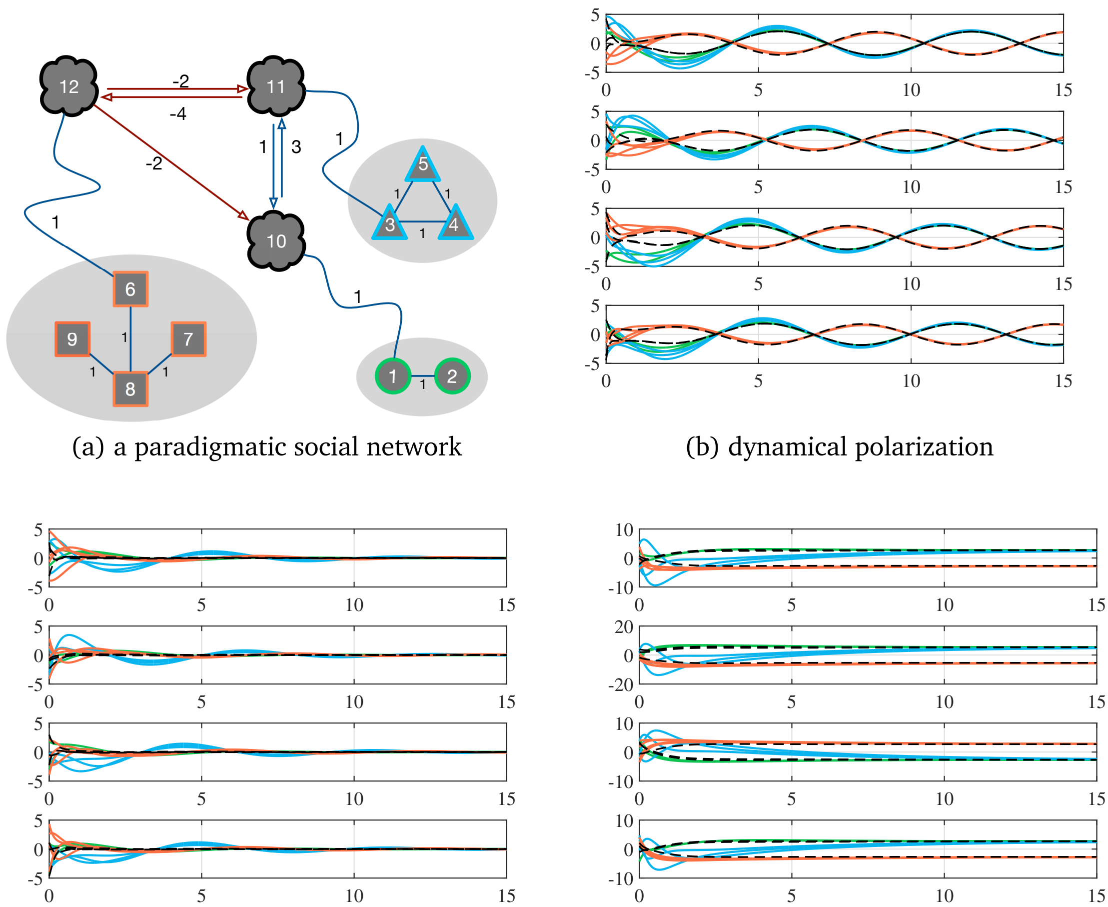

(a) a paradigmatic social network

(b) dynamical polarization

(c) neutralization

(d) stationary polarization

Figure 3.3: Numerics for opinion dynamics on cooperative networks under media influence.

The paradigmatic example of social networks is illustrated in Figure 3.3a comprising 3 media and 9 social actors which self-organize into 3 separate groups. The color configuration of the nodal border is applied correspondingly to the figures describing their state trajectories. In Figure 3.3a, the cooperative interrelation is drawn in blue (arrow)line and the competition is in red. Clearly, the network topology satisfies the connectivity requirement and is structurally balanced. Namely, the entities of the social networks split into two hostile camps. To save cliché, we consider the identity matrix for all input-to-state and state-to-output maps of actors $\mathbb{V}^a$ and media $\mathbb{V}^m$. Their system matrices are respectively given as

$$\boldsymbol{\Psi}_{\mathbb{V}^m} = \begin{bmatrix} -2 & 1 & \frac{11}{5} & \frac{9}{25} \\ \frac{3}{2} & -\frac{9}{10} & -\frac{17}{50} & -\frac{7}{50} \\ \frac{1}{2} & -2 & -\frac{3}{2} & \frac{1}{2} \\ -\frac{27}{10} & \frac{19}{10} & \frac{16}{5} & -\frac{3}{5} \end{bmatrix}, \qquad \boldsymbol{F}_{\mathbb{V}_1^a} = \begin{bmatrix} \frac{1}{2} & -1 & \frac{1}{2} & -\frac{1}{2} \\ 2 & -\frac{3}{2} & -1 & 0 \\ \frac{1}{2} & -1 & \frac{1}{2} & -\frac{3}{2} \\ \frac{3}{2} & -\frac{5}{4} & 1 & -\frac{5}{2} \end{bmatrix},$$

$$\boldsymbol{F}_{\mathbb{V}_2^a} = \begin{bmatrix} \frac{2}{5} & -\frac{29}{20} & -\frac{1}{2} & \frac{3}{5} \\ 4 & -\frac{7}{2} & -3 & 0 \\ -\frac{4}{5} & -\frac{17}{20} & -\frac{1}{2} & \frac{4}{5} \\ 0.4 & -\frac{7}{10} & 1 & -\frac{7}{5} \end{bmatrix}, \qquad \boldsymbol{F}_{\mathbb{V}_3^a} = \begin{bmatrix} \frac{3}{4} & -\frac{37}{20} & -\frac{9}{10} & \frac{7}{10} \\ \frac{5}{2} & -\frac{13}{10} & -\frac{1}{10} & -\frac{7}{5} \\ \frac{5}{2} & -\frac{17}{5} & -\frac{18}{5} & \frac{9}{5} \\ \frac{5}{2} & \frac{21}{10} & \frac{2}{5} & -\frac{29}{10} \end{bmatrix},$$

which commonly have a pair of purely imaginary eigenvalues $\pm\imath$ and the others belong to the open left-half complex plane. In particular, the eigenspaces associated with the $\pm\imath$ share in common for all social entities in $\mathbb{V}$. In response to Theorem 3.6, the opinions of actors in the network reach output (state) polarization under the protocol (3.32b), as shown in Figure 3.3b which also demonstrates that the asymptotic states of the polarized opinions fall into a dynamic trajectory rather than a static value. To visualize the opinion neutralization, we set the weight of link $(10, 12)$ to be -2, thus violating the structural balance of graph $\mathcal{G}(\boldsymbol{\mathcal{L}})$. According to Theorem 3.7, the public opinions asymptotically turn into neutrality whatever their initial attitudes were. The trajectory curves of opinion variables in the neutralization case are plotted in Figure 3.3c.

Finally, we select the system matrices by

$$\boldsymbol{\Psi}_{\mathbb{V}^m} = \begin{bmatrix} -\frac{5}{2} & 1 & -\frac{3}{2} & -1 \\ 1 & 1 & -1 & -4 \\ -\frac{3}{2} & -1 & -\frac{5}{2} & 1 \\ 1 & 1 & -1 & -4 \end{bmatrix}, \qquad \boldsymbol{F}_{\mathbb{V}_1^a} = \begin{bmatrix} -1 & 0 & -1 & 0 \\ 6 & 2 & 4 & -6 \\ -2 & -2 & -4 & 2 \\ 3 & 0 & -1 & -4 \end{bmatrix},$$

$$\boldsymbol{F}_{\mathbb{V}_2^a} = \begin{bmatrix} 2 & 3 & -3 & -11 \\ 5 & 3 & -5 & -16 \\ -2 & -3 & 1 & 9 \\ 3 & 3 & -3 & -12 \end{bmatrix}, \qquad \boldsymbol{F}_{\mathbb{V}_3^a} = \begin{bmatrix} -\frac{7}{2} & 4 & \frac{1}{2} & -4 \\ -1 & 4 & 1 & -6 \\ 0.5 & -4 & -\frac{7}{2} & 4 \\ -1 & 4 & 1 & -6 \end{bmatrix},$$

whose eigenvalues all have negative real eigenvalues except the common semi-simple eigenvalues at zero. In particular, all nodes have an isomorphic eigenspace associated to the common zero eigenvalues. As discussed in Remark 3.5, the opinions of actors and media split into two polarized camps with two stationary equilibrium values whose signs are opposite. See Figure 3.3d for a graphic illustration.

3.3 Literature Review

Before concluding this chapter, we present a short overview of the literature relevant to our investigation.

The LTI system (3.26) describing dynamical diffusion processes has been widely adopted in analyzing the collective behavior of multi-agent systems on cooperative networks, including agreement- [MZ10; XS16] and disagreement-problems [XC11]. Only very recently in the context of coopetitive networks have researchers started to employ a state-feedback LTI model to study bipartite consensus [VM14; ZC17]. In the special case of zero matrix $\boldsymbol{F}_i$ and identity matrix $\boldsymbol{G}_i$ and $\boldsymbol{H}_i$, the model (3.26) of opinion evolving on single topic degenerates to Altafini-type model [Alt13]. Furthermore, a nonlinear counterpart of the model (3.26a) with the controller (3.26b) is proposed in [PC16]. All those cited literature is dedicated to studying the opinion formation problems of scalar-valued variables. Other research work on the vector-valued opinions appears in recent publications [VM14; FPTP16; PPTF17].

The quorum-sensing communication architecture, despite arising from different social contexts, motivates the focused study of opinion dynamics in this chapter. Along with this line of research, most literature focus on the understanding of the opinion-forming processes under the impact of stubborn leaders [GS14] or an exogenous constant signal [HK15]. Other works [QCS14; MJB14] take into account the importance of audiences on media and suggest using a bounded confidence model (BCM) to formulate the communication links. The truncation effect of BCM, however, prevents the use of commonly available tools for analyzing dynamical systems.

3.4 Summary

In this chapter, we develop a model of opinion dynamics governed by endogenous (self-dynamics) and exogenous (inflowing information) factors. First of all, the criteria for the stationary bipartite consensusablity and neutralizability, in terms of sufficient and necessary conditions, are provided, respectively. Among those conditions, the constraints on individuals' self-dynamics are of key importance that is different from the existing results proposed in the relevant literature which mainly focus on the topological properties of the underlying graphs. Then, we investigate how external media influence individuals' opinions through different strategies. In connection with output-regulation problem in control theory, we propose a mathematical model to describe the dynamics of autocratic media who dominate the outcome of opinion discussion. The numerical tests demonstrate the obtained results.

... that our self-concepts are formed as reflections of the responses and evaluations of others in our environment.

V. Gecas and M.L. Schwalbe

Chapter 4

Opinion Dynamics and Self-Appraisal of Social Power on Signed Networks

This chapter addresses the analysis of individuals' opinion-forming processes along a sequence of issues. The shifting from single-issue opinion formation to opinion evolution over sequential issues relaxes the assumption that the interpersonal influence network is static. More specifically, individuals can modify their relative influence structure in response to their self-appraisals of social power. The major focus of this chapter is on exploring the coevolution of opinion dynamics and social power over social networks containing antagonistic interconnections. The emergence of positive and negative interpersonal influence attributes to the individuals' interpersonal appraisal along the issue sequence. This more general view is also corroborated by the social phenomena of the coexistence of various contrasting relationships (friendly/hostile, like/dislike, trust/distrust, etc.). Hence, we develop a succinct mathematical treatment for the evolution of social power, self-evaluation, and interpersonal influences on signed social networks. By applying classical Lyapunov theory to the tangent bundle, a rigorous mathematical analysis is conducted to examine the convergence behavior and to demonstrate the existence and uniqueness of the equilibrium. We also study the non-stationary convergence property or dynamic appraisal networks using Lyapunov-based contraction analysis leading to the insight that group members forget their initial perception of social influence and the long-term configuration of their social power is completely determined by the underlying topological property of the appraisal networks. Furthermore, a graph-theoretic interpretation of individuals' social power is provided to expose topologically how individuals allocate their relative importance to others through influence networks. This interpretation facilitates the extension of obtained results to networks with weaker topology constraints.

The remainder of this chapter is organized as follows. In Section 4.1, the mathematical models, spectral properties of the influence matrix, explicit mathematical formulation of social power are presented. Section 4.2 contains a complete mathematical analysis of the convergence properties of the proposed models. Section 4.3 illustrates the graph-theoretic description of social power over signed networks and develops some further theoretical extensions. Illustrative simulations are presented in Section 4.4. Section 4.5 presents a literature overview of related works and Section 4.6 eventually concludes this article.

4.1 Problem Formulation

Before embarking this section, we introduce some basic concepts and fix the notation. The set of n-dimensional vectors whose 1-norm is 1 forms the surface of an n-dimensional *cross-polytope* or *orthoplex*, i.e., $\mathbb{D}^n := \{\boldsymbol{z} \in \mathbb{R}^n | -1 \le \boldsymbol{z} \le 1, \|\boldsymbol{z}\|_1 = 1\}$, which has an interior $\operatorname{int}(\mathbb{D}^n) := \{\boldsymbol{z} \in \mathbb{R}^n | -1 < \boldsymbol{z} < 1, \|\boldsymbol{z}\|_1 = 1\}$. To save triviality, the orthoplex manifold with the exclusion of vertices is given by $\nabla\mathbb{D}^n := \mathbb{D}^n \backslash \{\pm\boldsymbol{e}_1, \dots, \pm\boldsymbol{e}_n\}$. The n-dimensional simplex is given by $\mathbb{S}^n := \{\boldsymbol{z} \in \mathbb{R}^n | \boldsymbol{z} \ge 0, \mathbf{1}_n^\top \boldsymbol{z} = 1\}$ with the interior $\operatorname{int}(\mathbb{S}^n) = \{\boldsymbol{z} \in \mathbb{R}^n | \boldsymbol{z} > 0, \mathbf{1}_n^\top \boldsymbol{z} = 1\}$ and the tangent space $T_z\mathbb{S}^n = \{\delta\boldsymbol{z} \in \mathbb{R}^n | \mathbf{1}_n^\top \delta\boldsymbol{z} = 0\}$. Finally, we denote $\nabla\mathbb{S}^n := \mathbb{S}^n \backslash \{\boldsymbol{e}_1, \dots, \boldsymbol{e}_n\}$.

4.1.1 Mathematical Modeling

The starting point of this section is the extension of Altafini's opinion model [Alt13] on a single issue to the opinion-forming process over a sequence of issues $\mathbb{I} = \{0, 1, 2, \dots\}$. On the issue $s \in \mathbb{I}$, each agent $i \in \{1, \dots, n\}$ $(n \ge 2)$ is associated with a time-dependent and issue-dependent variable $x_i(s,t) \in \mathbb{R}$ that represents his or her attitude on issue s at time t. Agents update their opinions according to the following rule

$$x_i(s, t+1) = p_{ii}(s) x_i(s,t) + \sum_{j \ne i}^{n} p_{ij}(s) x_j(s,t) \tag{4.1}$$

where $p_{ii}(s) \in [0,1]$ is the self-weight and $p_{ij}(s) \in [-1,1]$ is the interpersonal influence weight that agent i attaches to the opinion of agent j such that $\sum_{j=1}^{n} |p_{ij}(s)| = 1$ on each issue s. Here, $p_{ij}(s)$ is issue-dependent and remains fixed for each issue under discussion.

By defining $\boldsymbol{x} = [x_1, \dots, x_n]^\top$, the opinion dynamics of the entire group can be reformulated to a compact form

$$\boldsymbol{x}(s, t+1) = \boldsymbol{P}(s)\boldsymbol{x}(s,t), \quad \boldsymbol{x}(s,0) \in \mathbb{R}^n \tag{4.2}$$

where $\boldsymbol{P}$ is referred to as the so-called *influence matrix* which has non-negative diagonals. In an unsigned setting, the update rule (4.2) on a single issue reduces to the well-known DeGroot model [DeG74] of opinion dynamics, in which the influence matrix $\boldsymbol{P} \in \mathbb{R}_{\ge 0}^{n \times n}$ satisfies the row-stochasticity. In this chapter, however, $\boldsymbol{P}$ usually needs not to be row-stochastic, unless edges are all with non-negative weights.

In reference to the dynamic model (4.2), the diagonal and non-diagonal entries of the influence matrix have distinct roles in opinion assimilation. The self-weights p_{ii} of $\boldsymbol{P}$ are designated as the individual self-appraisal (self-worth, self-confidence, self-esteem) indicator which corresponds to the degree of assertiveness to their own opinions, whereas the interpersonal weight p_{ij} $(j \ne i)$ represents individual i's extent of trust-distrust to the displayed opinion of individual j. The reflected appraisal mechanism of Friedkin [Fri11] illustrates that individuals intentionally revise their interpersonal influence structure based on the prior issue negotiation, thereby adjusting the interpersonal allocation of influence networks. Besides, our work in this chapter involves an interpersonal appraisal mechanism [GS83] in assisting the self-appraisal process. This elementary psychological mechanism describes that before embarking on a new issue discussion, individuals naturally prefer to evaluate their social ties – friendships and enmities – with others. As such, the influence weight p_{ij} that the i-th individual entails on the neighbor j's conveyed opinion is modified according to $p_{ij}(s)=(1-p_{ii}(s))q_{ij}(s)$, where $q_{ij}(s)$ corresponds to individual i's (positive or negative) appraisal of individual j on previous issue discussion. In other words, individuals allocate the aggregate relative influence $1-p_{ii}$ to other neighboring members in correspondence with the interpersonal appraisal q_{ij}. With the definition $q_{ii}=0$, the interpersonal appraisal mechanism is encoded by a matrix $\boldsymbol{Q}(s):=[q_{ij}(s)]\in\mathbb{R}^{n\times n}$ which satisfies $\sum_j^n |q_{ij}(s)|=1$ for all $i\in\{1,\dots,n\}$ and consequently ensures $\sum_j^n |p_{ij}(s)|=1$. Note that the matrix $\boldsymbol{Q}$ is an issue-specific variable and its non-diagonal entries describing appraisals that individuals grant peers are not always positive and may be negative. Moreover, zero non-diagonal entry q_{ij} $(j\neq i)$ means individual i does not know individual j. Central in the sequel of this chapter is to characterize the evolutionary property of individuals' self-appraisals along the sequence of issues, so we use the shorthand notation $z_i(s):=p_{ii}(s)$ for $i\in\mathbb{V}$ for an easy exposition. As a result, the influence matrix along the issue sequence is recast by

$$\boldsymbol{P}(\boldsymbol{z},\boldsymbol{Q})=\mathsf{diag}\big(\boldsymbol{z}(s)\big)+\big(\boldsymbol{I}_n-\mathsf{diag}(\boldsymbol{z}(s))\big)\boldsymbol{Q}(s). \tag{4.3}$$

Throughout this chapter, we sometimes drop the explicit dependence of matrix $\boldsymbol{P}$ on $\boldsymbol{z}$ and $\boldsymbol{Q}$ and thus simply write $\boldsymbol{P}(s)$.

It is well-known that in the unsigned scenario where $\boldsymbol{P}$ is row stochastic on each issue, the strong connectedness of graph $\mathcal{G}(\boldsymbol{P}(s))$ implies the existence of a unique normalized left eigenvector $\boldsymbol{p}(s)\in\mathbb{R}^n_{>0}$ associated to the dominant eigenvalue 1 such that $\lim_{t\to\infty}\boldsymbol{P}^t(s)=\mathbf{1}_n\boldsymbol{p}^\top(s)$. This is an application of Perron-Frobenius theorem[1] [GR01] to irreducible nonnegative matrices. Accordingly, the issue discussion process (4.2) on issue s asymptotically reaches an opinion conformity

$$\lim_{t\to\infty}\boldsymbol{x}(s,t+1)=\big(\lim_{t\to\infty}\boldsymbol{P}^t(s)\big)\boldsymbol{x}(s,0)=\big(\boldsymbol{p}^\top(s)\boldsymbol{x}(s,0)\big)\mathbf{1}_n.$$

Namely, the beliefs of social actors converge to a common value as time progresses, which is equal to a convex combination of individuals' initial thoughts. Unlike the unsigned case, however, the signed influence matrix $\boldsymbol{P}(s)$ may not always have a dominant eigenvalue 1, even when the underlying topology $\mathcal{G}(\boldsymbol{P}(s))$ is strongly connected. Therefore, we now try to characterize the properties of the influence matrix.

Lemma 4.1: Properties of The Influence Matrix

Consider an interpersonal appraisal matrix $\boldsymbol{Q}(s)=[q_{ij}(s)]\in\mathbb{R}^{n\times n}$ on issue $s\in\mathbb{I}$, which has zero diagonal entries and satisfies $\sum_{j=1}^n |q_{ij}(s)|=1$ for all $i\in\mathbb{V}$. If the associated graph $\mathcal{G}(\boldsymbol{Q})$ is strongly connected and structurally balanced, then the following claims hold for the influence matrix $\boldsymbol{P}(\boldsymbol{z},\boldsymbol{Q})$ defined in (4.3)

(i) $\boldsymbol{P}$ has a simple eigenvalue 1 which is strictly larger than the magnitude of all other eigenvalues;

(ii) there exist a unique vector $\boldsymbol{p}(\boldsymbol{z},\boldsymbol{Q})\in\mathbb{D}^n$ and a vector $\boldsymbol{\rho}(s)=[\rho_i(s)]\in\{-1,1\}^n$ satisfying $\boldsymbol{Q}\boldsymbol{\rho}=\boldsymbol{\rho}$, such that $\boldsymbol{p}^\top\boldsymbol{P}=\boldsymbol{p}^\top$, $\boldsymbol{P}\boldsymbol{\rho}=\boldsymbol{\rho}$, and $\lim_{t\to\infty}\boldsymbol{P}^t=\boldsymbol{\rho}\boldsymbol{p}^\top$;

[1] The formal definition is reviewed in Section A.2.

(iii) $\boldsymbol{p}(\mathbf{1}/n, \boldsymbol{Q}) = \boldsymbol{\rho}(s)/n$ if and only if $\mathcal{G}(\boldsymbol{Q})$ is balanced;

(iv) $\mathcal{G}(\boldsymbol{P})$ is structurally balanced;

(v) if $\boldsymbol{z} = \boldsymbol{e}_i$ for some $i \in \{1, \ldots, n\}$, then $\mathcal{G}(\boldsymbol{P}(\boldsymbol{e}_i, \boldsymbol{Q}))$ has only one root at node i and $\boldsymbol{p}(\boldsymbol{e}_i, \boldsymbol{Q}) = \rho_i(s)\boldsymbol{e}_i$;

(vi) if $\boldsymbol{z} \in \nabla\mathbb{S}^n$, the graph $\mathcal{G}(\boldsymbol{P})$ is strongly connected and $\mathrm{diag}(\boldsymbol{\rho})\boldsymbol{p} > 0$.

Proof. To make this treatment self-contained, the proof is not presented in the same order as the claims appearing in the lemma. First, we note that when $\boldsymbol{z} = \boldsymbol{e}_i$ for some $i \in \mathbb{V}$ or more concretely, let $i = n$ without loss of generality, the matrix $\boldsymbol{P}$ can be calculated by

$$\boldsymbol{P} = \mathrm{diag}(0, \ldots, 0, 1) + \mathrm{diag}(1, \ldots, 1, 0)\boldsymbol{Q} = \begin{bmatrix} \tilde{\boldsymbol{Q}}^\top & \boldsymbol{e}_n \end{bmatrix}^\top \tag{4.4}$$

where the matrix $\tilde{\boldsymbol{Q}} \in \mathbb{R}^{(n-1)\times n}$ is obtained by removing the n-th row from $\boldsymbol{Q}$. As $\mathcal{G}(\boldsymbol{Q})$ is strongly connected, each node of $\mathcal{G}(\boldsymbol{Q})$ has paths connecting to others. The observation that the associated graph of $\boldsymbol{P}$ given in (4.4) has no other root except for node n, which implies $\mathcal{G}(\boldsymbol{P})$ is only quasi-connected in the case $\boldsymbol{z} = \boldsymbol{e}_i$. By simply calculating, one can show $\boldsymbol{p}(\boldsymbol{e}_i, \boldsymbol{Q}) = \rho_i \boldsymbol{e}_i$. This completes the proof of statement (v). Meanwhile, $\mathcal{G}(\boldsymbol{P})$ here can be obtained from $\mathcal{G}(\boldsymbol{Q})$ by removing all incoming edges of node i and thus inherits the same structural balance from $\mathcal{G}(\boldsymbol{Q})$.

Regarding claim (vi), condition $\boldsymbol{z} \in \nabla\mathbb{S}^n$ implies the graph $\mathcal{G}(\boldsymbol{P} - \mathrm{diag}(\boldsymbol{z}))$ has the same sign pattern on the edge set as $\mathcal{G}(\boldsymbol{Q})$'s, namely, $\mathcal{G}(\boldsymbol{P} - \mathrm{diag}(\boldsymbol{z}))$ is strongly connected and structurally balanced. As the self-appraisals is $z_i \in [0, 1)$ for all $i \in \{1, \ldots, n\}$, the graph $\mathcal{G}(\boldsymbol{P})$ is also strongly connected and structurally balanced. The statements (iv) and the first part of statement (vi) are proved.

Next, the structural balance of $\mathcal{G}(\boldsymbol{P})$ implies the node set can be split into two disjoint subsets that the negatively weighted edges only exist between nodes belonging to distinct groups. By associating a vector $\boldsymbol{\rho} \in \{-1, 1\}^n$ to graph $\mathcal{G}(\boldsymbol{P})$, an observed relation is $p_{ij} = |p_{ij}|\rho_i\rho_j$ for all $i, j \in \mathbb{V}$, and thus one has

$$\mathrm{diag}(\boldsymbol{\rho})\boldsymbol{P}\,\mathrm{diag}(\boldsymbol{\rho}) = |\boldsymbol{P}|.$$

It is not difficult to show that $|\boldsymbol{P}|$ is a non-negative matrix and is row-stochastic. Thanks to the similar transformation, $\boldsymbol{P}$ and $|\boldsymbol{P}|$ share the same spectrum. Therefore, the application of the Perron-Frobenius theorem to $|\boldsymbol{P}|$ shows indirectly the existence, uniqueness, and other properties of the dominant left eigenvector $\boldsymbol{p}$ of matrix $\boldsymbol{P}$, as well as the spectral property. This is the proof of statement (i). Note that $\mathrm{diag}(\rho)\boldsymbol{p}$ is the left-eigenvector associated to eigenvalue 1 of $|\boldsymbol{P}|$, namely,

$$\boldsymbol{p}^\top \mathrm{diag}(\rho)|\boldsymbol{P}| = \boldsymbol{p}^\top \mathrm{diag}(\rho).$$

Therefore, if $\mathcal{G}(\boldsymbol{P})$ is strongly connected, as is $\mathcal{G}(|\boldsymbol{P}|)$, then the matrix $|\boldsymbol{P}|$ admits a unique (up to a scaling) left eigenvector $\mathrm{diag}(\rho)\boldsymbol{p} > 0$. The second part of statement (vi) is proved.

Moreover, direct calculation shows that

$$\sum_j^n p_{ij}\rho_j = \sum_j^n |p_{ij}|\rho_i = \rho_i, \quad i \in \mathbb{V},$$

as the 1-norm of each row of $\boldsymbol{P}$ equals to 1. Therefore, it holds $\boldsymbol{P}\boldsymbol{\rho}=\boldsymbol{\rho}$. The final asymptotic behavior $\lim_{t\to\infty}\boldsymbol{P}^t=\boldsymbol{\rho}\boldsymbol{p}^\top$ is an immediate consequence of claim (i), so the proof of claim (ii) is completed.

Finally, in regard to claim (iii), a direct computation is conducted on (4.3) by

$$\boldsymbol{P}(\mathbf{1}_n/n,\boldsymbol{Q})=\mathsf{diag}(\mathbf{1}_n/n)+(n-1)\boldsymbol{Q}/n,$$

of which by left multiplying $\boldsymbol{\rho}^\top/n$ to both sides, one can obtain $\boldsymbol{\rho}^\top\boldsymbol{P}(\mathbf{1}_n/n,\boldsymbol{Q})/n=\boldsymbol{\rho}^\top\mathsf{diag}(\mathbf{1}_n/n)/n+(n-1)\boldsymbol{\rho}^\top\boldsymbol{Q}/n^2$. As a result, if $\boldsymbol{p}(\mathbf{1}_n/n,\boldsymbol{Q})=\boldsymbol{\rho}^\top/n$, then $\boldsymbol{\rho}_n^\top\boldsymbol{Q}=\boldsymbol{\rho}_n^\top$, i.e., $\mathcal{G}(\boldsymbol{Q})$ is balanced according to the definition. Meanwhile, if $\mathcal{G}(\boldsymbol{Q})$ is balanced, one can immediately prove that $\boldsymbol{\rho}^\top\boldsymbol{P}(\mathbf{1}_n/n,\boldsymbol{Q})/n=\boldsymbol{\rho}^\top/n$, i.e., $\boldsymbol{p}=\boldsymbol{\rho}/n$. □

First, we focus on the networks $\mathcal{G}(\boldsymbol{Q})$ that are strongly connected and structurally balanced on each issue. As one will see, networks with weaker topological constraints are also covered, thus making the developments applicable to a wider range of real networks. An immediate consequence of claim (ii) in Lemma 4.1 is that the opinion dynamics (4.2) on signed influence networks converge after each issue discussion

$$\lim_{t\to\infty}\boldsymbol{x}(s,t)=\left(\boldsymbol{p}^\top(s)\boldsymbol{x}(s,0)\right)\boldsymbol{\rho}(s) \tag{4.5}$$

where $\boldsymbol{\rho}(s)\in\{-1,1\}^n$ and $\boldsymbol{p}(s)\in\mathbb{D}^n$ are the dominant right- and left-eigenvector of the influence matrix $\boldsymbol{P}(s)$ during issue s, respectively. Different from opinion consensus on cooperative networks, the individuals may not agree to a common (absolute) value but polarize themselves in two opposite groups.

The most important message of the convergence limit (4.5) is that the coefficient vector $\boldsymbol{p}(s)$ mathematically specifies the social contribution of individuals made to the final decision making. In other words, $\boldsymbol{p}(s)$ can be regarded as a social metric that measures the ability of individuals to relatively control the outcome of opinion discussion processes. As suggested by Cartwright in [Car56], this control ability is closely related to personal social power. In the spirit similar to the DeGroot-Friedkin model [JMFB15], we also equivalently refer the relative control and social power of agent $i\in\mathbb{V}$ to the entry $p_i(s)$, the stack vector form of which is formally defined by

$$\boldsymbol{p}(s)=\left(\lim_{t\to\infty}\left(\boldsymbol{P}^t(s)\right)\right)^\top\boldsymbol{\rho}(s)/n, \tag{4.6}$$

which is evidently coincident with the dominant left-eigenvector of $\boldsymbol{P}(s)$ on strongly connected and structurally balanced networks.

It is worthwhile to note that individuals may have some identical magnitude of social power but with distinct signs according to Lemma 4.1. This is slightly different from the sense of social power arising in the cooperative context [Car56]. It is customary to endow the social power with an orientation system such that the relative control exerting along the forward direction leads to a positive effect on issue discussions, while a negative influence along the backward direction, as addressed in [PPS16]. In fact, the sign pattern of social power could be more significant than their exact values in practical scenarios. For example, in information systems, to name a few, media industries including traditional mass media, e.g., TV, radio, and newspaper, and the recently emerged socio-technical platforms, e.g., blogs, Facebook and Twitter, are of fundamental importance in information distribution and news reporting. On some occasions, biased media with high audience rating may release misleading reports for political or commercial reasons, and manage

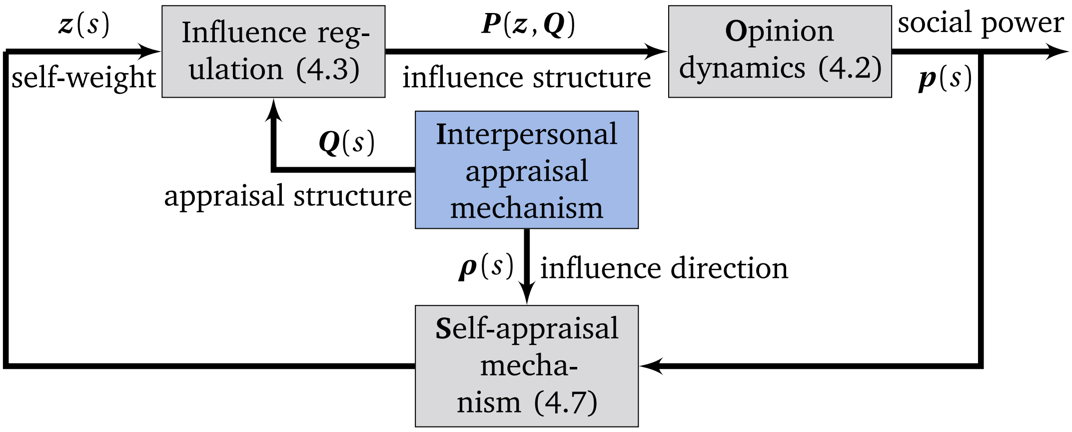

Figure 4.1: The schematic diagram of the coevolution of opinion dynamics and self-appraisal mechanism.

to persuade people to believe a perceived truth which is probably very far away from the actual fact. The social power entraining negative influence accounts for this phenomenon that media seeks to divert the public opinions away from the real truth. An example is the shifting of U.S. public attitudes from "unjustified" to "justified" on the 2003 invasion of Iraq after Powel's speech [FPTP16]. From this point of view, the dominant right eigenvector $\boldsymbol{\rho}$ is as informative as the dominant left eigenvector $\boldsymbol{p}$. Moreover, note that the oriented effect of social power is argued in a relative sense; that is, the positiveness and negativeness of individual power are defined in a relative coordinate but do not imply its absolute direction. For instance, although Powel's speech fulfills a passive function on shaping the public opinion of the Iraq invasion, it plays an active role from the perspective of a few politicians.

Now, our aim is to deliberate how the self-confidence level $s \mapsto \boldsymbol{z}(s)$ evolves along the issue sequence. In an influence network with antagonism, the self-weight of individuals is updated after each issue discussion according to the following rule

$$\boldsymbol{z}(s+1) = \mathsf{diag}\big(\boldsymbol{\rho}(s)\big)\boldsymbol{p}(s) \tag{4.7}$$

where $\boldsymbol{p}(s) \in \mathbb{D}^n$ and $\boldsymbol{\rho}(s) \in \{-1, 1\}^n$ are the dominant left- and right- eigenvectors of the influence matrix $\boldsymbol{P}(s)$, respectively. Note that the update rule (4.7) involving the normalized vector $\boldsymbol{p}$, i.e., $||\boldsymbol{p}||_1 = 1$, implies that the elements of self-confidence level $\boldsymbol{z}$ are nonnegative and have unit sum $\mathbf{1}_n^\top \boldsymbol{z} = 1$, i.e., $\boldsymbol{z}(s) \in \mathbb{S}^n$. The self-appraisal process (4.7) imitates Friedkin's *reflected appraisal* mechanism [Fri11] and more details about its psychological interpretations and empirical verifications can be found in the seminal work [FJB16]. The design philosophy of the entire framework is illustrated in Figure 4.1, in which the outputs of the interpersonal appraisal systems govern the coevolutionary networks involving the feedback loop of influence structure and opinion dynamics.

Hence, the model (4.7) exposes how the interpersonal influence system affects individuals' perception of social power along the issue sequence. Furthermore, the development in (4.7) reflects the psychological fact that there may be a dramatic discrepancy between self-perception and reality [Fri11]. Indeed, the self-appraisal vector of individuals takes values in $\mathbb{S}^n$ for all issues, while the social power metric $\boldsymbol{p}(s)$ allows negative vectors in $\mathbb{D}^n$ in the light of Lemma 4.1. Such deviation in the sign agrees with the sociological and psychological fact that self-esteem reflects individuals' subjective but not necessarily objective assessment of his or her own power [LS11]. On one hand, the individual generally has a positive self-impression [Fri11]. On the other hand, the network-wide calculator concerning social power represents what the actual appraisals of others on each agent are, and is an objective study of the net effect. As such, the self-appraisal mechanism (4.7) aims to adaptively modify the status of individuals (assertion vs. reconciliation, confidence vs. uncertainty) in response to their absolute power over prior issue outcomes.

When the underlying network has no edge with negative weight, the self-appraisal model (4.7) reduces to the traditional DeGroot-Friedkin model examined in [JMFB15; FJB16], wherein the dominant left- and right-eigenvector here degenerate to a non-negative vector and $\mathbf{1}_n$, respectively. Therefore, the DeGroot-Friedkin framework that unfolds on a cooperative network can be treated as a special case of our investigation.

4.1.2 Explicit Formulas

At the end of this section, we explore the explicit formula of the evolutionary dynamics of self-weights and social power.

Proposition 4.1: Explicit Formulation

For each issue $s \in \mathbb{I}$, let $\boldsymbol{q}(s)$ be the dominant left eigenvector of $\boldsymbol{Q}(s) \in \mathbb{R}^{n\times n}$ that per-issue has zero diagonal entries and an induced graph $\mathcal{G}(\boldsymbol{Q})$ that is strongly connected and structurally balanced. The dynamics of self-appraisal (4.7) are equivalent to the discrete-time system

$$\boldsymbol{z}(s+1) = \boldsymbol{f}(\boldsymbol{z}, s), \tag{4.8}$$

where $f : \mathbb{S}^n \times \mathbb{I} \to \mathbb{S}^n$ is a smooth map defined by

$$\boldsymbol{f}(\boldsymbol{z}, s) = \theta(\boldsymbol{z}, s)\Big[\frac{\rho_1(s)q_1(s)}{1 - z_1(s)}, \cdots, \frac{\rho_n(s)q_n(s)}{1 - z_n(s)}\Big]^\mathsf{T} \tag{4.9}$$

where

$$\theta(\boldsymbol{z}, s) = 1 / \sum_{i=1}^{n} \frac{\rho_i(s)q_i(s)}{1 - z_i(s)}$$

is a scaling factor and $\boldsymbol{\rho}(s) := [\rho_1(s), \ldots, \rho_n(s)]^\mathsf{T} \in \{-1, 1\}^n$ satisfies $\boldsymbol{Q}(s)\boldsymbol{\rho}(s) = \boldsymbol{\rho}(s)$.

Proof. First, we have already known that $\boldsymbol{z}(s+1) = \boldsymbol{e}_i$ if $\boldsymbol{z}(s) = \boldsymbol{e}_i$ according to statement (v) of Lemma 4.1. For the self-weight $\boldsymbol{z}(s) \in \nabla\mathbb{S}^n$ at issue $s \in \mathbb{I}$, an immediate deduction from (4.7) is

$$\boldsymbol{P}^\mathsf{T}(s)(\boldsymbol{z}(s))\mathsf{diag}(\boldsymbol{\rho}(s))\boldsymbol{z}(s+1) = \mathsf{diag}(\boldsymbol{\rho}(s))\boldsymbol{z}(s+1).$$

In conjunction with the forming of influence matrix given in (4.3), straightforward computation shows

$$\boldsymbol{Q}^\mathsf{T}(s)\,\mathsf{diag}(\mathbf{1}_n - \boldsymbol{z}(s))\,\mathsf{diag}(\boldsymbol{\rho}(s))\boldsymbol{z}(s+1) = \mathsf{diag}(\mathbf{1}_n - \boldsymbol{z}(s))\,\mathsf{diag}(\boldsymbol{\rho}(s))\boldsymbol{z}(s+1),$$

which means that $\mathsf{diag}(\mathbf{1}_n - \boldsymbol{z}(s))\mathsf{diag}(\boldsymbol{\rho}(s))\boldsymbol{z}(s+1)$ is a left eigenvector corresponding to eigenvalue 1 of $\boldsymbol{Q}$. Bearing in mind $\boldsymbol{z}(s+1) \in \mathbb{S}^n$, one can acquire

$$\rho_i(s)(1 - z_i(s))z_i(s+1) = \theta(\boldsymbol{z}, s)q_i(s) \quad \forall\, i \in \mathbb{V},$$

wherein the scaling coefficient $\theta(\boldsymbol{z},s)=1/\sum_{i=1}^{n}\frac{\rho_i(s)q_i(s)}{1-z_i(s)}$ guarantees $\boldsymbol{z}(s+1)\in\mathbb{S}^n$.

Since the map $\boldsymbol{f}:\mathbb{S}^n\times\mathbb{I}\to\mathbb{S}^n$ has an analytic expression for $\boldsymbol{z}\in\mathbb{S}^n$, the continuity of $\boldsymbol{f}$ on $\mathbb{S}^n$ is clear. The remaining task is to prove the differentiability of map $\boldsymbol{f}$ at the vertices of the simplex. At issue $s\in\mathbb{I}$, consider the self-weight variables in a neighborhood of $\boldsymbol{e}_i$. For any $\boldsymbol{z}\in\{\boldsymbol{z}\in\mathbb{S}^n|\mathrm{d}_{\mathbb{S}}(\boldsymbol{z},\boldsymbol{e}_i)\le c,\boldsymbol{z}\neq\boldsymbol{e}_i\}$ where $\mathrm{d}_{\mathbb{S}}:\mathbb{S}^n\times\mathbb{S}^n\to\mathbb{R}$ is a metric on $\mathbb{S}^n$ and $c>0$ is a constant scalar, entries of $\boldsymbol{z}$ satisfy $z_j<1$ for all $j\in\{1,,\cdots,n\}$ which allows for the computation of the Jacobian of the vector field $\boldsymbol{f}$ in this neighborhood. To obviate the emergence of zero value in the denominators of $\boldsymbol{f}$ given in (4.9) as $\boldsymbol{z}\to\boldsymbol{e}_i$, we rewrite the vector field into the following pattern

$$\begin{aligned}\boldsymbol{f}(\boldsymbol{z},s)=\Big[\frac{\theta(\boldsymbol{z})}{1-z_i(s)}\frac{\rho_1(s)q_1(s)(1-z_i(s))}{1-z_1(s)},\ldots,\frac{\theta(\boldsymbol{z})\rho_i(s)q_i(s)}{1-z_i(s)},\\ \ldots,\frac{\theta(\boldsymbol{z})}{1-z_i(s)}\frac{\rho_n(s)q_n(s)(1-z_i(s))}{1-z_n(s)}\Big]^{\mathsf{T}},\end{aligned}$$

from which its Jacobian matrix evaluated at $\boldsymbol{e}_i$ can be obtained by

$$\frac{\partial\boldsymbol{f}}{\partial\boldsymbol{z}}(\boldsymbol{z},s)=\begin{bmatrix}0&\cdots&-\frac{\rho_1(s)q_1(s)}{\rho_i(s)q_i(s)}&\cdots&0\\ \vdots&&\vdots&&\vdots\\ 0&\cdots&\frac{1-\rho_i(s)q_i(s)}{\rho_i(s)q_i(s)}&\cdots&0\\ \vdots&&\vdots&&\vdots\\ 0&\cdots&-\frac{\rho_n(s)q_n(s)}{\rho_i(s)q_i(s)}&\cdots&0\end{bmatrix}\tag{4.10}$$

which implies that $\boldsymbol{f}$ is differentiable at $\boldsymbol{e}_i$. Obviously, the first order partial derivative of $\boldsymbol{f}$ is continuous for $\boldsymbol{z}\in\mathbb{S}^n$. The higher order differentiability of function $\boldsymbol{f}$ can be deduced in the same manner. Therefore, the smoothness of $\boldsymbol{f}$ is the immediate consequence of the differentiability for all orders and thus, the proof is completed. □

Lastly, we specify two distinct configurations of social power: *autocracy* and *democracy*. The autocratic power structure features the existence of a dictator-like individual who dominantly holds all the absolute social power and other members of the organization are dramatically vulnerable to the interpersonal influence. On the other end of the spectrum, the democratic social power configuration characterizes the members of social networks equally involving in making the final decision.

4.2 Convergence Analysis

In this section, we first examine the convergence of the proposed self-appraisal model on constant networks and then develop the extension to dynamic networks in an appealing generic setting.

4.2.1 Constant Interpersonal Appraisal with Structure Balance

In this subsection, we concentrate on an invariant interpersonal appraisal structure under which issue discussants are stubborn and along the issue sequence they stick to their first impressions of others. The self-appraisal dynamics (4.8) correspondingly degenerate to a nonlinear autonomous system. With the same assumption as in the previous section, the graph modeling the interpersonal appraisal structure is strongly connected and structurally balanced.

We first study an extreme situation in which the underlying graph $\mathcal{G}(\boldsymbol{Q})$ is a star graph. Some special properties emerge in this scenario.

Lemma 4.2: Properties of Star Graph

Suppose that $n \geq 3$ and the digraph $\mathcal{G}(\boldsymbol{Q})$ is a strongly connected and structurally balanced. Let $\boldsymbol{q}$ be the dominant left eigenvector of $\boldsymbol{Q}$ associated to eigenvalue 1. Then, the following statements hold

(i) $|q_i| \leq 1/2$ for all $i \in \{1, \ldots, n\}$;

(ii) there exists a node i with $|q_i| = 1/2$ if and only if $\mathcal{G}(\boldsymbol{Q})$ is a star centered at node i. Moreover, the self-weights $\boldsymbol{z}$ governed by the dynamics (4.7) converge to $\boldsymbol{e}_i$ for arbitrary $\boldsymbol{z}(0) \in \nabla\mathbb{S}^n$ and the social power $\boldsymbol{p}(\boldsymbol{e}_i)$ given in (4.6) converges to $\rho_i \boldsymbol{e}_i$ for all initial conditions $\boldsymbol{z}(0) \in \nabla\mathbb{S}^n$.

Proof. The proof here resembles the one of Lemma 2.3 in [JMFB15]. From the definition of the dominant left eigenvector, one can straightforwardly calculate $q_i = \sum_{j=1, j\neq i}^{n} q_j q_{ji}$. As $|q_{ij}| \leq 1$ for $i, j \in \mathbb{V}$ from the notation and $\|\boldsymbol{q}\|_1 = 1$, one can obtain

$$|q_i| \leq \sum_{j=1, j\neq i}^{n} |q_j||q_{ji}| \leq \sum_{j=1, j\neq i}^{n} |q_j| = 1 - |q_i|,$$

which implies $|q_i| \leq 1/2$ for all $i \in \mathbb{V}$. This is the proof of statement (i).

For statement (ii), we first note that a signed graph with star topology is always structurally balanced. Let individual i be the node with $|q_i| = \frac{1}{2}$ without loss of generality. An immediate consequence is to make

$$\sum_{j=1, j\neq i}^{n} |q_j q_{ji}| = \sum_{j=1, j\neq i}^{n} |q_j|,$$

which is equivalent to

$$\sum_{j=1, j\neq i}^{n} |q_j||q_{ji}| = \sum_{j=1, j\neq i}^{n} |q_j|$$

thanks to graph structural balance $|q_{ji}| = \rho_i \rho_j q_{ji}$, where $\rho_i, \rho_j \in \{-1, 1\}$. Since the strong connectivity assumption of $\mathcal{G}(\boldsymbol{Q})$ implies $q_i \neq 0$ for all $i \in \mathbb{V}$, the node i has $|q_i| = 1/2$ if and only if $|q_{ji}| = 1$ for all $j \in \mathbb{V}$. The fact that the 1-norm of each row of matrix $\boldsymbol{Q}$ is equal to zero uncovers $q_{jk} = 0$ for all $j, k \in \mathbb{V} \backslash \{i\}$ evidences that node i is the center vertex and $\mathcal{G}(\boldsymbol{Q})$ is a star graph.

Next, we elaborate on the convergence analysis of the self-appraisal dynamics (4.8) under the interpersonal appraisal structure with a star topology. Let agent n be the center node of graph $\mathcal{G}(\boldsymbol{Q})$, without loss of generality. The observation that $\boldsymbol{f}(\boldsymbol{e}_i) = \boldsymbol{e}_i$ for all $i \in \mathbb{V}$ exposes that $\{\boldsymbol{e}_1, \ldots, \boldsymbol{e}_n\}$ are fixed points of self-appraisal dynamics (4.8). To demonstrate the nonexistence of equilibria in $\nabla\mathbb{S}^n$ when $\mathcal{G}(\boldsymbol{Q})$ is a star graph, we assume on the contrary that there exists a vector $\boldsymbol{z}^* \in \nabla\mathbb{S}^n$ such that $\boldsymbol{z}^* = \boldsymbol{f}(\boldsymbol{z}^*)$ or individually, $z_i^*(1-z_i^*) = \theta(\boldsymbol{z}^*)\rho_i q_i$ for all $i \in \mathbb{V}$. Note that $\theta(\boldsymbol{z}^*) > 0$ for $\boldsymbol{z}^* \in \nabla\mathbb{S}^n$. Thanks to the Perron-Frobenius Theorem [GR01], the graph $\mathcal{G}(\boldsymbol{Q})$ that is strongly connected and structurally balanced, yields $\rho_i q_i > 0$ for all $i \in \mathbb{V}$, thereby deriving $0 < z_i^* < 1$. It is already known that the center node n entails

$$\rho_n q_n = |q_n| = 1 - \sum_{j=1}^{n-1} |q_j| = 1/2,$$

thus

$$\sum_{j=1}^{n-1} z_j^*(1-z_j^*) = \theta(\boldsymbol{z}^*) \sum_{j=1}^{n-1} |q_i| = \rho_n q_n \theta(\boldsymbol{z}^*) = z_n^*(1-z_n^*). \tag{4.11}$$

On the other hand, $z_n^* < 1 - z_j^*$ as $n \geq 3$ and $z_i^* > 0$ for all $i \in \mathbb{V}$. Hence, $z_n^* z_j^* < z_j^*(1-z_j^*)$ for all $j \in \mathbb{V}\backslash\{n\}$. This implies

$$\sum_{j=1}^{n-1} z_j^*(1-z_j^*) > \sum_{j=1}^{n-1} z_n^* z_j^* = z_n^*(1-z_n^*),$$

which contradicts (4.11). Thus, there does not exist such an equilibrium in $\nabla\mathbb{S}^n$ when graph $\mathcal{G}(\boldsymbol{Q})$ has a star topological structure.

Regarding the second half of statement (ii), it is already known so far that if $\boldsymbol{z}(s_1) = \boldsymbol{e}_n$ at certain issue $s_1 \in \mathbb{I}$, then the self-weights remain invariant $\boldsymbol{z}(s) = \boldsymbol{e}_n$ for $s > s_1$. Now, it remains to show the convergence of the self-appraisal mechanism in the non-trivial situation $\boldsymbol{z}(0) \in \nabla\mathbb{S}^n$ which divides into two cases: 1) $z_n(0) = 0$ and 2) $z_n(0) > 0$. For the first case, it is easy to obtain

$$z_n(1) := \theta(\boldsymbol{z}(0)) \frac{\rho_n q_n}{1 - z_n(0)} = \frac{1}{1 + \sum_{j=1}^{n-1} \frac{\rho_j q_j}{1-z_j}} > 0,$$

where $\rho_n q_n = 1/2$ as shown in above. Ordinarily, one has $z_n(s+1) > z_n(s)$ for any $z_n(s) = 0$. As $0 < z_n(s) < 1$, the immediate consequence $1 - z_j(s) \geq z_n(s)$ for any $j \in \{1, \ldots, n-1\}$ leads to

$$\sum_{j=1}^{n-1} \frac{\rho_j q_j}{1-z_j} \leq \frac{1}{z_n} \sum_{j=1}^{n-1} \rho_j q_j = \rho_n q_n / z_n.$$

Now, we rule out the possibility of equality $\sum_{j=1}^{n-1} \frac{\rho_j q_j}{1-z_j} = \rho_n q_n / z_n$ which implies there exists $k \in \{1, \ldots, n-1\}$ such that $1 - z_k = z_n$ and $z_j = 0$ for other $j \neq k$. Then, one can infer that

$$\sum_{j=1}^{n-1} \frac{\rho_j q_j}{1-z_j} = \frac{\rho_k q_k}{1-z_k} + \sum_{j=1, j\neq k}^{n-1} \frac{\rho_j q_j}{1-z_j} = \frac{\rho_k q_k}{z_n} + (\rho_n q_n - \rho_k q_k) < \frac{\rho_n q_n}{z_n}, \tag{4.12}$$

where the fact that $\rho_n q_n > \rho_k q_k$ is taken into account. The inequality (4.12) enables us to obtain $\theta(\boldsymbol{z}) > z_n(1-z_n)/\rho_n q_n$, as well as the more important result that $z_n(s+1) - z_n(s) > 0$ for $z_n(s) \in]0, 1[$. In summary, one can acquire that $z_n(s+1) - z_n(s) > 0$ for $z_n(s) \in [0, 1[$ and $z_n(s+1) = z_n(s)$ when $z_n(s) = 1$.

Next, we consider a Lyapunov function candidate by

$$V(\boldsymbol{z}(s)) = \frac{1}{2}\|\boldsymbol{z}(s) - \boldsymbol{e}_n\|_1, \quad \text{for } \boldsymbol{z} \in \mathbb{S}^n$$

which has the difference

$$V(\boldsymbol{z}(s+1)) - V(\boldsymbol{z}(s)) = z_n(s) - \frac{\theta(\boldsymbol{z}(s))\rho_n q_n}{1 - z_n(s)}, \tag{4.13}$$

where $\theta(\boldsymbol{z})$ is well defined and $\theta(\boldsymbol{z}) > 0$ for $\boldsymbol{z}(s) \in \nabla\mathbb{S}^n$.

In the trivial case $z_n(s) = 0$, the difference of Lyapunov function (4.13) leads to $V(\boldsymbol{z}(s+1)) < V(\boldsymbol{z}(s))$. For the nontrivial situation $z_n(s) > 0$, the factor $\theta(\boldsymbol{z})$ has a lower bound as follows

$$\theta(\boldsymbol{z}) = \frac{1}{\frac{\rho_n q_n}{1 - z_n(s)} + \sum_{j=1}^{n-1} \frac{\rho_j q_j}{1 - z_j(s)}} \geq \frac{1}{\frac{\rho_n q_n}{1 - z_n(s)} + \frac{\rho_n q_n}{z_n(s)}} = \frac{z_n(1 - z_n)}{\rho_n q_n}, \tag{4.14}$$

where the inequality is derived from $1 - z_j \geq z_n$ for $j \in \mathbb{V}\backslash\{n\}$ and $\rho_n q_n = \sum_{j=1}^{n-1} \rho_j q_j$. Additionally, we underline the lower bound is given in a strict sense. Supposed there exists $k \in \mathbb{V}\backslash\{n\}$ such that $1 - z_k = z_n$, one can obtain that

$$\sum_{j}^{n-1} \frac{\rho_j q_j}{1 - z_j(s)} = \frac{\rho_k q_k}{1 - z_k(s)} + (\rho_n q_n - \rho_k q_k) < \frac{\rho_n q_n}{z_n},$$

wherein the property $|q_n| > |q_k|$ for all $k \in \mathbb{V}\backslash\{n\}$ is used. Hence, one can draw conclusion on the difference of Lyapunov function along the issue sequence as $V(\boldsymbol{z}(s+1)) < V(\boldsymbol{z}(s))$, $\forall \boldsymbol{z}(s) \in \nabla\mathbb{S}^n$, where $V(\boldsymbol{z}(s)) > 0$ for all $\boldsymbol{z}(s) \in \nabla\mathbb{S}^n$. In conclusion, we claim that $\boldsymbol{e}_n$ is the asymptotically stable equilibrium point for self-appraisal dynamic (4.8) in the case of $\mathcal{G}(\boldsymbol{Q})$ having a star topology. This is a direct application of Lyapunov stability theory to a discrete-time system [Kha02]. Therefore, given the center node of graph $\mathcal{G}(\boldsymbol{Q})$ being i and $\lim_{s\to\infty} \boldsymbol{z}(s) = \boldsymbol{e}_i$, one can immediately compute that $\rho_i \boldsymbol{e}_i$ is the appropriate dominant left eigenvector of $\boldsymbol{P}(\boldsymbol{e}_i)$, which is equivalent to $\lim_{s\to\infty} \boldsymbol{p}(\boldsymbol{z}(s)) = \rho_i \boldsymbol{e}_i$. The proof is complete. □

Lemma 4.2 features the predictable emergence of autocratic configuration in individuals' social power for the interpersonal appraisal network with a star topology across the issues. More fundamentally, social power tends to accumulate at the center node that represents the dictator-like individual, for almost every initial conditions except for the vertices of the simplex. As the number of issues grows, the outcome of opinion formation at each issue is determined exclusively by the initial attitude of the autocrat actor.

Next, we embark on the quest of convergence and stability of the self-appraisal mechanism (4.9) with a relatively more generic setting.

Theorem 4.1: Convergence and Stability of Constant Non-star Appraisal Structure

For $n \geq 3$, consider the self-appraisal system (4.8) and social power formula (4.6). Assume the underlying interaction graph $\mathcal{G}$ associated with the interpersonal appraisal matrix $\boldsymbol{Q}$ is not a star graph and is strongly connected and structurally balanced. Then, the following claims hold

(i) Fixed points: the set of equilibrium points of $\boldsymbol{f}$ is $\{\boldsymbol{e}_1, \dots, \boldsymbol{e}_n, \boldsymbol{z}^*\}$, where $\boldsymbol{z}^* \in \mathrm{int}(\mathbb{S}^n)$;

(ii) Convergence: for any $\boldsymbol{z}(0) \in \nabla\mathbb{S}^n$, the self-weights $\boldsymbol{z}(s)$ converges exponentially to the equilibrium configuration $\boldsymbol{z}^* \in \mathrm{int}(\mathbb{S}^n)$ and the network-scale social power $\boldsymbol{p}(\boldsymbol{z}^*)$ converges exponentially to $\mathrm{diag}(\boldsymbol{\rho})\boldsymbol{z}^* \in \mathrm{int}(\mathbb{D}^n)$ as $s \to \infty$;

(iii) Stability: the fixed point in the interior of simplex is the unique stable equilibrium for nonlinear dynamics (4.8) in $\mathbb{S}^n$.

Proof. From the analytic expression (4.9), the vertices $\boldsymbol{e}_i$ $(i \in \mathbb{V})$ of $\mathbb{S}^n$ are naturally fixed points of the map $\boldsymbol{f}$. Furthermore, the factor $\theta(\boldsymbol{z})$ is strictly positive for $\boldsymbol{z}(s) \in \nabla\mathbb{S}^n$, which suffices to ensure $\boldsymbol{z}(s+1) > 0$. Namely, no fixed point exists on the boundary of simplex $\mathbb{S}^n$.

We define a compact set by

$$\mathbb{A}^n = \{\boldsymbol{z} \in \mathbb{S}^n | 0 \le z_i \le 1 - r, \forall i \in \mathbb{V}\},$$

where $r \in \mathbb{R}_{>0}$ is an extremely small scalar and satisfies

$$0 < r \le \min_{i \in \mathbb{V}} \frac{1 - 2\rho_i q_i}{1 - \rho_i q_i}.$$

Note that the properties of the dominant left eigenvector $\boldsymbol{q}$ developed in Lemma 4.2 ensure that $(1-2\rho_i q_i)/(1-\rho_i q_i) > 0$ for all $i \in \mathbb{V}$ and graphs $\mathcal{G}(\boldsymbol{Q})$ with a non-star topology.

We first calculate the i-th entry of vector field $\boldsymbol{f}(\boldsymbol{z})$ by

$$f_i(\boldsymbol{z}) = \frac{\rho_i q_i}{(1-z_i)\sum_j^n \frac{\rho_j q_j}{1-z_j}} = \frac{1}{1 + \frac{\sum_{j\neq i}^n \frac{\rho_j q_j}{1-z_j}}{\rho_i q_i / 1 - z_i}} \le \frac{1}{1 + \frac{r}{\rho_i q_i} \sum_{j \neq i}^n \frac{\rho_j q_j}{(1-z_j)}}, \tag{4.15}$$

as $1 - z_i \ge r$. Since it is already known $1 - z_j < 1$ for $\boldsymbol{z} \in \nabla\mathbb{S}^n$ and $\rho_i q_i = 1 - \sum_{j \neq i}^n \rho_j q_j$, the formula (4.15) further becomes

$$\begin{aligned} f_i(\boldsymbol{z}) < \frac{\rho_i q_i}{r + (1-r)\rho_i q_i} &= \frac{(1-\rho_i q_i) r^2 + (2\rho_i q_i - 1) r}{r + (1-r)\rho_i q_i} + 1 - r \\ &= \frac{r(1-\rho_i q_i)(r - \frac{1-2\rho_i q_i}{1-\rho_i q_i})}{r + (1-r)\rho_i q_i} + 1 - r \le 1 - r, \end{aligned}$$

where the last inequality is based on the fact that $r \le \frac{1-2\rho_i q_i}{1-\rho_i q_i}$ for all $i \in \mathbb{V}$. Hence, one can derive the conclusion that $\boldsymbol{f}(\mathbb{A}^n) \subset \mathbb{A}^n$. In what follows, we restrict the consideration of self-appraisal dynamics to this compact set $\mathbb{A}^n$.

In response to the primal system (4.8), there exists a prolonged system as follows

$$\begin{cases} \boldsymbol{z}(s+1) = \boldsymbol{f}(\boldsymbol{z}) \\ \delta\boldsymbol{z}(s+1) = \frac{\partial \boldsymbol{f}}{\partial \boldsymbol{z}}(\boldsymbol{z}) \delta\boldsymbol{z}(s) \end{cases} \tag{4.16}$$

where the infinitesimal displacement is $\delta\boldsymbol{z} \in T_{\boldsymbol{z}}\mathbb{S}^n$ and the Jacobian matrix of vector field $\boldsymbol{f}$ has the form

$$\left[\frac{\partial \boldsymbol{f}}{\partial \boldsymbol{z}}\right]_{ij}(\boldsymbol{z}) = \begin{cases} \frac{z_i(s+1)(1-z_i(s+1))}{1-z_i(s)} & \text{if } j = i \\ -\frac{z_i(s+1) z_j(s+1)}{1-z_j(s)} & \text{if } j \neq i, \end{cases} \tag{4.17}$$

where the relation $\frac{\partial \theta(z)}{\partial z_i} = -\frac{\rho_i q_i \theta^2(z)}{(1-z_i)^2}$ is an intermediate for the computation.

For each $s \in \mathbb{I}$, $\boldsymbol{z} \in \mathbb{A}^n$, and $\boldsymbol{\delta z} \in T_{\boldsymbol{z}}\mathbb{A}^n$, we consider a candidate Finsler-Lyapunov function of the form

$$V(\boldsymbol{z}(s), \boldsymbol{\delta z}(s)) = \sum_{i=1}^{n} \left| \frac{\delta z_i(s)}{1 - z_i(s)} \right|, \tag{4.18}$$

which is well defined in $\nabla\mathbb{S}^n$ and satisfies conditions of Definition 2.2. In what follows, we denote the diagonal matrix by

$$\boldsymbol{\Pi}(\boldsymbol{z}(s)) := \mathsf{diag}(1/(1-z_1(s)), \ldots, 1/(1-z_n(s)))$$

for clarity of presentation. The Finsler-Lyapunov function then can be rewritten to a form $V = \|\boldsymbol{\Pi}(\boldsymbol{z}(s))\boldsymbol{\delta z}(s)\|_1$ in terms of the 1-norm, which has a difference calculation along the issue sequence

$$\begin{aligned} &V(\boldsymbol{z}(s+1), \boldsymbol{\delta z}(s+1)) - V(\boldsymbol{z}(s), \boldsymbol{\delta z}(s)) \\ &\qquad = \|\boldsymbol{\Pi}(\boldsymbol{z}(s+1))\frac{\partial \boldsymbol{f}}{\partial \boldsymbol{z}}(\boldsymbol{z}(s))\boldsymbol{\delta z}(s)\|_1 - \|\boldsymbol{\Pi}(\boldsymbol{z}(s))\boldsymbol{\delta z}(s)\|_1 \\ &\qquad = \|\boldsymbol{K}(\boldsymbol{z}(s+1)\boldsymbol{\Pi}(\boldsymbol{z}(s))\boldsymbol{\delta z}(\boldsymbol{z}(s))\|_1 - \|\boldsymbol{\Pi}(\boldsymbol{z}(s))\boldsymbol{\delta z}(s)\|_1 \end{aligned} \tag{4.19}$$

where $\boldsymbol{K}(\boldsymbol{z}(s))$ represents the matrix with entries

$$[\boldsymbol{K}]_{ij}(\boldsymbol{z}(s)) = \begin{cases} z_i(s) & \text{if } j = i \\ -\frac{z_i(s) z_j(s)}{1 - z_i(s)} & \text{if } j \neq i. \end{cases} \tag{4.20}$$

From the facts that $0 < z_i \leq 1 - r$ for all $i \in \{1, \ldots, n\}$ and $\sum_i z_i = 1$, one can obtain $z_i/1 - z_j < 1$ for arbitrary $j \neq i$. As a result, the 1-norm of each column of the matrix $\boldsymbol{K}(\boldsymbol{z}(s))$ has a strict upper bound, i.e., $z_i(s) + \sum_{j=1, j\neq i}^{n} \frac{z_i(s) z_j(s)}{1 - z_j(s)} < 1$, for all $i \in \mathbb{V}$, which guarantees, as well as the compactness of the set $\mathbb{A}^n$, $\|\boldsymbol{K}(\boldsymbol{z}(s))\|_1 < 1 - \kappa$ for some $0 < \kappa < 1$ for all $\boldsymbol{z}(s) \in \mathbb{A}^n$. Therefore, the difference inequality (4.19) can be reformulated by

$$\begin{aligned} &V(\boldsymbol{z}(s+1), \boldsymbol{\delta z}(s+1)) - V\big(\boldsymbol{z}(s), \boldsymbol{\delta z}(s)\big) \\ &\qquad < (1-\kappa)\|\boldsymbol{\Pi}(\boldsymbol{z}(s))\boldsymbol{\delta z}(s)\|_1 - \|\boldsymbol{\Pi}(\boldsymbol{z}(s))\boldsymbol{\delta z}(s)\|_1 = -\kappa V(\boldsymbol{z}(s), \boldsymbol{\delta z}(s)), \end{aligned} \tag{4.21}$$

which means the differential Lyapunov function V decreases non-trivially along the trajectories of the prolong system (4.16). As a consequence of Theorem 2.1, the self-appraisal system (4.7) is incrementally exponentially stable on $\nabla\mathbb{S}^n \subset \mathbb{S}^n$ with respect to the contraction measure V given in (4.18).

The remaining issue is to prove the existence and uniqueness of the equilibrium point in the interior of the simplex. The construction of the distance $\mathrm{d}_{\mathbb{S}}$ in terms of curve integration (2.7) endows $\mathbb{S}^n$ with the structure of metric space. Specifically, the distance function $\mathrm{d}_{\mathbb{S}}$ induced by $F(\boldsymbol{z}, \delta(z)) = V(\boldsymbol{z}, \delta(z))$ in coordinates reads

$$\mathrm{d}_{\mathbb{S}}(\boldsymbol{z}_1, \boldsymbol{z}_2) = \inf_{\Gamma(\boldsymbol{z}_1, \boldsymbol{z}_2)} \int_J V\left(\gamma(\tau), \frac{\partial \gamma(\tau)}{\partial \tau}\right) d\tau \tag{4.22}$$

where $\Gamma(\boldsymbol{z}_1, \boldsymbol{z}_2)$ is the collection of piecewisely differential curves $\gamma : J \to \nabla\mathbb{S} \subset \mathbb{S}$, $J := \{\tau \in \mathbb{R} | 0 \leq \tau \leq 1\}$, connecting $\boldsymbol{z}_1$ to $\boldsymbol{z}_2$, namely, $\gamma(0) = \boldsymbol{z}_1$ and $\gamma(1) = \boldsymbol{z}_2$. For any initial conditions

$\boldsymbol{z}_1$ and $\boldsymbol{z}_2$, and any given converging sequence $\{\chi_1,\ldots,\chi_k,\ldots\}\in\mathbb{R}_{>0}$ with $\lim_{k\to\infty}\chi_k=0$, one can develop a sequence of continuously differential curves $\gamma_k: J_k\to\mathbb{S}^n$ such that

$$\lim_{k\to\infty}\int_{J_k} V\Big(\gamma_k(\tau),\frac{\partial\gamma_k(\tau)}{\partial\tau}\Big)d\tau \le \lim_{k\to\infty}(1+\chi_k)\mathrm{d}_{\mathbb{S}}(\boldsymbol{z}_1,\boldsymbol{z}_2)=d_{\mathbb{S}}(\boldsymbol{z}_1,\boldsymbol{z}_2). \tag{4.23}$$

From (4.21), one can get $V\big(\boldsymbol{z}(s),\delta\boldsymbol{z}(s)\big)\le(1-\kappa)^s V\big(\boldsymbol{z}(0),\delta\boldsymbol{z}(0)\big)$, for all $s\ge 0$, which together with (4.23) implies that in the limit of $k\to\infty$, for arbitrary initial conditions $\boldsymbol{z}_1,\boldsymbol{z}_2\in\nabla\mathbb{S}^n$,

$$\mathrm{d}_{\mathbb{S}}(\boldsymbol{\phi}(s;0,\boldsymbol{z}_1),\boldsymbol{\phi}(s;0,\boldsymbol{z}_2))\le\int_{J_k} V^{\frac{1}{l}}(\gamma_k(\tau),\frac{\partial\gamma_k(\tau)}{\partial\tau})d\tau\le(1-\kappa)^{\frac{s}{l}}\mathrm{d}_{\mathbb{S}}(\boldsymbol{z}_1,\boldsymbol{z}_2),$$

where $l\ge 1$. Since the Lipschitz constant $(1-\kappa)^{s/l}$ is strictly smaller than 1, the map $\boldsymbol{f}:\mathbb{S}^n\to\mathbb{S}^n$ is a contraction mapping on $\mathbb{S}^n$. Thereby, the employment of *Banach fixed-point theorem* [Kha02] to the complete metric space $(\nabla\mathbb{S}^n,\mathrm{d}_{\mathbb{S}})$ suffices to prove the existence and uniqueness of a fixed point $\boldsymbol{z}^*\in\nabla\mathbb{S}^n$ such that $\boldsymbol{z}^*=\boldsymbol{f}(\boldsymbol{z}^*)$. Since the previous examination has addressed that there is no other fixed-point on the boundary of the simplex, this non-vertex equilibrium $\boldsymbol{z}^*$ only appears in the interior $\boldsymbol{z}^*\in\mathrm{int}(\mathbb{S}^n)$. The proof of statement (i) is achieved.

Hence, one can draw the conclusion that the trajectory of the solutions to $\boldsymbol{z}(s+1)=\boldsymbol{f}(\boldsymbol{z}(s))$ converge exponentially to a unique equilibrium point $\boldsymbol{z}^*\in\mathrm{int}(\mathbb{S}^n)$. As a by-product of the convergence of self-weights, the social power indicators $\boldsymbol{p}(\boldsymbol{z}(s))$ converges exponentially to a unique fixed point $\boldsymbol{p}^*(\boldsymbol{z}^*)\in\mathrm{int}(\mathbb{D}^n)$ as the issue sequence progresses. The statement (ii) is finished.

The stability of the fixed point in the interior of simplex has been addressed in the above statement. That is, the fixed point $\boldsymbol{z}^*\in\mathrm{int}(\mathbb{S}^n)$ is an exponentially stable equilibrium point for the self-appraisal dynamics. It remains to elucidate that the vertices $\boldsymbol{e}_i$ $(i\in\{1,\ldots,n\})$ are unstable fixed points. The Jacobian matrix evaluated at the vertex of simplex can be found in the proof of Proposition 4.1. Without loss of generality, for any $i\in\mathbb{V}$, the virtual system with the Jacobian (4.10) at $\boldsymbol{z}=e_i$ characterizes the linearization of (4.8) about the vertex $\boldsymbol{z}=e_i$. In particular, this Jacobian has a single eigenvalue at $(1-|q_i|)/|q_i|$ and all other eigenvalues are zero. From Lemma 4.2, the entry q_i of the influence matrix satisfies $|q_i|<1/2$ if the graph $\mathcal{G}(\boldsymbol{Q})$ has no star topology, thus implying $(1-|q_i|)/|q_i|>1$. Hence, the vertices of simplex are unstable equilibrium points for the self-appraisal dynamics Proposition 4.1 according to the adoption of Lyapunov's indirect method [Kha02] to a discrete-time setting. The statement (iii) is claimed and this is the entire proof. □

The above convergence and stability analysis benefits substantially from the aid of the differential Lyapunov framework. The equivalence relation between incremental exponential stability and contraction, e.g., see Theorem 14 in [TRK16], facilitates the statement on the existence and uniqueness of the equilibrium. Another trait rooted in the differential structure is the exponential convergence of nonlinear dynamics in question, whereas previous results in [JMFB15; JFB17] are stated in an asymptotic sense. Moreover, the convergence property of contractive systems, which is independent of initial conditions, implies that individuals exponentially forget their original self-appraisal of relative control along the issue sequence. Analogous arguments can be addressed for the centralized assessment of social power $\boldsymbol{p}(\boldsymbol{z})\in\mathbb{D}^n$.

In the pioneering literature of cooperative networks [FJB16], social power is in connection with the eigenvector centrality of a graph, thus providing some ranking implications for relative control of individuals at the equilibrium point. Similar conclusions also can be drawn in the case of signed graphs. Following Theorem 4.1, the self-weight (social power) for each individual exponentially converges to a stable fixed point $\boldsymbol{z}^* \in \operatorname{int}(\mathbb{S}^n)$ ($\boldsymbol{p}^* \in \operatorname{int}(\mathbb{D}^n)$) along the issue sequence. Moreover, the self-weight score (social power) at the equilibrium configuration is parallel to the eigenvector centrality ranking: $z_i^* < z_j^*$ ($|p_i^*| < |p_i^*|$) if and only if $|q_i| < |q_j|$ for any pair of i and j, and $z_i^* = z_j^*$ ($|p_i^*| = |p_j^*|$) if and only $|q_i| = |q_j|$, where $\boldsymbol{q} \in \mathbb{D}^n$ and $\boldsymbol{q}^\top \boldsymbol{Q} = \boldsymbol{q}^\top$. The notable fact is that each column of the interpersonal appraisal matrix $\boldsymbol{Q}$ collects others' assessments of the corresponding individual. The elements of the product $\boldsymbol{q}^\top \boldsymbol{Q}$ imply in some sense, the collective appraisal of others on the individual group members. Thereby, one can also refer to the centrality $\boldsymbol{q}$ as a consensual appraisal of individuals. Another vector-based index arising from this context is an average interpersonal appraisal $\boldsymbol{q}_{\text{ave}} := \boldsymbol{Q}^\top \boldsymbol{\rho}/n$. Those influence metrics provide profound implications to the equilibrium ranking of individual social power and will be empirically demonstrated in the numerical testing.

Moreover, the proof of Theorem 4.1 shows that the set $\mathbb{A}^n = \{\boldsymbol{z} \in \mathbb{S}^n | 0 \le z_i \le 1 - r\} \subset \nabla\mathbb{S}$ with $r \le \min_{i\in\mathbb{V}} \frac{1-2\rho_i q_i}{1-\rho_i q_i}$ is forward $\boldsymbol{f}$-invariant and the stable equilibrium point $\boldsymbol{z}^*$ exists in this contraction region. It is reasonable to predict an upper bound for the absolute social power of individuals at the equilibrium point, that is, $0 < |p_i^*| < |q_i|/(1 - |q_i|)$. Obviously, a smaller $|q_i|$ entails a tighter upper bound for the equilibrium social power $|p_i^*|$ of each individual. Additionally, one can acquire a threshold value $q_{\text{threshold}} = 1/3$ such that if $|q_i| < q_{\text{threshold}}$ for all $i \in \mathbb{V}$, then there is no such agent who holds more than half of the total absolute power after each issue discussion, i.e., $|p_i| < 1/2$ for all $i \in \mathbb{V}$.

Remark 4.1. *In the proof of Lemma 4.2, a Lyapunov-based method is applied to conduct the convergence analysis of self-appraisal dynamics in the scenario when $\mathcal{G}(\boldsymbol{Q})$ is a star graph. The implicit prediction or prior knowledge of the equilibrium point at the autocratic state allows for the applicability of Lyapunov theory. However, the first challenge encountered in using the Lyapunov methodology to non-autocratic networks is that the explicit calculation of the equilibrium may be an intractable task due to the nonlinear form of dynamics. The customized remedy here does not directly seek a Lyapunov-based metric on the state space. Instead, a differential framework by lifting the Lyapunov function to the tangent bundle is employed to investigate the contraction of infinitesimal dynamics, thus obtaining the equilibrium-independent convergence of the self-appraisal dynamics.*

Remark 4.2. *Inspired by the geometric property of the state manifold $\mathbb{S}^n$, the 1-norm is exploited to construct the Lyapunov function and Finsler-Lyapunov function in the proofs of Lemma 4.2 and Theorem 4.1, respectively. In general, the first choice of Lyapunov-like function is a quadratic form in terms of the matrix 2-norm, which endows a Riemannian structure on $\mathbb{S}^n$. However, the 2-norm metric in this chapter fails to guarantees the convergence of the nonlinear dynamics in question. Other investigations of a Riemannian structure on probability space, e.g., using 2-Wasserstein metric, can be found in [AGS08] and references therein, indicating the potential to develop the gradient-flow structure in the evolutionary framework of social power.*

4.2.2 Dynamic Interpersonal Appraisal Mechanism

In this subsection, we begin to examine the convergence behavior of the proposed self-appraisal mechanism in a general context in which the interpersonal appraisal structure does not remain unchanged along the issue sequence.

A paradigmatic example of variant appraisal structure is a congress in the governance system where the representatives of different nations, constituent states, or independent social groups regularly assemble to deal with issues in multiple domains involving national security, diplomatic policy, legislative initiative, and other economic and political matters. Stemming from the common political and social benefit orientation, participants may form conglomerates on some fixed issues while contesting with other opposition factions. The "unbreakable" relationship, however, is not inherently stable, and as the discussed topic changes, conventioneers may realign themselves with others, or possibly even cooperate with the opponents on prior issues. The consideration of dynamic appraisal topology is consistent with the political maxim: "no eternal allies, no perpetual enemies, only eternal and perpetual interests".

The paradigm shift from a static structure of appraisal relation to a dynamic network of interpersonal appraisal makes the self-appraisal dynamic (4.8) become a nonlinear non-autonomous system. To clarify the presentation, the following finite set encapsulates all interpersonal appraisal matrices under consideration

$$\mathbb{Q} := \{\boldsymbol{Q} \in \mathbb{R}^{n\times n} \,|\, \mathcal{G}(\boldsymbol{Q}) \text{ is SC and SB non-star graph}\}. \tag{4.24}$$

For some technical reasons, we assume that $\boldsymbol{Q}(s)$ is independent of $\boldsymbol{z}(s_1)$ where $s_1, s \in \mathbb{I}$ and $s_1 < s$.

Theorem 4.2: Convergence Analysis of Dynamic Non-star Appraisal Structure

For $n \geq 3$, consider the self-appraisal system (4.8) on $\mathbb{S}^n$ and the interpersonal appraisal matrix $\boldsymbol{Q}(s) \in \mathbb{Q}$ at issue $s \in \mathbb{I}$. With initial conditions $\boldsymbol{z}(0) \in \nabla\mathbb{S}^n$, the self-weights $\boldsymbol{z}(s) \in \mathbb{S}^n \cup \{\boldsymbol{0}\}$ governed by the nonlinear map $\boldsymbol{f}$ in (4.9) converge exponentially to a steady state trajectory $\boldsymbol{z}^*(s) \in \mathsf{int}(\mathbb{S}^n)$. The network-scale social power $\boldsymbol{p}(\boldsymbol{z}) \in \mathbb{D}^n$ converges exponentially to the trajectory $\mathsf{diag}(\boldsymbol{\rho}(s))\boldsymbol{z}^*(s) \in \mathsf{int}(\mathbb{D}^n)$ as $s \to \infty$.

Proof. Note that with $\boldsymbol{z}(0) \in \nabla\mathbb{S}^n$, the appraisal graph $\mathcal{G}(\boldsymbol{Q}(0))$ for $\boldsymbol{Q}(0) \in \mathbb{Q}$ being structurally balanced and strongly connected entails $\boldsymbol{z}(1) \in \mathsf{int}(\mathbb{S}^n)$. Indeed, the factor here becomes $\theta(\boldsymbol{z}, 0) > 0$ as a result of $q_i(0)\rho_i(0) > 0$ for all $i \in \mathbb{V}$. Hence, we only need to concern the ultimate asymptotic behavior of $\boldsymbol{z}(s)$ in the interior of simplex.

It is straightforward to conduct the convergence analysis by following the proofs of Theorem 4.1. In particular, one can treat the self-appraisal dynamics with vector field (4.9) as a switching system and then employ the function (4.18) as a common (differential) Lyapunov function in the studying of stability. The contraction region here is modified by

$$\mathbb{A}^n = \{\boldsymbol{z} \in \mathbb{S}^n | 0 \leq z_i \leq 1 - r, \forall i \in \mathbb{V}\},$$

where $r \leq \inf_{i\in\mathbb{V}, s\in\mathbb{I}} \frac{1-2\rho_i(s)q_i(s)}{1-\rho_i(s)q_i(s)}$. The rest of proof can be induced issue-wise from the proof of Theorem 4.1 and is omitted in order to save triviality. Since $\mathbb{A}^n$ is convex and compact, by incremental exponential stability, the solution $\boldsymbol{z}(s) \in \mathsf{int}(\mathbb{S}^n)$ exponentially approaches to a limiting trajectory $\boldsymbol{z}^*(s) \in \mathsf{int}(\mathbb{S}^n)$ being independent of its initial conditions.

Finally, we sum up that the limit set of $\boldsymbol{z}(s)$ is a trajectory in the interior of the simplex and the social power $\boldsymbol{p}(\boldsymbol{z})$ converges either to a limiting trajectory $\boldsymbol{p}(\boldsymbol{z}^*) \in \mathsf{int}(\mathbb{D}^n)$. The proof is completed. $\square$

As illustrated in Figure 4.1, the left- $\boldsymbol{q}(s)$ and right-eigenvector $\boldsymbol{\rho}(s)$ can be treated as exogenous signals for the self-appraisal dynamics (4.8), which encode the topologically structural information of graph $\mathcal{G}(\boldsymbol{Q}(s))$ on the issue $s \in \mathbb{I}$. Therefore, the steady-state solution $\boldsymbol{z}^*(s)$, in some sense, is specified implicitly by the interpersonal appraisal mechanism.

In general, the self-appraisal system exhibits the non-equilibrium asymptotic behavior because of the issue-varying interpersonal appraisal mechanism. In some special scenarios, however, the self-weight may coincidentally reach a stationary fixed point. We first explore an equivalence relation $\simeq_e$ in the set $\mathbb{Q}$ such that for arbitrary $\boldsymbol{Q}_1, \boldsymbol{Q}_2 \in \mathbb{Q}$, it holds $\boldsymbol{Q}_1 \simeq_e \boldsymbol{Q}_2$ if $\boldsymbol{Q}_1$ and $\boldsymbol{Q}_2$ share the same left-eigenvector $\boldsymbol{q}$ and right-eigenvector $\boldsymbol{\rho}$. Such relation enables us to define an equivalent class $[\boldsymbol{Q}]_{\simeq_e}$ of matrix $\boldsymbol{Q} \in \mathbb{Q}$.

Corollary 4.1: Stationary Configuration of Equilibrium Social Power

For arbitrary initial appraisal matrix $\boldsymbol{Q}(0) \in \mathbb{Q}$ which has the left eigenvector $\boldsymbol{p}(0)$ and right eigenvector $\boldsymbol{\rho}(0)$ associated to eigenvalue 1, if it holds $\boldsymbol{Q}(s) \in [\boldsymbol{Q}(0)]_{\simeq_e}$ over the sequence of issue $\mathbb{I}$, then the self-weight $\boldsymbol{z}(s)$ governed by the vector field (4.9) converges exponentially to a static equilibrium point $\boldsymbol{z}^* \in \mathsf{int}(\mathbb{S}^n)$ and the social power $\boldsymbol{p}(\boldsymbol{z}, \boldsymbol{Q})$ has an equilibrium configuration $\boldsymbol{p}^* \in \mathsf{int}(\mathbb{D}^n)$. Moreover, there is the ranking implication of the equilibrium self-weights (social powers) of individuals as follows: $z_i^* < z_j^*$ ($|p_i^*| < |p_i^*|$) if and only if $|q_i| < |q_j|$ for any pair of i and j, and $z_i^* = z_j^*$ ($|p_i^*| = |p_j^*|$) if and only if $|q_i| = |q_j|$.

The proof can be straightforwardly derived from Theorem 4.2 and therefore is omitted here. Although the developed results of Corollary 4.1 provide preferable ranking implication for the equilibrium social power, we have to admit such static configuration of relative control is a rare case, while self-appraisal mechanism of social power exposes mostly the stationary non-equilibrium dynamical behavior.

4.2.3 Constant Interpersonal Appraisal with Structural Unbalance

Until now, we usually postulate explicitly or implicitly the structural balance for the interpersonal appraisal structure in the study of opinion dynamics and self-esteem mechanism. This condition, however, may not always be satisfied in many real-life social networks. For example, large-scale online social networks typically have complex and multidimensional appraisal structures. Hence, the interpersonal appraisal graph arising from such networks hardly satisfy the structural balance condition. So in what follows, we investigate the evolution of social power with a structurally unbalanced interpersonal appraisal mechanism.

On the issue $s \in \mathbb{I}$, the social actors forming opinions on an influence network which is strongly connected and structurally unbalanced, tend towards neutrality no matter what individuals' initial ideas are, i.e., $\lim_{t\to\infty} \boldsymbol{x}(s,t) = \boldsymbol{0}$, for any $\boldsymbol{x}(s,0) \in \mathbb{R}^n$. In reference to (4.6), social power in opinion neutrality leads to $\boldsymbol{p}(s) = \boldsymbol{0}$ as a result of $\lim_{t\to\infty}(\boldsymbol{P}^t(s)) = \boldsymbol{0}$. Here, the magnitude of all eigenvalues of the influence matrix $\boldsymbol{P}(\boldsymbol{z}(s))$ is strictly smaller than 1. In other words, the neutral opinion dynamics features n individuals making no direct contribution to the issue discussion and hence, the self-weights here are accordingly set to 0 for everyone.

Theorem 4.3: Evolution of Social Power over Appraisal Networks with Structural Unbalance

For $n \geq 3$, consider the self-appraisal system (4.8) and social power formula (4.6). Assume the associated graph $\mathcal{G}(\boldsymbol{Q})$ of the interpersonal appraisal matrix $\boldsymbol{Q}$ is aperiodic, strongly connected, and structurally unbalanced. The map $\boldsymbol{f}$ on $\mathbb{S}^n \cup \{\mathbf{0}\}$ in (4.8) is then defined by

$$\boldsymbol{f}(\boldsymbol{z}) = \begin{cases} \boldsymbol{e}_i & \text{if } \boldsymbol{z}(s) = \boldsymbol{e}_i, \text{ for all } i \in \mathbb{V}, \\ \mathbf{0} & \text{if } \boldsymbol{z} \in \nabla\mathbb{S}^n \cup \{\mathbf{0}\}. \end{cases} \tag{4.25}$$

Furthermore, the equilibrium points of $\boldsymbol{f}$ belong to $\{\boldsymbol{e}_1, \ldots, \boldsymbol{e}_n, \mathbf{0}\}$. For arbitrary initial condition $\boldsymbol{z}(0) \in \nabla\mathbb{S}^n \cup \{\mathbf{0}\}$, the self-weights $\boldsymbol{z}(s)$ (social powers $\boldsymbol{p}(\boldsymbol{z})$) of individuals are constantly $\mathbf{0}$ for $s \in \{1, 2, \ldots\}$.

Proof. For $\boldsymbol{z} \in \nabla\mathbb{S}^n \cup \{\mathbf{0}\}$, the graph $\mathcal{G}(\boldsymbol{P}(\boldsymbol{z}))$ is strongly connected and structurally unbalanced according to the notation (4.3) since strongly connected graph $\mathcal{G}(\boldsymbol{Q})$ is structurally unbalanced. Therefore, we have the formulation $\boldsymbol{f} = \mathbf{0}$ in $\nabla\mathbb{S}^n \cup \{\mathbf{0}\}$.

Moreover, if $\boldsymbol{z} = \boldsymbol{e}_i$ for some $i \in \mathbb{V}$ (without loss of generality, let $i = n$), then the associated graph of the corresponding influence matrix is quasi-strongly connected, as node n is the only root vertex in $\mathcal{G}(\boldsymbol{P}(\boldsymbol{z}))$. Two cases are considered. First, if $\mathcal{G}(\boldsymbol{P}(\boldsymbol{z}))$ is structurally balanced, it equivalently means that removing one or multiple incoming edges of node n in $\mathcal{G}(\boldsymbol{Q})$ retrieves the structural balance. Thus, the vector field, in this case, has the same form as in the situation when $\mathcal{G}(\boldsymbol{Q})$ is quasi-strongly connected and structurally balanced, i.e., $\boldsymbol{f}(\boldsymbol{e}_i) = \boldsymbol{e}_i$. Second, if $\mathcal{G}(\boldsymbol{P}(s))$ is structurally unbalanced, there exists one, and only one isolated structurally balanced (ISB) component definitely containing n in $\mathcal{G}(\boldsymbol{P})$. By contradiction, assume there exists another ISB component $\mathcal{H}$ in $\mathcal{G}(\boldsymbol{P}(\boldsymbol{z}))$. Since node n as a root has a path to contact any nodes belonging to $\mathcal{H}$, so $\mathcal{H}$ has at least one inward edge, which contradicts the definition of in-isolated subgraph. In this situation, $\boldsymbol{P}(\boldsymbol{z})$ has a dominant eigenvalue 1 associated with a (up to scaling) left eigenvector $\boldsymbol{e}_i$. Thus, we have $\boldsymbol{f}(\boldsymbol{e}_i) = \boldsymbol{e}_i$ for some $i \in \mathbb{V}$.

Finally, following the fact that $\boldsymbol{f}$ keeps constantly zero in $\nabla\mathbb{S}^n \cup \{\mathbf{0}\}$, one can immediately show $\lim_{s\to\infty} \boldsymbol{z}(s) = \mathbf{0}$ and $\lim_{s\to\infty} \boldsymbol{p}(s) = \mathbf{0}$. □

In the above development, the special case of initial condition $\boldsymbol{z}(0) = \mathbf{0}$ mirrors a natural interpretation from a psychological context. Before acknowledging the specific issue in discussion, social actors usually behave in an unbiased fashion. More interestingly, there are several distinct emergent behaviors of opinion dynamics that unfold in structurally unbalanced networks. On one hand, the non-autocratic configuration of initial conditions leads to the situation where individuals do not take sides on any issue across the issues. On the other hand, the development in the proof of Theorem 4.3 shows that the presence of autocratic social power can generate diverse collective behavior in opinion forming including a consensus outcome, two opposite settled opinions, or a set of unreconciled opinions [Fri15]. This finding may open up avenues for driving the occurrence of clustering in human populations [MFH10] with self-perception of their relative control.

4.3 Transient Characterization of Social Power

The above study of interpersonal influence with constant $\boldsymbol{Q}$ shows that the equilibrium ordering of self-weight and social power can be conducted in relation to eigenvector centrality rather than waiting until the end of the issue sequence. Nevertheless, this interrelated correspondence is usually not that useful, when the appraisal structure turns into a non-constant situation. In addition, even in the constant scenario, appropriate methods to compute the precise equilibrium vector are still missing, with a few exceptions, such as the appraisal graph being star topology or balanced. The latter case in which $\boldsymbol{p}^* = \boldsymbol{\rho}/n$ and $\boldsymbol{z}^* = \mathbf{1}/n$ leads to the democratic configuration of personal social power.

Alternatively, in this section, we characterize the transient properties of social power during each issue discussion. The core of our methodology is the accommodation of *Kirchhoff's matrix tree theorem* [MG13] that is extended to the signed case.

Following the proof of Lemma 4.1, $\mathrm{diag}(\boldsymbol{\rho})\boldsymbol{p}$ is known to be the dominant left eigenvector of matrix $|\boldsymbol{P}| = \mathrm{diag}(\boldsymbol{\rho})\boldsymbol{P}\,\mathrm{diag}(\boldsymbol{\rho})$, from which one can form a Laplacian by $\boldsymbol{L} = \boldsymbol{I} - |\boldsymbol{P}|$. It is obvious that $\mathcal{G}(\boldsymbol{L})$ is (quasi)-strongly connected, provided that $\mathcal{G}(\boldsymbol{P})$ is (quasi)-strong connected and structurally balanced, so that $\dim\ker(\boldsymbol{L}^\top) = 1$ and $(\mathrm{diag}(\boldsymbol{\rho})\boldsymbol{p})^\top \boldsymbol{L} = \mathbf{0}_n$. Let $\mathrm{cof}(\boldsymbol{L})$ be the cofactor matrix associated to Laplacian $\boldsymbol{L}$, where $[\mathrm{cof}(\boldsymbol{L})]_{ij}$ is the (i,j)-th cofactor of $\boldsymbol{L}$ equaling to $(-1)^{i+j} b_{ij}$ (b_{ij} is the determinant of the (i,j)-th minor of $\boldsymbol{L}$). A well-known fact is that

$$\mathrm{cof}(\boldsymbol{L}) \cdot \boldsymbol{L}^\top = \det(\boldsymbol{L})\boldsymbol{I}_n = \mathbf{0}_{n\times n}.$$

Since the sum of the rows of the Laplacain $\boldsymbol{L}$ is zero, i.e, $\boldsymbol{L}\mathbf{1}_n = \mathbf{0}_n$, the characteristics of the determinant function reveal that the entries of each column of $\mathrm{cof}(\boldsymbol{L})$ are uniform. That is to say, $[\mathrm{cof}(\boldsymbol{L})]_{ij}$ is independent of i and without loss of generality, let $[\mathrm{cof}(\boldsymbol{L})]_{ij} = \rho_j p_j \geq 0$. In particular, the Kirchhoff matrix tree theorem tells us that $\rho_i p_i$ is equal to the sum, over all spanning tree rooted at node i in $\mathcal{G}(\boldsymbol{L})$, of the products of weights of edges traversing each tree [vdS17]. This finding provides several insights into the evaluation of social power of individuals.

The first hint is that when the appraisal network $\mathcal{G}(\boldsymbol{Q})$ is strongly connected and structurally balanced, there exists at least one individual in the social network, whose social power is nonzero on each issue. In the configuration space $\boldsymbol{z}(s) \in \nabla\mathbb{S}^n$, the social power of agents is non-zero, since for strongly connected influence network every node on $\mathcal{G}(|\boldsymbol{P}(s)|)$ has at least one spanning tree rooted at it. Especially, the absolute social power $|p_i(s)|$ for $s \in \mathbb{I}$ is equal to the sum of the products of absolute weights ($|p_{ij}(s)|$) of all the spanning trees starting from i in the graph $\mathcal{G}(\boldsymbol{P}(s))$ without self-loop. It should be emphasized that the positive and negative weighted interactions are treated equally without discrimination in the evaluation of social power, although the total effect of social power may be positive or negative. Moreover, the individual influence is usually not imposed via a single pathway, but through all available paths reaching others. In reference to the constraint $\boldsymbol{p}(s) \in \mathbb{D}^n$, the relative control p_i (up to sign) represents the ratio of the amount of spanning tree products that start from i to the total number of the spanning tree products in the influence network.

In addition, the introduction of the Kirchhoff matrix tree theorem to a signed setting enables us to extend previous Theorem 4.1 on strongly connected appraisal networks to the scenario that $\mathcal{G}(\boldsymbol{Q})$ is not strongly connected, but with multiple root nodes.

Theorem 4.4: Evolution of Social Power over Appraisal Networks with Multiple Root Nodes

For $n \geq m \geq 2$, consider the social power formula (4.6) and self-appraisal system (4.7). Assume the associated graph $\mathcal{G}(\boldsymbol{Q})$ is structurally balanced and quasi-strongly connected. Let $\{1,\dots,m\}$ be the set of root nodes in $\mathcal{G}(\boldsymbol{Q})$ and let $\boldsymbol{q}$ be the dominant left eigenvector of $\boldsymbol{Q}$. The map $\boldsymbol{f}:\mathbb{S}^n \to \mathbb{S}^n$ in (4.8) is then reformulated to

$$\boldsymbol{f}(\boldsymbol{z}) = \begin{cases} \boldsymbol{e}_i & \text{if } \boldsymbol{z}(s) = \boldsymbol{e}_i,\ \forall i \in \{1,\cdots,m\}, \\ \boldsymbol{g}_i & \text{if } \boldsymbol{z}(s) = \boldsymbol{e}_i,\ \forall i \in \{m+1,\cdots,n\}, \\ \theta_m(\boldsymbol{z}) \begin{bmatrix} \frac{\rho_1 q_1}{1-z_1(s)} \\ \vdots \\ \frac{\rho_m q_m}{1-z_m(s)} \\ 0 \\ \vdots \\ 0 \end{bmatrix} & \text{otherwise,} \end{cases}$$

where $\theta_m(\boldsymbol{z}) = 1/\sum_{j=1}^{m} \frac{\rho_j q_j(s)}{1-z_j(s)}$ and $\boldsymbol{g}_i := [g_i^1,\dots,g_i^m,0,\dots,0,g_i^i,0,\dots,0]^\top \in \mathbb{S}^n$ with appropriate strictly positive scalars $\{g_i^1,\dots,g_i^m,g_i^i\}$. The map $\boldsymbol{f}$ is continuous in $\mathbb{S}^n \backslash \{\boldsymbol{e}_{m+1},\dots,\boldsymbol{e}_n\}$. Furthermore, when $m=2$, the fixed points of $\boldsymbol{f}$ have the form $[(1-\beta),\beta,0,\dots,0]^\top$ with $\beta \in [0,1]$, and the self-confidence $\boldsymbol{z}(s)$ and the social power $\boldsymbol{p}(\boldsymbol{z}(s))$ respectively converges to an appropriate equilibrium point independent of initial condition $\boldsymbol{z}(0) \in \mathbb{S}^n$. In the case of $m \geq 3$,

(i) when $\mathcal{G}(\boldsymbol{Q})$ is a star graph centered at vertex i where $i \in \{1,\dots,m\}$, the fixed points of $\boldsymbol{f}$ are $\{\boldsymbol{e}_1,\dots,\boldsymbol{e}_m\}$; there are $\lim_{s\to\infty} \boldsymbol{z}(s) \to \boldsymbol{e}_i$ and $\lim_{s\to\infty} \boldsymbol{p}(\boldsymbol{s}) \to \rho_i \boldsymbol{e}_i$ for arbitrary initial condition $\boldsymbol{z}(0) \in \mathbb{S}^n \backslash \{\boldsymbol{e}_1,\dots,\boldsymbol{e}_m\}$ where $\rho_i \in \{-1,1\}$;

(ii) when $\mathcal{G}(\boldsymbol{Q})$ is not a star graph, the fixed points of $\boldsymbol{f}$ are $\{\boldsymbol{e}_1,\dots,\boldsymbol{e}_m,\boldsymbol{z}^*\}$, where $\boldsymbol{z}^* \in \nabla\mathbb{S}^n$ has the entries satisfying $z_i^* > 0$ for $i \in \{1,\dots,m\}$ and $z_i^* = 0$ for $i \in \{m+1,\dots,n\}$. Moreover, for an arbitrary initial condition $\boldsymbol{z}(0) \in \nabla\mathbb{S}^n$, the self-weights $\boldsymbol{z}(s)$ converge exponentially to the stable equilibrium point $\boldsymbol{z}^*$ and the social power $\boldsymbol{p}(\boldsymbol{z}(s))$ converges exponentially to $\mathrm{diag}(\boldsymbol{\rho})\boldsymbol{z}^*$.

Proof. The majority of the proof of Theorem 4.4 is the derivation of the Kirchhoff matrix tree theorem in conjunction with the proofs of Proposition 4.1 and Theorem 4.1. More importantly, the Kirchhoff matrix tree theorem is indicative of those nodes $i \in \{m+1,\dots,n\}$ who are constantly powerless on a specific issue, because they are continuously non-root vertex in the influence graph. That is, those individuals that have no spanning tree starting from them in influence network to impose their influence on opinion formation processes, are regarded as powerless actors in social networks. Thus, it is not difficult to acquire the formula of $\boldsymbol{f}$ in $\mathbb{S}^n \backslash \{\boldsymbol{e}_1,\dots,\boldsymbol{e}_m\}$ in reference to Proposition 4.1, as well as its continuity in $\mathbb{S}^n \backslash \{\boldsymbol{e}_1,\dots,\boldsymbol{e}_m\}$.

When $z(s) = e_i$ for $i \in \{m+1,\dots,n\}$ (let $i = n$ to simplify the presentation), the influence matrix $\boldsymbol{P}(e_n)$ here has the form

$$\boldsymbol{P}(\boldsymbol{e}_i) = \mathsf{diag}(\boldsymbol{e}_n) + \mathsf{diag}(\mathbf{1}_n - \boldsymbol{e}_i)\boldsymbol{Q} = [\boldsymbol{Q}^{\top}_{\{1,\dots,n-1\}}, \boldsymbol{e}_n^{\top}]^{\top} \tag{4.26}$$

where the $(n-1)\times n$ matrix $\boldsymbol{Q}_{\{1,\dots,n-1\}}$ is obtained by removing the last row from $\boldsymbol{Q}$. The resultant influence graph $\mathcal{G}(\boldsymbol{P}(\boldsymbol{e}_n))$ is disconnected, as vertex i is not reachable for other nodes in $\mathbb{V}\backslash\{n\}$. Thus, the above derivation in terms of the Kirchhoff matrix tree theorem is inapplicable to this case. Especially, $\boldsymbol{P}(\boldsymbol{e}_n)$ has multiple dominant left eigenvectors associated with eigenvalue 1, which disallows the uniqueness of an indicator vector for social power. The issue discussion on such influence networks exhibits opinion separation rather than consensus or polarity.

Note that the formal definition of social power in (4.6) still holds here, and the calculated result $\left(\lim_{k\to\infty} \boldsymbol{P}^k(\boldsymbol{e}_i)\right)^{\top} \boldsymbol{\rho}/n$ is treated as an alternative of eigenvector-based metric of social power in disconnected graphs. The analytic solution to this limitation can be computed in the light of the proof of Lemma 3.1 proposed in [JFB17], in which an unsigned influenced network is taken into account. Due to the similarity, we save the detailed computation to avoid repetition. As a result, one can obtain

$$\boldsymbol{f}(\boldsymbol{e}_i) = \mathsf{diag}(\boldsymbol{\rho})\Big(\lim_{k\to\infty} \boldsymbol{P}^k(\boldsymbol{e}_i)\Big)^{\top} \boldsymbol{\rho}/n,$$

which by normalizing, leads to the vector $[g_i^1,\dots,g_i^m,0,\dots,0,g_i^i,0,\dots,0]^{\top}$. Obviously, $\boldsymbol{f}(\boldsymbol{z})$ is not continuous on the vertices $\{\boldsymbol{e}_{m+1},\dots,\boldsymbol{e}_n\}$ as $f_i(\boldsymbol{z}) > 0$ when $\boldsymbol{z} = \boldsymbol{e}_i$ with $i \in \{m+1,\dots,n\}$ which mismatches $f_i(\boldsymbol{z}) \equiv 0$ for $\boldsymbol{z} \in \nabla\mathbb{S}^n$.

By noticing that although $\boldsymbol{z}(1)$ is unlikely to an equilibrium point for initial condition $\boldsymbol{z}(0) = \boldsymbol{e}_i$ where $i \in \{m+1,\dots,n\}$, whereas this initial configuration is assimilated into the scenario of $\boldsymbol{z} \in \nabla\mathbb{S}^n$. Thus, the convergence analysis on initials $\boldsymbol{z}(0) \in \mathbb{S}^n\backslash\{\boldsymbol{e}_1,\dots,\boldsymbol{e}_m\}$ is parallel to the proof of Theorem 4.1, thereby acknowledging the stable equilibrium point $\boldsymbol{z}^* \in \mathbb{S}^n\backslash\{\boldsymbol{e}_1,\dots,\boldsymbol{e}_m\}$ with $z_i^* > 0$ for all $i \in \{1,\dots,m\}$ and $z_i^* = 0$ for all $i \in \{m+1,\dots,n\}$ □

It is worth mentioning that the accumulated vector $\mathsf{diag}(\boldsymbol{\rho})\boldsymbol{g}_i$ – a local property – is not the dominant left-eigenvector – a global property – of $\boldsymbol{P}(\boldsymbol{e}_i)$ associated to eigenvalue 1 for some $i \in \{m+1,\dots,n\}$. The employment of $\mathsf{diag}(\boldsymbol{\rho})\boldsymbol{g}_i$ to feature the social power of individuals is actually a micro-level mechanism that only reflects the relative influence of actors on shaping the opinions of other members in the vicinity. Moreover, the structural characteristic of $\boldsymbol{z}^*$ shows that those individuals with few network-wide interpersonal connections (namely, non-root nodes) are vulnerable groups in social activities, even if they are empowered the supreme power.

4.4 Simulation Evaluations

In this section, several simulations serve to illustrate the proposed mathematical models and demonstrate the theoretical results.

A small-size social network of interpersonal ties is reported in [Thu79]. To fit our consideration, we make a slight modification such that the antagonism is also involved as shown in Figure 4.2. The office consists of 15 members in which the cooperative interrelation is drawn in blue arrowline and competition is in red. Obviously, {Ann, Tina, Katy, Lisa, Pete, Amy} and {Presendent, Rose, Mary, Mike, Emma, Peg, Minna, Andy, Bill} are two hostile cliques. We encode their interpersonal appraisals into the interpersonal appraisal matrix $\boldsymbol{Q}_1$. Apparently, the graph $\mathcal{G}(\boldsymbol{Q}_1)$ is strongly connected and structurally connected, which has a dominant right-eigenvector

$$\boldsymbol{\rho} = [1,1,-1,1,1,1,-1,-1,1,1,-1,-1,1,1,-1]^{\mathsf{T}},$$

and a unique dominant left-eigenvector

$$\boldsymbol{q} = [0.027, 0.026, -0.106, 0.027, 0.164, 0.111, -0.148, -0.066, 0.027, \\ 0.027, -0.140, -0.048, 0.014, 0.009, -0.058]^{\mathsf{T}}.$$

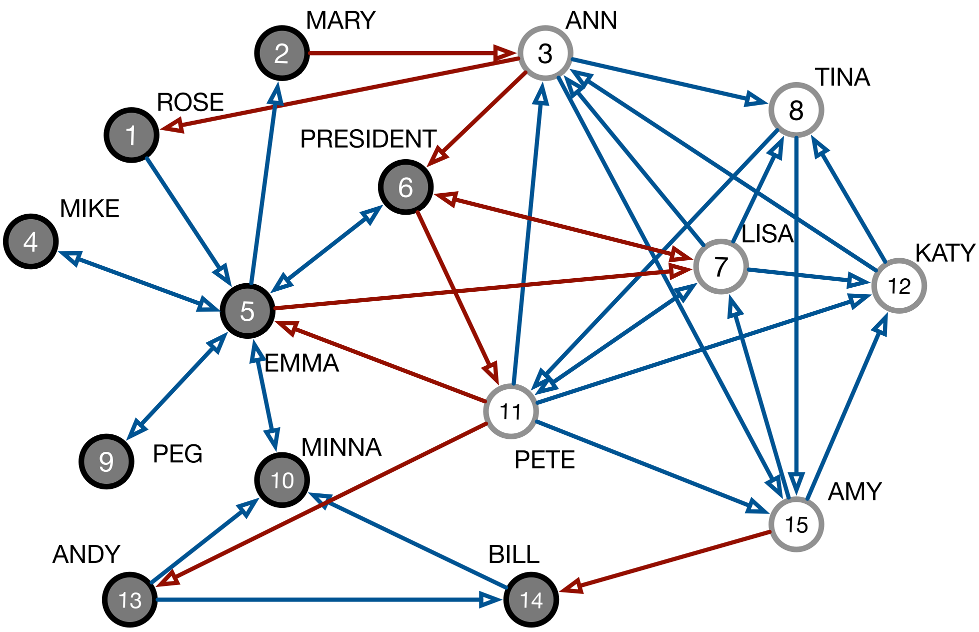

Figure 4.2: Signed Thurman's informal network of interpersonal ties among 15 staffs.

We numerically study the proposed self-appraisal framework on this modified small-size social network. For illustrative purpose, we conduct the simulation in a Monte-Carlo (MC) trial of 200 initial conditions. The dynamical trajectories of the self-confidence of individuals are illustrated in Figure 4.3a which shows the self-weights converge exponentially to an equilibrium point, independent of initially perceived appraisals. Especially, all self-weights strictly belong to the domain $]0,1[$, evidencing that the equilibrium self-confidence lies in the interior of the simplex $\mathbb{S}_n$. The numerical tests are consistent with the statements in Theorem 4.1.

Furthermore, comparisons among different social power metrics of individuals along the issue sequence are provided in Figure4.3b. We introduce two additional measures of relative influence: a mean interpersonal appraisal $\boldsymbol{q}_{\text{ave}} = \boldsymbol{Q}_1^{\mathsf{T}}\boldsymbol{\rho}/n$ and a vector of social power bound $\boldsymbol{p}_{\text{bd}} = [\frac{q_i}{1-\rho_i q_i}]$ $(i \in \mathbb{V})$. The first observation is that Emma is maximally close to interpersonal influence, while Bill lies at the lowest power layer in the office. Second, as discussed in Subsection 4.2.1, the absolute social power of individuals is strictly upper bounded by $\boldsymbol{p}_{\text{bd}}$, i.e., $|p_i^*| < \frac{|q_i|}{1-|q_i|}$ for all $i \in \mathbb{V}$. Although those influence metrics (final perceived social power $\boldsymbol{p}^*$, consensual appraisal $\boldsymbol{q}$, average appraisal $\boldsymbol{q}_{\text{ave}}$) are different in the exact value, they share the same ordering of the importance ranking, that is $p_i^* > p_i^*$

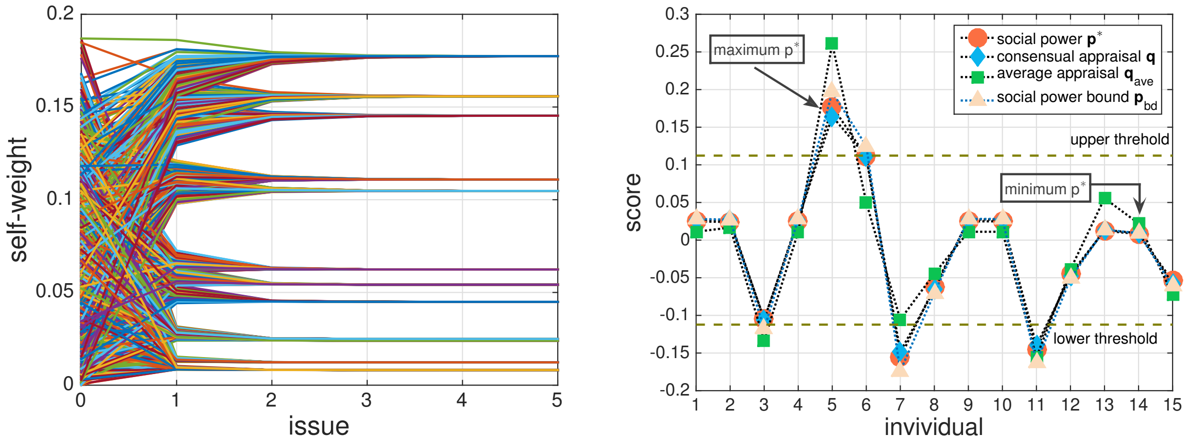

(a) Monte Carlo trial of self-weight dynamics with 200 initial conditions

(b) Comparison of different evaluation metrics

Figure 4.3: Numerical iillustration of developed results on strongly connected and structurally balanced influence networks.

if and only if $q_i > q_j$ ($q^i_{\text{ave}} > q^j_{\text{ave}}$) for $i, j \in \mathbb{V}$. Since all eigenvector centralities are lower than 1/3 in modulus, nobody in the office possesses more than half of the total social power at equilibrium. Even though there is no predominant actor in this organization, the experiment retains the "iron law of oligarchy" in sociological studies [Mic15]. By defining a threshold at the equilibrium by $1-\theta(\boldsymbol{z}^*)$ which equals 0.1123 here, the social power accumulation can be observed from Figure 4.3b wherein $|p^*_i| > |q_i|$ if $|q_i| > 0.1123$. Therefore, Emma, Pete and Lisa eventually develop into the power oligarchies at the top of the hierarchy. This finding is also consistent in spirit with Proposition 4.2 of [JMFB15].

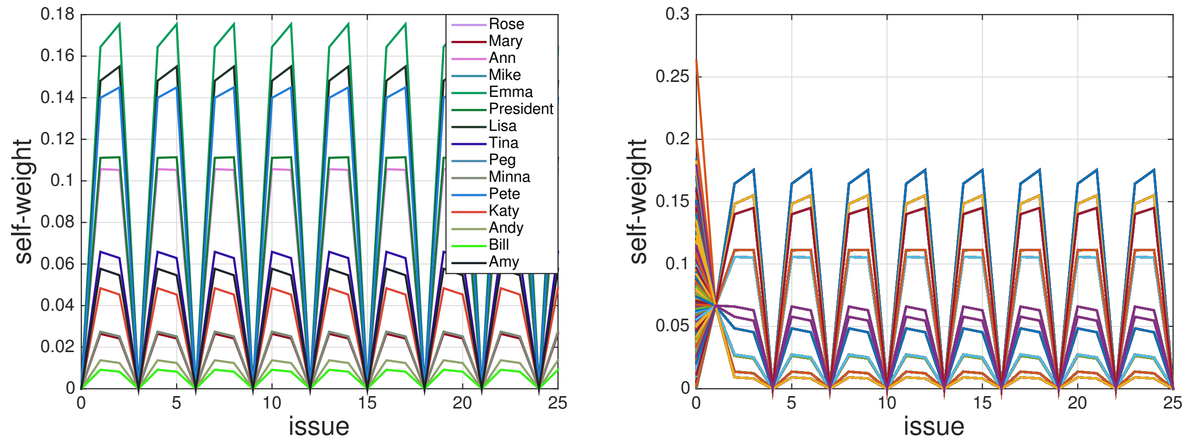

(a) Zero initial condition

(b) Monte Carlo trial

Figure 4.4: Evolution of self-weigths over dynamic interpersonal appraisal networks.

Next, to study the self-appraisal system (4.9) on a dynamic appraisal network, we construct two other interpersonal appraisal structures from the network Figure 4.2. The first one defined by matrix $\boldsymbol{Q}_2$ is derived by converting all edges with negative weights into the positively weighted ones. The graph $\mathcal{G}(\boldsymbol{Q}_2)$ is unsigned and strongly connected. By

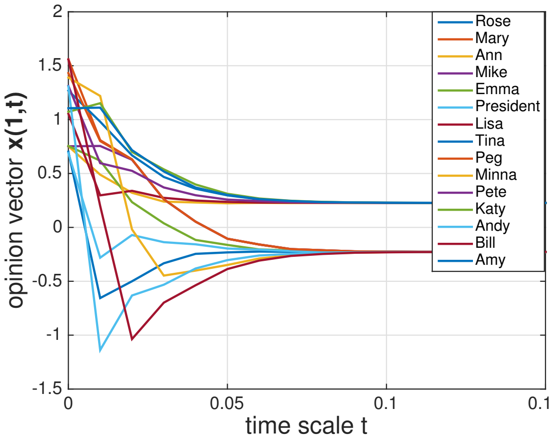

(a) Opinion polarity on issue 1

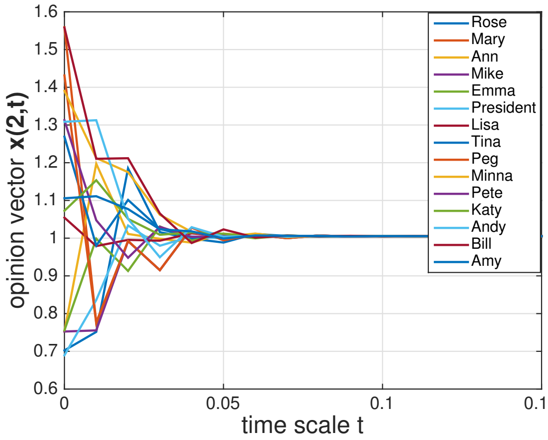

(b) Opinion conformity on issue 2

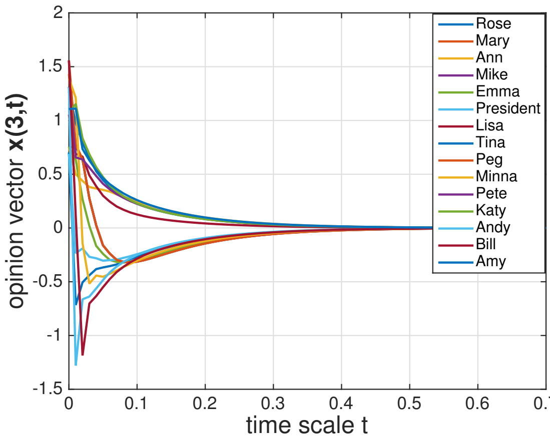

(c) Opinion neutrality on issue 3

Figure 4.5: Evolution of opinion dynamics on first three issues.

replacing the positive weight of link $(7,5)$ of the network in Figure 4.2 by a negative value, one can build up another interpersonal appraisal matrix $\boldsymbol{Q}_3$ whose associated graph is strongly connected and structurally unbalanced. Then, we implement the dynamics (4.9) on a periodically switching appraisal networks $\{\boldsymbol{Q}_1, \boldsymbol{Q}_2, \boldsymbol{Q}_3\}$. By setting $\boldsymbol{z}(0) = \boldsymbol{0}$ and the initial interpersonal appraisal structure by a completely positively connected topology, the dynamical trajectories of the self-weights are plotted in Figure 4.4a which exposes the self-weights asymptotically fall into an attractor system which relies on the setup of the interpersonal appraisal mechanism. Meanwhile, the Monte Carlo trial in Figure 4.4b shows the contraction property of the trajectories is independent of the setup of the initially perceived states $\boldsymbol{z}(0)$. Note that it is generally difficult to draw any conclusions on the ordering of social power since there does not exist a static equilibrium point in the case of dynamic topology.

In addition, we examine the evolution of opinion dynamics over a sequence of issues. Figure 4.5 presents the opinion-forming processes on the first three issues, which exhibit diversified tendencies of the settled opinions of group members on each issue including polarization Figure 4.5a, consensus Figure 4.5b, and neutrality Figure 4.5c. With the interpersonal appraisal matrix $\boldsymbol{Q}_3$, we also study the forming process of opinions under the autocratic configuration of social power. Allocation of dominant power at nodes results in community cleavages of opinion on issues as shown in Figure 4.6. What is intriguing is the case $\boldsymbol{x}(s) = \boldsymbol{e}_3$ depicted in Figure 4.6b in which the opinions of Ann and Rose polarize at the exact opposite values and the opinions of all other members in the office lie in between these two polarized values. The perception of social power $\boldsymbol{x}(s) = \boldsymbol{e}_7$ gives rise to that the attitudes of the entire office evolve into two polarized camps.

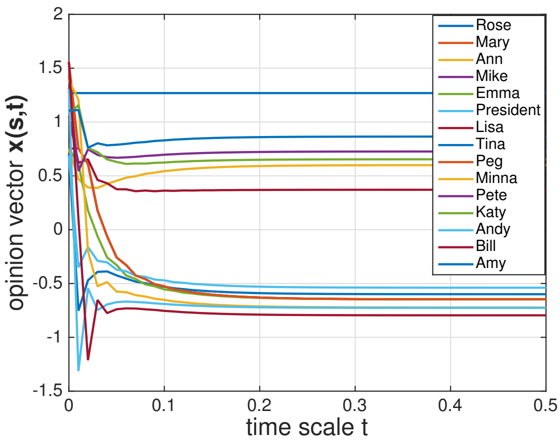

(a) Opinion clustering for $\boldsymbol{x}(s) = \boldsymbol{e}_8$

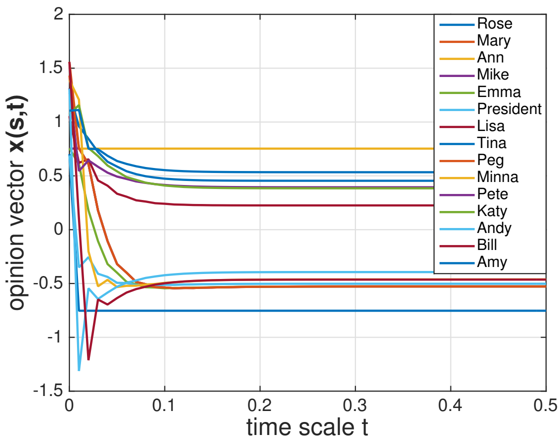

(b) Opinion separation for $\boldsymbol{x}(s) = \boldsymbol{e}_3$

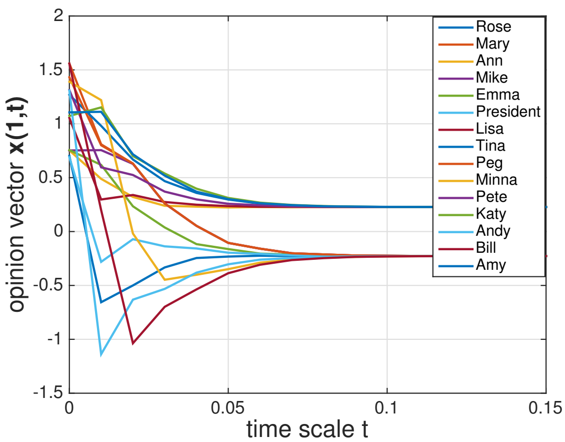

(c) Opinion polarization for $\boldsymbol{x}(s) = \boldsymbol{e}_7$

Figure 4.6: Evolution of opinion dynamics with autocratic social power.

For the last testing, we modify the toy social network in Figure 4.2 by breaking up links (4, 5), (10, 14), (10, 13) and building up links (14, 10), (13, 10) such that there is no spanning tree starting from the members {Mike, Andy, Bill}. Thus, the resulting graph of the interpersonal appraisal structure here is quasi-strongly connected but still structurally balanced. We explore the interpersonal appraisal matrix $\boldsymbol{Q}_4$ from this network, which has the dominant right-eigenvector

$$\boldsymbol{\rho} = [1, 1, -1, 0, 1, 1, -1, -1, 1, 1, -1, -1, 0, 0, -1]^{\mathsf{T}},$$

and a unique dominant left-eigenvector

$$\boldsymbol{q} = [0.035, 0.029, -0.114, 0, 0.177, 0.119, -0.151, -0.064, 0.035, \\ 0.035, -0.137, -0.050, 0, 0, -0.055]^{\mathsf{T}}.$$

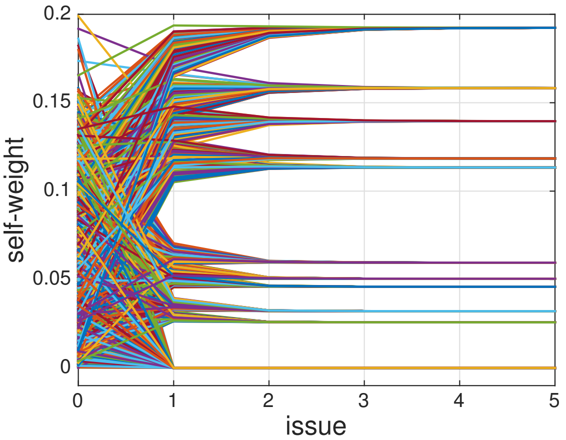

(a) Monte Carlo trial of self-weight dynamics with 200 initial conditions

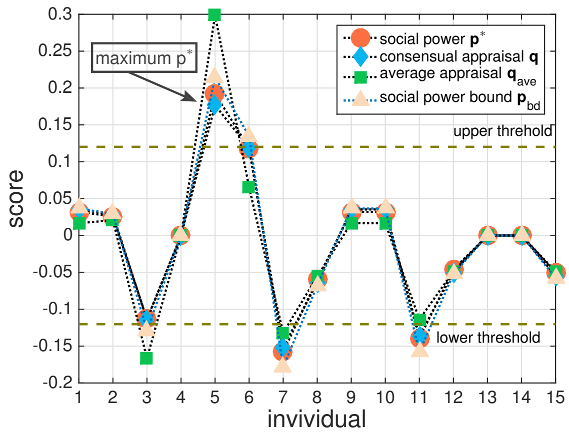

(b) Comparsion of different evaluation metrics.

Figure 4.7: Numerical illustration of the developed results on quasi-strongly connected and structurally balanced influence networks.

Similarly, the dynamical trajectories of the self-weights with 200 randomly initial conditions are illustrated in Figure 4.7a. Individuals asymptotically forget their originally perceived social influence. In analogy with the strongly connected case, Emma still has the maximum equilibrium social power and the statements on the ordering of the social power ranking at equilibrium point hold, as illustrated in Figure 4.7b. The observation that Mike, Andy, and Bill have zero social power in the equilibrium configuration verifies statement (ii) of Theorem 4.4.

4.5 Literature Review

Similar to the previous chapter, we introduce some literature related to the work of this chapter before making a conclusion. The seminal work of French in the 1950s [Fre56] initiated the investigation of the total (direct and indirect) influence of each individual's initial idea on the final collective opinion outcome. By shifting the focus on opinion dynamics on a single issue to successive issues, the DeGroot-Friedkin (DF) model was proposed in [JMFB15] to study the evolution of individuals' social power along the issue sequence. Central in the dynamic evolution is the theory of reflected appraisal [Fri11]. Empirical validation of the Degroot-Friedkin model can be found in [FJB16]. Other research efforts on developing the DeGroot-Friedkin model include relaxation to reducible influence networks [JFB17], extensions to dynamic interaction topology [YLA+18], distributed modeling in both continuous time [CLB+17] and discrete time [XLJB16].

4.6 Summary

In this chapter, we examine a social group of actors discussing and forming opinions over a sequence of issues on the evolutionary influence networks. A self-regulation of individuals' attachments to their initial beliefs along the issue sequence is of central importance in the evolution of interpersonal influence. The adjustment of individuals' degrees of openness-closure rests in a well-accepted sociological observation - the “reflected appraisal mechanism”. This mechanistic explanation is also responsible for the evaluation of individual social power in controlling the outcome of opinions. A significant advance of this chapter is to employ an interpersonal appraisal mechanism to involve in the configuration of influence relationships among social entities. This employment provides a natural, plausible explanation for the emergence of positiveness and negativeness in social interrelations. As a consequence, the opinion dynamics evolving over this class of networks exhibits diverse outcomes of the sequential issue discussions. These settled behaviors include not only consensus in common with unsigned cases, but also neutrality, polarity, and dissension. From the sociological and psychological perspective, our investigation is thus more in line with “real-life” issue discussions in social organizations. Moreover, we emphasize the functional role of the dominant left eigenspace of influence/appraisal structure on Friedkin’s reflected appraisal mechanism, as well as the dominant right eigenspace. At the stage of convergence analysis, the accommodation of differential Lyapunov theorem establishes the contraction properties of the proposed self-appraisal system and associated dynamics of social power. Especially, the self-confidence weights of individuals exponentially converge to a unique, static configuration in the interior of the probability simplex. Besides, individuals gradually forget their initial perception of relative importance in the networks as the sequence of issues enlarges. For better applicability, we also examine the developed framework under the consideration of influence networks with different topological hypotheses. The theoretical and numerical illustrations confirm the specifications of the postulated dynamics in this chapter.

Any complex network can be represented by a graph and any graph can be represented by an adjacency matrix, from which other matrices such as the Laplacian are derived.

Piet van Mieghem

Chapter 5

Distributed Topology Operations for Enhancing Network Performance

This chapter addresses the second aspect of this thesis, namely the distributed optimal design of network topology concerning specific performance criteria. In general, the problems of topology design to optimize network metrics are NP-hard and are traditionally solved by heuristics and approximation algorithms. While numerous methods to design network topology already exist, these approaches are commonly based on complete full information of the network model and a centralized manner. In an attempt to eliminate the dependence on high-level knowledge about the network, we propose a unified distributed strategy to distributively compute a (sub)-optimal solution to link-operation problems. More specifically, an eigenvalue-sensitivity analysis is sought to formulate an optimization problem involving the eigenvectors of network matrices. A distributed power-iteration scheme is then developed to estimate the eigenvector of interest, and a distributed identification process is carried out to find the near-optimal solution of the topology-design problem. Some emerging techniques coming from communication and computation science, including event-based control, parallel algorithm design, and distributed learning, play a key role in the development of distributed strategies. More importantly, we revisit the link-operation problem from the perspective of coevolutionary networks and discuss the optimality of the proposed methods compared the original combinatorial problem from the viewpoint of topological graph theory.

The remainder of this chapter is organized as follows. Section 5.1 considers a robust distributed controller design for interconnected systems with topological uncertainty. In Section 5.2, we provide a distributed algorithm for optimal link addition operation with local knowledge of the network topology. With the particular focus on mitigating epidemic spreading over networks by link removal or rewiring, we improve the proposed distributed strategy from the perspective of low-power communication and efficient algorithm design in Section 5.3. We present a literature overview of related works and conclude with a summary in Section 5.5 and in Section 5.4, respectively.

5.1 Robust Control Design for Interconnected Systems under Topological Uncertainty

The individual subsystems in a large-scale interconnected system are physically coupled; typically the overall system has a specific sparse structure. For such large-size systems, centralized or conventional control methods become unfeasible, since they assume that a single centralized controller has instantaneous access to all measurements. Advances in digital communication technologies allow for communication among subsystems and thereby, distributed control schemes come to researchers. One of the challenges in designing distributed control laws is the topological uncertainty due to the physical or communication link failures. Such uncertainty may harm the stability and performance of the entire system. Thus, the main contribution of this section is to propose a design approach for an optimal robust distributed control law for interconnected systems under topology fluctuation.

5.1.1 Problem Formulation

Consider an interconnected system of n linear time-invariant (LTI) subsystems with dynamics described by the following differential equations

$$\begin{aligned}\dot{\boldsymbol{x}}_i(t) &= \boldsymbol{F}_i\boldsymbol{x}_i(t)+\sum_{j=1}^{n} a^p_{ij}\boldsymbol{F}_{ij}\boldsymbol{x}_j(t)+\boldsymbol{G}^i_1\boldsymbol{w}_i(t)+\boldsymbol{G}^i_2\boldsymbol{u}_i(t),\\ \boldsymbol{z}_i(t) &= \boldsymbol{H}_i\boldsymbol{x}_i(t), \qquad i=1,2,\ldots,n\end{aligned} \tag{5.1}$$

where $\boldsymbol{x}_i \in \mathbb{R}^{n_x}$, $\boldsymbol{u}_i \in \mathbb{R}^{n_u}$ are respectively the state and state-feedback input of subsystem i, and matrices $\boldsymbol{F}_i$, $\boldsymbol{F}_{ij}$, $\boldsymbol{G}^i_1$, $\boldsymbol{G}^i_2$ and $\boldsymbol{H}_i$ are real and of compatible dimensions. For convenient illustration, we consider the dimension for all subsystems to be equal but the approach can be straightforwardly extended to different dimensions. The performance output $\boldsymbol{z}_i \in \mathbb{R}^{n_z}$ represents an error signal and the exogenous signal $\boldsymbol{w}_i \in \mathbb{R}^{n_w}$ denotes all external inputs, including sensor noise, disturbance, and commands. The term $\sum_{j=1}^{n} a^p_{ij}\boldsymbol{F}_{ij}\boldsymbol{x}_j$ represents the physical coupling with neighboring subsystems and matrix $\boldsymbol{F}_{ij}$ is the coupling strength between subsystem i and j, respectively. The physical coupling architecture is encoded by an adjacency matrix $\boldsymbol{A}^p=[a^p_{ij}]\in\mathbb{R}^{n\times n}_{\geq 0}$. In many practical situations, the physical coupling between any two subsystems may not always be available or fixed due to the failure of physical devices, geographical limitations or environmental changes. Motivated by recent technological advances in wired and wireless communication, remote non-local information can be used to implement the following local control law

$$\boldsymbol{u}_i(t)=\boldsymbol{K}_i\boldsymbol{x}_i(t)+\sum_{j=1}^{n} a^c_{ij}\boldsymbol{K}_{ij}\boldsymbol{x}_j(t), \qquad i=1,\ldots,n, \tag{5.2}$$

where $\boldsymbol{K}_i$ and $\boldsymbol{K}_{ij}$ is the self- and neighboring-feedback gain. Another adjacency matrix $\boldsymbol{A}^c=[a^c_{ij}]\in\mathbb{R}^{n\times n}_{\geq 0}$ describes the communication structure among subsystems. The physically coupled system (5.1) together with the communication-based control law (5.2) is illustrated in Figure 5.1 wherein solid blue lines represent physical coupling, solid black lines are locally state-feedback, and solid red lines correspond to the communication links among subsystems.

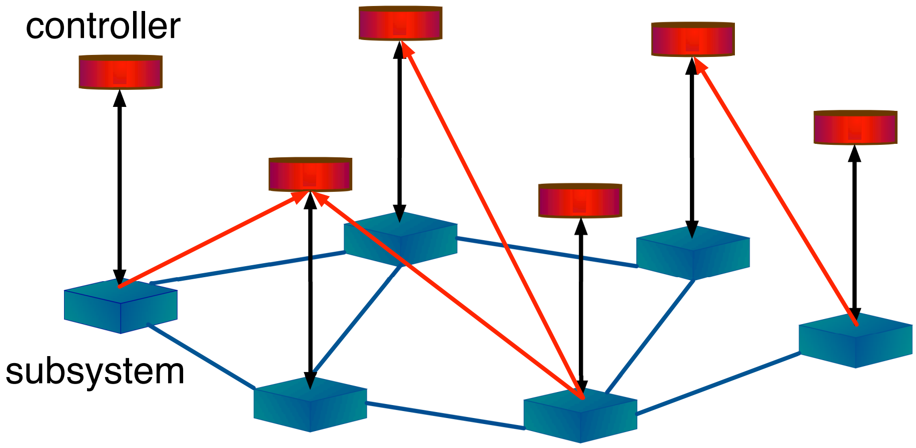

Figure 5.1: An illustrative diagram for a synthesized network of physical coupling and communication topology.

A joint simple graph[1] $\mathcal{G} = (\mathbb{V}, \mathbb{E}^p \cup \mathbb{E}^c, \boldsymbol{A} \in \{0,1\}^{n\times n})$ represents the integrated interconnection relationships of the physical couplings among subsystems and the communication structure in the distributed controllers. $\mathbb{V} = \{1,\dots,n\}$ is a set of nodes, and $\mathbb{E}^p$ and $\mathbb{E}^c$ are the set of edges in coupling and communicating topologies, respectively. When $\mathbb{E}^c = \emptyset$, the control law reduces to a *decentralized* control[2] and the graph $(\mathbb{V}, \mathbb{E}^c, \boldsymbol{A}^c)$ being a complete graph corresponds to a centralized control. For some reasons, such as for computation and communication resource constraints, the underlying interconnection of practical systems has a sparsity. In the sequel of this section, we characterize the network sparsity by imposing a connectivity bound $\bar{d}$ on the degree $\mathrm{deg}_i := \sum_{j=1}^{n} a_{ij}$ of each subsystem i, i.e., $1 \le \mathrm{deg}_i \le \bar{d}$ for all $i \in \mathbb{V}$, resulting in the following admissible set of network topology,

$$\mathbb{G}(\bar{d}) = \{\mathcal{G} | \mathcal{G} \text{ is connected and } 1 \le \mathrm{deg}_i(\mathcal{G}) \le \bar{d},\ \forall i \in \mathbb{V}\}, \tag{5.3}$$

which corresponds to the definition of topological uncertainty. In the extreme case of $\bar{d} = n-1$, the set $\mathbb{G}(\bar{d})$ contains arbitrary topologies for a given number of vertices. A smaller $\bar{d}$ reduces the cardinality of the set and imposes a stronger restriction on the admissible interconnection structure.

After giving the aggregated state vector $\boldsymbol{x} = [\boldsymbol{x}_1^\top, \dots, \boldsymbol{x}_n^\top]^\top$, the closed-loop dynamics of the entire system can be written as

$$\dot{\boldsymbol{x}}(t) = \big(\boldsymbol{F} + \boldsymbol{G}_2\boldsymbol{K}\big)\boldsymbol{x}(t) + \boldsymbol{G}_1\boldsymbol{w}(t), \qquad \boldsymbol{z}(t) = \boldsymbol{H}\boldsymbol{x}(t), \tag{5.4}$$

where $\boldsymbol{z} = [\boldsymbol{z}_1^\top, \dots, \boldsymbol{z}_n^\top]^\top$, $\boldsymbol{G}_1 = \mathrm{diag}(\boldsymbol{G}_1^1, \dots, \boldsymbol{G}_1^n)$, $\boldsymbol{G}_2 = \mathrm{diag}(\boldsymbol{G}_2^1, \dots, \boldsymbol{G}_2^n)$, $\boldsymbol{H} = \mathrm{diag}(\boldsymbol{H}_1, \dots, \boldsymbol{H}_n)$ and

$$\boldsymbol{F} = \boldsymbol{F}_{\mathrm{ind}} + \boldsymbol{A}^p \circ \boldsymbol{F}_{\mathrm{int}} = \mathrm{diag}(\boldsymbol{F}_1, \cdots, \boldsymbol{F}_n) + \boldsymbol{A}^p \circ \begin{bmatrix} 0 & \boldsymbol{F}_{12} & \cdots & \boldsymbol{F}_{1n} \\ \boldsymbol{F}_{21} & 0 & \cdots & \boldsymbol{F}_{2n} \\ \vdots & \vdots & \ddots & \vdots \\ \boldsymbol{F}_{n1} & \boldsymbol{F}_{n2} & \cdots & 0 \end{bmatrix},$$

[1] Through this section, we confine ourselves to simple graphs whose edges are undirected, unweighted and unsigned as introduced in Section A.1.1

[2] Every subsystem uses only local measurement signal $\boldsymbol{x}_i$ to compute the control signal $\boldsymbol{u}_i$, and there is no measurement information exchange between the individual subsystems.

where $\circ$ is the Hadamard product. The control gain matrix has an analogous decomposition into a local and an interacted term as

$$\boldsymbol{K} = \boldsymbol{K}_{\text{ind}} + \boldsymbol{A}^c \circ \boldsymbol{K}_{\text{int}}. \tag{5.5}$$

The additional assumption that $(\boldsymbol{F}, \boldsymbol{G}_2)$ is stabilizable and $(\boldsymbol{F}, \boldsymbol{H})$ is detectable, is taken into account in the following.

The goal of this section is to design the communication structure $\boldsymbol{A}^c$ and the feedback gain matrix $\boldsymbol{K}_{\text{ind}}$ and $\boldsymbol{K}_{\text{int}}$ in (5.5) such that 1). the stability of the entire system is preserved in the presence of topological uncertainty, and 2). the control performance (robustness) is guaranteed at the desired level.

5.1.2 Control Law Design for $\mathcal{H}_\infty$ Robust Topology

To deal with external disturbances and topological uncertainty, we first identify a set of distributed control laws which ensures a certain $\mathcal{H}_\infty$ performance level for all graphs $\mathcal{G} \in \mathbb{G}(\bar{d})$.

Denote $\boldsymbol{T}_{zw}$ as the transfer function matrix from the disturbance $\boldsymbol{w}$ to the controlled output $\boldsymbol{z}$ of the interconnected system (5.4), i.e. $\boldsymbol{z} = \boldsymbol{T}_{zw}\boldsymbol{w}$. The classical $\mathcal{H}_\infty$ problem can be stated as follows: given a desired scalar $\gamma > 0$, find an appropriate control protocol $\boldsymbol{u} = \boldsymbol{K}\boldsymbol{x}$, such that the entire system is stable, while $\|\boldsymbol{T}_{zw}\|_\infty < \gamma$. When there is no structural constraint on matrix $\boldsymbol{K}$, *Kalman-Yakubovich-Popov* lemma [DGZ96] shows the condition $\|\boldsymbol{T}_{zw}\|_\infty < \gamma$ being satisfied for the system (5.4) usually means that there exists a positive-definite matrix $\boldsymbol{P}$ such that the following *Riccati* inequality holds

$$(\boldsymbol{F} + \boldsymbol{G}_2\boldsymbol{K})\boldsymbol{P} + \boldsymbol{P}(\boldsymbol{F} + \boldsymbol{G}_2\boldsymbol{K})^\top + \boldsymbol{G}_1\boldsymbol{G}_1^\top + \frac{1}{\gamma^2}\boldsymbol{P}\boldsymbol{H}^\top\boldsymbol{H}\boldsymbol{P} \prec 0. \tag{5.6}$$

This conclusion is usually difficult to extend to the case when the matrix $\boldsymbol{K}$ has a specific topological structure.

To render the problem computationally tractable, we restrict our attention to the matrix $\boldsymbol{P}$ of a diagonal form, i.e., $\boldsymbol{P} = \text{diag}(\boldsymbol{P}_1, \dots, \boldsymbol{P}_n)$, where $\boldsymbol{P}_i$ is positive definite for all $i = 1, \dots, n$. In addition, we denote a new matrix variable $\boldsymbol{Q} = \boldsymbol{K}\boldsymbol{P}$ which entails the following form

$$\boldsymbol{Q} = \boldsymbol{Q}_{\text{ind}} + \boldsymbol{A}^c \circ \boldsymbol{Q}_{\text{int}} = \text{diag}(\boldsymbol{Q}_1, \dots, \boldsymbol{Q}_N) + \boldsymbol{A}^c \circ \begin{bmatrix} 0 & \boldsymbol{Q}_{12} & \cdots & \boldsymbol{Q}_{1n} \\ \boldsymbol{Q}_{21} & 0 & \cdots & \boldsymbol{Q}_{2n} \\ \vdots & \vdots & \ddots & \vdots \\ \boldsymbol{Q}_{n1} & \boldsymbol{Q}_{n2} & \cdots & 0 \end{bmatrix},$$

where $\boldsymbol{Q}_i = \boldsymbol{K}_i\boldsymbol{P}_i$ and $\boldsymbol{Q}_{ij} = \boldsymbol{K}_{ij}\boldsymbol{P}_j$. The Riccati inequality (5.6) can be rewritten as

$$\boldsymbol{F}\boldsymbol{P} + \boldsymbol{P}\boldsymbol{F}^\top + \boldsymbol{G}_2\boldsymbol{Q} + \boldsymbol{Q}^\top\boldsymbol{G}_2^\top + \boldsymbol{G}_1\boldsymbol{G}_1^\top + \frac{1}{\gamma^2}\boldsymbol{P}\boldsymbol{H}^\top\boldsymbol{H}\boldsymbol{P} \prec 0. \tag{5.7}$$

Since the matrix $\boldsymbol{P}$ is diagonal, the i, j block of (5.7) reads

$$\begin{aligned} &\text{for } i = j: \quad && \boldsymbol{F}_i\boldsymbol{P}_i + \boldsymbol{P}_i\boldsymbol{F}_i^\top + \boldsymbol{G}_2^i\boldsymbol{Q}_i + \boldsymbol{Q}_i^\top(\boldsymbol{G}_2^i)^\top + \boldsymbol{G}_1^i(\boldsymbol{G}_1^i)^\top + \frac{1}{\gamma^2}\boldsymbol{P}_i\boldsymbol{H}_i^\top\boldsymbol{H}_i\boldsymbol{P}_i, \\ &\text{for } i \neq j: \quad && a_{ij}^p\boldsymbol{F}_{ij}\boldsymbol{P}_j + a_{ji}^p\boldsymbol{P}_i\boldsymbol{F}_{ji}^\top + a_{ij}^c\boldsymbol{G}_2^i\boldsymbol{Q}_{ij} + a_{ji}^c\boldsymbol{Q}_{ji}^\top(\boldsymbol{G}_2^j)^\top. \end{aligned}$$

Fact 5.1 ([CL04]). *Let a Hermitian matrix $\boldsymbol{M}$ be partitioned into blocks $\boldsymbol{M}_{ij}$, where $i, j = 1, \ldots, n$. Suppose the number of nonzero off-diagonal blocks in i-th row of $\boldsymbol{M}$ is m_i. Without loss of generality, there exist at least one nonzero off-diagonal block in each row. If the relation*

$$\begin{bmatrix} \frac{1}{m_i}\boldsymbol{M}_{ii} & \boldsymbol{M}_{ij} \\ \boldsymbol{M}_{ji} & \frac{1}{m_j}\boldsymbol{M}_{jj} \end{bmatrix} \succ 0 \tag{5.8}$$

holds for all $i, j = 1, \ldots, n$, $i \neq j$, then one has $\boldsymbol{M} \succ 0$.

In the following theorem, a distributed control algorithm is proposed to determine when the interconnected system has a robust $\mathcal{H}_\infty$ performance for any graph $\mathcal{G} \in \mathbb{G}(d)$.

Theorem 5.1: Robust $\mathcal{H}_\infty$ Controller Design

Consider the interconnected system (5.4) and the admissible set of topology $\mathbb{G}(\bar{d})$ given in (5.3). If $\boldsymbol{P}_i \succ 0$, $\boldsymbol{Q}_i$, $\boldsymbol{Q}_{ij}$ $(i, j = 1, \ldots, n)$ are the solutions of the following linear matrix inequalities:

$$\begin{aligned} &\tilde{\boldsymbol{F}}_{ij}\hat{\boldsymbol{P}}_{ij} + \hat{\boldsymbol{P}}_{ij}\tilde{\boldsymbol{F}}_{ij}^\top + \hat{\boldsymbol{G}}_2^{ij}\tilde{\boldsymbol{Q}}_{ij} + \tilde{\boldsymbol{Q}}_{ij}^\top(\hat{\boldsymbol{G}}_2^{ij})^\top + \hat{\boldsymbol{G}}_1^{ij}(\hat{\boldsymbol{G}}_1^{ij})^\top + \frac{1}{\gamma^2}\hat{\boldsymbol{P}}_{ij}\hat{\boldsymbol{H}}_{ij}^\top\hat{\boldsymbol{H}}_{ij}\hat{\boldsymbol{P}}_{ij} \prec 0 \\ &\tilde{\boldsymbol{F}}_{ij}\hat{\boldsymbol{P}}_{ij} + \hat{\boldsymbol{P}}_{ij}\tilde{\boldsymbol{F}}_{ij}^\top + \hat{\boldsymbol{G}}_2^{ij}\hat{\boldsymbol{Q}}_{ij} + \hat{\boldsymbol{Q}}_{ij}^\top(\hat{\boldsymbol{G}}_2^{ij})^\top + \hat{\boldsymbol{G}}_1^{ij}(\hat{\boldsymbol{G}}_1^{ij})^\top + \frac{1}{\gamma^2}\hat{\boldsymbol{P}}_{ij}\hat{\boldsymbol{H}}_{ij}^\top\hat{\boldsymbol{H}}_{ij}\hat{\boldsymbol{P}}_{ij} \prec 0 \\ &\hat{\boldsymbol{F}}_{ij}\hat{\boldsymbol{P}}_{ij} + \hat{\boldsymbol{P}}_{ij}\hat{\boldsymbol{F}}_{ij}^\top + \hat{\boldsymbol{G}}_2^{ij}\tilde{\boldsymbol{Q}}_{ij} + \tilde{\boldsymbol{Q}}_{ij}^\top(\hat{\boldsymbol{G}}_2^{ij})^\top + \hat{\boldsymbol{G}}_1^{ij}(\hat{\boldsymbol{G}}_1^{ij})^\top + \frac{1}{\gamma^2}\hat{\boldsymbol{P}}_{ij}\hat{\boldsymbol{H}}_{ij}^\top\hat{\boldsymbol{H}}_{ij}\hat{\boldsymbol{P}}_{ij} \prec 0 \end{aligned} \tag{5.9}$$

with the performance level $\gamma > 0$ and

$$\tilde{\boldsymbol{F}}_{ij} = \begin{bmatrix} \boldsymbol{F}_i & \bar{d}\boldsymbol{F}_{ij} \\ \bar{d}\boldsymbol{F}_{ji} & \boldsymbol{F}_j \end{bmatrix} \quad \hat{\boldsymbol{F}}_{ij} = \begin{bmatrix} \boldsymbol{F}_i & \boldsymbol{0} \\ \boldsymbol{0} & \boldsymbol{F}_j \end{bmatrix} \quad \hat{\boldsymbol{G}}_1^{ij} = \begin{bmatrix} \boldsymbol{G}_1^i & \boldsymbol{0} \\ \boldsymbol{0} & \boldsymbol{G}_1^j \end{bmatrix} \quad \hat{\boldsymbol{G}}_2^{ij} = \begin{bmatrix} \boldsymbol{G}_2^i & \boldsymbol{0} \\ \boldsymbol{0} & \boldsymbol{G}_2^j \end{bmatrix}$$

$$\tilde{\boldsymbol{Q}}_{ij} = \begin{bmatrix} \boldsymbol{Q}_i & \bar{d}\boldsymbol{Q}_{ij} \\ \bar{d}\boldsymbol{G}_{ji} & \boldsymbol{Q}_j \end{bmatrix} \quad \hat{\boldsymbol{Q}}_{ij} = \begin{bmatrix} \boldsymbol{Q}_i & \boldsymbol{0} \\ \boldsymbol{0} & \boldsymbol{Q}_j \end{bmatrix} \quad \hat{\boldsymbol{P}}_{ij} = \begin{bmatrix} \boldsymbol{P}_i & \boldsymbol{0} \\ \boldsymbol{0} & \boldsymbol{P}_j \end{bmatrix} \quad \hat{\boldsymbol{H}}_{ij} = \begin{bmatrix} \boldsymbol{H}_i & \boldsymbol{0} \\ \boldsymbol{0} & \boldsymbol{H}_j \end{bmatrix},$$

then the distributed control law (5.2) with $\boldsymbol{K}_i = \boldsymbol{Q}_i\boldsymbol{P}_i^{-1}$, and $\boldsymbol{K}_{ij} = \boldsymbol{Q}_{ij}\boldsymbol{P}_j^{-1}$ stabilizes the system (5.1) and guarantees $\|\boldsymbol{T}_{zw}\|_\infty < \gamma$, for all $\mathcal{G} \in \mathbb{G}(\bar{d})$.

Proof. The three matrix inequalities in (5.9) are equivalent to

$$\begin{bmatrix} \frac{1}{\bar{d}}\boldsymbol{\Phi}_i & \boldsymbol{\theta}_k^\top\boldsymbol{\Lambda}_{ij} \\ \boldsymbol{\theta}_k^\top\boldsymbol{\Lambda}_{ji} & \frac{1}{\bar{d}}\boldsymbol{\Phi}_j \end{bmatrix} \prec 0, \qquad k = 1, 2, 3, \quad i, j = 1, \ldots, n \tag{5.10}$$

where $\boldsymbol{\Lambda}_{ij} = [\boldsymbol{P}_j^\top\boldsymbol{F}_{ij}^\top, \boldsymbol{F}_{ji}^\top\boldsymbol{P}_i^\top, \boldsymbol{Q}_{ij}^\top(\boldsymbol{G}_2^i)^\top, \boldsymbol{G}_2^j\boldsymbol{Q}_{ji}]^\top$, $\boldsymbol{\theta}_1 = [\boldsymbol{1}^\top, \boldsymbol{1}^\top, \boldsymbol{1}^\top, \boldsymbol{1}^\top]^\top$, $\boldsymbol{\theta}_2 = [\boldsymbol{1}^\top, \boldsymbol{1}^\top, \boldsymbol{0}^\top, \boldsymbol{0}^\top]^\top$, $\boldsymbol{\theta}_3 = [\boldsymbol{0}^\top, \boldsymbol{0}^\top, \boldsymbol{1}^\top, \boldsymbol{1}^\top]^\top$, and

$$\boldsymbol{\Phi}_i = \boldsymbol{F}_i\boldsymbol{P}_i + \boldsymbol{P}_i\boldsymbol{F}_i^\top + \boldsymbol{G}_2^i\boldsymbol{Q}_i + \boldsymbol{Q}_i^\top(\boldsymbol{G}_2^i)^\top + \boldsymbol{G}_1^i(\boldsymbol{G}_1^i)^\top + \frac{1}{\gamma^2}\boldsymbol{P}_i\boldsymbol{H}_i^\top\boldsymbol{H}_i\boldsymbol{P}_i.$$

Based on Fact 5.1 and the fact $\deg_i \le \bar{d}$, if the following linear matrix inequalities

$$\begin{bmatrix} \frac{1}{\deg_i}\boldsymbol{\Phi}_i & \boldsymbol{a}_{ij}^\top \boldsymbol{\Lambda}_{ij} \\ \boldsymbol{a}_{ji}^\top \boldsymbol{\Lambda}_{ji} & \frac{1}{\deg_j}\boldsymbol{\Phi}_j \end{bmatrix} \prec 0, \quad \text{where } \boldsymbol{a}_{ij} = [a_{ij}^p, a_{ji}^p, a_{ij}^c, a_{ji}^c]^\top, \quad i \neq j, \tag{5.11}$$

holds for all $i, j = 1, \ldots, n$, then the inequality (5.7) is achieved. To examine inequality (5.11), we investigate all possibility: 1). $a_{ij}^p = a_{ji}^p = a_{ij}^c = a_{ji}^c = 1$; 2). $a_{ij}^p = a_{ji}^p = a_{ij}^c = a_{ji}^c = 0$; 3). $a_{ij}^p = a_{ji}^p = 1, a_{ij}^c = a_{ji}^c = 0$; 4).$a_{ij}^p = a_{ji}^p = 0, a_{ij}^c = a_{ji}^c = 1$. The case 1) and 2) can be easily confirmed by inequality (5.10) with $\boldsymbol{\theta}_1$. The inequalities (5.10) with $\boldsymbol{\theta}_2$ and $\boldsymbol{\theta}_3$ can be used to verify the case 3) and 4), respectively. In conclusion, the inequality (5.11) holds for all $i \neq j$. Thus, the interconnected system is stable, while $\|\boldsymbol{T}_{zw}\|_\infty < \gamma$ for all graph $\mathcal{G} \in \mathbb{G}(\bar{d})$. This completes the proof. □

The results of Theorem 5.1 offer some additional insights into the manipulation of the large-scale interconnected systems. Under local degree constraints, we are allowed to add or remove communication links to a certain degree. The link gains can be calculated independently in a distributed manner from the LMIs (5.9). In fact, this criterion (5.9) can be tested on each subsystem in a distributed way. As such, the design framework is very appealing for practical systems, for example, in a smart grid consisting of renewable energy resources such as wind or solar. The developed design procedure will guarantee the given robustness level for any graph topology satisfying a pre-determined degree bound. Moreover, in the procedure of allocating communication links, the restriction on the maximal interconnection of each subsystem can balance the link distribution among the subsystems, i.e., prevent a fraction of subsystem from being highly connected in contrast to others, reduce the risk of the network to be inoperable due to subsystem failures.

5.1.3 Optimal Robust Communication Topology Design

Within the scope of optimal control design for interconnected systems, the identification of the most favorable interconnection structure under a given performance level is desirable. In contrast to $\mathcal{H}_\infty$, the $\mathcal{H}_2$ norm control design is more appealing for control engineers to achieve the desired control performance. In particular, the $\mathcal{H}_2$ theory is well-understood and associated with many mature and efficient numerical algorithms. A suboptimal $\mathcal{H}_2$ performance with a guaranteed worst-case performance is considered here, which leads to a suboptimal strategy for allocating the communication links. In addition, a trade-off between the performance improvement and communication cost incorporates into the topology design.

The cost function of $\mathcal{H}_2$ optimal control problem is given by

$$J(\boldsymbol{A}^c) = \mathrm{tr}\left(\int_0^\infty \boldsymbol{G}_1^\top e^{(\boldsymbol{F}+\boldsymbol{G}_2(\boldsymbol{K}_{\mathrm{int}}+\boldsymbol{A}^c\circ\boldsymbol{K}_{\mathrm{ind}}))^\top t} \boldsymbol{H}^\top \boldsymbol{H} e^{(\boldsymbol{F}+\boldsymbol{G}_2(\boldsymbol{K}_{\mathrm{int}}+\boldsymbol{A}^c\circ\boldsymbol{K}_{\mathrm{ind}}))t} \boldsymbol{G}_1 dt \right)$$

where the adjacency matrix $\boldsymbol{A}^c$ is the only decision variable in the cost function and its entries a_{ij}^c relies implicitly on the degree limitation $\bar{d}$ and the physical coupling index a_{ij}^p. According to the Theorem 5.1, the feedback controller $\boldsymbol{u}(t) = \boldsymbol{K}\boldsymbol{x}(t)$ based on the underlying topology $\mathcal{G} \in \mathbb{G}(\bar{d})$ stabilizes the system. That is, the above integral is bounded and it can be evaluated by solving the Lyapunov equation

$$\left(\boldsymbol{F} + \boldsymbol{G}_2(\boldsymbol{K}_{\mathrm{int}} + \boldsymbol{A}^c \circ \boldsymbol{K}_{\mathrm{ind}})\right)^\top \boldsymbol{\Gamma} + \boldsymbol{\Gamma}\left(\boldsymbol{F} + \boldsymbol{G}_2(\boldsymbol{K}_{\mathrm{int}} + \boldsymbol{A}^c \circ \boldsymbol{K}_{\mathrm{ind}})\right) = -\boldsymbol{H}^\top \boldsymbol{H}, \tag{5.12}$$

where the matrix $\boldsymbol{\Gamma}(\boldsymbol{A}^c)$ is the observability Gramian of the overall system (5.4) and is relevant to the communication topology.

To this end, the optimal robust network design problem can be formulated to the following minimization

$$\begin{aligned}\min_{\boldsymbol{A}^c\in\{0,1\}^{n\times n}} \quad & \mathrm{tr}\Big(\boldsymbol{G}_1^\top\boldsymbol{\Gamma}(\boldsymbol{A}^c)\boldsymbol{G}_1\Big)+\frac{\rho}{2}\mathbf{1}^\top\boldsymbol{A}^c\mathbf{1} \\ \text{s.t.} \quad & 1\le\sum_{j=1}^{n}\Big(1-(1-a_{ij}^p)(1-a_{ij}^c)\Big)\le\bar{d},\ \forall i,j\in\{1,\dots,n\} \quad \text{and (5.12) holds.}\end{aligned}\tag{P1a}$$

The second term on the right-hand side of the objective function in the optimization problem (P1a) calls for the communication penalty. In particular, the factor ρ weights the trade-off between control performance and communication cost. In general, a larger value of ρ encourages fewer communication links but at the expense of worse system performance. The $\mathcal{H}_2$ optimal problem incorporated with communication constraints in minimization problem (P1a) results in a combinatorial problem. Despite the existence of nonconvex constraints, the digital software can still be employed to achieve the locally optimal solution.

Furthermore, Theorem 5.1 renders that the closed-loop interconnected system (5.4) preserves robust $\mathcal{H}_\infty$ performance, and hence the inverse matrix of $(\boldsymbol{F}+\boldsymbol{G}_2\boldsymbol{K})$ exists. Right multiplying $(\boldsymbol{F}+\boldsymbol{G}_2\boldsymbol{K})^{-1}$ at both sides, the Lyapunov equation (5.12) becomes:

$$(\boldsymbol{F}+\boldsymbol{G}_2\boldsymbol{K})^\top\boldsymbol{\Gamma}(\boldsymbol{F}+\boldsymbol{G}_2\boldsymbol{K})^{-1}+\boldsymbol{\Gamma}=-\boldsymbol{H}^\top\boldsymbol{H}(\boldsymbol{F}+\boldsymbol{G}_2\boldsymbol{K})^{-1}.$$

Using the cyclic permutations of trace function, the following equation can be obtained from the above equation

$$\mathrm{tr}(\boldsymbol{\Gamma})=-\frac{1}{2}\,\mathrm{tr}\Big(\boldsymbol{H}^\top\boldsymbol{H}(\boldsymbol{F}+\boldsymbol{G}_2\boldsymbol{K})^{-1}\Big).$$

Supposed the weighted matrix of disturbance $\boldsymbol{G}_1$ is an identity matrix, $\mathrm{deg}_i^p=\sum_{j=1}^n a_{ij}^p$ and $\mathrm{deg}_i^c=\sum_{j=1}^n a_{ij}^c$, optimization problem (P1a) can be reformulated to the following mixed-integer semi-defininte program (MISDP)

$$\begin{aligned}\min_{\boldsymbol{A}^c\in\{0,1\}^{n\times n}} \quad & \mathrm{tr}(\boldsymbol{\Xi})+\rho\mathbf{1}^\top\boldsymbol{A}^c\mathbf{1} \\ \text{s.t.} \quad & \begin{bmatrix}\boldsymbol{\Xi} & \boldsymbol{H}^\top \\ \boldsymbol{H} & \boldsymbol{F}+\boldsymbol{G}_2\boldsymbol{K}(\boldsymbol{A}^c)\end{bmatrix}\preceq 0, \\ & \boldsymbol{I}_n\preceq\mathrm{diag}(\mathrm{deg}_1^p,\dots,\mathrm{deg}_n^p)+\mathrm{diag}(\mathrm{deg}_1^c,\dots,\mathrm{deg}_n^c)+\boldsymbol{I}_n\circ(\boldsymbol{A}^p\boldsymbol{A}^c)\preceq\bar{d}\boldsymbol{I}_n,\end{aligned}\tag{P1b}$$

which is based on the property $\boldsymbol{A}+\boldsymbol{G}_2\boldsymbol{K}\succ 0$ and *Schur complement* and can be solved using sophisticated algorithms, e.g., branch-and-bound method [KV12].

5.1.4 Numerical Evaluations

In this subsection, the developed robust controller design criterion is evaluated via numerical examples. We consider a system consisting of 5 scalar subsystems with undirected physical couplings which are shown by solid black lines in Figure 5.2. Let $\gamma=0.5$ and

Table 5.1: $\mathcal{H}_2$ performance vs. communication cost

ρ	communication links	$\mathcal{H}_2$ norm
3×10^{-5}	$(2,3)$, $(3,4)$, $(4,5)$	0.3977
5×10^{-5}	$(2,3)$, $(3,4)$	0.3978
1.2×10^{-4}	$(3,4)$	0.3979

$\bar{d}=2$ in this case. Other matrices of interest are respectively given by $\boldsymbol{G}_1=\boldsymbol{I}$, $\boldsymbol{G}_2=\boldsymbol{I}/3$, $\boldsymbol{H}=\mathrm{diag}(1.6,\ 0.8,\ 2.4,\ 3.2,\ 1.6)$,

$$\boldsymbol{F}=\begin{bmatrix}-2&1&1&2&1\\0.5&-2&1&1.5&0.5\\1&1&-4&1.5&0.5\\1.5&1&1.5&-3&0.5\\1&0.5&1&0.5&-2\end{bmatrix},\quad\text{and}\quad \boldsymbol{K}=\begin{bmatrix}-73.1&-0.9&-1.8&-3.7&-1.4\\-1.8&-67.1&-2.8&-3.9&-1.0\\-1.3&-1.0&-71.2&-2.7&-0.8\\-1.9&-1.0&-2.0&-75.3&-0.5\\-1.7&-0.6&-1.4&-1.3&-71.1\end{bmatrix},$$

where the feedback gain matrix derived from the adoption of YALMIP toolbox [Lof04] and SDPT3 toolbox [TTT01] to solve the LMIs (5.9). Thus, the $\mathcal{H}_\infty$ performance of the interconnected systems is guaranteed for any graph in $\mathbb{G}(\bar{d})$. Next, the optimal communication topology is determined by solving the $\mathcal{H}_2$ optimal problem presented in (P1b) with the penalty weight $\rho=5\times10^{-5}$. The consequent communication topology is shown in Figure 5.2 by the red dash lines. The $\mathcal{H}_2$ norm, in this case, equals to 0.3978.

Finally, the trade-off between the achievable performance and the required communication cost is under investigation. As shown in Table 5.1, employing more communication links results in a smaller $\mathcal{H}_2$ performance but at the price of higher communication cost. Figure 5.2 shows the corresponding communication architectures by the red dashed line.

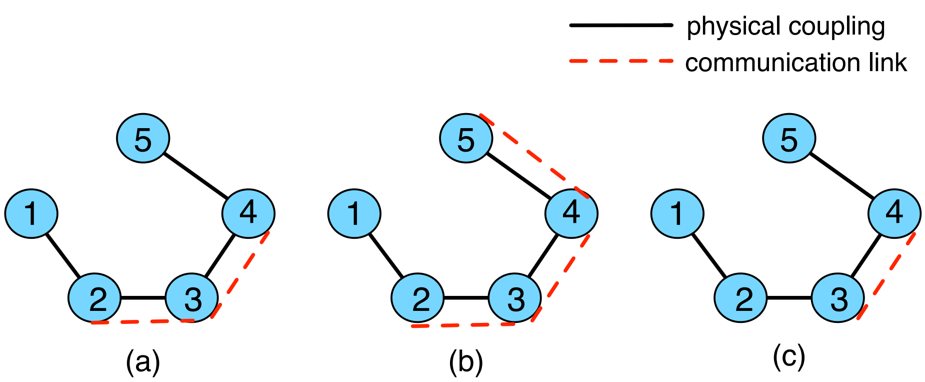

Figure 5.2: An interconnected system consisting of 5 subsystems: (a) $\rho=5\times10^{-5}$; (b) $\rho=3\times10^{-5}$; (c) $\rho=1.2\times10^{-4}$.

5.2 Distributed Link Addition Using Local Estimation of Network Topology

As mentioned in the previous section, many existing methods including greedy heuristics and approximation approaches can be used to solve the combinatorial problem efficiently in a centralized fashion. However, the performance of those approaches depends highly on the knowledge of network topology which is unlikely to accumulate in real large-scale networks due to geographical constraints or privacy concerns. In this section, we devote ourselves to developing new distributed algorithms to solve such network-based optimization problems in the absence of information on the global network structure. Particular focus is on the link-operation problems for reinforcing the network resilience against malicious attacks. Among other metrics, the algebraic connectivity is one of the most prominent parameters to evaluate how well a network defends and restores to a stable state in the presence of random failures and targeted attacks. An effective preventive approach for enhancing network resilience is to add edges into the network.

5.2.1 Problem Formulation

Consider a connected simple graph $\mathcal{G}_0 = (\mathbb{V}, \mathbb{E}_0, \boldsymbol{A}_0)$ with a Laplacian $\boldsymbol{L}_0$ and a neighboring set $\mathbb{V}_0^i$ for each node $i \in \mathbb{V}$. Our goal is to add m_a number of links $\Delta\mathbb{E}^+$ from the set $\overline{\mathbb{E}}_0$ such that the algebraic connectivity[3] of the resulting graph $\mathcal{G}_{m_a}^+ = (\mathbb{V}, \mathbb{E}_0 \cup \Delta\mathbb{E}^+, \boldsymbol{A}_{m_a}^+)$ is maximized. The problem in general can be formulated as the following optimization problem

$$\begin{aligned} \max_{\Delta\mathbb{E}^+ \subseteq \overline{\mathbb{E}}_0} \quad & \lambda_2(\boldsymbol{L}_{m_a}^+) \\ \text{s.t.} \quad & |\Delta\mathbb{E}^+| = m_a, \end{aligned} \tag{P2a}$$

where $\boldsymbol{L}_{m_a}^+$ represents the Laplacian associated to $\mathcal{G}_{m_a}^+$. Drawing upon the edge labeling $\bar{l}_{ij} \sim (j,i) \in \overline{\mathbb{E}}_0$ on the complement graph $\overline{\mathcal{G}}_0$ and Laplacian factorization, the optimization problem (P2a) can be recast as

$$\begin{aligned} \max_{\bar{\boldsymbol{y}} \in \{0,1\}^{|\overline{\mathbb{E}}_0|}} \quad & \lambda_2(\boldsymbol{L}_0 + \Delta\boldsymbol{L}_{m_a}^+) \\ \text{s.t.} \quad & \Delta\boldsymbol{L}_{m_a}^+ = \sum_{\bar{l}=1}^{|\overline{\mathbb{E}}_0|} \bar{y}_{\bar{l}_{ij}} \bar{\boldsymbol{\delta}}_{\bar{l}_{ij}} \bar{\boldsymbol{\delta}}_{\bar{l}_{ij}}^\top, \quad \boldsymbol{1}^\top \bar{\boldsymbol{y}} = m_a, \end{aligned} \tag{P2b}$$

where $\bar{\boldsymbol{\delta}}$ is the edge vector adjunct to $\overline{\mathcal{G}}_0$ and for $\bar{l}_{ij} \sim (j,i) \in \overline{\mathbb{E}}_0$, its elements are defined as

$$[\bar{\boldsymbol{\delta}}_{\bar{l}_{ij}}]_k = \begin{cases} 1 & \text{if } k = i, \\ -1 & \text{if } k = j, \\ 0 & \text{otherwise} \end{cases} \qquad \text{for } k = \{1, \dots, n\}. \tag{5.13}$$

Moreover, $\bar{\boldsymbol{y}} = [\bar{y}_1, \dots, \bar{y}_{|\overline{\mathbb{E}}_0|}]^\top$ is defined as a Boolean vector whose $\bar{l}_{ij}$-th entry is one when the edge labeling $\bar{l}_{ij} \sim (j,i) \in \overline{\mathbb{E}}_0$ is added into the graph $\mathcal{G}_0$ and is zero otherwise.

[3] As described in Section A.1.1, the second smallest eigenvalue of the Laplacian matrix measures the algebraic connectivity of a graph.

The optimization problem (P2b) is a combinatorial problem whose global optimum can be extracted by exhaustively searching all possibilities or a suboptimal solution by using a greedy heuristic in polynomial time [SCL16]. One common assumption in solving (P2b) is that the global knowledge of network topology is available. However, this prerequisite is often insubstantial in practice because of computational restrictions and privacy concerns. Hence, the remainder of this section focuses on developing a distributed computation algorithm to solve the optimization problem (P2b) individually by nodes based on the gathered local information.

5.2.2 Distributed Link Addition Algorithm

In this subsection, we formulate an approximation to provide a suboptimal solution to optimization (P2b) and describe a method to solve it in a distributed fashion.

To circumvent the NP-hard nature of the optimization (P2b), we first employ the matrix perturbation analysis [SS90] to provide an approximation of the original problem. Matrix perturbation theory provides an insight into the behavior of the eigenvalues of a matrix while perturbing the matrix. The magnitude of the eigenvalue sensitivity informs about the range of the eigenvalue displacement in the complex plane. The following lemma quantifies the variation of eigenvalues under perturbation.

Fact 5.2 ([GR01]). *Consider a symmetric matrix $\boldsymbol{C}$ perturbed by a symmetric matrix $\Delta\boldsymbol{C}$. The first order approximation of the eigenvalues of $\boldsymbol{C}+\Delta\boldsymbol{C}$ can be expressed as*

$$\lambda_i(\boldsymbol{C}+\Delta\boldsymbol{C}) \approx \lambda_i(\boldsymbol{C}) + \Delta\lambda_i(\boldsymbol{C},\Delta\boldsymbol{C}) \tag{5.14}$$

where the approximated eigenvalue displacement $\Delta\lambda_i(\boldsymbol{C},\Delta\boldsymbol{C}) = \boldsymbol{\eta}_i^\top \Delta\boldsymbol{C}\boldsymbol{\eta}_i/\|\boldsymbol{\eta}_i\|^2$ and $\boldsymbol{\eta}_i$ is the eigenvector of the matrix $\boldsymbol{C}$ with respect to the eigenvalue $\lambda_i(\boldsymbol{C})$.

In the case of link addition, the matrix $\Delta\boldsymbol{L}^+_{m_a}$ can be treated as a perturbation added to the matrix $\boldsymbol{L}_0$. Then, a suboptimal solution to the optimization problem (P2b) can be acquired by solving the following approximation.

Lemma 5.1: Approximation Algorithm for Link addition

The optimization problem (P2b) can be solved approximately by

$$\begin{aligned} \max_{\bar{\boldsymbol{y}}} \quad & \Delta\lambda_2(\boldsymbol{L}_0,\Delta\boldsymbol{L}^+_{m_a}) \\ \text{s.t.} \quad & \Delta\lambda_2(\boldsymbol{L}_0,\Delta\boldsymbol{L}^+_{m_a}) = \sum_{\bar{l}_{ij}=1}^{|\bar{\mathbb{E}}_0|} \bar{y}_{\bar{l}_{ij}}(v_2^i - v_2^j)^2, \quad \mathbf{1}^\top\bar{\boldsymbol{y}} = m_a, \quad \bar{\boldsymbol{y}} \in \{0,1\}^{|\bar{\mathbb{E}}_0|} \end{aligned} \tag{P2c}$$

where $\bar{l}_{ij} \sim (j,i) \in \bar{\mathbb{E}}_0$ and $\boldsymbol{v}_2(\boldsymbol{L}_0) = [v_2^1,\dots,v_2^n]^\top$ is the eigenvector corresponding to the eigenvalue $\lambda_2(\boldsymbol{L}_0)$.

Proof. A well-known fact is that the algebraic connectivity of a connected graph is a non-decreasing function for the edge addition [GB06]. According to Fact 5.2, the first order expansion of the second smallest eigenvalue of $\boldsymbol{L}_0+\Delta\boldsymbol{L}^+_{m_a}$ can be computed as

$$\lambda_2(\boldsymbol{L}_0+\Delta\boldsymbol{L}^+_{m_a}) \approx \lambda_2(\boldsymbol{L}_0) + \frac{\boldsymbol{v}_2^\top \Delta\boldsymbol{L}^+_{m_a}\boldsymbol{v}_2}{\boldsymbol{v}_2^\top\boldsymbol{v}_2},$$

which enables us to approximate the objective function in (P2b) by

$$\max_{\bar{y}} \lambda_2(\boldsymbol{L}^+_{m_a}) \approx \lambda_2(\boldsymbol{L}_0) + \frac{\max_{\bar{y}} \boldsymbol{v}_2^\top \Delta \boldsymbol{L}^+_{m_a} \boldsymbol{v}_2}{\|\boldsymbol{v}_2\|_2^2}.$$

Upon the factorization of $\boldsymbol{L}^+_{m_a}$, we arrive at the approximate algorithm (P2c) and the proof is complete. □

Lemma 5.1 means that the edge-addition method is to select links possessing the largest deviation $|v_2^i - v_2^j|$ from $\bar{l}_{ij} \sim (j,i) \in \overline{\mathbb{E}}_0$. Thus, the optimal solution of the primary problem (P2b) is related to algebraic-graph conditions. Noteworthily, the aggregated squared difference of Fiedler vector elements, i.e., $\sum_{j\in\mathbb{N}^i}(v_2^i - v_2^j)^2$, also appears as a metric to assess the criticality of node i in [ALQR16]. Thus far, the original combinatorial problems (P2b) is approximated by (P2c) which involve the eigenvector associated to the second smallest eigenvalue of the Laplacian matrix. Nevertheless, the complete topological knowledge is necessary to compute those eigenvectors in question, thus preventing performing the topology manipulation process in a distributed fashion.

Power iteration (PI) method [GL12] has been widely used to estimate the simple largest eigenvalue and its associated eigenvector of a symmetric matrix $\boldsymbol{C}$,

$$\hat{\boldsymbol{\eta}}_n(t+1) = \frac{\boldsymbol{C}\hat{\boldsymbol{\eta}}_n(t)}{\|\boldsymbol{C}\hat{\boldsymbol{\eta}}_n(t)\|}, \tag{5.15}$$

where $\hat{\boldsymbol{\eta}}_n(t)$ is the variable of PI estimator at time t. As time evolves, the sequence $\{\hat{\boldsymbol{\eta}}_n(t)\}_{t\in\mathbb{R}_{\geq 0}}$ approaches asymptotically to the principal eigenvector of matrix $\boldsymbol{C}$. For more details on power iteration, see Section A.3. One of the major challenges that arise in the application of PI approach for sizable networks is an intermediate normalization in each iteration step. Yet, this intermediate operation is indispensable for settling the overflow problem, so that the estimates are unlikely to grow to infinity when $\lambda_n(\boldsymbol{C}) > 1$ or shrink to zero when $\lambda_n(\boldsymbol{C}) < 1$. Moreover, we aim to pursue an estimation of the eigenvector corresponding to the second smallest eigenvalue of Laplacian rather than the largest one.

In the sequel of this section, we develop a complete distributed PI method to support sufficient estimation of $\boldsymbol{v}_n$. To get down to bedrock, let consider a network $\mathcal{G} = (\mathbb{V}, \mathbb{E}, \boldsymbol{A})$ with the Laplacian matrix $\boldsymbol{L}$ and the neighborhood set $\mathbb{N}^i$ for each node $i \in \mathbb{V}$ when introducing the distributed computation of the Fiedler vector. First, we define Perron matrix $\boldsymbol{P}$ of a graph by $\boldsymbol{P} = \boldsymbol{I}_n - \beta \boldsymbol{L}$ where $0 < \beta < 1/\max_{i\in\mathbb{V}} \lambda_i(\boldsymbol{L})$. The upper bound on β guarantees the power iteration on Perron matrix converges to the non-negative dominant eigenvalue. The upper bound $1/\max_{i\in\mathbb{V}} \lambda_i(\boldsymbol{L})$ and others such as $1/n$ and $1/(\max_{i\in\mathbb{V}}|\mathbb{N}|^i + \min_{i\in\mathbb{V}}|\mathbb{N}|^i)$ [Zha07] can be estimated/computed in a distributed manner [ASD+12; GVJ12].

Since we aim to estimate the spectrum associated to the second smallest eigenvalue of Laplacian, a matrix deflation is conducted on Perron matrix as $\boldsymbol{Q} = \boldsymbol{P} - \mathbf{1}\mathbf{1}^\top/n$ whose dominant eigenvector coincides with the one associated to $\lambda_2(\boldsymbol{L})$. Note that the deflated Perron matrix entails row and column sums equal to zero. The eigenstructures of Laplacian matrix, Perron matrix, and its deflated matrix are summarized in Table 5.2 wherein the symbols λ_i and $\boldsymbol{v}_i$ for $i \in \mathbb{V}$ represent the eigenvalues and eigenvectors associated to the Laplacian matrix, respectively.

Now,let $\hat{\boldsymbol{v}}_2(t) = [\hat{v}_2^1(t), \ldots, \hat{v}_2^n(t)]^\top$ be the estimation variable of $\boldsymbol{v}_2$ corresponding to the simple second smallest eigenvalue of Laplacian matrix at iteration t. After initializing

Table 5.2: Spectrum of matrices

	$\boldsymbol{L}$		$\boldsymbol{P}$		$\boldsymbol{Q}$	
i	eigenvalue	eigenvector	eigenvalue	eigenvector	eigenvalue	eigenvector
1	0	$\frac{1}{\sqrt{n}}$	$1-\beta\lambda_n$	$\boldsymbol{v}_n$	0	$\frac{1}{\sqrt{n}}$
2	λ_2	$\boldsymbol{v}_2$	$1-\beta\lambda_{n-1}$	$\boldsymbol{v}_{n-1}$	$1-\beta\lambda_n$	$\boldsymbol{v}_n$
$\vdots$	$\vdots$	$\vdots$	$\vdots$	$\vdots$	$\vdots$	$\vdots$
n	λ_n	$\boldsymbol{v}_n$	1	$\frac{1}{\sqrt{n}}$	$1-\beta\lambda_2$	$\boldsymbol{v}_2$

$\hat{\boldsymbol{v}}_2(0)$ with a random non-zero vector, each node updates individual estimate by using the following iterative principle,

$$\hat{v}_2^i(t+1)=\alpha(t)\Big[\hat{v}_2^i(t)-\beta\sum_{j\in\mathbb{N}^i}^{n}(\hat{v}_2^i(t)-\hat{v}_2^j(t))-\frac{\boldsymbol{1}^\top\hat{\boldsymbol{v}}_2(t)}{n}\Big], \tag{5.16}$$

where $\alpha(t)=1/\max_{i\in\mathbb{V}}|\sum_{j=1}^{n}[\boldsymbol{Q}]_{ij}\hat{v}_2^j(t)|$ implies that the infinity norm is adopted to the power iteration (5.15). In this iteration mechanism (5.16), the normalization factor α and the matrix deflation require that each node has access to some network-wide vectors. To obviate this requirement, one can first notice that

$$\boldsymbol{1}^\top\hat{\boldsymbol{v}}_2(t)=\prod_{k=0}^{t}\alpha(t-k)\boldsymbol{1}^\top\boldsymbol{Q}^t\hat{\boldsymbol{v}}_2(0)=0,\quad \forall\, t\in\mathbb{Z}_{\geq 0}, \tag{5.17}$$

which bases on the fact that $\boldsymbol{1}$ is the left eigenvector of $\boldsymbol{Q}$ associated to the eigenvalue 0. We adjust slightly the initial condition to

$$\hat{\boldsymbol{v}}_2(0)=\boldsymbol{L}\boldsymbol{p},\quad \hat{v}_2^i(0)=\sum_{j\in\mathbb{N}^i}(p_i-p_j), \tag{5.18}$$

where $\boldsymbol{p}=[p_1,\ldots,p_n]^\top$ is a random non-zero vector, so one can obtain $\boldsymbol{1}^\top\hat{\boldsymbol{v}}_2(0)=0$. Note that the modified initialization can also be achieved in a distributed realization. Moreover, since the graph compatible[4] with matrix $\boldsymbol{Q}$ is connected, the factor $\alpha(t)$ can be computed distributively by min-consensus algorithm via finite iterations [OCR14]

$$x_i(s+1)=\min_{j\in\mathbb{N}^i\cup\{i\}}x_j(s),\quad x_i(0)=1/\Big|\sum_{j=1}^{n}[\boldsymbol{Q}]_{ij}\hat{v}_2^j(t)\Big|. \tag{5.19}$$

To this end, the update rule (5.16) can be implemented in a fully distributed fashion with the aid of the initialization (5.18) and min-consensus algorithm (5.19). As an inheritance of centralized PI method introduced in Section A.3, the estimate $\hat{\boldsymbol{v}}_2(t)$ converges exponentially to the Fiedler vector of Laplacian $\boldsymbol{L}$ at the rate $(1-\beta\lambda_3(\boldsymbol{L}))/(1-\beta\lambda_2(\boldsymbol{L}))$.

Algorithm 5.1 contains the pseudo-code of the distributed algorithm to compute a suboptimal solution to (P2b) in the case of a single link $m_a=1$.

At the end of Algorithm 5.1, each node acquires a binary flag f_i indicating whether node i is an endpoint of the selected link (i^*,j^*) ($f_i=1$) or not ($f_i=0$). In addition, the label of the selected suboptimal link to be added into the network is stored locally at $\bar{l}_{ij^*}$ for future utility.

[4] The defintion of a graph compatible with a matrix, please refer to Section A.2.

Algorithm 5.1: Distributively adding one link at a time to $\mathcal{G}_0$

Input : $\mathcal{G}_0$ is connected, $\boldsymbol{e}_i$ is the i-th column vector of $\boldsymbol{I}$
Output : f_i, $\bar{l}_{ij^*}$

1 Initialization: set $t \leftarrow 0$, $f_i \leftarrow 1$ and choose randomly a non-zero vector $\boldsymbol{p} \in \mathbb{R}^n$;
2 **while** 1 **do**
3   execute mean correction (5.17) with $\boldsymbol{p}$ to produce an initial condition $\hat{\boldsymbol{v}}_2(0)$;
4   estimate $\boldsymbol{v}_2$ distributively based on the initial vector $\hat{\boldsymbol{v}}_2(0)$ and the iterative algorithm (5.16), (5.19);
5   node assigns $\boldsymbol{\epsilon}_i \leftarrow \hat{v}_2^i \boldsymbol{e}_i$;
6   node transmits $\boldsymbol{\epsilon}_i$ to neighbors;
7   **if** $\boldsymbol{\epsilon}_i$ *has no component equal to zero* **then**
8   **break**;
9   **else**
10   **for** $j \in \mathbb{N}^i$ **do**
11   **for** $k = 1:1:n$ **do**
12   **if** $[\boldsymbol{\epsilon}_i]_k == 0$ *and* $[\boldsymbol{\epsilon}_j]_k \neq 0$ **then**
13           $[\boldsymbol{\epsilon}_i]_k \leftarrow [\boldsymbol{\epsilon}_j]_k$;
14   **end**
15   **end**
16   **end**
17   back to step 6;
18   **end**
19   node computes $\bar{l}_{ij^*} \leftarrow \arg\max_{j \notin \mathbb{N}_0^i} ([\boldsymbol{\epsilon}_i]_i - [\boldsymbol{\epsilon}_i]_j)^2$;
20   compute $\bar{l}^* \leftarrow \arg\max([\boldsymbol{\epsilon}_i]_i - [\boldsymbol{\epsilon}_i]_{j^*})^2$ with (i, j^*) using max-consensus algorithm $x_i(s+1) \leftarrow \max_{j \in \mathbb{V}_0^i \cup \{i\}} x_j(s)$ with $x_i(0) \leftarrow ([\boldsymbol{\epsilon}_i]_i - [\boldsymbol{\epsilon}_i]_{j^*})^2$;
21   **if** $\bar{l}_{ij^*} \neq \bar{l}^*$ **then**
22     $\bar{l}_{ij^*} \leftarrow \bar{l}^*$, $f_i \leftarrow 0$;
23   **end**
24 **end**

5.2.3 Numerical Evaluations

In this subsection, the proposed distributed algorithm to yield suboptimal solution is evaluated and compared with the centralized approach via a numerical example.

We consider a network of 10 nodes whose initial interconnection structure is shown by solid black lines in Figure 5.3a. First, we assess the proposed distributed estimation algorithm for the Fiedler vector. In Figure 5.3b, the solid colored lines describe the trajectories of $\hat{v}_2^i$ and the dashed black lines depict the corresponding true value $v_2^i(t)$. By observing, the estimator states converge exponentially to their corresponding true values.

To evaluate the distributed strategy for link addition, we vary the number m_a from 1 to 12. The resultant algebraic connectivity after adding m_a links into the network is shown in Figure 5.3c and those new links are drawn by orange dashed lines in Figure 5.3a. By comparison, the suboptimal solution derived from the successive application of Algorithm 5.1 is very close to the global optimizer by a brute-force search.

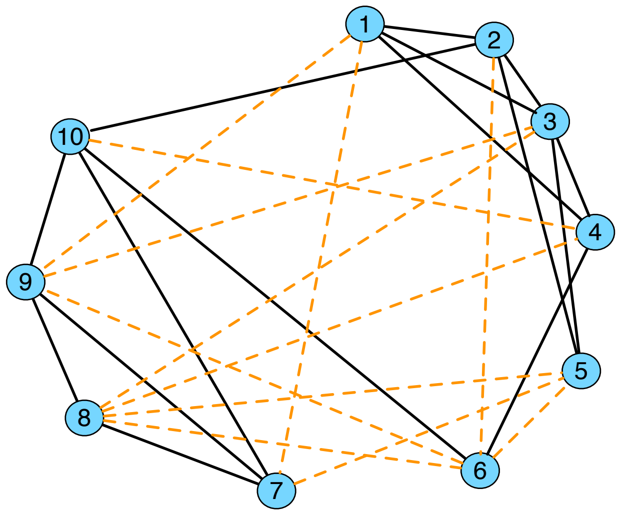

(a) A network consisting 10 nodes

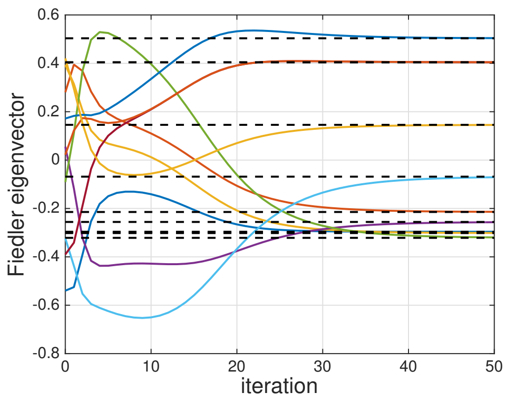

(b) The distributed PI estimation of $\boldsymbol{v}_2(\boldsymbol{L}_0)$

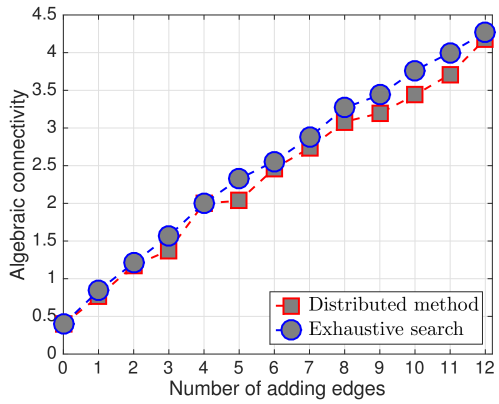

(c) Comparison of our solution vs. the global optimizer

Figure 5.3: An illustrative example to test the proposed distributed link addition algorithm.

5.3 Distributed Topology Manipulation to Control Epidemic Spread

The previous section provides a distributed strategy to solve the link-operation problem, yet there are still blemishes. One minor pitfall is that the link-selection procedure is implemented after the convergence of the distributed estimation algorithm, degrading the efficiency of the developed method. Another deficiency is the nested loops of intermediate normalization, highly increasing communication burden. Thus, this section is dedicated to improving the state-of-art of the distributed algorithm design and seeing the bigger picture of network-structure manipulation. As a motivating application, the primary focus is on the spectral radius minimization problem by removing/rewiring links to control epidemic spreading over networks without a central coordinator which collects network information and makes decisions.

5.3.1 Problem Formulation

Consider a network of n nodes represented by a connected undirected graph $\mathcal{G} = (\mathbb{V}, \mathbb{E}, \boldsymbol{A})$. Each node in the network is either *infected* or *healthy*. Each infected individual recovers naturally with a curing rate r_c and contaminates their healthy neighbors with an infection rate r_i. Epidemic dynamics are commonly modeled by stochastic diffusion processes [NPP16] and therein lies the following susceptible-infected-susceptible (SIS) model,

$$\dot{x}_k(t) = -r_c\, x_k(t) + r_i \sum_{j=1}^{n} [\boldsymbol{A}]_{kj}\, x_j(t)(1 - x_k(t)), \tag{5.20}$$

where $x_k \in [0,1]$ $(k \in \mathbb{V})$ represents the probability that individual k gets infected at time t. For more details on modeling, see [NPP16] and reference therein. The overarching point is that an epidemic dies out quickly if the effective spreading rate r_i/r_c is below a certain threshold that hinges on the model parameters; see [CWW+08] for a discussion on this threshold in real networks.

Fact 5.3 ([NPP16])**.** *Consider an SIS infection process on a graph $\mathcal{G}$ with adjacency matrix $\boldsymbol{A}$. Initial infection will extinguish exponentially if the effective spreading rate satisfies $r_i/r_c \leq \frac{1}{\mathsf{sr}(\boldsymbol{A})}$, where $\mathsf{sr}(\boldsymbol{A})$ is the spectral radius of the graph $\mathcal{G}$.*

Central in the above lemma is the connection between the epidemic eradication and the spectral property of underlying graphs. More fundamentally, a smaller spectral radius leads to a higher probability of networks against the spread of viruses. Instead, the violation of the condition in Fact 5.3 indicates that the disease may persist in the network for a long time. As such, a natural option to mitigate the spreading of disease effectively is to make the spectral radius of the underlying graph as small as possible. In the following, we focus on studying a distributed strategy for link operations to reduce $\mathsf{sr}(\boldsymbol{A})$.

Remark 5.1. *The result given in Fact 5.3 does not depend on the modeling of epidemics, our strategy has the broadest applicability to other epidemic models including (susceptible-infected-removed) SIR, (susceptible-infected-recovered-susceptible) SIRS and (susceptible-exposed-infected-recovered) SEIR [NPP16].*

Given a connected undirected graph $\mathcal{G}_0 = (\mathbb{V}, \mathbb{E}_0, \boldsymbol{A}_0)$, the problem of link removal is defined as follows: for a fixed budget $|\Delta\mathbb{E}^-| = m_d$ $(m_d \in \mathbb{Z}_{\geq 1})$, select a set of edges $\Delta\mathbb{E}^-$ from $\mathbb{E}_0$ such that the spectral radius of resulting graph $\mathcal{G}^-_{m_d} = \{\mathbb{V}, \mathbb{E}_0 \setminus \Delta\mathbb{E}^-, \boldsymbol{A}^-_{m_d}\}$ is minimal. As claimed in Proposition 3.1.1. of [BH12], the adoption of Perron-Frobenius theory given in Lemma A.1 to adjacency matrix[5] provides $\mathsf{sr}(\boldsymbol{A}) = \lambda_n(\boldsymbol{A}) > 0$. With the notation $\boldsymbol{A}^-_{m_d}$ as the adjacency matrix of graph $\mathcal{G}^-_{m_d}$, the problem is cast as the following optimization

$$\begin{aligned} \min_{\Delta\mathbb{E}^- \subseteq \mathbb{E}_0} \quad & \lambda_n(\boldsymbol{A}^-_{m_d}) \\ \text{s.t.} \quad & |\Delta\mathbb{E}^-| = m_d. \end{aligned} \tag{P3a}$$

[5] For the sake of a concise presentation, we suppose that $\lambda_n(\boldsymbol{A}) > |\lambda_i(\boldsymbol{A})|$ for $i = 1, \ldots, n-1$. Nevertheless, this pragmatic hypothesis is without loss of generality, as the development of distributed strategy in the sequel is applicable to the cases in which this assumption is violated. As we shall see, this is because the proposed algorithms rely on power iterations of a primitive matrix derived from the adjacency, leading to a 1-dimensional dominant eigenspace.

After labeling edges on graph $\mathcal{G}_0$ by $l_{ij} \sim (j,i) \in \mathbb{E}_0$, the optimization problem (P3a) can be rewritten as

$$\begin{aligned} \min_{\boldsymbol{y}\in\{0,1\}^{|\mathbb{E}_0|}} \quad & \lambda_n(\boldsymbol{A}_0 - \Delta\boldsymbol{A}^-_{m_d}) \\ \text{s.t.} \quad & \Delta\boldsymbol{A}^-_{m_d} = \sum_{l_{ij}=1}^{|\mathbb{E}_0|} y_{l_{ij}}(\boldsymbol{e}_i\boldsymbol{e}_j^\top + \boldsymbol{e}_j\boldsymbol{e}_i^\top), \quad \boldsymbol{1}^\top\boldsymbol{y} = m_d \end{aligned} \tag{P3b}$$

where $\boldsymbol{e}_i$ the i-th column vector of identity matrix $\boldsymbol{I}$ and the vector $\boldsymbol{y} = [y_1, \dots, y_{|\mathbb{E}_0|}]^\top$ encodes the information in the sense that $y_{l_{ij}} = 1$ for $l_{ij} \sim (j,i) \in \mathbb{E}_0$ means the edge $(j,i) \in \mathbb{E}_0$ is removed from $\mathbb{E}_0$.

In real-life networks, the link removal might physically be implemented by, e.g., limiting traffic/travel between cities, or restricting interactions between individuals.

Remark 5.2. *Note that the link-breaking optimization (P3a) can be reinterpreted equivalently to retard the information diffusion over networks. The fact that the convergence speed of such dynamical processes is a sub-modular set function of network topology means deleting an edge from the graph cannot accelerate the information diffusion [CH15]. Moreover, the distributed link-removing strategy can be extended to study transition behavior in large-scale networks of coupled phase oscillators [ROH05] in which the largest eigenvalue of the adjacent matrix stands for a critical quantity.*

Despite the instrumental effect on controlling the propagation of disease, the link-breaking scheme, in turn, degrades other network performances dramatically, such as robustness and coherence. Instead, a moderate method, called link rewiring/rerouting/re-location, has also been employed to mitigate the effects of the disease [DYL+15; CA16].

In specific, the nodes reconnect a portion of edges $1 \le m_r \le |\mathbb{E}_0|$ in graph $\mathcal{G}_0$ to minimize the spectral radius, leading to a new network structure $\widetilde{\mathcal{G}}_{m_r} = (\mathbb{V}, \widetilde{\mathbb{E}}, \widetilde{\boldsymbol{A}}_{m_r})$ with $|\widetilde{\mathbb{E}}| = |\mathbb{E}_0|$. This problem is formally stated as follows.

$$\begin{aligned} \min_{\widetilde{\mathbb{E}}} \quad & \lambda_n(\widetilde{\boldsymbol{A}}_{m_r}) \\ \text{s.t.} \quad & |\widetilde{\mathbb{E}} \cap \mathbb{E}_0| = |\mathbb{E}_0| - m_r,\ |\widetilde{\mathbb{E}}| = |\mathbb{E}_0|. \end{aligned} \tag{P4a}$$

Likewise, the optimization problem (P4a) can also be recast to

$$\begin{aligned} \min_{\bar{\boldsymbol{y}},\boldsymbol{y}} \quad & \lambda_n(\boldsymbol{A}_0 - \Delta\boldsymbol{A}^-_{m_r} + \Delta\boldsymbol{A}^+_{m_r}) \\ \text{s.t.} \quad & \Delta\boldsymbol{A}^-_{m_r} = \sum_{l_{ij}=1}^{|\mathbb{E}_0|} y_{l_{ij}}(\boldsymbol{e}_i\boldsymbol{e}_j^\top + \boldsymbol{e}_j\boldsymbol{e}_i^\top), \quad \boldsymbol{1}^\top\boldsymbol{y} = m_r, \\ & \Delta\boldsymbol{A}^+_{m_r} = \sum_{\bar{l}_{ij}=1}^{|\bar{\mathbb{E}}^-_{m_r}|} \bar{y}_{\bar{l}_{ij}}(\boldsymbol{e}_i\boldsymbol{e}_j^\top + \boldsymbol{e}_j\boldsymbol{e}_i^\top), \quad \boldsymbol{1}^\top\bar{\boldsymbol{y}} = m_r, \end{aligned} \tag{P4b}$$

where $\bar{l}_{ij} \sim (j,i) \in \bar{\mathbb{E}}^-_{m_r}$ is the edge index labeling on complement graph of $\mathcal{G}^-_{m_r}$, $l_{ij} \sim (j,i) \in \mathbb{E}_0$ is the edge label of graph $\mathcal{G}_0$, $\boldsymbol{y} = [y_1, \dots, y_{|\mathbb{E}_0|}]^\top \in \{0,1\}^{|\mathbb{E}_0|}$, and $\bar{\boldsymbol{y}} = [\bar{y}_1, \dots, \bar{y}_{|\bar{\mathbb{E}}|^-_{m_r}}]^\top \in \{0,1\}^{|\bar{\mathbb{E}}^-_{m_r}|}$.

The reformulation from the problem (P4a) to (P4b) gives rise to disconnecting m_r links in the graph $\mathcal{G}_0$ first and then establishing m_r new connection in the graph $\mathcal{G}^-_{m_r}$. Note that the link-creating operation in link-rerouting strategy, adding m_r new edges into the graph $\mathcal{G}^-_{m_r}$ such that the increment of the spectral radius is minimal, involves the link searching in the complement graph $\bar{\mathcal{G}}^-_{m_r} = (\mathbb{V}_0, \bar{\mathbb{E}}^-_{m_r}, \bar{\boldsymbol{A}}^-_{m_r})$ of the graph $\mathcal{G}^-_{m_r}$. As shown in [SSG13], reversing reciprocally the order of link deletion and addition in (P4b) results in the same minimum $\lambda^*_n(\widetilde{\boldsymbol{A}}_{m_r})$.

As mentioned in dealing with the link-adding problem (P2b), the optimization problems (P3b) and (P4b) are of combinatorial nature and can be solved by brute-force searching all possibility and selecting the best edge subset. However, the computation complexity grows factorially as the number of nodes increases and quickly becomes unfeasible even for moderate networks. Instead, this kind of problems is usually modified to be tractable using convex relaxation or heuristics. This line of methodologies assumes explicitly or implicitly the existence of a central coordinator that access to all network information and makes decisions. In practice, network systems commonly scatter around a broad region, with dozens more consisting of hundreds of ingredients in smart-sensor networks to millions of actors in social networks. Thus, these networks do not possess a fusion center for knowing the complete network's information. This lack of central point necessitates the development of new distributed strategies to solve (P3b) and (P4b) that go beyond the traditional (centralized) methods functioned under the umbrella of an existed central entities.

5.3.2 Distributed Link Removal/Rewiring Algorithms

In a spirit similar to the development of link addition problem in Section 5.2, we adopt matrix-perturbation theory to formulate an approximation for the original problem (P3b) and (P4b).

Lemma 5.2: Approximation Algorithm for Link removal

The optimization problem (P3b) can be approximately solved by

$$\begin{aligned} \max_{\boldsymbol{y}\in\{0,1\}^{|\mathbb{E}_0|}} \quad & \Delta\lambda_n(\boldsymbol{A}_0, \Delta\boldsymbol{A}^-_{m_d}) \\ \text{s.t.} \quad & \Delta\lambda_n(\boldsymbol{A}_0, \Delta\boldsymbol{A}^-_{m_d}) = \sum_{l_{ij}}^{|\mathbb{E}_0|} y_{l_{ij}} \omega^i_n \omega^j_n, \quad \mathbf{1}^\top \boldsymbol{y} = m_d, \end{aligned} \tag{P3c}$$

where $\boldsymbol{\omega}_n(\boldsymbol{A}_0) = [\omega^1_n, \ldots, \omega^n_n]^\top$ is the eigenvector associated to the eigenvalue $\lambda_n(\boldsymbol{A}_0)$ of the graph $\mathcal{G}_0$.

Proof. The proof follows along the same step as in the proof of Lemma 5.1 and is saved for triviality. □

Note that deleting a link does not increase the spectral radius of graphs in the setting of optimization (P3c), but this intuition is essentially not correct for the primal problem (P3a) due to its non-convexity. The optimization problem (P4b) has a similar approximation.

Lemma 5.3: Approximation Algorithm for Link relocation

The optimization (P4b) can be approximately solved by

$$\begin{aligned}\max_{\boldsymbol{y},\bar{\boldsymbol{y}}} \quad & \Delta\lambda_n(\boldsymbol{A}_0, \Delta\boldsymbol{A}^-_{m_r}) - \Delta\lambda_n(\boldsymbol{A}^-_{m_r}, \Delta\boldsymbol{A}^+_{m_r}) \\ \text{s.t.} \quad & \Delta\lambda_n(\boldsymbol{A}_0, \Delta\boldsymbol{A}^-_{m_r}) = \sum_{l_{ij}}^{|\mathbb{E}_0|} y_{l_{ij}} \omega^i_n \omega^j_n, \\ & \Delta\lambda_n(\boldsymbol{A}^-_{m_r}, \Delta\boldsymbol{A}^+_{m_r}) = \sum_{\bar{l}_{ij}=1}^{|\bar{\mathbb{E}}^-_{m_r}|} \bar{y}_{\bar{l}_{ij}} \xi^i_n \xi^j_n, \quad \mathbf{1}^\top \bar{\boldsymbol{y}} = \mathbf{1}^\top \boldsymbol{y} = m_r,\end{aligned} \tag{P4c}$$

where $l_{ij} \sim (j,i) \in \mathbb{E}_0$, $\boldsymbol{y} = [y_1, \dots, y_{|\mathbb{E}_0|}]^\top \in \{0,1\}^{|\mathbb{E}_0|}$, $\bar{l}_{ij} \sim (j,i) \in \bar{\mathbb{E}}^-_{m_r}$, and $\bar{\boldsymbol{y}} = [\bar{y}_1, \dots, \bar{y}_{|\bar{\mathbb{E}}^-_{m_r}|}]^\top \in \{0,1\}^{|\bar{\mathbb{E}}^-_{m_r}|}$. Moreover, $\boldsymbol{\omega}_n = [\omega^1_n, \dots, \omega^n_n]^\top$ and $\boldsymbol{\xi}_n = [\xi^1_n, \dots, \xi^n_n]^\top$ specify the eigenvector corresponding to the largest eigenvalue of adjacency matrix of graph $\mathcal{G}_0$ and graph $\mathcal{G}^-_{m_r}$, respectively.

In general, the solution to (P3c) and (P4c) is essentially an upper bound for the one to (P3b) and (P4b), respectively. So far, the original combinatorial problems (P3b) and (P4b) are heuristically approximated respectively by (P3c) and (P4c) which involve the eigenvectors of interests. Despite monitoring node-wise quantities only, yet, such approximations are indeed centralized owing to the need for complete topological information for computing the eigenvector in question. Moreover, one often postulates the existence of a central coordinator determining the candidates based on the computed variables.

In Section 5.2, a distributed power iteration method is proposed to estimate the dominant eigenvector of a matrix. However, this algorithm requires nested loops (a min-consensus algorithm between each iteration step) for the intermediate normalization which severely affects its efficiency in the aspect of communication frequency and convergence speed. In what follows, we devote ourselves to improving the distributed estimation algorithm that, in particular, involves event-triggered communication technology and parallel algorithm design.

For simplicity of exhibition, consider the network $\mathcal{G} = (\mathbb{V}, \mathbb{E}, \boldsymbol{A})$ with the Laplacian matrix $\boldsymbol{L}$ and the neighborhood set $\mathbb{N}^i$ for each node $i \in \mathbb{V}$. Let $\hat{\boldsymbol{\omega}}_n(t) = \left[\hat{\omega}^1_n(t), \dots, \hat{\omega}^n_n(t)\right]^\top$ be the estimate of the eigenvector $\boldsymbol{\omega}_n$ corresponding to $\lambda_n(\boldsymbol{A}(\mathcal{G}))$. Locally, each node $i \in \mathbb{V}$ maintains a component of the estimate $\hat{\omega}^i_n$ and exclusively accounts for computing the corresponding true value ω^i_n. As a consequence of Lemma A.1, $\boldsymbol{\omega}_n$ has all strictly positive components and hence, without loss of generality, the initialization can be randomly given by a positive-value vector $\hat{\boldsymbol{\omega}}_n(0) > 0$.

Let $\boldsymbol{C} \triangleq \boldsymbol{I} + \boldsymbol{A}$ in (5.15). Obviously, the matrix $\boldsymbol{C}$ is primitive and the Perron-Frobenius eigenvalue of $\boldsymbol{C}$ is simple. A modified distributed PI method with the following node-wise update rule is proposed,

$$\hat{\omega}^i_n(t+1) = r_i(t)[\hat{\omega}^i_n(t) + \sum_{j \in \mathbb{N}^i} [\boldsymbol{A}]_{ij} \hat{\omega}^j_n(t)] \tag{5.21}$$

where $r_i \in \mathbb{R}$ compensates the magnitude of node i and will be defined later. Since $\mathrm{sr}(\boldsymbol{C}) = \lambda_n(\boldsymbol{C}) > 1$, $\hat{\boldsymbol{\omega}}_n(t)$ may diverge infinitely as time evolves. It is, therefore, indispensable to scale $\hat{\boldsymbol{\omega}}_n(t)$ felicitously.

First, each node is assigned a variable $h_i(t) \in \mathbb{R}_{>0}$ to locally estimate the growth rate $\|\boldsymbol{C}\hat{\boldsymbol{\omega}}_n(t)\|/\|\hat{\boldsymbol{\omega}}_n(t)\|$ in each iteration, which is updated according to the following rule

$$h_i(t+1) = h_i(t) + \frac{\hat{\omega}_n^i(t)}{\min(\sigma, (\hat{\omega}_n^i)^2(t))}[(1-h_i(t))\hat{\omega}_n^i(t) + \sum_{j \in \mathbb{N}^i} [\boldsymbol{A}]_{ij}\hat{\omega}_n^j(t)] \tag{5.22}$$

where $\sigma > 0$ is a given threshold.

When $(\hat{\omega}_n^i)^2(t)$ exceeds the given upper threshold σ, node i triggers a timer to scale $\hat{\boldsymbol{\omega}}_n(t)$. Specifically, a flag signal $\pi_i(t) \in \{0,1\}$ of the event-trigger indicates whether or not to shrink $\hat{\omega}_n^i(t)$ at time t, i.e.,

$$\pi_i(t) = \begin{cases} 1, & \text{if } (\hat{\omega}_n^i)^2(t) > \sigma \\ 0, & \text{otherwise} \end{cases}, \quad i \in \mathbb{V}. \tag{5.23}$$

To ensure all nodes reaching an agreement on r_i, nodes run a max-consensus algorithm [OCR14] on the variables $h_i(t)$ across the network as such

$$x_i(t+k+1) = \max_{j \in \mathbb{N}^i \cup \{i\}} x_j(t+k), \quad x_i(t) = h_i(t), \tag{5.24}$$

where $k \in \mathbb{Z}_{\geq 0}$. Algorithm (5.24) will end after a mixing time[6] T_d of a random walk on graph $\mathcal{G}$ and then, all nodes attain the maximum of the inputs $h_i(t)$ over the network

$$x_1(t+T_d) = \cdots = x_n(t+T_d) = \max_{j \in \mathbb{V}} h_j(t). \tag{5.25}$$

As a consequence, the compensation variable $r_i(t)$ is given by

$$r_i(t) = \begin{cases} \frac{1}{\max_{j \in \mathbb{V}} h_j(t-T_d)} & \text{if } \pi_i(t-T_d) = 1 \\ 1 & \text{otherwise} \end{cases}. \tag{5.26}$$

Note that nodes keep on computing their local $h_j(t)$ ($j \in \mathbb{V}$) after $\pi_i(t) = 1$ as the max-consensus (5.24) executes in parallel to the growth-rate estimation algorithm (5.22).

The following theorem summarizes that the output of the proposed method ultimately converges to $\boldsymbol{\omega}_n$.

Theorem 5.2: Convergence of Distributed Event-based PI algorithm

Given a connected graph $\mathcal{G}$, the eigenvector $\boldsymbol{\omega}_n$ corresponding to $\lambda_n(\boldsymbol{A}(\mathcal{G}))$ can be computed distributively and component-wisely by running (5.21)-(5.26).

Proof. As matrix $\boldsymbol{C}$ is primitive, the sequences $\{\max_{i \in \mathbb{V}} \hat{\omega}_n^i(t+1)/\hat{\omega}_n^i(t)\}$ converges asymptotically to $\mathrm{sr}(\boldsymbol{C})$, namely,

$$\mathrm{sr}(\boldsymbol{C}) \leq \cdots \leq \max_{i \in \mathbb{V}} \frac{\hat{\omega}_n^i(2)}{\hat{\omega}_n^i(1)} \leq \max_{i \in \mathbb{V}} \frac{\hat{\omega}_n^i(1)}{\hat{\omega}_n^i(0)}; \tag{5.27}$$

[6] It can be chosen as the network diameter and could be a prior knowledge to every node since there are distributed algorithms to compute the diameter of a graph, e.g., [GVJ12; HJOV14].

see [WO03] and references therein. Note that between any consecutive event-triggered time instants, the update rule (5.22) exactly reduces to

$$h_i(t+1) = \frac{\hat{\omega}_n^i(t+1)}{\hat{\omega}_n^i(t)}. \tag{5.28}$$

As the magnitude scaling occurs only at designated event-time by a common value, it does not change the direction of iteration in (5.21). In conjugation with max-consensus (5.24) and its convergence (5.27), it is not very difficult to deduce that

$$\lim_{t\to\infty} h_i(t) = \lim_{t\to\infty} \frac{\|\boldsymbol{C}\hat{\boldsymbol{\omega}}_n(t)\|}{\|\hat{\boldsymbol{\omega}}_n(t)\|} = 1 + \lambda_n(\boldsymbol{A}), \quad \forall\, i \in \mathbb{V}, \tag{5.29}$$

which indicates $r_i(t) \to 1/(1+\lambda_n(\boldsymbol{A}))$ for all $i \in \mathbb{V}$ when $t \to \infty$. Eventually, the distributed power-based iteration (5.21) in a compact form converges to the true eigenvector corresponding to the leading eigenvalue of the adjacency matrix. That is,

$$\lim_{t\to\infty} \hat{\boldsymbol{\omega}}_n(t+1) = \lim_{t\to\infty} \frac{(\boldsymbol{I}+\boldsymbol{A})\hat{\boldsymbol{\omega}}_n(t)}{1+\lambda_n(\boldsymbol{A})} = \boldsymbol{\omega}_n. \tag{5.30}$$

The proof is completed. □

In view of (5.29), the maximal eigenvalue of the adjacency matrix is also available for each node when the algorithm establishes convergence, i.e., $\lambda_n(\boldsymbol{A}) \leftarrow h(t)-1$ as $t \to \infty$. In network science [CPS17], the principal adjacency eigenvalue and its associated eigenvector of a network suggest the topological structure of the network, as well as the behavior of dynamical systems on networks. Thus, our developed methodology has wider applications in the study of network systems.

In the special case that $(\hat{\omega}_n^i)^2(t) > \sigma$ holds for every $t = 1, 2, \cdots$, the iteration (5.21) keeps on updating the norm compensation $r_i(t)$ over time after the first T_d steps. As such, the proposed algorithm (5.21)-(5.24) in this scenario is identical to the conventional PI method (5.15) but with a distributed implementation of the intermediate normalization at each iteration step.

Remark 5.3. *As suggested in [BM13], a cooperative diffusion method can be employed to improve the convergence of* (5.22). *Namely, one can run the following algorithm to estimate the growth rate* $\|\boldsymbol{C}\hat{\boldsymbol{\omega}}_n(t)\|/\|\hat{\boldsymbol{\omega}}_n(t)\|$ *instead of the operation* (5.22),

$$\begin{aligned} \underline{h}_i(t+1) &= h_i(t) + \frac{\hat{\omega}_n^i(t)}{\min(\sigma, (\hat{\omega}_n^i)^2(t))}[(1-h_i(t))\hat{\omega}_n^i(t) + \sum_{j\in\mathbb{N}^i}[\boldsymbol{A}]_{ij}\hat{\omega}_n^j(t)] \\ h_i(t+1) &= [\underline{h}_i(t+1) + \sum_{j\in\mathbb{N}^i}\underline{h}_j(t+1)]/(1+|\mathbb{N}^i|) \end{aligned} \tag{5.31}$$

which provides fairly more robustness to the estimation by sacrificing transmission expense.

The remaining problem is how to choose the threshold σ. When an event is triggered at the time t due to $(\hat{\omega}_n^i)^2(t) = \sigma$, a plausible principle is that the estimates $\hat{\omega}_n^i(t+T_d)$ cannot grow infinitely or exceed a critical bound $\sigma_{\max}$, namely,

$$\sigma \cdot n^{T_d} < \sigma_{\max}, \tag{5.32}$$

which is based on the fact $\lambda_n(\boldsymbol{A}(\mathcal{G})) \le n-1$. Furthermore, other bounds on spectral radius of graphs, e.g., in [vMi11; BH12], can be used to explore the more precise value of σ. Evidently, a larger value $\sigma_{\max}$ means a wider inter-event interval and thus less computation and fewer data transmissions across the network.

Now, we provide the overall distributed strategy for the edge removal/rewiring within a formal computational context. To unravel the underlying design principle of the developed strategy, we focus on the edge-removing problem with $m_d = 1$. For the multi-edges scenario $m_d > 1$, one could repeatedly invoke the operations of this illustrative example. The detailed pseudo-code of the edge-removing strategy is exhibited in Algorithm 5.2.

Algorithm 5.2: Distributed link-wise removal strategy to solve (P3c)

Input : $\mathcal{G}_0$ is connected, $\sigma \cdot n^{T_d} < \sigma_{\max}$
Output : f_i, l_{ij^*}
Initialization: set $t \leftarrow 0$, $r_i(0) \leftarrow 1$, $\pi_i \leftarrow 0$, $\mu_i \leftarrow -1$, $\beta_i \leftarrow 1$, $w_i \leftarrow 0$, $h_i(0) \leftarrow 1 + \max_{i,j\in\mathbb{V}} \sqrt{|\mathbb{N}_0^i||\mathbb{N}_0^j|}/2$, $\forall i \in \mathbb{V}$, and choose $\hat{\boldsymbol{\omega}}_n(0) \in \mathbb{R}^n_{>0}$ randomly;
while 1 **do**
    $t \leftarrow t+1$;
    if $\pi_i = 1$ **then**
        $\mu_i \leftarrow \mu_i - 1$;
        if $\mu_i = 0$ **then**
            $r_i(t) \leftarrow x_i(t)$, $\pi_i \leftarrow 0$;
        else if $|\hat{\omega}_n^i(t)| > \sigma$ **then**
            $\pi_i \leftarrow 1$, $\mu_i \leftarrow T_d$, $x_i(t) = h_i(t)$;
        end
    end
    if $\exists \pi_j = 1 \ j \in \mathbb{N}_0^i$ **then**
        $k \leftarrow \arg\min_{j\in\mathbb{N}_0^i\cup\{i\}} \{\pi_j\}$, $\pi_i \leftarrow \pi_k$, $x_i(t) \leftarrow x_k(t)$, $\pi_i = 1$;
    end
    each node transmits its data to neighbors and updates $\hat{\omega}_n^i$ and h_i according to (5.21) and (5.22), respectively;
    if $t \mod T_d = 0$ **then**
        $f_i \leftarrow \beta_i$;
    else if $t \mod T_d = 1$ **then**
        $w_i \leftarrow \max_{j\in\mathbb{N}_0^i} \hat{\omega}_n^i \hat{\omega}_n^j$, $l_{ij^*} \leftarrow l_{i \arg\max_{j\in\mathbb{N}_0^i} \hat{\omega}_n^i \hat{\omega}_n^j}$;
    end
    each node transmits w_i and l_{ij^*} to neighbors;
    if $\max_{j\in\mathbb{N}_0^i} \hat{\omega}_n^i \hat{\omega}_n^i < \max_{j\in\mathbb{N}_0^i\cup\{i\}} w_j$ **then**
        $\beta_i \leftarrow 0$, $w_i \leftarrow \max_{j\in\mathbb{N}_0^i\cup\{i\}} w_j$, $l_{ij^*} \leftarrow l_{\arg\max_{j\in\mathbb{N}_0^i\cup\{i\}} w_j \, j^*}$;
    end
end

In Algorithm 5.2, the meanings of some data transmitted among nodes are exhibited as below

- $\hat{\omega}_n^i(t)$ – estimate state of ω_n^i on node i at time t;
- $r_i(t)$ – scale factor (5.26) for shrinking $\hat{\omega}_n^i(t)$ at time t;

- μ_i – timer with 0 means shrinking $\hat{\omega}_n^i(t)$ with $r_i(t) \neq 1$;
- $\pi_i(t)$ – flag bit for event-trigger;
- $x_i(t)$ – variable of max-consensus algorithm;

Moreover, each node is assigned a binary flag f_i indicating whether node i is an endpoint of the selected optimal edge $l_{i^* j^*}$ ($f_i = 1$) or not ($f_i = 0$) at the end of the algorithm. Lines 4–14 are the pseudo-codes of the compensation mechanism to avoid the infinity of estimation vector, while line 15 is the parallel distributed power iteration. The process of lines 16–24 distributively identifies the candidate edge whose breaking suspends the evolution of epidemic extremely. In particular, this neighborhood identification process is implemented in parallel with the distributed PI. That is, the identification operation does not need to wait for the distributed computation to finish, and hence it is appealing to the case of a large m_d. After the algorithm converges, the pair of nodes with $f_i = 1$ will self-consciously break the link indicated by the label $l_{i^* j^*}$. The proposed strategy behaves indeed in a purely distributed fashion since it needs not a fusion center to gather information and to make a decision throughout the entire process.

Remark 5.4. *In real applications, an empirical bound $T_{\max}$ of the total iteration could be found and used as the stopping time for Algorithm 5.2. More practically, the following condition can be set as the stopping criteria to further accelerate the estimation*

$$|\hat{\omega}_n^i(t+1) - \hat{\omega}_n^i(t)| < \epsilon, \qquad \forall i \in \mathbb{V}, \tag{5.33}$$

where $\epsilon > 0$ is a small predefined tolerance. The consideration that the solution to the problem (P3c) relies on a product of two relative values, means no need to end up with the exact values of ω_n^i for all $i \in \mathbb{V}$. Recently, a distributed stopping criterion for the power iteration is presented in [RLM15], which can seamlessly incorporate with Algorithm 5.2 and support efficient computation and communication in link manipulation.

To this end, the entire profile of the distributed strategy in a generic setting is concluded in the following.

Proposition 5.1: Strategy 1 for Distributed Link Removal

For $m_d \in \mathbb{Z}_{\geq 1}$ link-removing from the network, Algorithm 5.2 is implemented link-wisely on the undergoing topology for m_d rounds. At the end of each round, a single candidate edge is removed based on the output of Algorithm 5.2.

Next, we study how the network evolves when a sequence of existing links is being rerouted in a distributed and iterative manner. Focusing on the $m_r = 1$ case, individuals first cut one connection by using the link-breaking Algorithm 5.2 and simultaneously create a new connection. The pseudo-code for the distributed link-rewiring is shown in Algorithm 5.3.

By inspection of the problem (P4c), the requirement of the complete topological information is the main challenge arising in the link-creating process. In the link-removing case, the product $\hat{\omega}_n^i \hat{\omega}_n^j$ of existed links is accessible locally. However, to pursue this product of the nonexistent links in present network amounts to a formidable computational task, especially, in a distributed fashion. That is to say, the topological information of the complement graph of current interconnection becomes indispensable. To deal with this

Algorithm 5.3: Distributed link-wise rewiring strategy to solve (P4c)

Input : $\mathcal{G}_0$ is connected, $\sigma \cdot n^{T_d} < \sigma_{\max}$

Output : $f_i,\ l_{ij^*},\ \tilde{f}_i,\ \bar{l}_{ij^*}$

1 Initialization: set $t \leftarrow 0$, $r_i(0) \leftarrow 1$, $\pi_i \leftarrow 0$, $\mu_i \leftarrow -1$, $\beta_i \leftarrow 1$, $w_i \leftarrow 0$, $h_i(0) \leftarrow 1 + \max_{i,j \in \mathbb{V}} \sqrt{|\mathbb{N}_0^i||\mathbb{N}_0^j|}/2$, $\tilde{\beta}_i \leftarrow 1$, $\tilde{w}_i \leftarrow 0$, $p_i \leftarrow i$, $\tilde{q}_i \leftarrow 0$, $\forall i \in \mathbb{V}$, and choose $\hat{\boldsymbol{\omega}}_n(0) \in \mathbb{R}^n_{>0}$ randomly;

2 **while** 1 **do**

3 $\quad t \leftarrow t+1$;

4 $\quad$ execute line 4–24 in Algorithm 5.2;

5 $\quad$ **if** $t \mod 2T_d = 0$ **then**

6 $\quad\quad \tilde{f}_i \leftarrow \tilde{\beta}_i$;

7 $\quad$ **else if** $t \mod 2T_d <= T_d$ **then**

8 $\quad\quad$ **if** $t \mod 2T_d = 1$ **then**

9 $\quad\quad\quad \mathbb{W}_i \leftarrow \cup_{j \in \mathbb{N}_0^i \cup \{i\}} \{(\hat{\omega}_n^j, j)\}$;

10 $\quad\quad$ **end**

11 $\quad\quad$ each node transmits $\mathbb{W}_i$ to neighbors and computes $\mathbb{W}_i \leftarrow \cup_{j \in \mathbb{N}_0^i \cup \{i\}} \mathbb{W}_j$;

12 $\quad\quad$ search for $(\hat{\omega}_n^j, j) \in \mathbb{W}_i$ and compute

13 $\quad\quad \alpha_i \leftarrow \min_{j \notin \mathbb{N}_0^i} \hat{\omega}_n^j$, $\hat{\alpha}_i \leftarrow \arg\min_{j \notin \mathbb{N}_0^i} \hat{\omega}_n^j$;

14 $\quad$ **else**

15 $\quad\quad$ **if** $t \mod T_d = 1$ **then**

16 $\quad\quad\quad w_i \leftarrow \hat{\omega}_n^i \alpha_i$, $\bar{l}_{ij^*} \leftarrow \bar{l}_{i\hat{\alpha}_i}$;

17 $\quad\quad$ **end**

18 $\quad\quad$ each node transmits w_i and $\bar{l}_{i\hat{\alpha}_i}$ to neighbors and computes

19 $\quad\quad w_i \leftarrow \min_{j \in \mathbb{N}_0^i \cup \{i\}} w_j \neq 0$, $p_i \leftarrow \arg\min_{j \in \mathbb{N}_0^i \cup \{i\}} w_j \neq 0$;

20 $\quad\quad$ **if** $\hat{\omega}_n^i \alpha_i > w_i$ **then**

21 $\quad\quad\quad \tilde{\beta}_i \leftarrow 0$, $\bar{l}_{ij^*} \leftarrow \bar{l}_{p_i \hat{\alpha}_{p_i}}$;

22 $\quad\quad$ **end**

23 $\quad$ **end**

24 **end**

problem, a link addition algorithm with the weakest growth in spectral radius is introduced in lines 5-23 of Algorithm 5.3. Compared to link-breaking process, an extra period T_d corresponding to lines 7-14 is demanded to compute a local minimum $\min_{j \notin \mathbb{N}_0^i} \hat{\omega}_n^j$ for each node i. In the second phase line 15-23, a distributed algorithm is developed to search the global minimum of the value $\hat{\omega}_n^i \min_{j \notin \mathbb{N}_0^i} \hat{\omega}_n^j$ wherein $(j,i) \notin \mathbb{E}_0$. At the end of Algorithm 5.3, the pair of nodes with $f_i = 1$ breaks up the link connecting them automatically. Meanwhile, the pair of nodes with $\tilde{f}_i = 1$ establishes their connection locally.

We summarize the entire distributed link-rewiring strategy in the following proposition.

Proposition 5.2: Strategy 2 for Distributed Link Rewiring

To reroute $1 \leq m_r \leq |\mathbb{E}_0|$ links of the network, Algorithm 5.3 is implemented for m_d rounds and in each round, an existing edge is relocated based on the output of Algorithm 5.3.

Remark 5.5. *In many real-life networks, such as power grids [ETV13] and air transmission systems, they are typically spatially distributed under geographical constraints. A modification of the link-rerouting strategy based on spatial proximity is necessary [RBK14]. For instance, the link $l_{i^* j^*}$ is supposed to be cut as a consequence of Algorithm 5.2, while simultaneously nodes i^* and/or j^* create a connection with another available node within a given radius rather than crossing over the entire network.*

5.3.3 A Coevolutionary Network Picture of Topology Operation

Literally speaking, the proposed methodology to solve the distributed edge manipulation problem falls into the research field of coevolutionary networks [GB08] which feedback loop the dynamics on and of networks. In particular, we could provide a natural interpretation for the link removal/rerouting problem by referring to opinion dynamics along a sequence of issues [JFB17].

Figure 5.4 shows that the topology structure and dynamics on nodes loop in a feedback fashion. Iterative deleting/reallocating multiple links can be treated as a sequence of issues. On each issue, a distributed identification process is called for finding the candidate edges. On the one hand, central in this link recolonization is a distributed PI dynamics which unfolds on the current interconnection network. On the other hand, the network topology renews at the end of each issue processing based on the output of estimation dynamics.

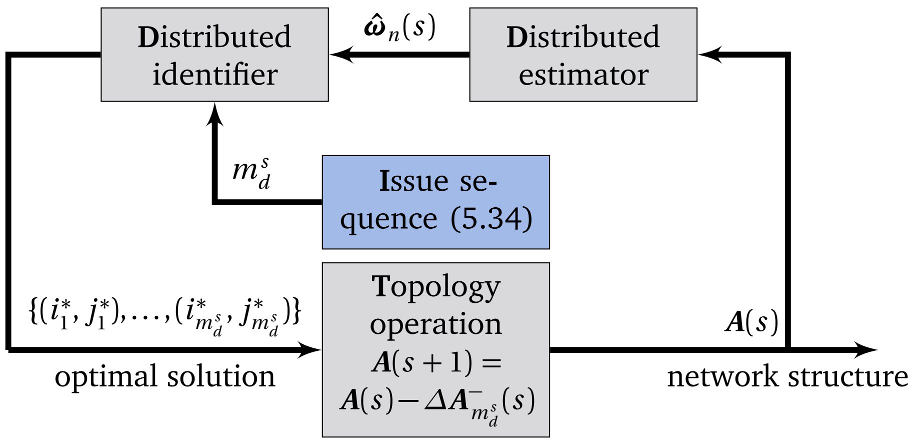

Figure 5.4: The schematic diagram of the coevolution of distributed compution processes over networks and network topology.

Strategy 1 given in Proposition 5.1 is apt to remove the m_d targeted links one-by-one. The above coevolution picture of link operation allows substantial flexibility for arranging multi-link deletion in one round. In particular, one could modify the issue sequence from the trivial case of strategy 1

$$\{\underbrace{\text{one link deletion}, \cdots, \text{one link deletion}}_{m_d \text{ link deletion}}\}$$

to a more flexible task assignment

$$\{m_d^1 \text{ links deletion}, \cdots, m_d^{\bar{s}} \text{ links deletion}\} \tag{5.34}$$

Algorithm 5.4: Distributed multi-link strategy to solve (P1c)

Input : $\mathcal{G}_0$ is connected, m_d^s, $\sigma \cdot n^{T_d} < \sigma_{\max}$
Output : f_i, $\mathbb{E}_i$
1 Initialization: set $t \leftarrow 0$, $r_i(0) \leftarrow 1$, $\xi_i \leftarrow 0$, $\mu_i \leftarrow -1$, $\beta_i \leftarrow 1$, $w_i \leftarrow 0$, $h_i(0) \leftarrow 1 + \max_{i,j\in\mathbb{V}} \sqrt{|\mathbb{V}_0^i||\mathbb{V}_0^j|/2}$, $\mathbb{E}_i \leftarrow \{\}$, and choose $\hat{\boldsymbol{\omega}}_n(0) \in \mathbb{R}^n_{>0}$ randomly;
2 **while** 1 **do**
3 $\quad t \leftarrow t+1$;
4 $\quad$ execute steps 4–14 in Algorithm 5.2;
5 $\quad$ **if** $t \mod T_d = 0$ **then**
6 $\quad\quad f_i \leftarrow \beta_i$, $\mathbb{W}_i \leftarrow \{\}$, $\mathbb{N}_i^{\text{temp}} \leftarrow \mathbb{V}_0^i$;
7 $\quad$ **else if** $t \mod T_d = 1$ **then**
8 $\quad\quad$ **for** $e = 1$ **to** m_d^s **do**
9 $\quad\quad\quad$ **if** $\mathbb{N}_i^{temp} = \emptyset$ **then**
10 $\quad\quad\quad\quad$ go to steps 16;
11 $\quad\quad\quad$ **end**
12 $\quad\quad\quad \mathbb{W}_i \leftarrow \mathbb{W}_i \cup \{\max_{j\in\mathbb{N}_i^{\text{temp}}} \hat{\omega}_n^i \hat{\omega}_n^j\}$;
13 $\quad\quad\quad j^* \leftarrow \arg\max_{j\in\mathbb{N}_i^{\text{temp}}} \hat{\omega}_n^i \hat{\omega}_n^j$;
14 $\quad\quad\quad \mathbb{E}_i \leftarrow \mathbb{E}_i \cup l_{ij^*}$, $\mathbb{N}_i^{\text{temp}} \leftarrow \mathbb{N}_i^{\text{temp}} \setminus \{j^*\}$;
15 $\quad\quad$ **end**
16 $\quad\quad \mathbb{W}_i^{\text{temp}} \leftarrow \mathbb{W}_i$, $\mathbb{E}_i^{\text{temp}} \leftarrow \mathbb{E}_i$;
17 $\quad$ **end**
18 $\quad$ each node transmits $\mathbb{W}_i^{\text{temp}}$ and $\mathbb{E}_i^{\text{temp}}$ to neighbors;
19 $\quad \mathbb{W}_i^{\text{temp}} \leftarrow$ the top m_d^s values in $\cup_{j\in\mathbb{V}_0^i\cup\{i\}} \mathbb{W}_j^{\text{temp}}$;
20 $\quad \mathbb{E}_i^{\text{temp}} \leftarrow$ associated link labels in $\cup_{j\in\mathbb{V}_0^i\cup\{i\}} \mathbb{E}_j^{\text{temp}}$;
21 $\quad$ **if** $\mathbb{E}_i \cap \mathbb{E}_i^{temp} = \emptyset$ **then**
22 $\quad\quad \beta_i \leftarrow 0$;
23 $\quad$ **end**
24 **end**
25 $\mathbb{E}_i \leftarrow \mathbb{E}_i^{\text{temp}}$;

where $\sum_{s=1}^{\bar{s}} m_d^s = m_d$. The pseudo-code of deleting multiple links simultaneously in one round is given in Algorithm 5.4.

Drawing upon Algorithm 5.4, we propose another distributed link-removing strategy in the next proposition.

Proposition 5.3: Strategy 3 for Distributed Link Removal

Consider $m_d \in \mathbb{Z}_{\geq 1}$ link-removing operation and the set of task assignment in (5.34). Algorithm 5.4 is called for $\bar{s}$ rounds and at each s-th round, m_d^s links are selected simultaneously to break up based on the result of Algorithm 5.4.

Strategy 3 for distributively removing links is likely to invoke the distributed computation algorithm with less frequency compared to Strategy 1 in Proposition 5.1 and thus, substantial computation efforts are saved. In fact, Strategy 1 is a special case of Strategy 3 where $m_d^s = 1$ for all $k = 1, \ldots, \bar{k}$. In the extreme case $m_d^1 = m_d$, the distributed strategy in Proposition 5.3 launches Algorithm 5.4 only once. It is, however, imperative to degrade the optimality in comparison to the implementation of Strategy 1. Since the exact leading eigenvalue of the perturbed adjacency can be computed by [SS90]

$$\lambda_n(\boldsymbol{A}^-_{m_d}) = \lambda_n(\boldsymbol{A}_0) - \hat{\boldsymbol{\omega}}_n^\top(\boldsymbol{A}_0)\Delta\boldsymbol{A}^-_{m_d}\hat{\boldsymbol{\omega}}_n(\boldsymbol{A}_0) - \sum_{k=1}^{n-1}\frac{[\boldsymbol{\omega}_k^\top(\boldsymbol{A}_0)\Delta\boldsymbol{A}^-_{m_d}\hat{\boldsymbol{\omega}}_n(\boldsymbol{A}_0)]^2}{\lambda_n(\boldsymbol{A}_0)-\lambda_k(\boldsymbol{A}_0)} + \mathbf{O}(\|\Delta\boldsymbol{A}^-_{m_d}\|^3) \tag{5.35}$$

which evidences our pioneering statement that the first order approximation (P3c) is an upper bound for the optimal solution of (P3b).

In general, it is troublesome to provide a quantitative study of the optimality gap between the approximated solution derived from Proposition 5.3 and the global optimal solution of the optimization (P3b). Nonetheless, the formula (5.35) provides prescient insights on this gap which depends jointly on the computation accuracy of the distributed estimation of eigenvectors and the influence of the higher-order terms. On the one hand, the approach of multi-link removal in each round elevates the impact of higher-order terms and leads to a considerable deviation by using the first-order approximation (P3c). Instead, Strategy 1 uses the distributed computation of the principal eigenvector using the newest topological information. This way to iteratively remove single edge in each round dampens this approximated error. On the other hand, the observation of the higher-order terms in (5.35) relates the optimality performance to the spectral gap $\lambda_n(\boldsymbol{A}_0)-\lambda_{n-1}(\boldsymbol{A}_0)$ of the adjacency matrix. When the spectral gap is large enough, the eigenvalues and eigenvectors other than the leading counterparts make little contribution to the approximation. The quality-of-service is primarily determined by the efficiency of the distributed estimation of the dominant eigenvector. As mentioned, the convergence rate of the distributed PI algorithm also relies a great deal on the spectral gap. Namely, the convergence speed of distributed estimation accelerates as the spectral gap grows. In summary, we can argue that the developed distributed scheme of link operation offers the desired level of performance, as long as the networks are of a large spectral gap.

Furthermore, the leading eigenvector of the adjacency matrix, also known as eigenvector centrality, is often used to characterize the ability of nodes to spread epidemics over networks [MSMH14]: Large value comes great power. Consequently, the product of each pair of eigenvector elements specifies the crucial role of the corresponding links in the propagation of disease. As such, the development in this section is intriguingly consistent with the intuitive instruction that the deletion of the edges connecting the nodes with higher centrality increases the probability of rehabilitating a network from diseases. Therefore, untying the strong links is preferable than cutting weak links in controlling the epidemic spread. Empirical findings also show the epidemic scale is still dramatically wide by removing links connecting nodes with low centrality [MSK+11; TK12].

Besides, it is necessary to remark that the efficiency of the distributed strategy by employing Algorithm 5.4 reduces gradually as the round step progresses. Following the undock of edges among nodes with high centrality ω_n^i from the network, the discriminating power of the principal eigenvector weakens continuously. In connection with graph irregularity [GR01], the developed distributed strategy for link operation tends to regularize the resulting network. A similar claim by empirical validations also appears in [MSK+11]. Good news is that networks extracting from real-world applications are far from being highly regular, so our approach is applicable to a significantly broader range.

5.3.4 Distributed Link Removal with Connectedness-Concerning

It is worth noting that when the number of deleted links m_d is close to *edge connectivity*[7], the resulting network after removing a certain amount of links may be disconnected. From the perspective of post-disaster reconstruction, networks tend to retain as a whole rather than splitting into isolated fractions, although the second scenario usually appears with a lower epidemic size. Therefore, a growing concern raises about preserving the connectedness of networks in the course of topology operation [POJ11; SBS12].

With the requirement on maintaining connectedness in mind, we reformulate the problem (P3c) as follows

$$\begin{aligned} \max_{\boldsymbol{y}\in\{0,1\}^{|\mathbb{E}_0|}} \quad & \Delta\lambda_n(\boldsymbol{A}_0, \Delta\boldsymbol{A}^-_{m_d}) \\ \text{s.t.} \quad & \Delta\lambda_n(\boldsymbol{A}_0, \Delta\boldsymbol{A}^-_{m_d}) = \sum_{l_{ij}}^{|\mathbb{E}_0|} y_{l_{ij}} \omega_n^i \omega_n^j, \quad \mathbf{1}^\top \boldsymbol{y} = m_d, \quad \mathcal{G}^-_{m_d} \text{ is connected.} \end{aligned} \tag{P3d}$$

To solve optimization (P3d), the main challenge is how to anticipate the connectedness of the resulting network in the event of link deletion, especially, in a distributed manner. The detailed pseudo-code of connectedness verification is exhibited in Algorithm 5.5.

Algorithm 5.5: Distributed connectedness examination for $\mathcal{G}^-_{l_{ij}} = (\mathbb{V}, \mathbb{E}_0 \setminus \{(j,i)\})$

Input : $\mathcal{G}_0$ is connected
Output : connectedness of $\mathcal{G}^-_{l_{ij}}$

Initialization: set $z_i \leftarrow 1$, $z_j \leftarrow -1$ and $z_k \leftarrow 0$ for all $k \in \mathbb{V} \setminus \{i, j\}$;
execute max- and min-consensus algorithm for z_i $(i \in \mathbb{V})$ over $\mathcal{G}^-_{l_{ij}}$;
set $z_i \leftarrow \text{output}_i^{\max} + \text{output}_i^{\min}$ for all $i \in \mathbb{V}$;
run max-consensus algorithm for z_i over $\mathcal{G}_0$;
if *output of* max-*consensus algorithm* **then**
  $\mathcal{G}^-_{l_{ij}}$ is disconnected;
else
  $\mathcal{G}^-_{l_{ij}}$ is connected;
end

Algorithm 5.5 reads that by assuming the edge to be deleted is (i^*, j^*), node i^* and j^*, and others of $\mathbb{V} \setminus \{i^*, j^*\}$ are assigned a test signal 0, 1 and −1, respectively. Then, the network runs simultaneously max-consensus and min-consensus protocol for the assigned signal variables over the network $\mathcal{G}^-_1 := (\mathbb{V}, \mathbb{E}_0 \setminus \{(i^*, j^*)\})$. In the end, each node adds up the eventual outputs of max- and min-consensus algorithm, respectively. If all the summations on nodes amount to zero, then $\mathcal{G}^-_1$ is connected; otherwise disconnected.

Finally, Algorithm 5.5 facilitates the extension of Strategy 1 given in Proposition 5.1 for preserving the network connectedness in the process of link removing. This connectedness-concerning strategy is abbreviated to Strategy 4 whose detailed pseudo-code is provided in Algorithm 5.6.

[7] Edge connectivity is denoted as the minimum number of edges whose deletion from a graph disconnects the graph.

Algorithm 5.6: Distributed connectedness-concerning strategy to solve (P3d)

Input : $\boldsymbol{y} = [0,\ldots,0] \in \mathbb{R}^{|\mathbb{E}_0|}$, a connected graph $\mathcal{G}_0$
Output : $\boldsymbol{y}$
1 Initialization: set **for** $s = 1,\ldots,m_d$ **do**
2   use Theorem 5.2 to compute $\hat{\boldsymbol{\omega}}_n(\boldsymbol{A}_{s-1}^{-})$;
3   set $\mathbb{E}_{s-1}^{\text{temp}} \leftarrow \mathbb{E}_{s-1}$;
4   select the candidate edge $(i^*, j^*) \in \mathbb{E}_{s-1}^{\text{tem}}$ using line 16−24 of Algorithm 5.2;
5   check connectedness of graph $(\mathbb{V}, \mathbb{E}_{s-1}^{\text{tem}} \setminus \{(i^*, j^*)\})$ by using Algorithm 5.5;
6   **if** $(\mathbb{V}, \mathbb{E}_{s-1}^{tem} \setminus \{(i^*, j^*)\})$ *is disconnected* **then**
7         $\mathbb{E}_{s-1}^{\text{tem}} \leftarrow \mathbb{E}_{s-1}^{\text{tem}} \setminus \{(i^*, j^*)\}$;
8   return to step 4;
9   **end**
10     $y_{l_{i^* j^*}} \leftarrow 1$, $\mathcal{G}_s^{-} \leftarrow (\mathbb{V}, \mathbb{E}_{s-1} \setminus \{(i^*, j^*)\})$;
11 **end**

5.3.5 Numerical Evaluations

In this section, we report simulation results for the proposed strategies of link operation over several empirical and real networks with different scales and topologies.

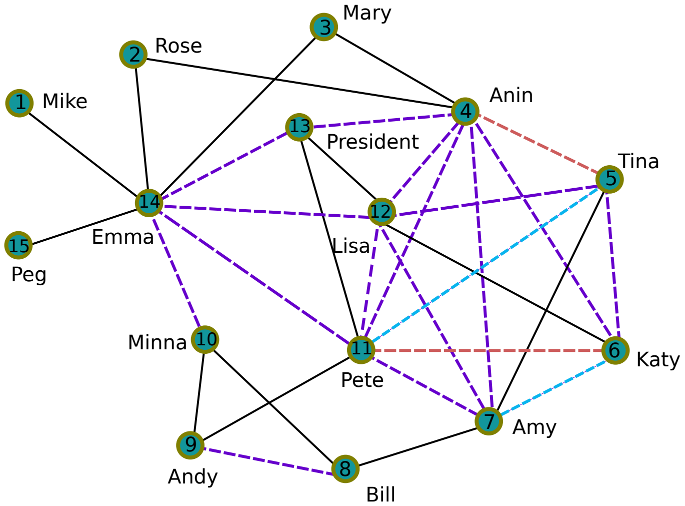

Figure 5.5: A network of social ties in an office.

First, we elucidate the development of distributed protocols and compare them with the centralized method on the condition that the information of global network topology is accessible. The case studied here is that malicious rumors spread through a small network of social ties in the office of an overseas branch of a large international organization [EHB12]. As shown in Figure 5.5, the network consists of 15 members and their initial interrelation structure is represented by both solid and dashed lines. To control the dissemination of fake messages efficiently, we remove (rewire) $m_d = 17$ ($m_r = 17$) links from the network.

As we studied in this section, central in the distributed strategy is a distributed PI algorithm which affords credible estimates of the centrality eigenvector. As such, we examine the effectiveness of the event-triggered distributed PI algorithm over this small social network. The trajectories of the estimation variables $\hat{\omega}_n^i$ are depicted by colored solid

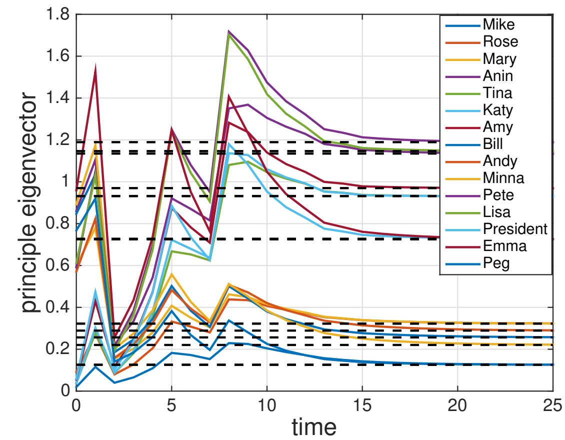

(a) The distributed PI estimation for $\boldsymbol{\omega}_n(\boldsymbol{A}_0)$.

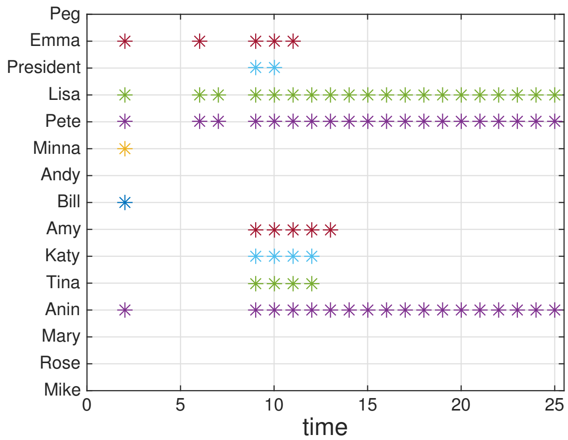

(b) A diagram of the event-triggered time instants

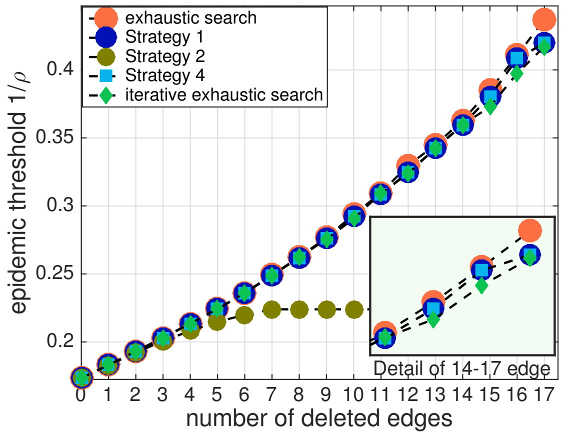

(c) Comparison of different strategies

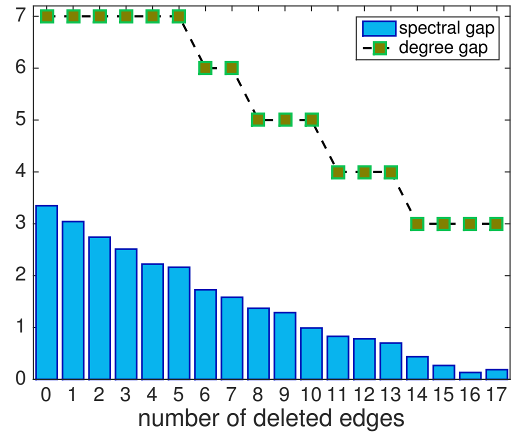

(d) The variation of spectral gap and degree

Figure 5.6: Simulation on a small-size network.

lines in Figure 5.6a, whereby black dashed lines describe the corresponding components of the true principal eigenvector. It can be observed that the estimate states converge to their corresponding true values in a fast manner. In this process, the compensation for magnitude in (5.21) does not occur continuously but acts only at some necessary moments. In the test, the event-trigger threshold is set to $\sigma = 1$ and the sequence of event-triggered instants is plotted in Figure. 5.6b. In comparison to constant transmissions, event-based implementation indeed offers some overt advantages in computation and communication. Even so, we need to point out that the event-trigger on Lisa, Pete, and Anin continues to be on after convergence because the equilibrium estimates corresponding to these three actors exceed $\sigma = 1$. An ad-hoc remedy is to endow a tailored threshold value σ_i for each node $i \in \mathbb{V}$, which, however, requisites for some prior knowledge of graph spectrum.

Under the same topological network, Figure 5.6c shows the comparison of the proposed distributed strategy with other approaches for link operation to control virus spreading. For link-deleting scheme, we focus on Strategy 1 developed in Proposition 5.1, as well as the connectedness-preserving Strategy 4. At each round $s = \{1, \ldots, m_d\}$, a single link is removed according to the output of Algorithm 5.2. The simulation results exhibit that Strategy 1 provides a near-optimal solution to the optimization problem (P3a), although the quality-of-service reduces slightly as the number m_d increases. The diagrammatic sketch of the resulting network after link removal in Figure 5.5 also corroborates the efficiency of Strategy 1, where the dashed lines in purple and red color are the global solution, while those in purple and blue color are the sub-optimal solution of Strategy 1. Notably, there is a mere two links difference between Strategy 1 and brute-force search. The second observation is that the reallocation of existed edges performs not as well as link-deleting scheme. Figure 5.6c also delivers another implicit message that the resultant network after deleting $m_d = 17$ links preserves connectedness since Strategy 1 and Strategy 4 enhance the epidemic controlling at the same level. Figure 5.6d shows the impact of removing links from the network on the graph indices including spectral gap $\lambda_n(\boldsymbol{A}) - \lambda_{n-1}(\boldsymbol{A})$ and degree gap $\max_{i\in\mathbb{V}} \deg_i - \min_{j\in\mathbb{V}} \deg_j$. Both indices take on a descending tendency as the amount of the deleted links augments. This phenomenon implies, in some sense, that the link-deleting operation relieves irregularity of graphs. As discussed in Subsection 5.3.3, the performance loss of Strategy 1 is attributed to reducing the spectral gap.

Next, we report simulation results for the distributed strategies over three synthetic networks: 1). *Gilbert* stochastic model (Gi) ($|\mathbb{V}| = 100$, $|\mathbb{E}| = 268$); 2). *Barabási-Albert* Scale Free model (BA) ($|\mathbb{V}| = 100$, $|\mathbb{E}| = 281$); and 3). *Watts-Strogatz* model (WS) ($|\mathbb{V}| = 100|$, $|\mathbb{E}| = 308$). In this simulation study, we compare the proposed strategies with random link removal as the globally optimal configuration is inaccessible in this case. From the exposition of Figure5.7a-5.7c, the developed distributed Strategy 1 in Proposition 5.1 significantly outperforms the random link-removal strategy over all three random networks. The simulation results also solidify the intuition that rewiring the existed links by using Strategy 2 in Proposition 5.2 is furnished with relatively unsatisfactory performance, especially, on the WS network which has a minor discrepancy in nodal degrees, as reported in Figure 5.7d.

Moreover, we revise the link-deleting scheme by using Strategy 3 in Proposition 5.3 where 5 links, 10 links, 20 links and 30 links are removed at each round, respectively. The results are depicted in Figure 5.7a-5.7c. Despite saving computational efforts, the growth of the quantity m_d^s at each round deteriorates the effect of the link-removing operation for all random networks. In particular, it is observed from Figure 5.7c, somehow surprisingly, the performance of Strategy 3 is worse than the random link removal on the WS model which has an even degree distribution as shown in Figure 5.7d. In conjunction with the fluctuation of the network metrics shown in Figure 5.7e, this observation is in accordance with the statement addressed in Subsection 5.3.3. That is, a small spectral gap amplifies the inaccuracy of the distributed estimation algorithm. In analogy with the results in the small-size networks, Figure 5.7e reveals that link-removing scheme makes the resulting random networks increasingly regular.

Table 5.3: Elapsed time (/s)

	$m_d^s = 1$	$m_d^s = 5$	$m_d^s = 10$	$m_d^s = 20$	$m_d^s = 30$
Gi network	2.4575	0.4849	0.2298	0.0926	0.0627
BA network	2.5882	0.5912	0.2335	0.0638	0.0378
WS network	3.51	0.7472	0.3910	0.1342	0.082

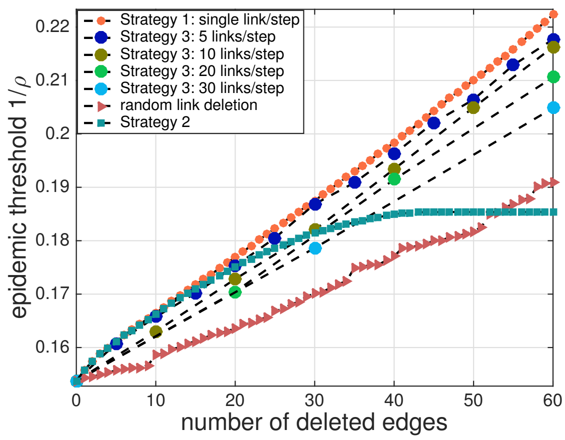

(a) Gilbert stochastic network

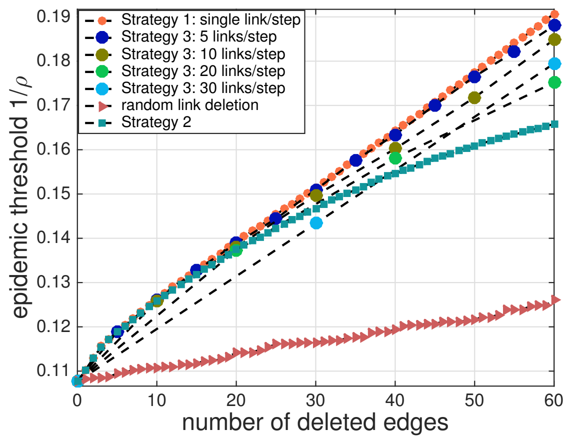

(b) Barabási-Albert scale free network

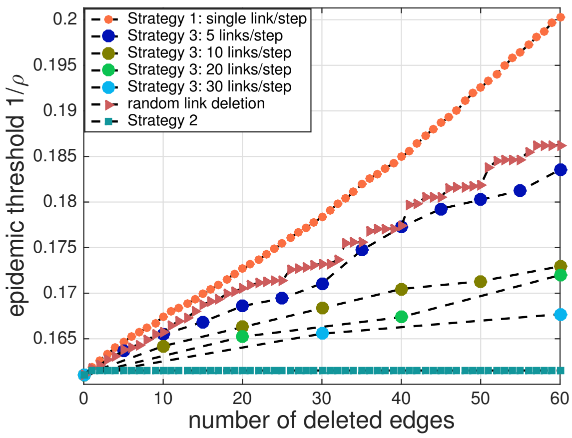

(c) Watts-Strogatz small world network

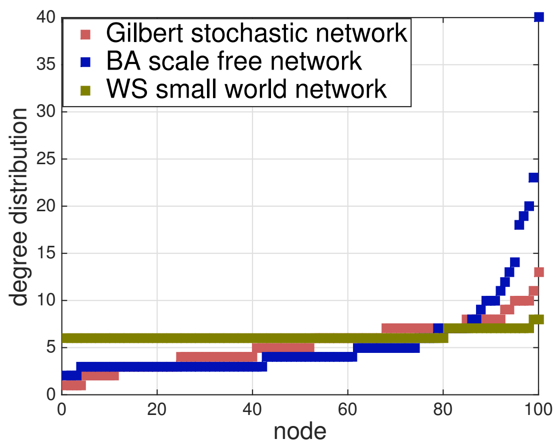

(d) Degree distribution of random networks

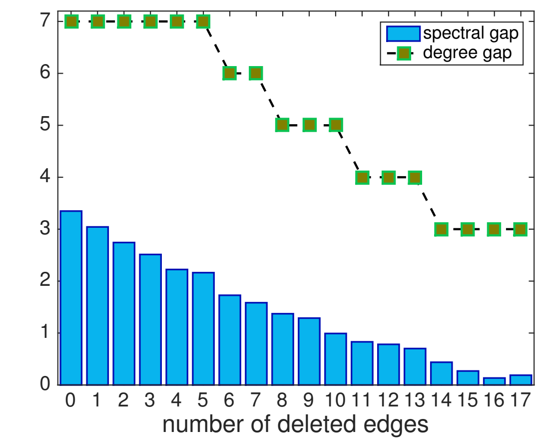

(e) The variation of spectral gap and degree gap

Figure 5.7: Comparison of different strategies for link-removing scheme in three random network.

Finally, Table 5.3 displays the elapsed time of the distributed link-removal strategy with different link-removal number m_d^s. Despite the evident benefits arising in the case of small m_d^s, it comes at the cost of high iteration times.

5.4 Literature Review

Numerous efforts have been directed towards developing distributed algorithms for computing eigenvalue and eigenvector of network-induced matrices. For example, a decentralized orthogonal iteration approach is proposed in [KM08] to estimate some leading eigenvectors but with a restriction of centralized initialization. Based on the power iteration approach, a method is introduced in [YFG+10] to estimate the components of the Fiedler vector and the Fiedler value in a continuous-time fashion. However, the continuous time nature of the algorithm makes its implementation in a real-world scenario particularly challenging. In the work of [LQ13], the authors propose a distributed approach for the estimation of the eigenvalues of the weight matrix and comparable work can be found in [ASD+12]. Both achievements require nested averaging loops which severely affects its efficiency on the aspect of convergence speed and communication cost. To circumvent this intermediate normalization in power iteration, a method, based on the normalized least-mean-square algorithm, is proposed in [BM13]. Unfortunately, this method assumes the existence of a global beacon implicitly and thus does not conduct a fully distributed manner. With the aid of the distributed algorithm for solving linear equations [MLM15], the recent literature [GQ17] provides a method to estimate all the eigenvalues and eigenvectors of an irreducible matrix. Nevertheless, this method enforces each node to estimate an entire vector and is stuck in high consumption of computation and communication. In addition, with the fast development of researches on distributed power iteration, many new contexts, such as random graphs [LB14], switching topologies [LQ14], and finite-time convergence [CRJH16], have emerged. Other applications of power iteration include dimensionality reduction in data traffic [HSK16], node criticality assessment in network security [ALQR16], to name a few.

5.5 Summary

In this chapter, we start with the joint design of a distributed control law and the communication structure in a large-scale interconnected system in the presence of external disturbance and topological uncertainty. After identifying a set of distributed control laws guaranteeing system stability and the desired level of $\mathcal{H}_\infty$ performance, a centralized algorithm to solve the optimal $\mathcal{H}_2$ minimization problem is proposed.

Because global information on a network structure is often unavailable in reality, we develop a distributed method to efficiently solve the link-operation problem by mimicking the gradient-based approach. Central in the development is to execute link addition/removal/rewiring in an iterative manner based on the results of a distributed estimation scheme and an identification mechanism using local information. Indeed, the developed strategies enable us to efficiently acquire the suboptimal solution and to find directed applications in network problems, including community detection [CH15], node-criticality assessment [ALQR16], and resource allocation [XHC+17].

Finally, the reinterpretation of the link-operation problem in the context of coevolutionary networks allows us to treat research activities in opinion dynamics on social networks and topology-design problems of complex networks in the same picture.

The failures and reverses which
await men - and one after
another sadden the brow of
youth - add a dignity to the
prospect of human life, which
no Arcadian success would do.

Henry D. Thoreau

Chapter 6

Conclusions and Outlook

Distributed algorithm analysis and topology design in networked dynamical systems in and of themselves are significant challenges in network science. The two issues are usually investigated along two separate lines of research: complex network analysis and network system theory. The distributed analysis of network systems considers the different types of so-called processes (e.g., information diffusion and opinion formation) on networks, while topology-design problems of complex networks are concerned with various functionalities (e.g., robustness and connectivity) of networks. To integrate these two aspects into a theoretical framework is much more challenging. The overall problem is that the dynamical behaviors of such processes are profoundly affected by the dynamics of the network and vice versa. This begs the need for the development of new analytical points of view and theoretical supports. This thesis contributes to this endeavor by addressing the two issues separately at the outset. The distributed analysis aligns with the burgeoning trend toward filling the gap between control theory and social network analysis, paying close attention to cooperative-competitive interactions and self-appraisal mechanisms of social influences. The distributed-topology design problem is generally formulated as a distributed decision-making problem related to local computation and neighboring communication. For practical consideration, such as computational limitations and privacy concerns, the goal is to develop legitimate strategies for topology-manipulation without full knowledge of the network structure and a central decision-maker. Two paradigm shifts emerging in both directions play an important role in eliminating the separation. The first shift, rooted in social networks from single-issue opinion-evolution to opinion-formation along a sequence of issues, explores the coevolution between opinion dynamics and topology of influence networks. For topology-design problems, distributed computation algorithms and topology-reconstruction profit greatly from the other shift from the simultaneously operating multiple links to iteratively manipulating links.

We briefly summarize the major contributions and conclusions of each chapter in the next section.

6.1 Conclusions

Chapter 3

In this chapter, we investigated the evolution of opinion-formation processes over cooperative-competitive social networks from a control-theoretic point of view. The main contribution was the establishment of an opinion model describing the joint influence of the dynamical properties of social agents and the interactive relationships among them in shaping public opinions. Analogous to the controllability problem in control theory, the first contribution in this chapter was to examine the consensusability, polarizability, and neutralizability of the proposed model by providing sufficient and/or necessary conditions. Then, the mathematical development was considered in the context of exogenous influences, especially media exposure in the real world. In the system-analysis stage, the port-Hamiltonian representation of opinion dynamics gave prescient insights into information-diffusion across the interaction networks and implications of the connection between the passivity property in systems theory and internalization behavior in psychological studies. The results demonstrate that the leadership in a social environment can manipulate public opinions through different tactics. Furthermore, the algebraic graph-theoretic interpretation of individuals' contribution to collective decision-making reflects the social power of each actor.

Chapter 4

In this chapter, we studied how a social group of actors discusses and forms opinions over a sequence of issues on the signed influence networks. The first contribution in this chapter was the development of a systematic framework to enable individuals to assess their social powers subjectively, and a network to objectively evaluate the constituent entities' social influences. With the proposed architecture, social power entails an orientation system such that the relative control exerted in the forward direction leads to a positive effect on issue discussions, while a negative influence along the backward direction. With the adoption of the differential Lyapunov method to convergence analysis, the second contribution was to establish the contraction properties of the developed mathematical formulations. Such contraction shows that individuals gradually forget their initial recognition of their social influence. Another important contribution of this chapter was the interpretation of individuals' social influence from a graph-theoretic point of view, deepening our understanding of relative control in social activities. This allows the extension of the acquired results to a broader range of influence-network structures. Numerical results not only validate all theoretical developments in this chapter, but also show that opinion-forming processes across an issue sequence may display conformity, neutrality, polarity, and separation.

Chapter 5

In this chapter, we introduced completely distributed strategies for different link operations in complex networks. The initial focus was on the dynamics of networks concerning various performance measures such as robustness, connectivity, and resilience. The main contribution in this chapter was the development of distributed computation algorithms that do not need the full information of network topology and a central entity. Such distributed strategies themselves perform with the aid of local computation and a cooperative decision-making mechanism that is implemented in an ad hoc manner based on a nearest-neighbor rule. In particular, multiple technologies, including event-triggered information exchange and parallel algorithm design, save significant computational and communication resources. This chapter's most important contribution was the treatment of link operation as a sequence of issues, inspiring us to redesign the distributed strategies from the perspective of coevolutionary networks. The new distributed approach breaks a single task of multi-link operation down to a series of subtasks, effectively upgrading the quality of service.

6.2 Outlook

The present thesis serves as the first step toward distributed algorithm analysis and topology design in dynamical network systems. The displayed results have potentially profound implications for our understanding of coevolutionary networks. However, much work remains to be done along the lines of research in the thesis, and we summarize the main future topics as follows.

Rigorous theoretical and empirical studies for opinion dynamics model

The linear time-invariant model describing opinion dynamics is fairly novel and innovative, allowing many comprehensive mathematical analysis approaches and theoretical results of systems and control theory to fuel social network analysis. However, the branch of research employing control theory to address problems posed by social and behavioral sciences is still in an embryonic stage, and its contours remain obscure. For the same reason, the lack of adequate empirical evidence presents a major difficulty in applying the developed methodology to study opinion dynamics in real-life social networks. Furthermore, many conjectured sociological interpretations of the mathematical models need confirmation. For example, the nullification of actor-to-actor communication in the presence of autocratic media could be reminiscent of the ruling police during the era of slavery in the United States. Slave owners (like the media group in our model), safeguarded their authority by restricting slaves' intercommunication. Throughout history, endowing illiterate slaves with literacy was regarded as the pathway to democratic enlightenment. With the technical revolution in communication, especially the recent penetration of social-networking tools such as Facebook and Twitter, autocratic behavior can be mitigated dramatically as interpersonal communication is enhanced [JS17]. Another conjecture is the sociological explanation for the appearance of media states in the opinion protocols of actors. One possible reason is that the leadership in a system of governance usually implements some brainwashing policies to assert its dominance. In principle, central to these strategies is the reduction of people's ability to think self-consciously, encouraging them to submit to the demands of rulers. Another feasible interpretation is to contextualize terms in press reports. The perceived truth persuading citizens to believe is probably very far from the actual truth. Thus, this aspect of future work is relevant to research topics in sociology and psychology.

Characterization of interpersonal appraisal dynamics

In this thesis, we do not address the dynamics of the interpersonal-appraisal mechanism. As presented in Figure 4.1, we study the coevolution framework as a whole in an open-loop context, whereby the appraisal matrix and its associated dominant spectral properties are regarded as an exogenous signal. From the realm of social psychology, social actors preferably ask for opinions of peers (friends, and even enemies sometimes) on a specific individual toward whom they accord cognitive appraisals. We believe appropriate mathematical modeling of such psychological phenomena, e.g., [MKKS11; TDL13; JFB16], can be incorporated seamlessly in a closed loop with the developed results. Note that these dynamical models of the interpersonal appraisal structure account for the asymptotic emergence of structural balance.

Interpretation of negative probability in Markov chains

The study of the duality between DeGroot opinion dynamics and Markov chains [PT17] has a long history in mathematical sociology. A recent achievement [AFH+17] derives the dual relation between the DeGroot-Friedkin model and the reinforcement of Markov chains. A significant challenge encountered in the exploration of such duality is the possible appearance of negative values of the transition probability. The ongoing scientific debates around the legitimacy of negative probability in the fields of mathematics and physics [Fey87] may shed some light on the appropriateness of this duality.

Distributed self-appraisal mechanism

The self-assessment of individual importance in successive opinion formation is implemented in a centralized manner. From the viewpoint of networked systems, we aim to develop a rigorous mathematical methodology of the reflected appraisal mechanism in a distributed way. Potential ideas involve distributed computation of eigenvectors, as presented in Chapter 5, as well as other distributed learning approaches [Ned15].

Distributed optimal topology design problems

Until now, the distributed-topology design problems are focused on an undirected and unweighted graph. An immediate generalization would extend current results to networks with directed and (signed) weighted interaction structures. Further areas of optimal topology design include dynamic networks, noisy environments, and real data verification, e.g., in power grids and international airport networks. In addition, one daunting problem in this area of research is that the developed distributed algorithms exhibit an asymptotic convergence behavior that may not meet the requirement of rapid response, e.g., the abruptness of cascade failures in power grids. Although this thesis mentions several stopping rules for distributed computation, they still perform in a centralized fashion because of a dependence, more or less, on global quantities. Thus, another open direction for research is to accelerate the convergence speed of the distributed strategy to accommodate real-life networks.

Appendices

Appendix A

Appendix

A.1 Graph Theory

This appendix is intended to review some of the basic notions of graph theory. Rather than being exhaustive, it is meant to familiarize the readers with the main principles used throughout this thesis. The presentation follows the textbooks [GR01; BH12; vMi11].

A.1.1 Ordinary Graphs

The interaction structure of a network system is captured by a directed *graph* (digraph) $\mathcal{G}=(\mathbb{V},\mathbb{E},\boldsymbol{A})$ with a set of *nodes* (*vertices*) $\mathbb{V}=\{1,2,\ldots,n\}$ and a set of *edges* (*links*) $\mathbb{E}\subseteq\mathbb{V}\times\mathbb{V}$ which has elements as ordered pairs (j,i) (an arc from node j to node i). The graph $\mathcal{G}$ is said to be *undirected* if $(i,j)\in\mathbb{E}$ signifies $(j,i)\in\mathbb{E}$. Sometimes, we may assign a label to an edge in $\mathbb{E}$ by $l_{ij}\sim(j,i)\in\mathbb{E}$. $\boldsymbol{A}=[a_{ij}]\in\mathbb{R}^{n\times n}_{\geq 0}$ is the weighted *adjacency* matrix and if an element $(j,i)\in\mathbb{E}$, then $a_{ij}>0$; otherwise $a_{ij}=0$. Through this thesis, we confine ourselves to graphs that have no self-loops (i.e., $a_i i=0$ for all $i\in\mathbb{V}$). Define the neighborhood of a node i as $\mathbb{N}^i=\{j\in\mathbb{V}|(j,i)\in\mathbb{E}\}$. The *degree* of a node i is the value $\deg_i=\sum_{j\in\mathbb{N}^i}a_{ij}$. A graph is called balanced if $\deg_i=\sum_{j\in\mathbb{N}^i}a_{ji}$ for all $i\in\mathbb{V}$ and it is *symmetric* if $a_{ij}=a_{ji}$ for all $(j,i)\in\mathbb{E}$. Clearly, any symmetric graph is a undirected graph, but not necessarily the other way around. An *unweighted* graph denotes a graph with an unweighted adjacency matrix $\boldsymbol{A}$ where $a_{ij}=1$ if $(j,i)\in\mathbb{E}$; otherwise $a_{ij}=0$. *Simple* graph, also called a strict graph, is an unweighted and undirected graph. The *complement* graph $\overline{\mathcal{G}}=(\mathbb{V},\overline{\mathbb{E}},\bar{\boldsymbol{A}})$ of a graph $\mathcal{G}$ is defined as a graph with a same set of nodes as $\mathcal{G}$, with a set of edges such that $(i,j)\in\overline{\mathbb{E}}$ if and only if $(i,j)\notin\mathbb{E}$. A *subgraph* of a graph $\mathcal{G}=(\mathbb{V},\mathbb{E},\boldsymbol{A})$ is represented by a graph with the node set is an improper subset of $\mathbb{V}$, the edge set is an improper subset of $\mathbb{E}$, and the adjacency matrix is the corresponding submatrix of $\boldsymbol{A}$. Moreover, a graph $\mathcal{G}$ has a star topology if there exists an unique node, called the *center* node, such that the edges of $\mathcal{G}$ pointing either all to or all away from this center node. In addition, a graph is compatible with a matrix $\boldsymbol{C}\in\mathbb{R}^{n\times n}$, denoted by $\mathcal{G}(\boldsymbol{C})$, if for all $(j,i)\notin\mathbb{E}$ and $j\neq i$, there is $[\boldsymbol{C}]_{ij}=0$.

A directed *path* connecting nodes i and j is a sequence of distinct nodes $i_0:=i,i_1,\ldots,i_{k-1},i_k:=j$ $(k\in\mathbb{Z}_{>1})$ such that $(i_{l-1},i_l)\in\mathbb{E}$ for $l=1,\ldots,k$. The shortest path between two nodes in a graph is the path that has the minimum sum of the weights of its constituent links. A graph is *quasi-strongly connected* (QSC) if it has at least one node, called root, which can reach any other nodes of the graph by a path. A graph is disconnected if it is not quausi-strongly connected . A graph is *strongly connected* if any node can reach any other nodes of the graph with a path. A strongly connectedness of an undirected graph is simplified as connectedness for simplicity. Note that the strongly connected components of an arbitrary directed graph form a partition into subgraphs that are themselves strongly connected.

The *Laplacian* matrix of a graph is denoted by $\boldsymbol{L} = \mathrm{diag}(\mathrm{deg}_1, \ldots, \mathrm{deg}_n) - \boldsymbol{A}$ with row sum equal to zero. Notably, Laplacian is a positive semi-definite matrix and has at least one zero eigenvalue associates with a right-eigenvector $\mathbf{1}^\top$. When the graph is quasi-strongly connected, the Laplacian matrix has one, and only one, zero eigenvalue associated with a left-eigenvector whose entries are non-negative and become positive for a strongly connected graph.

A.1.2 Graph Measures

There are several graph measures of network performance.

- **Connectivity measure**:
  Node connectivity is equal to the minimum number of nodes that must be removed to disconnect the graph. *Edge connectivity* is the minimum number of edges whose removal from a graph disconnects the graph. *Algebraic connectivity* is the second smallest eigenvalue of graph Laplacian and is equal to zero if the graph is disconnected and it together with its corresponding eigenvector, also known as the *Fiedler vector* [Fie73], play an important in characterizing the topological properties of a graph [ASD+12; SSG13; LB14].

- **Centrality measure**:
  Degree centrality is the degree deg_i of node i. *Between centrality* for each node is the number of these shortest paths that pass through this node. *Closeness centrality* is equal to the sum of the length of the shortest paths between the node and all other nodes in the graph. *Eigenvector centrality* uses the entries of the dominant eigenvector of the adjacency matrix of a graph. As a result of Perron-Frobenius Theorem, these entries are all positive and unique for a strongly connected graph.

A.1.3 Signed Graphs

A signed graph $\mathcal{G} = (\mathbb{V}, \mathbb{E}, \boldsymbol{A})$ allows the edges $(j, i) \in \mathbb{E}$ to have a negative weight $a_{ij} < 0$, i.e., $\boldsymbol{A} \in \mathbb{R}^{n \times n}$. A signed graph being *digon sign-symmetric* [PMC16] means any undirected edge if exists, i.e., $(i, j) \in \mathbb{E} \Leftrightarrow (j, i) \in \mathbb{E}$ is identically signed $a_{ij} a_{ji} > 0$. Note that a graph $(\mathbb{V}, \mathbb{E}, |\boldsymbol{A}|)$ can regarded as the unsigned version of the signed graph $\mathcal{G} = (\mathbb{V}, \mathbb{E}, \boldsymbol{A})$.

Slightly different from conventional definition of the Laplacian matrix arising in unsigned graph, the Laplacian $\boldsymbol{L}$ of a signed graph is denoted by

$$[\boldsymbol{L}]_{ij} := \begin{cases} -a_{ij} & \text{if } j \neq i \\ \sum_{j=1}^{N} |a_{ij}| & \text{if } j = i \end{cases} \tag{A.1}$$

According to the Gershgorin disk theorem [HJ09], $\boldsymbol{L}$ has no eigenvalues in $\mathbb{C}_{<0}$ with the possible exception of eigenvalue 0. Unlike the unsigned case, Laplacian of graphs with negative coupling may have no eigenvalue 0. *Structural balance theory* is widely used to characterize the existence of eigenvalue 0 for the signed Laplacian. A directed signed graph $\mathcal{G}$ with vertex set $\mathbb{V}$ is *structurally balanced* if $\mathbb{V}$ can be split into two disjoint subsets (i.e., $\mathbb{V}^+ \cup \mathbb{V}^- = \mathbb{V}$, $\mathbb{V}^+ \cap \mathbb{V}^- = \emptyset$) such that weights of $(i,j) \in \mathbb{E}$ are positive $\forall i \in \mathbb{V}^+, j \in \mathbb{V}^+$ and $\forall i \in \mathbb{V}^-, j \in \mathbb{V}^-$ and weights of $(i,j) \in \mathbb{E}$ are negative $\forall i \in \mathbb{V}^+, j \in \mathbb{V}^-$ and $\forall j \in \mathbb{V}^+, i \in \mathbb{V}^-$. Therefore, when a signed graph is quasi-strongly connected and structurally balanced, the Laplacian matrix has and only has one zero eigenvalue and all other eigenvalues have a positive real part. We say a subgraph is *in-isolated* if no edge comes from outside nodes. A subgraph is an in-isolated structurally balanced (ISB) component of a signed digraph $\mathcal{G}$ if it is an in-isolated subgraph of $\mathcal{G}$ and structurally balanced and any other subgraph of $\mathcal{G}$ strictly containing this subgraph is not in-isolated and structurally balanced.

A.2 Matrix Algebra

In this appendix, we will review some of the basic definitions and concepts in matrix algebra which are used extensively through this thesis. This overview is based on the standard textbooks [Dat04; HJ09]. In the sequel of this section, unless otherwise mentioned, a $n \times n$ matrix $\boldsymbol{C}$ consists of n rows and n columns of real-valued elements $[\boldsymbol{C}]_{ij}$ where $i, j = 1, \ldots, n$.

For a square matrix $\boldsymbol{C}$, let $\lambda_i(\boldsymbol{C})$ denote the eigenvalue with the i-th smallest real part which is sorted in the increasing order $\lambda_1(\boldsymbol{C}) \leq \lambda_2(\boldsymbol{C}) \leq \ldots \leq \lambda_n(\boldsymbol{C})$ and $\mathsf{sr}(\boldsymbol{C}) := \mathsf{max}_i |\lambda_i(\boldsymbol{C})|$ is defined as its spectral radius. The spectrum of matrix $\boldsymbol{C}$ is given by $\mathsf{sp}(\boldsymbol{C}) = \{\lambda_1(\boldsymbol{C}), \lambda_2(\boldsymbol{C}), \ldots, \lambda_n(\boldsymbol{C})\}$

A matrix $\boldsymbol{C}$ is *non-negative* (*positive*), i.e. $\boldsymbol{C} \geq 0$ ($\boldsymbol{C} > 0$), if all its elements are non-negative (positive). The matrix $\boldsymbol{C}$ is *compatible* with a graph $\mathcal{G}(\boldsymbol{C})$ if $[\boldsymbol{C}]_{ij} = 0$ iff $(j, i) \notin \mathbb{E}$ and $j \neq i$. A non-negative matrix $\boldsymbol{C}$ is irreducible if and only if it is compatible with a connected graph $\mathcal{G}$. A non-negative matrix $\boldsymbol{C}$ is said to be *primitive* if there exists a positive integer k such that $\boldsymbol{C}^k > 0$. The *period* of a non-negative and irreducible matrix is define as the greatest common divisor of the lengths of the closed directed paths in its compatible graph. If the period is 1, $\boldsymbol{C}$ is *aperiodic*. In particular, a non-negative matrix $\boldsymbol{C}$ is primitive if it is irreducible and aperiodic (or has at least one positive diagonal element).

The *Perron-Frobenius theorem* states that a real square matrix with positive entries has a unique largest real eigenvalue and that the corresponding eigenvector can be chosen to have strictly positive components. This theorem is of significant importance in many matrix-based applications.

Lemma A.1. *Let $\boldsymbol{C}$ be an irreducible non-negative $n \times n$ matrix with period p and spectral radius $\mathsf{sr}(\boldsymbol{A}) = \rho$. Then the following statements hold.*

- *The number of ρ is a positive real number and it is an eigenvalue of the matrix $\boldsymbol{A}$, called the* Perron–Frobenius eigenvalue.
- *The Perron–Frobenius eigenvalue ρ is simple. Both right and left eigenspaces associated with ρ are one-dimensional.*
- *$\boldsymbol{C}$ has a right eigenvector $\boldsymbol{\omega}$ with eigenvalue ρ whose components are all positive.*
- *$\boldsymbol{C}$ has a left eigenvector $\boldsymbol{\nu}$ with eigenvalue ρ whose components are all positive.*
- *The only eigenvectors whose components are all positive are those associated with the eigenvalue $\boldsymbol{C}$.*
- *The matrix $\boldsymbol{C}$ has exactly p (where p is the period) complex eigenvalues with absolute value ρ. Each of them is a simple root of the characteristic polynomial and is the product of ρ with an p-th root of unity.*

See [Dat04; HJ09], and the references therein, for more details and the refined variants of the Perron-Frobenius theorem.

A.3 Power Iteration Algorithm

The power method is a well-known algorithm for estimating the simple largest eigenvalue and its associated eigenvector of a diagonalizable matrix. In this thesis, we restrict our attention to the case that $\boldsymbol{C}$ is a symmetric matrix and has an eigenvalue in magnitude that is strictly greater than its other eigenvalues, i.e.,

$$|\lambda_n(\boldsymbol{C})| > |\lambda_{n-1}(\boldsymbol{C})| \geq |\lambda_{n-2}(\boldsymbol{C})| \geq \cdots \geq |\lambda_2(\boldsymbol{C})| \geq |\lambda_1(\boldsymbol{C})|.$$

A comprehensive description and some refined variants of power iteration can be found in [GL12; BM12] and references therein. The iteration method is given by

$$\hat{\boldsymbol{x}}_n(t+1) = \frac{\boldsymbol{C}\hat{\boldsymbol{x}}_n(t)}{\|\boldsymbol{C}\hat{\boldsymbol{x}}_n(t)\|}, \tag{A.2}$$

where the initial vector has a nonzero component in the direction of the eigenvector associated with the dominant eigenvalue. As time progresses, the sequence $\{\hat{\boldsymbol{x}}_n(t)\}_{t\in\mathbb{R}_{\geq 0}}$ converges asymptotically to the right eigenvector $\boldsymbol{x}_n$ corresponding to the dominant eigenvalue $\lambda_n(\boldsymbol{C})$, at the rate $|\lambda_{n-1}(\boldsymbol{C})/\lambda_n(\boldsymbol{C})|$. In specific, the Jordan canonical form of $\boldsymbol{C}$ is supposed to be $\boldsymbol{C} = \boldsymbol{X}\boldsymbol{J}\boldsymbol{X}^{-1}$, where the first column of $\boldsymbol{V}$ is an eigenvector of $\boldsymbol{C}$ associated to the principal eigenvalue $\lambda_n(\boldsymbol{C})$. In particular, the initial condition can be formulated by $\hat{\boldsymbol{x}}_n(0) = c_1\boldsymbol{x}_1 + c_2\boldsymbol{x}_2 + \ldots + c_n\boldsymbol{x}_n$ with the assumption $c_n \neq 0$. As a result, one can calculate

$$\hat{\boldsymbol{x}}_n(t) = \frac{\boldsymbol{C}^t\hat{\boldsymbol{x}}_n(0)}{\boldsymbol{C}^t\hat{\boldsymbol{x}}_n(0)} = \frac{\boldsymbol{X}\boldsymbol{J}^t\boldsymbol{X}^{-1}\hat{\boldsymbol{x}}_n(0)}{\boldsymbol{X}\boldsymbol{J}^t\boldsymbol{X}^{-1}\hat{\boldsymbol{x}}_n(0)} = \frac{\lambda_n^t(\boldsymbol{C})}{|\lambda_n(\boldsymbol{C})|}\frac{c_n}{|c_n|}\frac{\boldsymbol{x}_n + \frac{1}{c_n}\boldsymbol{X}\frac{\boldsymbol{J}^t}{\lambda_n^t(\boldsymbol{C})}(c_1\boldsymbol{x}_1 + \cdots + c_{n-1}\boldsymbol{x}_{n-1})}{\|\boldsymbol{x}_n + \frac{1}{c_n}\boldsymbol{X}\frac{\boldsymbol{J}^t}{\lambda_n^t(\boldsymbol{C})}(c_1\boldsymbol{x}_1 + \cdots + c_{n-1}\boldsymbol{x}_{n-1})\|}.$$

By noticing the fact that $\lim_{t\to\infty}(\boldsymbol{J})^t/(\lambda_n^t(\boldsymbol{C})) = \mathsf{diag}(1, 0, \ldots, 0)$, the limiting behavior of the above expression reads

$$\lim_{t\to\infty}\hat{\boldsymbol{x}}_n(t) = \mathsf{sgn}(c_n)\lim_{t\to\infty}\frac{\lambda_n^t(\boldsymbol{C})}{|\lambda_n^t(\boldsymbol{C})|}\frac{\boldsymbol{x}_n(t)}{\|\boldsymbol{x}_n(t)\|},$$

which implies the vector $\hat{\boldsymbol{x}}_n(t)$ converges to the eigenvector $\boldsymbol{x}_n$ up to a scalar as $t \to \infty$.

Bibliography

[Abe64] R. Abelson, “Mathematical models of the distribution of attitudes under controversy,” *Contrib. Math. Psychol.*, vol. 14, pp. 1–160, 1964.

[AJB10] R. Albert, H. Jeong, and A. Barabási, “Error and attack tolearnce of complex networks,” *Nature*, vol. 406, pp. 378–382, 2010.

[AG14] A. Allahverdyan and A. Galstyan, “Opinion dynamics with confirmation bias,” *PLoS One*, vol. 9, no. 7, e99557 2014.

[All85] G. Allport, “The historical background of social psychology,” in *Handb. Soc. Psychol.*, G. Lindzey and E. Aronson, Eds., Random House, New York, 1985, pp. 1–46.

[Alt12] C. Altafini, “Dynamics of opinion forming in structurally balanced social networks,” *PLoS ONE*, vol. 7, no. 6, e38135, 2012.

[Alt13] ——, “Consensus problems on networks with antagonistic interactions,” *IEEE Transactions on Automatic Control*, vol. 58, no. 4, pp. 935–946, 2013.

[AGS08] L. Ambrosio, N. Gigli, and G. Savaré, *Gradient flows: In metric space and in the space of probability measures*. Birkhäuser, 2008.

[Ang02] D. Angeli, “A Lyapunov approach to incremental stability properties,” *IEEE Transaction on Automatic Control*, vol. 47, no. 3, pp. 410–421, 2002.

[ASD+12] R. Aragues, G. Shi, D. Dimarogonas, C. Sagues, and K. Johansson, “Distributed algebraic connectivity estimation for adaptive event-triggered consensus,” in *Proceeding of the 2012 American Control Conference*, Montreal, QC, USA, 2012, pp. 32–37.

[ALQR16] W. Asif, M. Lestas, H. Qureshi, and M. Rajarajan, “Optimization based spectral partitioning for node criticality assessment,” *Journal of Network and Computer Applications*, vol. 75, pp. 279–292, 2016.

[AFH+17] Z. Askarzadeh, R. Fu, A. Halder, Y. Chen, and T. Georgiou, “Stability theory in l_1 for nonlinear Markov chains and stochastic model for opinion dynamics over influence networks,” *ArXiv preprint: 1706.03158v1 [cs.SY]*, 2017.

[Bar16] L.-A. Barabási, *Network Science*. Cambridge University Press, 2016.

[BA99] L.-A. Barabási and R. Albert, “Energence of scaling in random networks,” *Science*, vol. 386, pp. 509–512, 1999.

[Bar04] M. Barthélemy, “Betweenness centrality in large complex networks,” *European Physical Journal B - Condensed Matter Complex Systems*, vol. 406, pp. 378–382, 2004.

[BM13] A. Bertrand and M. Moonen, "Distributed computation of the Fiedler vector with application to topology inference in ad hoc networks," *Signal Processing*, vol. 93, no. 5, pp. 1106–1117, 2013.

[BT89] D. Bertsekas and J. Tsitsiklis, *Parallel and distributed computation*. NJ:Prentice-Hall: Upper Saddle River, 1989.

[BKCM17] H. Bhuiyan, M. Khan, J. Chen, and M. Marathe, "Parallel algorithms for switching edges in heterogeneous graphs," *Journal of Parallel and Distributed Computing*, vol. 104, pp. 19–35, 2017.

[BS11] A. Bishop and I. Shames, "Link operations for slowing the spread of disease in complex networks," *Europhysics Letters*, vol. 95, no. 18005, 2011.

[BHT09] V. Blondel, J. Hnedrickx, and J. Tsitsiklis, "On Krause's multi-agent consensus model with state-dependent connectivity," *IEEE Transactions on Automatic Control*, vol. 54, no. 11, pp. 2586–2597, 2009.

[BT00] V. Blondel and J. Tsitsiklis, "A survey of computational complexity results in systems and control," *Automatica*, vol. 36, pp. 1249–1274, 2000.

[BV82] V. Borkar and P. Varaiya, "Asymptotic agreement in distributed estimation," *IEEE Transactions on Automatic Control*, vol. 27, pp. 650–655, 1982.

[BM12] S. Börm and C. Mehl, *Numerical methods for eigenvalue problems*. Walter de Gruyter, 2012.

[BHD10] M. Breakspear, S. Heitmann, and A. Daffertshofer, "Generative models of cortical oscillations: From Kuramoto to the nonlinear Fokker Planck equation," *Frontiers in Human Neuroscience*, vol. 4, no. 190, 10.3389/fnhum.2010.00190, 2010, issn: 1662-5161.

[BP98] S. Brin and L. Page, "The anatomy of a large-scale hypertextual Web search engine," *Computer Networks and ISDN Systems*, vol. 30, pp. 107–117, 1998.

[BH12] A. Brouwer and W. Haemers, *Spectra of graphs*. Springer-Verlag New York, 2012.

[CB06] A. Camilli and B. Bassler, "Bacterial small-molecule signaling pathways," *Science*, vol. 311, no. 5764, pp. 1113–1116, 2006.

[CL12] C. Canali and R. Lancellotti, "A quantitative methomethod based on component analysis to identify key users in social networks," *Internation Journal of Social Networks and Mining*, vol. 1, no. 1, pp. 27–50, 2012.

[Car56] D. Cartwright, *Studies in social power*. Research Center for Group Dynamics, Institute for Social Research, University of Michigan, 1956.

[CPS17] C. Castellano and R. Pastor-Satorras, "Relating topological determinants of complex networks to their spectral properties: Structural and dynamical effects," *Physical Review X*, vol. 7, p. 041 024, 2017.

[CWW+08] D. Chakrabarti, Y. Wang, C. Wang, J. Leskovec, and C. Faloutsos, "Epidemic thresholds in real networks," *ACM Transactions on Information and Systems Security*, vol. 10, no. 4, 2008.

[CA16] H. Chan and L. Akoglu, "Optimizing network robustness by edge rewiring: A general framework," *Data Mining and Knowledge Discovery*, vol. 30, pp. 1395–1425, 2016.

[CRJH16] T. Charalambous, M. Rabbat, M. Johansson, and C. Hadjicostis, “Distributed finite-time computation of digraph parameters: Left-eigenvector, out-degree and spectrum,” *IEEE Transactions on Control of Network Systems*, vol. 3, no. 2, pp. 137–148, 2016.

[CH15] P. Chen and A. Hero, “Deep community detection,” *IEEE Transactions on Signal Processing*, vol. 63, no. 21, pp. 5706–5719, 2015.

[CWL+16] W. Chen, D. Wang, J. Liu, T. Başar, L. Qiu, K. Johansson, and L. Qiu, “On semidefiniteness of signed Laplacian with application to microgrids,” in *Proceedings of 6th IFAC Workshop on Distributed Estimation and Control in Networked Systems*, vol. 49, 2016, pp. 97–102.

[CLB+17] X.-D. Chen, J. Liu, M.-A. Belabbas, Z. Xu, and T. Başar, “Distributed evaluation and convergence of self-appraisal in social networks,” *IEEE Trans. Automat. Control*, vol. 62, no. 1, pp. 291–304, 2017.

[CS09] S.-J. Chung and J.-J. Slotine, “Cooperative robot control and concurrent synchronization of Lagrangian systems,” *IEEE Transactions on Robotics*, vol. 25, no. 3, pp. 686–700, 2009.

[CBP14] A. Clark, L. Bushnell, and R. Poovendran, “A supermodular optimization framework for leader selction under link noise in linear multi-agent systems,” *IEEE Transactions on Automatic Control*, vol. 59, no. 2, pp. 283–296, 2014.

[CP11] A. Clark and R. Poovendran, “A submodular optimizaiton framework for leader-selection in linear multi-agent systems,” in *Proceedings of 50th IEEE Conference on Decision and Control/European Control Conference*, 2011, pp. 3614–3621.

[CL04] R. Cogill and S. Lall, “Control design for topology-independent stability of interconnected systems,” in *Proceedings of American Control Conference*, 2004, pp. 3717–3722.

[Cor08] J. Cortes, “Distributed algorithms for reaching consensus on general functions,” *Automatica*, vol. 44, no. 3, pp. 726–737, 2008.

[CDH+16] J. Cortés, G. Dullerud, S. Han, J. L. Ny, S. Mitra, and G. Pappas, “Differential privacy in control and network systems,” in *Proceedings of 55th IEEE Conference on Decision and Control*, 2016, pp. 4252–4272.

[DM11] R. Dai and M. Mesbahi, “Optimal topology design for dynamic networks,” in *Proceedings of 50th IEEE Conference on Decision and Control/European Control Conference*, 2011, pp. 1280–1285.

[DMPTH10] T. Danino, O. Mondragón-Palomino, L. Tsimring, and J. Hasty, “A synchronized quorum of genetic clocks,” *Nature*, vol. 463, pp. 326–330, 2010.

[Dat04] K. Datta, *Matrix and linear algebra*. Prentice-Hall Of India Pvt. Limited, 2004.

[BM16] M. H. de Badyn and M. Mesbahi, “Growing controllable networks via whiskering and submodular optimization,” in *Proceedings of 55th IEEE Conference on Decision and Control (CDC)*, 2016, pp. 867–872.

[DeG74] M. DeGroot, “Reaching a consensus,” *Journal of the American Statistical Association*, vol. 69, no. 345, pp. 118–121, 1974.

[DK07] S. DellaVigna and E. Kaplan, “The fox news effect: Media bias and voting,” *Quarterly Journal of Economics*, vol. 122, pp. 1187–1234, 2007.

[DLR15] J.-C. Delvenne, R. Lambiotte, and L. Rocha, “Diffusion on networked systems is a question of time or structure,” *Nature Communications*, vol. 6, no. 7366, pp. 1–10, 2015.

[DS14] J.-C. Delvenne and H. Sandberg, “Finite-time thermodynamics of port-Hamiltonian systems,” *Physica D*, vol. 267, pp. 123–132, 2014.

[DMUH15] F. Deroo, M. Meinel, M. Ulbrich, and S. Hirche, “Distributed stability tests for large-scale systems with limited model information,” *IEEE Transactions on Control of Network Systems*, vol. 3, no. 3, pp. 298–309, 2015.

[DS05] J. Dillard and L. Shen, “On the nature of reactance and is role in persuasive health communication,” *Communication Monographs*, vol. 72, no. 2, pp. 144–168, 2005.

[DYL+15] C. Dong, Q. Yin, W. Liu, Z. Yan, and T. Shi, “Can rewiring strategy control the epidemic spreading?” *Physica A*, vol. 438, pp. 169–177, 2015.

[DB14] F. Dörfler and F. Bullo, “Synchronization in complex networks of phase oscillators: A survey,” *Automatica*, vol. 50, pp. 1539–1564, 2014.

[DGZ96] J. Doyle, K. Glover, and K. Zhou, *Robust and optimal control*. Upper Saddle River, NJ, USA: Prentice-Hall, Inc., 1996.

[EK10] D. Easley and J. Kleinberg, *Networks, Crowds, and Markets. Reasoning about a Highly Connected World*. Cambridge, U.K.: Cambridge Univ. Press, 2010.

[ESM+11] W. Ellens, F. Speksma, P. Mieghem, A. Jamakovic, and R. Kooij, “Effective graph resistence,” *Linear algebraic and its applications*, vol. 435, pp. 2419–2506, 2011.

[ETV13] T. Erseghe, S. Tomasin, and A. Vigato, “Topology estimation for smart microgirds via power communication,” *IEEE Transactions on Signal Processing*, vol. 61, no. 13, pp. 3368–3377, 2013.

[EH08] E. Estrada and N. Hatano, “Communicability in complex networks,” *Physical Review E*, vol. 77, pp. 1–12, 036111 2008.

[EHB12] E. Estrada, N. Hatano, and M. Benzi, “The physics of communicability in complex networks,” *Physics Reports*, vol. 514, pp. 89–119, 2012.

[ERV05] E. Estrada and J. Rodriguez-Velázquez, “Subgraph centrality in complex networks,” *Physical Review E*, vol. 056103, pp. 1–9, 2005.

[FIA11] G. Facchetti, G. Iacono, and C. Altafini, “Computing global structural balance in large-scale signed social networks,” *PNAS*, vol. 108, no. 52, pp. 20 953–20 958, 2011.

[FLJ14] M. Fardad, F. Lin, and M. Jovanović, “Design of optimal sparse interconnection graphs for synchronization of oscillators networks,” *IEEE Transactions on Automatic Control*, vol. 59, no. 9, pp. 2457–2562, 2014.

[Fey87] R. Feynman, “Negativity probability,” *In Quantum Implications: Essays in Honour of David Bohm*, pp. 235–248, 1987.

[FOSS13] S. Fiaz, D. Ortega, J. Scherpen, and A. van der Schaft, "A port-Hamiltonian approach to power network modeling and analysis," *European Journal of Control*, vol. 19, pp. 477–485, 2013.

[Fie73] M. Fiedler, "Algebraic connectivity of graphs," *Czechoslovak Mathematics Journal*, vol. 23(98), pp. 298–305, 1973.

[FS14] F. Forni and R. Sepulchre, "A differential Lyapunov framework for contraction analysis," *IEEE Trans. Automat. Control*, vol. 59, no. 3, pp. 614–628, 2014.

[FSS13] F. Forni, R. Sepulchre, and A. van der Schaft, "On differential passivity of physical systems," in *Proceedings of 52nd IEEE Conference on Decision and Control*, 2013, pp. 6580–6585.

[For10] S. Fortunato, "Community dection in graphs," *Physics Reports*, vol. 486, pp. 75–174, 2010.

[FW76] B. Francis and W. Wonham, "The internal model principle of control theory," *Automatica*, vol. 12, pp. 457–465, 1976.

[FIRT15] P. Frasca, H. Ishii, C. Ravazzi, and R. Tempo, "Distributed randomized algorithms for opinion formation, centrality computation and power systems estimation: A tutorial overview," *European Journal of Control*, vol. 24, pp. 2–13, 2015.

[Fre56] J. French, "A formal theory of social power," *Psychol. Rev.*, vol. 63, pp. 181–194, 1956.

[Fri11] N. Friedkin, "A formal theory of reflected appraisals in the evolution of power," *Administrative Science Quarterly*, vol. 56, no. 4, pp. 501–529, 2011.

[Fri15] ——, "The problem of social control and coordination of complex systems in sociology: A look at the community cleavage problem," *IEEE Control Systems Magazine*, vol. 35, no. 3, pp. 40–51, 2015.

[FJB16] N. Friedkin, P. Jia, and F. Bullo, "A theory of the evolution of social power: Natural trajectories of interpersonal influence systems along issue sequences," *Sociological Science*, vol. 3, pp. 444–472, 2016.

[FPTP16] N. Friedkin, A. Proskurnikov, R. Tempo, and S. Parsegov, "Network science on belief system dynamics under logic constraints," *Science*, vol. 354, no. 6310, pp. 321–326, 2016.

[GVJ12] F. Garin, D. Varagnolo, and K. Johansson, "Distributed estimation of diameter, radius and eccentricities in anonymous networks," in *Proceeding of 3rd IFAC Workshop on Distributed Estimation and Control in Networked Systems*, Santa Barbara, CA, USA, 2012, pp. 13–18.

[GS83] V. Gecas and M. Schwalbe, "Beyond the looking-glass self: Social structure and efficacy-based self-esteem," *Social Psychology Quarterly*, vol. 46, pp. 77–88, 1983.

[GS14] J. Ghaderi and R. Srikant, "Opinion dynamics in social networks with stubborn agents: Equilibrium and convergence rate," *Automatica*, vol. 50, pp. 3209–3215, 2014.

[GB06] A. Ghosh and S. Boyd, “Growing well-connected graphs,” in *Proceedings of the 45th IEEE Conference on Decision and Control*, San Diego, CA, USA, 2006, pp. 6605–6611.

[GN02] M. Girvan and M. Newman, “Community structure in social and biological networks,” *Proceedings of National Academy of Sciences of the United States of America*, vol. 99, no. 12, pp. 7821–7826, 2002.

[GR01] C. Godsil and G. Royle, *Algebraic graph theory*. Springer, 2001.

[GL12] G. Golub and C. van Loan, *Matrix computations*, 4th Edition. Johns Hopkins University Press, 2012.

[GB08] T. Gross and B. Blasius, “Adaptive coevolutionary networks: A review,” *Journal of The Royal Society Interface*, vol. 5, pp. 259–271, 2008.

[GH83] J. Guckenheimer and P. Holmes, *Nonlinear oscillations, dynamical systems, and bifurcations of vector fields*. Springer, 1983.

[GQ17] A. Gusrialdi and Z.-H. Qu, “Distributed estimation of all the eigenvalues and eigenvectors of matrices associated with strongly connected digraph,” *IEEE Control Systems Letters*, vol. 1, no. 2, pp. 328–333, 2017.

[GQH18] A. Gusrialdi, Z.-H. Qu, and S. Hirche, “Distributed link remval using local estamtion of network topology,” *IEEE Transactions on Network Science and Engineering*, 2018, accepted.

[HCS+17] X. Han, S. Cao, Z. Shen, B. Zhang, W.-X. Wang, R. Cressman, and H. Stanley, “Emergence of communities and diversity in social networks,” *PNAS*, vol. 114, no. 11, pp. 2887–2891, 2017.

[Har59] F. Harary, “A criterion for unanimity in French’s theory of social power,” in *Studies in Social Power*, D. Cartwright, Ed., University of Michigan, 1959.

[HCFS15] T. Hatanaka, N. Chopra, M. Fujita, and M. Spong, *Passivity-based control and estimation in network robotics*. Springer, 2015.

[HK15] R. Hegselmann and U. Krause, “Opinion dynamics under the influence of radical groups, charismatic leaders, and other constant signals: A simple unifying model,” *Networks and Heterogeneous Media*, vol. 10, no. 3, pp. 477–509, 2015.

[Hei46] F. Heider, “Attitudes and cognitive orgainzation,” *The Journal of Psychology*, vol. 21, pp. 107–122, 1946.

[Hei58] ——, *The psychology of interpersonal relations*. Lawrence Erlbaum Associates, New Jersey, USA, 1958.

[HJOV14] J. Hendrickx, R. Jungers, A. Olshevsky, and G. Vankeerberghen, “Graph diameter, eigenvalue and minimum-time consensus,” *Automatica*, vol. 50, pp. 635–640, 2014.

[HO16] J. Hendrickx and A. Olshevsky, “On symmetric continuum opinion dynamics,” *SIAM Journal on Control and Optimization*, vol. 54, no. 5, pp. 2893–2918, 2016.

[HK02] P. Holme and B. Kim, “Attack vulnerability of comlex networks,” *Physical Review E*, vol. 65, 056109 2002.

[HJ09] R. Horn and C. Johnson, *Matrix analysis*. New York: Cambridge University Press, 2009.

[HSK16] T.-S. Huang, H. Sethu, and N. Kandasamy, “A new approach to dimensionality reduction for anomaly detection in data traffic,” *IEEE Transactions on Network and Service Management*, vol. 13, no. 3, pp. 651–665, 2016.

[HH08] Q. Hui and W.-M. Haddad, “Distributed nonlinear control algorithms for network consensus,” *Automatica*, vol. 44, pp. 2375–2381, 2008.

[JLM03] A. Jadbabaie, J. Lin, and A. Morse, “Coordination of groups of mobiles autonomous agents using nearest neighbor rules,” *IEEE Transactions on Automatic Control*, vol. 48, no. 3, pp. 988–1001, 2003.

[JMBO01] H. Jeong, S. Mason, A. Barabási, and Z. Oltvai, “Lethality and centrality in protein networks,” *Nature*, vol. 411, no. 6833, pp. 41–42, 2001.

[JS17] C. Jha and S. Sarangi, “Does social media reduce corruption?” *Information Economics and Policy*, vol. 39, pp. 60–71, 2017.

[JFB16] P. Jia, N. Friedkin, and F. Bullo, “The coevolution of appraisal and influence networks leads to structural balance,” *IEEE Transactions on Network Science and Engineering*, vol. 3, p. 4, 2016.

[JFB17] ——, “Opinion dynamics and social power evolution over reducible influence networks,” *SIAM Journal on Control and Optimization*, vol. 55, no. 2, pp. 1280–1301, 2017.

[JMFB15] P. Jia, A. MirTabatabaei, N. Friedkin, and F. Bullo, “Opinion dynamics and the evolution of social power in influence networks,” *SIAM Review*, vol. 57, no. 3, pp. 367–397, 2015.

[JBYJZ10] W. Jun, M. Barahona, T. Yue-Jin, and D.-H. Zhong, “Natural connectivity of complex networks,” *Chinese Physics Letters*, vol. 27, no. 7, 2010.

[KK10] A. Kchiche and F. Kamoun, “Centrality-based access-points deployment for vehicular networks,” *Proceedings of IEEE International Conference of Telecommunication*, pp. 700–706, 2010.

[KM08] D. Kempe and F. McSherry, “A decentralized algorithm for spectral analysis,” *Journal of Computer and System Sciences*, vol. 74(1), pp. 70–83, 2008.

[Kha02] H. Khalil, *Nonlinear systems - Third Edition*. Pearson, 2002.

[KM06] Y. Kim and M. Mesbahi, “On maximizing the second smallest eigenvalue of a state-dependent graph Laplacian,” *IEEE Transactions on Automatic Control*, vol. 51, no. 1, pp. 116–120, 2006.

[KV12] B. Korte and J. Vygen, *Combinartorial optimization: Theory and algorithms*. Springer, 2012.

[KKM97] D. Kratsch, T. Kloks, and H. Muller, “Measuring the vulnerability of classes of intersection graphs,” *Discrete Applied Mathematics*, vol. 77, pp. 259–270, 3 1997.

[Laz01] D. Lazer, “The co-evolution of individual and network,” *The Journal of Mathematical Sociology*, vol. 25, pp. 69–108, 1 2001.

[LBB+18] D. Lazer, M. Baum, Y. Benkler, A. Berinsky, K. Greenhill, F. Menczer, M. Metzger, B. Nyhan, G. Pennycook, D. Rothschild, M. Schudson, S. Sloman, C. Sunstein, E. Thorson, D. Watts, and J. Zittrain, “The science of fake news,” *Schience*, vol. 359, pp. 1094–1096, 6380 2018.

[LQ13] C. Li and Z.-H. Qu, “Distributed estimation of algebraic connectivity of directed networks,” *Systems & Control Letters*, vol. 62, pp. 517–524, 2013.

[LQ14] ——, “Distributed finite-time consensus of nonlinear systems under switching topologies,” *Automatica*, vol. 50, pp. 1626–1631, 2014.

[LFJ14] F. Lin, M. Fardad, and M. Jovanović, “Algorithms for leader selection in stochastically fforce consensus networks,” *IEEE Transactions on Automatic Control*, vol. 59, no. 7, pp. 1789–1802, 2014.

[LXHB18] F.-Z. Liu, D. Xue, S. Hirche, and M. Buss, “Polarizability, consensusability and neutralizability of opinion dynamics on coopetitive networks,” *IEEE Transactions on Automatic Control*, 2018, to appear.

[LSB11] Y.-Y. Liu, J.-J. Slotine, and A. Barabási, “Controllability of complex networks,” *Nature*, vol. 473, pp. 167–173, 2011.

[LSB13] ——, “Observability of complex networks,” *PNAS*, vol. 110, no. 7, pp. 2460–2465, 2013.

[Lof04] J. Lofberg, “YALMIP: A toolbox for modelling and optimization in MATLAB,” in *Proceedings of IEEE International Symposium on Computer Aided Control Systems Design*, 2004.

[LS98] W. Lohmiller and J.-J. Slotine, “On contraction analysis for non-linear systems,” *Automatica*, vol. 34, no. 6, pp. 683–696, 1998.

[LS11] S. Lopez and C. Snyder, *The Oxford handbook of positive psychology - 2nd Edition*. Oxford University Press, 2011.

[LB14] P. D. Lorenzo and S. Barbarossa, “Distributed estimation and control of algebraic connectivity over random graphs,” *IEEE Transactions on Signal Processing*, vol. 62, no. 1, pp. 5616–5628, 2014.

[Lun15] J. Lunze, “Self-organizing disturbance attenuation for synchronized agents with individual dynamics,” *International Journal of Control*, vol. 88, no. 3, pp. 469–483, 2015.

[LMSM17] S.-J. Luo, F. Morone, C. Sarraute, and H. Makse, “Inferring personal economic status from social network location,” *Nat. Commun.*, vol. 8, e15227, 2017.

[MZ10] C.-Q. Ma and J.-F. Zhang, “Necessary and sufficient conditions for consensusability of linear multi-agent systems,” *IEEE Transactions on Automatic Control*, vol. 55, no. 5, pp. 1263–1268, 2010.

[MXH18] H. Mangesius, D. Xue, and S. Hirche, “Consensus driven by the geometric mean,” *IEEE Transactions on Control of Networked Systems*, vol. 5, pp. 251–261, 1 2018.

[MKKS11] S. Marvel, J. Kleinberg, R. Kleinberg, and S. Strogatz, “Continuous-time model of structural balance,” *PNAS*, vol. 108, no. 5, pp. 1771–1776, 2011.

[MFH10] M. Mäs, A. Flache, and D. Helbing, "Individualization as driving force of clustering phenomena in humans," *Plos Computational Biology*, vol. 6, no. 10, e1000959, 2010.

[MB10] I. Matei and J. Baras, "Consensus-based distributed linear filtering," in *Proceedings of IEEE Conference on Decision and Control*, 2010, pp. 7009–7014.

[MSLC01] M. McPherson, L. Smith-Lovin, and J. Cook, "Birds of a feather: Homophily in social networks," *Ann. Rev. Sociol.*, vol. 27, pp. 415–444, 2001.

[MB16] W.-J. Mei and F. Bullo, "Sequential decision aggregation with social networks," *Mathematics of Control, Signals, and Systems*, vol. 28, no. 3, pp. 1–16, 2016.

[Mes05] M. Mesbahi, "On state-dependent dynamic graphs and their controllability properties," *IEEE Transactions on Automatic Control*, vol. 50, pp. 387–392, 2005.

[ME10] M. Mesbahi and M. Egerstedt, *Graph theoretic methods in multi-agent networks*. Princeton University Press, 2010.

[Mic15] R. Michels, *Political parties: A sociological study of the oligarchical tendencies of modern democracy*. Hearst's International Library Co., 1915.

[MH07] J. Miller and J. Hyman, "Effective vaccination strategies for ealistic social networks," *Physica A: Statistical Mechanics and its Applications*, vol. 386, pp. 780–785, 2007.

[MJB14] A. Mirtabatabaei, P. Jia, and F. Bullo, "Eulerian opinion dynamics with bounded confidence and exogenous inputs," *SIAM Journal on Applied Dynamical Systems*, vol. 13, no. 1, pp. 425–446, 2014.

[MG13] I. Mirzaev and J. Gunawardena, "Laplacian dynamics on general graphs," *Bull Math Biol*, vol. 75, no. 11, pp. 2118–49, 2013.

[MSMH14] G. Moores, P. Shakarian, B. Macdonald, and N. Howard, "Finding near-optimal groups of epidemic spreaders in a complex network," *Plos One*, vol. 9, no. 4, e90303, 2014.

[MK14] F. Morbidi and A. Kibangou, "A distributed sloution to the network reconstruction problem," *Systems & Control Letters*, vol. 70, pp. 85–91, 2014.

[MT14] S. Motsch and E. Tadmor, "Heterophilious dynamics enhances consensus," *SIAM Review*, vol. 56, no. 4, pp. 577–621, 2014.

[MLM15] S. Mou, J. Liu, and A. Morse, "A distributed algorithm for solving a linear algebraic equation," *IEEE Transactions on Automatic Control*, vol. 60, no. 1, pp. 2863–2878, 2015.

[MGTH09] M. Moussaid, S. Garnier, G. Theraulaz, and D. Helbing, "Collective information processing and pattern formation in swarms, flocks, and crowds," *Top. Cogn. Sci.*, vol. 1, no. 3, pp. 469–497, 2009.

[MCP+13] A. Mukherjee, M. Choudhury, F. Peruani, N. Ganguly, and B. Mitra, *Dynamics on and of complex networks, Applications to time-varying dynamical systems*, in *Modeling and Simulation in Science, Engineering and Technology*, N. Bellomo, Ed. Birkhäuser Basel, 2013, vol. 2.

[Ned15] A. Nedić, "Convergence rate of distributed averaging dynamic and optimization in networks," *Foundations and Trends in System and Control*, vol. 2, no. 1, pp. 1–100, 2015.

[NV12] T. Nepusz and T. Vicsek, "Controlling edge dynamics in comple networks," *Nature Physics*, 2012.

[New00] M. Newman, "Models of small world," *Journal of Statistical Physics*, vol. 101, pp. 819–841, 2000.

[NWX13] W. Ni, X.-L. Wang, and C. Xiong, "Consensus controllability, obervability and robust design for leader-following linear multi-agent systems," *Automatica*, vol. 49, pp. 2199–2205, 2013.

[NPP16] C. Nowzari, V. Preciado, and G. Pappas, "Analysis and control of epidemics: A survey of spreading process on complex networks," *IEEE Control Systems Magazine*, vol. 36, no. 1, pp. 26–46, 2016.

[OSM04] R. Olfati-Saber and R. Murray, "Consensus problems in networks of agents with switching topology and time-delays," *IEEE Transactions on Automatic Control*, vol. 49, pp. 1520–1533, 9 2004.

[OCR14] B. Oreshkin, M. Coates, and M. Rabbat, "Optimization and analysis of distributed averaging with short node memory," *IEEE Transactions on Signal Process*, vol. 58, no. 5, pp. 2850–2865, 2014.

[PPTF17] S. Parsegov, A. Proskurnikov, R. Tempo, and N. Friedkin, "Novel multidimensional models of opinion dynamics in social networks," *IEEE Transactions on Automatic Control*, vol. 62, no. 5, pp. 2270–2285, 2017.

[PPS16] G. Pereira, R. Prada, and P. Santos, "Integrating social power into the decision-making of cognitive agents," *Artificial Intelligence*, vol. 241, pp. 1–44, 2016.

[PJ14] C. D. Persis and B. Jayawardhana, "On the internal model priniple in the coordination of nonlinear systems," *IEEE Transactions on Control of Network Systems*, vol. 1, no. 3, pp. 272–282, 2014.

[PG16] M. Porter and J. Gleeson, *Dynamical systems on networks*. Springer International Publishing, 2016.

[PYSL16] I. Poulakakis, G. Young, L. Scardovi, and N. Leonard, "Information centrality and ordering of nnode for accuracy in noisy decision-making networks," *IEEE Transactions on Automatic Control*, vol. 61, no. 4, pp. 1040–1045, 2016.

[POJ11] V. Preciado, J. Oh, and A. Jadbabaie, "Spectral design of dynamics networks via local operations," *Arxiv preprint: 1112.0765*, 2011.

[PZE+14] V. Preciado, M. Zargham, C. Enyioha, A. Jadbabaie, and G. Pappas, "Optimal resource allocation for network protection against spreading processes," *IEEE Transactions on Control of Network Systems*, vol. 1, no. 1, pp. 99–109, 2014.

[PRD18] A. Proskurnikov, C. Ravazzi, and F. Dabbene, "Dynamics and structure of social networks from a systems and control viewpoint: A survey of Roberto Tempo's contributions," *Online Soc. Net. Med.*, vol. 000, pp. 1–15, 2018.

[PC16] A. V. Proskurnikov and M. Cao, "Polarization in coopetitive networks of heterogeneous nonlinear agents," in *Proceedings of IEEE 55th Conference on Decision and Control (CDC)*, Las Vegas, US, 2016, pp. 6915–6920.

[PMC16] A. Proskurnikov, A. Matveev, and M. Cao, "Opinion dynamics in social networks with hostile camps: Consensus vs. polarization," *IEEE Transactions on Automatic Control*, vol. 61, no. 6, pp. 1524–1536, 2016.

[PT17] A. Proskurnikov and R. Tempo, "A tutorial on modeling and analysis of dynamic social networks. Part I," *Annual Review in Control*, vol. 43, pp. 65–79, 2017.

[PT18] ——, "A tutorial on modeling and analysis of dynamic social networks. Part II," *ArXiv:1801.06719v2 [cs.SI]*, 2018.

[QCS14] W. Quattrociocchi, G. Caldarelli, and A. Scala, "Opinion dynamics on interacting networks: Media competition and social influence," *Scientific Reports*, vol. 4, no. 4938, pp. 1–7, 2014.

[RCW16] P Ramazi, M. Cao, and F. Weissing, "Evolutionary dynamics of homophily and heterophily," *Scientific Reports*, vol. 6, no. 22766, pp. 1–9, 2016.

[RLM15] E. Ramirez-Llanos and S. Martinez, "Distributed stopping criterion for the power iteration applied to virus mitigation," in *Proceedings of 49th Asilomar Conference on Signals, Systems and Computers*, 2015, pp. 1328–1332.

[RBK14] P. Rattana, L. Berthouze, and I. Kiss, "Impact of constrained rewiring on network structure and node dynmics," *Physical Review E*, vol. 90, no. 052806, 2014.

[RFTI15] C. Ravazzi, P. Frasca, R. Tempo, and H. Ishii, "Ergodic randomized algorithms and dynamics over networks," *IEEE Trans. Control Netw. Syst.*, vol. 2, no. 1, pp. 78–87, 2015.

[RA05] W. Ren and E. Atkins, "Second-order consensus protocols in multiple vehicle system with local interactions," in *Proceedings of the AIAA Guidance, Navigation, and Control Conference and Exhibit*, 2005, pp. 1–13.

[RB05] W. Ren and R. Beard, "Consensus seeking in multiagent systems under dynamically changing interaction topologies," *IEEE Transactions on Automatic Control*, vol. 50, no. 5, pp. 655–661, 2005.

[RB08] ——, *Distributed consensus in multi-Vehicle cooperative control - Theory and applications*. Springer London, 2008.

[RC11] W. Ren and Y.-C. Cao, *Distributed coordination of multi-Agent networks - Emergent Problems, Models, and Issues*. Springer-Verlag London, 2011.

[ROH05] J. G. Restrepo, E. Ott, and B. Hunt, "Onset of synchronization in large networks of coupled oscillators," *Physcial Review E*, vol. 71, no. 036151, 2005.

[RMD15] C. Rougé, J.-D. Mathias, and G. Deffuant, "Vulnerability: From the conceptual to the operation using a dynamical system perpective," *Environmental Modeling & Software*, vol. 73, pp. 218–230, 2015.

[RS10] G. Russo and J. Slotine, "Global convergence of quorum-sensing networks," *Physical Review E*, vol. 82, p. 041 919, 2010.

[SAPV15] S. Saha, A. Adiga, B. Prakash, and A. Vullikanti, "Approximation algorithms for reducing the spectral radius to control epidemic spread," in *Proceeding of the 2015 SIAM International Conference on Data Mining*, 2015, pp. 568–576.

[SBS12] S. Sardellitti, S. Barbarossa, and A. Swami, "Optimal topology control and power allocation for minimum energy consumption in consensus networks," *IEEE Transactions on Signal Processing*, vol. 60, no. 1, pp. 383–399, 2012.

[SMHH11] C. Schneider, T. Mihaljev, S. Havlin, and H. Herrmann, "Suppressing epidemics with a limited amount of immunization units," *Physical Review E*, vol. 84, 061911 2011.

[Sep11] R. Sepulchre, "Consensus on nonlinear space," *Annual Reviews in Control*, vol. 35, no. 1, pp. 56–64, 2011.

[SSS14] M. Seslija, A. van der Schaft, and J. Scherpen, "Hamiltonian perspective on compartmental reaction-diffusion network," *Automatica*, vol. 50, pp. 737–746, 2014.

[SDJ13] G. Seyboth, D. Dimarogonas, and K. Johansson, "Event-based broadcasting for multi-agent average consensus," *Automatics*, vol. 49, no. 1, pp. 245–252, 2013.

[SS15] I. Shames and T. Summers, "Rigid network design via submodular set functions optimization," *IEEE Transactions on Network Science and Engineering*, vol. 2, no. 3, pp. 84–96, 2015.

[Sha11] Y.-L. Shang, "Local natural connectivity in complex networks," *Chinese Physical Letters*, vol. 28, no. 6, pp. 1–4, 068903 2011.

[SPB14] J. Simpson-Porco and F. Bullo, "Contraction theory on Riemannian manifolds," *Systems & Control Letters*, vol. 65, pp. 74–80, 2014.

[SS07] G. Stan and R. Sepulchre, "Analysis of interconnected oscillators by dissipativity theory," *IEEE Transactions on Automatic Control*, vol. 52, no. 2, pp. 256–270, 2007.

[SS90] G. Stewart and J. Sun, *Matrix perturbation theory*. Boston: Academic Press, 1990.

[SSLD15] T. Summers, I. Shames, J. Lygeros, and F. Dörfler, "Topology design for optimal network coherence," in *Proceedings of 2015 European Control Conference (ECC)*, 2015, pp. 575–580.

[SCL16] T. Summers, F. Cortesi, and J. Lygeros, "On submodularity and controllability in complex dynamical networks," *IEEE Transactions on Control of Network Systems*, vol. 3, pp. 91–101, 1 2016.

[SSG13] A. Sydney, C. Scoglio, and D. Gruenbacher, "Optimizing algebraic connectivity by edge rewiring," *Applied Mathematics and Computation*, vol. 219, pp. 5465–5479, 2013.

[Thu79] B. Thurman, "In the office: Networks and coalitions," *Social Networks*, vol. 2, no. 1, pp. 47–63, 1979.

[TK12] I. Tomovski and L. Kocarev, "Simple algorithm for virus spreading control on complex networks," *IEEE Transactions on Circuits and Systems-I: Regular Papers*, vol. 59, no. 4, pp. 763–771, 2012.

[TPER12] H. Tong, B. Prakash, and T. Eliassi-Rad, "Gelling, and melting, large graph by edge manipulation," Proceedings of the 21st ACM international conference on Information and knowledge management, 2012, pp. 245–254.

[Tot13] C. Toth, "Rationality and irrationality in understanding human behaviors: An evaluation of the methodological consequence of conceptualising irrationality," *Journal of Comparative Research in Anthropology and Sociology*, vol. 4, no. 1, pp. 85–104, 2013.

[TDL13] V. Traag, P. V. Dooren, and P. D. Leenheer, "Dynamical models explaining social balance and evolution of cooperation," *Plos one*, vol. 8, no. 4, e60063, 2013.

[TRK16] D. Tran, B. Rüffer, and C. Kellett, "Convergence properties for discrete-time nonlinear systems," *ArXiv preprint:1612.05327*, 2016.

[TSH01] H. Trentelman, A. Stoorvogel, and M. Hautus, *Control theory for linear systems*. Springer, 2001.

[TBA86] J. Tsitsiklis, D. Bertsekas, and M. Athans, "Distributed asynchronous determinstic and stochastic greadient optimization algorithms," *IEEE Transactions on Automatic Control*, vol. 31, pp. 803–812, 9 1986.

[TTT01] R. Tütüncü, K. Toh, and M. Todd. (2001). SDPT3 — A Matlab software package for semidefinite-quadraticlinear programming, Version 3.0, [Online]. Available: `http://www.math.nus.edu.sg/Ëœmattohkc/..`

[VM14] M. E. Valcher and P. Misra, "On the consensus and bipartite consensus in high-order multi-agent dynamical systems with antagonistic interactions," *System* & *Control Letters*, vol. 66, pp. 94–103, 2014.

[VPS+16] T. Valente, L. Palinkas, S.C., K.-H Chu, and C. Brown, "Fragmentation versus stability in bimodal coalitions," *Plos One*, vol. 10, no. 6, e0131712, 2016.

[vMi11] P. van Mieghem, *Graph spectra for complex networks*. Cambridge University Press, 2011.

[MSK+11] P. van Mieghem, D. Stevanović, F. Kuipers, C. Li, R. van de Bovenkamp, D. Liu, and H. Wang, "Deceasing the spectral radius of a graph by link removals," *Physical Review E*, vol. 84, no. 016101, 2011.

[vdS14] A. van der Schaft, "Port-Hamiltonian systems theory: An introductory overview," *Foundations and Trends in Systems and Control*, vol. 1, no. 2-3, pp. 173–378, 2014.

[vdS17] ——, "Modeling of physical network systems," *System* & *Control Letters*, vol. 101, pp. 21–27, 2017.

[SRJ16] A. van der Schaft, S. Rao, and B. Jayawardhana, "A network dynamics approach to chemical reaction networks," *International Journal of Control*, vol. 89, no. 4, pp. 731–745, 2016.

[SM13] A. van der Schaft and B. Machke, "Port-Hamiltonian systems on graphs," *SIAM Journal on Control and Optimization*, vol. 51, pp. 906–937, 2 2013.

[VBZ+16] M. D. Vicario, A. Bessi, F. Zollo, F. Petroni, A. Scala, G. Caldarelli, H. Stanley, and W. Quattrociocchi, "The spreading of misinformation online," *PNAS*, vol. 113, no. 3, pp. 554–559, 2016.

[WLY14] P. Wang, J. Lü, and X. Yu, "Identification of important nnode in directed biological networks: A network motif approach," *Plos ONE*, e106132, vol. 9, no. 8, 2014.

[WS98] D. Watts and S. Strogatz, "Collective dynamics of "small-world" networks," *Nature*, 1998.

[WSA11] P. Wieland, R. Sepulchre, and F. Allgäwer, "An internal model principle is necessary and sufficient for linear output synchronization," *Automatica*, vol. 47, pp. 1068–1074, 2011.

[WO03] R. Wood and M. O'Neill, "An always convergent method for finding the spectral radius of an irreducible non-negative matrix," *ANZIAM Journal*, vol. 45, pp. 474–485, 2003.

[XS16] T. Xia and L. Scardovi, "Output-feedback synchronizability of linear time-invariant systems," *Systems & Control Letters*, vol. 94, pp. 152–158, 2016.

[XC11] W.-G. Xia and M. Cao, "Clustering in diffusively coupled networks," *Automatica*, vol. 47, pp. 2395–2405, 2011.

[XCJ16] W.-G. Xia, M. Cao, and K. Johansson, "Structural balance and opinion separation in trust-mistrust social networks," *IEEE Transaction on Control of Network Systems*, vol. 3, no. 1, pp. 46–56, 2016.

[XLJB16] W.-G. Xia, J. Liu, K. Johansson, and T. Başar, "Convergence rate of the modified Degroot-Friendkin model with doubly stochastic relative interaction matrices," in *Conf. Proc. Amer. Control*, Boston, USA, 2016, pp. 1054–1059.

[XW06] F. Xiao and L. Wang, "State consensus for multi-agent systems with switching topologies and time-varying delays," *International Journal of Control*, vol. 79, no. 10, pp. 1277–1284, 2006.

[Xia10] L. W. F. Xiao, "Finite-time consensus problems for networks of dynamic agents," *IEEE Transactions on Automatic Control*, vol. 55, no. 4, pp. 950–955, 2010.

[XHC+17] Y. Xu, T. Han, K. Cai, Z. Lin, G. Yan, and M. Fu, "A distributed algorithm for resource allocation over dynamic digraphs," *IEEE Transactions on Signal Processing*, vol. 65, no. 10, pp. 2600–2612, 2017.

[XGH13] D. Xue, A. Gusrialdi, and S. Hirche, "Robust distributed control design for interconnected systems under topology uncertainty," in *Proceedings of American Control Conference (ACC)*, 2013, pp. 6541–6546.

[XGH14] ——, "A distributed strategy for near-optimal network topology design," in *Proceedings of the 21st International Symposium on Mathematical Theory of Networks and Systems (MTNS)*, Groningen, The Netherlands, 2014, pp. 7–14.

[XH13] D. Xue and S. Hirche, "Event-triggered consensus of heterogeneous multi-agent systems with double integrator dynamics," in *Proceedings of 2013 European Control Conference*, 2013, pp. 1162–1167.

[XH18a] ——, "Distributed topology manipulation to control epidemic spreading over networks," *IEEE Transactions on Signal Processing*, 2018, under review.

[XH18b] ——, "Finite-time distributed topology design for optimal network resilience," *IET Control & Applications*, 2018, under review.

[XHC18a] D. Xue, S. Hirche, and M. Cao, "Opinion behavior analysis in social networks with coopetitive interactions and media influence," *IEEE Transactions on Network Science and Engineering*, 2018, submitted.

[XHC18b] ——, "Opinion dynamics and self-appraisal of social power in signed networks," *IEEE Transactions on Automatic Control*, 2018, under review.

[YFG+10] P. Yang, R. Freeman, G. Gordon, K. Lynch, S. Srinivasa, and R. Sukthankar, "Decentralized estimation and control of graph connectivity for mobile sensor networks," *Automatica*, vol. 46(2), pp. 390–396, 2010.

[YCFC18] Q. Yang, M. Cao, H. Fang, and J. Chen, "Constructing universally rigid tensegrity fframework with application in multi-agent formation control," *IEEE Transactions on Automatic Control*, 2018. doi: 10.1109/TAC.2018.2829687.

[YLA+18] M.-B. Ye, J. Liu, B. Anderson, C.-B. Yu, and T. Başar, "Evolution of social power in social networks with dynamic topology," *IEEE Trans. Automat. Control*, 2018. doi: 10.1109/TAC.2018.2805261.

[YSC+13] G. Young, L. Scardovi, A. Cavagna, I. Giardina, and N. Leonard, "Starling flock networks manage uncertainty in consensus at low cost," *PlOS Communication Biology*, vol. 9, no. e1002894, 1 2013.

[YSL15] G. Young, L. Scardovi, and N. Leonard, "A new notion of effective resistence for directed graphs - Part I: Definition and properties," *IEEE Transactions on Automatica Control*, vol. 61, pp. 1727–1736, 7 2015.

[YSL16] ——, "A new notion of effective resistence for directed graphs - Part II: Computing resistence," *IEEE Transactions on Automatic Control*, vol. 61, pp. 1737–1752, 7 2016.

[You16] K. Young, *Handbook of social psychology*. 2016.

[Zas82] T. Zaslavsky, "Signed graphs," *Discrete Appl. Math.*, vol. 4, no. 1, pp. 47–74, 1982.

[ZC17] H. Zhang and J. Chen, "Bipartite consensus of multi-agent systems over signed graphs: State feedback and output feedback control approaches," *Int. J. Robust Nonlinear Control*, vol. 27, no. 1, pp. 3–14, 2017.

[Zha07] X.-D. Zhang, "The Laplacian eigenvalues of graphs: A survey," *Linear Algebra Research Advances*, pp. 201–228, 2007.

[ZT10] Y. Zhang and Y.-P. Tian, "Consensus of data-sampled milti-agent systems with random communication delay and packet loss," *IEEE Transactions on Automatic Control*, vol. 55, no. 4, pp. 939–943, 2010.

[ZX16] L. Zhao and D. Xue, "An operator-theoretic approach to synchronization of dynamically coupled biological," in *Proceedings of 35th Chinese Control Conference*, 2016, pp. 9342–9348.

[ZC16] Y. Zhao and J. Cortés, "Gramian-based reachability metric for bilinear networks," *IEEE Transactions on Control of Network Systems*, vol. 4, pp. 620–631, 3 2016.

[ZGP13] Y. Zhao, A. Goldsmith, and H. Poor, "Fundamental limits of cyber-physical security in smart power grids," in *Proceedings of 52nd Conference on Decision and Control*, 2013, pp. 200–205.